A novel role for the chromosomal passenger complex in DNA replication and damage response

Dissertation
zur Erlangung des Doktorgrades
Dr. rer. nat.

der Fakultät für Biologie
an der Universität Duisburg-Essen

vorgelegt von
Stefanie Mosel
aus Münster

April 2018

DOI: 10.17185/duepublico/46551
URN: urn:nbn:de:hbz:465-20250107-124626-5

Die der vorliegenden Arbeit zugrunde liegenden Experimente wurden am Zentrum für medizinische Biotechnologie in der Abteilung für Molekularbiologie II der Universität Duisburg-Essen durchgeführt.

1. Gutachter:	Prof. Dr. Shirley Knauer
2. Gutachter:	Prof. Dr. Georg Iliakis
3. Gutachter:	
Vorsitzender des Prüfungsausschusses:	Prof. Dr. Christian Johannes
Tag der mündlichen Prüfung:	27.06.2018

Table of contents

List of abbreviations

°C	degrees celsius
µ	micro
53BP1	p53-binding protein
5-AzaC	5-azacytidine
9-1-1	Rad9-Rad1-Hus1
A	ampere
aa	amino acid
AA	Antibiotic-Antimycotic
AF	Alexa Fluor
AID	auxin-inducible degron
AIR-2	Aurora/Ipl1-related kinase
Akt	AKT Serine/Threonine Kinase
Ankle1	Ankyrin Repeat And LEM Domain Containing 1
APC/C	anaphase-promoting complex/cyclosome
APH	aphidicolin
APS	ammonium peroxydisulfate
ASF1	anti-silencing function 1
ATAD5	ATPase Family, AAA Domain Containing 5
ATM	ataxia telangiectasia mutated
ATP	adenosine triphosphate
ATR	ataxia telangiectasia and Rad3-related
ATRIP	ATR-interacting protein
BER	base excision repair
BIR	baculoviral IAP repeat
bp	base pair
BRCA1, 2	breast cancer type 1, 2 susceptibility protein
BrdU	bromodeoxyuridine
BSA	bovine serum albumin
Bub1	Budding Uninhibited By Benzimidazoles 1
CAF1	chromatin assembly factor 1
CCAN	constitutive centromere-associated network
CD	chromo domain
CD34	cluster of differentiation 34
Cdc25	cell division cycle 25
Cdc6	cell division recognition complex 6
CDCA8	cell division cycle associated 8
CDK	cyclin-dependent kinase
CDKi	cyclin-dependent kinase inhibitor
Cdt1	Cdc10-dependent transcription factor 1
CENP-A	centromere protein A
Chk1, 2	checkpoint kinase 1, 2
CldU	chlorodeoxyuridine
CMG	Cdc45-MCM2-7-GINS

co-IP	co-immunoprecipitation
CPC	chromosomal passenger complex
CPT	camptothecin
crasiRNA	centromere repeat-associated small interacting RNA
CRISPR/Cas	Clustered Regularly Interspaced Short Palindromic Repeats/CRISPR-associated
Crm1	chromosomal region maintenance 1
CSD	chromoshadow domain
CSK	cytosceletal
Ctf18	chromosome transmission fidelity protein 18
Da	dalton
Dbf4	Dumbbell former 4 protein
ddH2O	double-distilled water
DMEM	Dulbecco's Modified Eagle Medium
DMSO	dimethyl sulfoxide
DNA	deoxyribonucleic acid
DNA-PKcs	catalytic subunit of the DNA dependent protein kinase
dNTP	deoxynucleotide triphosphate
DPBS	Dulbecco's phosphate-buffered saline
DSB	double strand break
dsDNA	double-stranded DNA
DTT	dithiothreitol
E2F	E2 factor
EDTA	ethylenediaminetetraacetic acid
EdU	5-ethynyl-2'-deoxyuridine
EGTA	ethylene glycol-bis(β-aminoethyl ether)-N,N,N',N'-tetraacetic acid
ESCO1, 2	establishment of sister chromatid cohesion 1/2
ESCRT-III	endosomal sorting complexes required for transport-III
FA	fanconi anemia
FACT	facilitates chromatin transcription
FANCD2	Fanconi anemia group D2 protein
FBH1	F-box DNA helicase 1
FCS	fetal calf serum
Fen1	flap structure-specific endonuclease
FITC	Fluorescein isothiocyanate
FlAsH-EDT$_2$	fluorescein arsenical hairpin binder
FoxM1	forkhead box M1
FRET	Förster/fluorescecne resonance energy transfer
fw	forward
G_1, G_2, G_0 phase	gap or growth phase 1, 2, 0
GFP	green fluorescent protein
GINS	"go-ichi-ni-san", japanese for 5, 1, 2, 3
Gy	Gray
h	hour
H3K9me3	histone H3 trimethylated on Lys9
HA	hemagglutinin

HBB	human *beta-globin*
HBXIP	hepatitis B X-interacting protein
HDAC	histone deacetylase
HEPES	4-(2-hydroxyethyl)-1-piperazineethanesulfonic acid
HP1	heterochromatin protein 1
HR	homologous recombination
HRP	horseradish peroxidase
HU	hydroxyl urea
IAP	inhibitor of apoptosis
IARC	International Agency for Research on Cancer
IdU	iododeoxyuridine
IF	immunofluorescence
INCENP	Inner centromere protein
IP	immunoprecipitation
iPOND	isolation of proteins on nascent DNA
k	kilo
Kif2A	kinesin family member 2A
KLD	kinase, ligase, DpnI
KMN	KNL1/Mis12/Ndc80
KNL1	Kinetochore-null protein 1
l	liter
LB	Luria-Bertani
LCR	locus control region
LMB	Leptomycin B
m	meter
m	milli
M	molar; mol/liter
M phase	mitotic phase
MCC	mitotic checkpoint complex
MCM	mini-chromosome maintenance
MEM	minimal essential medium
min	minute
Mis12	Mum2p-Ime4p-Slz1p
Mklp1	mitotic kinesin-like protein 2
MOPS	3-Morpholinopropane-1-sulfonic acid
Mre11	meiotic recombination 11
MRN	Mre11-Rad50-Nbs1
mRNA	messenger RNA
mTOR	mammalian target of rapamycin
n	nano
Nbs1	Nijmegen breakage syndrome protein-1
ncRNA	non-coding RNA
Ndc80	Nuclear division cycle 80
NEAA	Non-Essential Amino Acids Solution
NER	nucleotide excision repair
NES	nuclear export signal

NHEJ	non-homologous end-joining
NP-40	Nonidet P40
NPM	nucleophosmin/nucleoplasmin
ORC	origin recognition complex
OsTIR1	*Oryza sativa* transport inhibitor response 1
PARP1	poly(ADP-ribose) polymerase1
PBS	phosphate-buffered saline
pCCC	PCNA chromobody
PCNA	proliferating cell nuclear antigen
PCR	polymerase chain reaction
PEI	polyethylenimine
PFA	paraformaldehyde
pH	potentia Hydrogenii
pH3S10	histone H3 phosphorylated on Ser10
PIP	PCNA-interacting protein
PIPES	1,4-Piperazinediethanesulfonic acid
PLA	Proximity Ligation Assay
Plk1	polo-like kinase 1
PMSF	phenylmethylsulfonyl fluorid
Pol	polymerase
PP1	protein phosphatase 1
PP2A	protein phosphatase 2A
pre-RC	pre-recognition complex
PrimPol	DNA-directed primase/polymerase protein
Psf1, 2, 3	partner of sld five 1, 2, 3
PTM	post-translational modification
PVDF	polyvinylidene difluoride
Rb	retinoblastoma-associated protein
Rev1	Reversionless protein 1
RFC	replication factor C
RFP	red fluorescent protein
RhoA	Ras Homolog Family Member A
RIPA	radioimmunoprecipitation assay buffer
RISC	RNA-induced silencing complex
RNA	ribonucleic acid
RNAi	RNA interference
ROS	reactive oxygen species
RPA	replication protein A
RT	room temperature
rv	reverse
s	second
S phase	synthesis phase
SAC	spindle assembly checkpoint
SAH	single alpha helix
SAHA	suberoylanilide hydroxamic acid
SCF	Skp1-Cullin-F-Box ligase

SDS	sodium dodecylsulphate
SDS-PAGE	sodium dodecylsulphate-polyacrylamide gel electrophoresis
SENP3	Sentrin-specific protease 3
SETDB1	SET Domain Bifurcated 1
Sgo1, 2	shugoshin 1, 2
siRNA	small interfering RNA
SMARCAL	SWI/SNF-related matrix-associated actin-dependent regulator of chromatin subfamily A-like protein
SMC	structural maintenance of chromosome
SOC	super optimal broth with catabolite repression
SSB	single strand break
ssDNA	single-stranded DNA
SUV39H	Suppressor Of Variegation 3-9 Homolog
T2AA	T2 amino alcohol
TAE	Tris-acetate-EDTA TBS
TBS	Tris-buffered saline
TEMED	N,N,N’,N’-Tetramethylethylenediamine
Tip60	tat-interacting protein 60
TLS	translesion synthesis
TOPII	DNA topoisomerase II
Tris	Tris (hydroxymethyl) aminomethane
TS	template switch
TSA	Trichostatin A
UV	ultraviolet
V	Volt
v/v	vlume/volume
VCP	Valosin Containing Protein
w/v	weight per volume
WB	Western blot
WHO	World Health Organization
WRN	Werner syndrome homolog
wt	wildtype

List of figures

List of tables

Summary

The faithful genome duplication and segregation of the entire genome to progeny cells are the most fundamental elements of the continuity of life. Aberrant events promote genomic instability, a characteristic of cancer development. One well-studied example for regulating key mitotic events is a set of proteins called the chromosomal passenger complex (CPC), which includes the Aurora B kinase, Survivin, Borealin and INCENP. All CPC members are overexpressed in a multitude of cancers. They regulate key mitotic events, including correction of chromosome-microtubule attachment errors, activation of the spindle assembly checkpoint and construction and regulation of the contractile apparatus that drives cytokinesis. Besides its nuclear function during mitosis, a cytoplasmic fraction of Survivin, without CPC association, exhibits anti-apoptotic functions as a member of the inhibitor of apoptosis protein (IAP) family. In addition, recent studies have also shown an involvement of the CPC in the DNA damage response after irradiation. Overexpression of at least one CPC member is associated with high rates of tumor recurrence, abbreviated patient survival and resistance to chemo- and radiotherapy. Besides its function as a molecular marker for malignancies, this designates the CPC as a potential target for cancer therapy. In contrast to the localization and according functions of the CPC during mitosis, its function during interphase is still unknown. It is important to understand the underlying mechanism to improve cancer therapies. Thus, the present project aims to dissect the functional role of the CPC during interphase, especially during replication and after damage response.

Survivin was already expressed in early S phase and formed nuclear foci. Some of these foci were in close proximity or co-localized with PCNA, especially during late S phase. Similarly, Aurora B also accumulated in nuclear foci during S phase, co-localizing with PCNA. In order to track the formation of CPC foci, time-lapse studies were performed but need to be improved to obtain further evidence regarding the spatial and temporal regulation of CPC foci formation throughout the cell cycle. Since the CPC co-localized with PCNA especially during late S phase, when the constitutive heterochromatin is replicated, the localization referring to heterochromatin protein 1α (HP1α) was investigated in more detail. Both overexpressed and endogenous CPC proteins co-localized with heterochromatin in interphase cells. The CPC co-localized at replication sites defined by PCNA not only with HP1α, but also to centromeric chromatin defined by a staining with a specific centromere antiserum (CREST).

In order to address the question if the CPC is bound to the replisome via PCNA or to heterochromatin, an iPOND assay was performed. While Survivin seems to be bound to the newly synthesized DNA strand in the vicinity of the replisome, it is still unknown whether this link is provided through an interaction with chromatin or with replication proteins, respectively. PLA analysis demonstrated a close proximity of all CPC members to PCNA, indicative for an interaction. Indeed, also in co-IP experiments Aurora B-HA, Borealin-HA and myc-INCENP were detected in immunoprecipitates of PCNA. A conserved PCNA-interacting protein (PIP)-box motif was found in the human protein INCENP and comfirmed in PLA and co-IP experiments either by blocking the interaction via inhibitor treatment or by mutation of the PIP box. A disruption of the interaction by mutating the respective binding site did not result in localization changes of INCENP, thus indicating that the PIP box motif in INCENP is necessary for interaction with

PCNA but does not play a role in foci formation. Since the CPC proteins co-localized to the heterochromatin marker HP1α, co-IPs were conducted and revealed a potential binding of HP1α and Borealin, but still need to be confirmed by further studies.

To evaluate whether the CPC could be functionally implicated in processes during replication, flow cytometry was performed and has demonstrated that cells in G_2/M phase increased dramatically while the amount of S and G_1 phase cells decreased upon depletion of Survivin. However, in this case the mitotic and a potential replicative dysfunction can not be unambiguously distinguished from one another. Further functional analysis of replication fork velocities via fiber assay analysis revealed a reduced replication fork speed in Survivin-depleted cells but not after Aurora B inhibition.

Since Survivin depletion decelerated the replication fork, thus causing replication stress, the question arises whether induced replication stress reversely affects the CPC. After induction of replication stress by different chemicals and irradiation, all CPC proteins showed similar expression levels in all samples of whole cell lysates, indicating that the total protein quantity remains the same. Aurora B and Survivin were slightly increased only in the cytoplasmic fraction after CPT and APH treatment as well as after irradiation, which still needs to be elucidated in more detail. Both soluble nuclear and chromatin bound fractions showed similar levels independently of the type of treatment in contrast to previous results after irradiation. Likewise, quantitative analysis of immunostaining revealed only slight or no alterations in nuclear protein expression of Survivin and Aurora B after induction of replication stress. In addition to replication fork stalling, replication stress can also lead to fork collapse. In this case, replication stress leads to functional uncoupling of the helicase complex from the replicative polymerase resulting in dissociation of elongating factors from the replication fork. While PCNA dissociated from forks, CPC proteins still showed an accumulation after fork collapse. This leads to the assumption that even if the CPC can bind to PCNA, this interaction seems not to be sufficient for targeting the CPC to replication sites. Furthermore, recent studies have shown that in cases of replication stress without checkpoint activation, DNA synthesis takes place even during mitosis. However, INCENP was not detected on newly synthesized DNA in mitotic cells, indicating that CPC members conduct their mitotic function without a relocation to replication sites.

Taken together, these results indicate a novel role of the CPC in DNA replication or replication-associated processes as well as after damage response. The CPC accumulates in nuclear foci, especially during late S phase, and these proteins interact via a PIP box motif in INCENP with PCNA. In addition, these foci are also located at heterochromatin, more precisely at centromeres. Furthermore, Survivin-depletion affected replication fork velocities thus causing replication stress. Overall, these results emphasize the concept of the multifunctional nature of the CPC. This kind of multitasking accomplished by a single protein complex could be on the one hand much more economical for a cell than producing many different proteins or protein complexes to regulate different tasks during the cell cycle. On the other hand, this vast array of tasks in maintaining genomic stability also support the CPC's importance for cancer therapy as treatment against one single protein complex can multiply its effect by targeting a multitude of cellular processes.

Zusammenfassung

Die gewissenhafte Genomverdoppelung und -verteilung des gesamten Genoms auf die nachkommenden Zellen stellen die grundlegendsten Elemente für den Fortbestand des Lebens dar. Das Auftreten von Fehlern in diesen Prozessen fördert die genomische Instabilität und damit auch die Krebsentwicklung. Ein gut untersuchtes Beispiel für die Regulation wichtiger mitotischer Ereignisse ist der so genannte *chromosomal passagenger complex* (CPC), welcher die Proteine Aurora B Kinase, Survivin, Borealin und INCENP beinhaltet. Alle CPC-Mitglieder sind in einer Vielzahl von Krebsarten überexprimiert. Sie regulieren wichtige mitotische Ereignisse, einschließlich der Korrektur von Anheftungsfehlern der Mikrotubuli an die Chromosomen, der Aktivierung des Kontrollpunkts der Spindelanordnung und der Bildung und Regulierung des kontraktilen Apparates, welcher schließlich die Zytokinese vorantreibt. Neben seiner nukleären Funktion während der Mitose existiert eine zytoplasmatische Fraktion von Survivin, welche ohne CPC-Assoziation als Mitglied der Inhibitoren der Apoptose Protein (IAP, *inhibitor of apoptosis*)-Familie anti-apoptotische Funktionen wahrnimmt. Darüber hinaus konnten neuere Studien auch eine Beteiligung des CPCs an der DNA-Schadensantwort nach Bestrahlung nachweisen. Die Überexpression mindestens eines CPC-Mitglieds in Krebszellen ist mit hohen Tumorrezidiven, verkürztem Überleben des Patienten und einer Resistenz gegenüber Chemo- und Strahlentherapie verbunden. Damit stellt der CPC, neben seiner Funktion als molekularer Marker für maligne Erkrankungen, auch ein potentielles Ziel für die Krebstherapie dar. Im Gegensatz zur Lokalisation und den entsprechenden Funktionen des CPC während der Mitose ist die Funktion des CPC während der Interphase noch unbekannt. Um Krebstherapien zu verbessern, ist es wichtig, die zugrunde liegenden Mechanismen zu verstehen. Ziel der vorliegenden Arbeit war daher, die funktionelle Rolle des CPC während der Interphase, insbesondere während der Replikation und nach der DNA-Schadensantwort, aufzuklären.

Survivin wird bereits in der frühen S-Phase exprimiert und bildet nukleäre Foci. Einige dieser Foci befinden sich in unmittelbarer Nähe von oder co-lokalisierten mit PCNA, insbesondere während der späten S-Phase. In ähnlicher Weise akkumuliert Aurora B während der S-Phase in nukleären Foci, ebenfalls gemeinsam mit PCNA. Um die Bildung der CPC-Foci während des gesamten Zellzyklus zu verfolgen, wurden Studien im zeitlichen Verlauf durchgeführt, die jedoch weiter verfeinert werden müssen, um deren räumliche und zeitliche Entwicklung zweifelsfrei darlegen zu können. Da der CPC vor allem während der späten S-Phase mit PCNA co-lokalisiert, also zum Zeitpunkt der Replikation des konstitutiven Heterochromatins, wurde die Lokalisation anhand des Heterochromatin-Proteins 1α (HP1α) genauer untersucht. Sowohl überexprimierte als auch endogene CPC-Proteine co-lokalisieren mit Heterochromatin in Interphase-Zellen. Der CPC co-lokalisiert an Replikationsstellen, die durch PCNA definiert wurden, nicht nur mit HP1α sondern auch mit centromerischem Chromatin, das durch eine Färbung mit einem spezifischen Centromer-Antiserum (CREST) definiert wurde.

Mithilfe der Durchführung eines iPOND-Assays sollte der Frage nachgegangen werden, ob der CPC über PCNA an das Replisom oder an das Heterochromatin gebunden ist. Während Survivin vermutlich an den neu synthetisierten DNA-Strang in der Nähe des Replisoms bindet, wurde noch nicht geklärt, ob diese Verbindung durch eine Interaktion mit dem Chromatin oder

mit Replikationsproteinen erfolgt. Die PLA-Analyse zeigte eine unmittelbare Nähe aller CPC-Mitglieder zu PCNA, was auf eine Interaktion hindeutet. Tatsächlich wurden auch in Co-IP-Experimenten Aurora B-HA, Borealin-HA und myc-INCENP in Immunopräzipitaten von PCNA nachgewiesen. Ein konserviertes PIP (PCNA-interacting protein)-Box-Motiv wurde im humanen Protein INCENP gefunden und in PLA- und Co-IP-Experimenten entweder durch Blockierung der Interaktion durch Inhibitor-Behandlung oder mittels Mutation der PIP-Box bestätigt.

Eine Verhinderung der Interaktion durch Mutation der Interaktionsstelle führte allerdings nicht zu Lokalisationsänderungen von INCENP, was darauf hindeutet, dass das PIP-Box-Motiv in INCENP für die Interaktion mit PCNA zwar notwendig ist, aber keine Rolle bei der Foci-Bildung spielt. Aufgrund der Tatsache, dass die CPC-Proteine zusammen mit dem Heterochromatinmarker HP1α lokalisieren, wurden co-IPs durchgeführt und diese zeigten eine potentielle Bindung von HP1α und Borealin, die aber noch weiter bestätigt werden muss.

Um zu klären, ob der CPC eine funktionelle Rolle in Replikationsprozessen spielt, wurden durchflusszytometrische Analysen durchgeführt. Hier zeigte sich, dass die Anzahl von Zellen in der G_2/M-Phase dramatisch anstieg, während die Menge an S- und G_1-Phasenzellen nach Survivin-Depletion abnahm. In diesem Fall können die mitotische und eine potentielle replikative Dysfunktion jedoch nicht eindeutig voneinander unterschieden werden. Weitere funktionelle Analysen mittels *Fiber Assays* zeigten eine reduzierte Geschwindigkeit der Replikationsgabel in Survivin-depletierten Zellen, jedoch nicht nach Aurora B Kinase Inhibition.

Da die Survivin-Depletion die Replikationsgabel verlangsamte und somit Replikations-Stress verursachte, stellte sich die Frage, ob induzierter Replikations-Stress umgekehrt auch den CPC beeinflusst. Nach Induktion von Replikations-Stress durch verschiedene Chemikalien und Bestrahlung zeigten alle CPC-Proteine ähnliche Expressionsniveaus in allen Proben von Zell-Lysaten, was darauf hindeutet, dass die Gesamtproteinmenge konstant bleibt. Aurora B und Survivin waren nur in der zytoplasmatischen Fraktion nach Camptothecin- und Aphidicolin-Behandlung sowie nach Bestrahlung leicht erhöht, was allerdings noch genauer untersucht werden muss. Sowohl lösliche nukleäre als auch Chromatin-gebundene Fraktionen zeigten unabhängig von der Art der Behandlung ähnliche Werte, im Gegensatz zu früheren Ergebnissen nach Bestrahlung. In ähnlicher Weise zeigte eine quantitative Analyse der Immunfärbung nur geringe oder keine Veränderungen in der nukleären Proteinexpression von Survivin und Aurora B nach Induktion von Replikationsstress. Zusätzlich zum Pausieren der Replikationsgabel kann Replikations-Stress auch zum Zusammenbruch der Replikationsgabel führen. In diesem Fall führt der Stress zu einer funktionellen Abkopplung des Helikase-Komplexes von der replikativen Polymerase, was zur Dissoziation der Elongationsfaktoren von der Replikationsgabel führt. Während PCNA von den Gabeln dissoziierte, zeigten die CPC-Proteine immer noch eine Akkumulation nach dem Zusammenbruch der Replikationsgabel. Dies führt zu der Annahme, dass, selbst wenn der CPC an PCNA binden kann, diese Interaktion nicht ausreicht, um den CPC fest an Replikationsstellen zu adressieren. Darüber hinaus haben neuere Studien gezeigt, dass in Fällen von Replikations-Stress ohne Aktivierung des Kontrollpunktes die DNA-Synthese sogar noch während der Mitose stattfinden kann. Jedoch wurde INCENP nicht an neu synthetisierter DNA in mitotischen Zellen nachgewiesen, was darauf hindeutet, dass CPC-Mitglieder ihre mitotische Funktion ohne eine Verlagerung zu Replikationsstellen ausführen.

Zusammengefasst zeigen diese Ergebnisse eine neue Rolle des CPC bei der DNA-Replikation oder Replikations-assoziierten Prozessen sowie nach einer Schadensantwort. Der CPC akkumuliert in nukleären Foci, insbesondere während der späten S-Phase, und diese Proteine interagieren über ein PIP-Box Motiv in INCENP mit PCNA. Außerdem befinden sich diese Foci in heterochromatischen Bereichen, genauer gesagt an Zentromeren. Darüber hinaus beeinflusste die Survivin-Depletion die Geschwindigkeit der Replikationsgabel und verursachte auf diese Weise Replikations-Stress. Insgesamt unterstreichen diese Ergebnisse das Konzept des multifunktionalen Charakters des CPC. Dias gleichzeitige Erfüllen mehrerer Aufgaben während des Zellzyklus durch nur einen einzigen Proteinkomplex könnte einerseits für die Zelle viel wirtschaftlicher sein als die Herstellung vieler verschiedener Proteine oder Proteinkomplexe. Auf der anderen Seite unterstreichen diese vielfältigen Aufgaben bei der Aufrechterhaltung der genomischen Stabilität auch die Bedeutung des CPCs für die Krebstherapie, da die Behandlung gegen einen einzigen Proteinkomplex den Behandlungseffekt multiplizieren kann, indem eine Vielzahl zellulärer Prozesse beeinflusst wird.

1 Introduction

1.1 Cancer

Cancer is a major public health problem around the world. According to WHO (World Health Organization) and the latest global cancer statistics (2015), there were 14.1 million new cancer cases in 2012 worldwide and the corresponding estimates for total cancer deaths were 8.2 million. Globally, nearly 1 in 6 deaths is due to cancer. According to the latest Worldwide Cancer Statistics from Cancer Research UK, the top 5 most common cancer sites are lung, breast, colorectum, prostate and stomach, with more than 6.9 million new cases reported in 2012 (**Fehler! Verweisquelle konnte nicht gefunden werden.** A). Correspondingly, the top 5 most common cancer deaths are lung, liver, stomach, colorectum and breast, accounting for more than half of total cancer death (Figure 1 B; Ferlay et al., 2015).

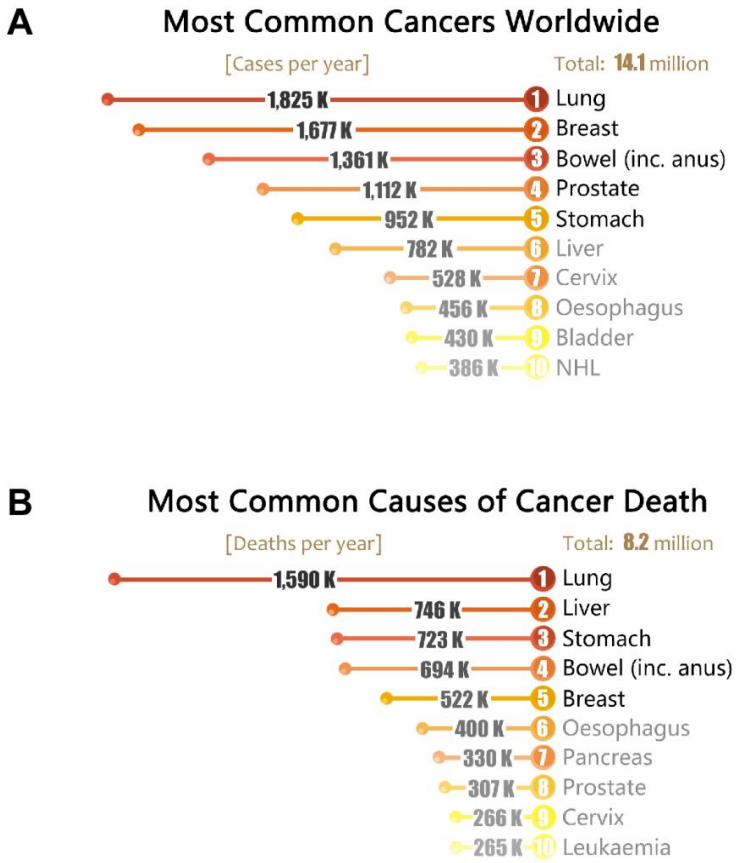

Figure 1: 10 most common cancers and causes of cancer death.
A) Estimated global numbers of new cases (incidence) worldwide. **B)** Estimated numbers of cancer death (mortality) worldwide. Adapted from "NJU-China", 2018.

In the GLOBOCAN 2008 report, the International Agency for Research on Cancer (IARC) and the WHO predict that according to the forecasted country-specific changes in population growth and aging future cancer incidence will increase by 69 % (2008: 12.7 million; 2030: 21.4 million new cases) and mortality burden by 72 % (2008: 7.6 million, 2030: 13.2 million deaths from cancer) until 2030. The probability to develop cancer rises with increasing age. Today, every second man and 43 % of all women have to expect to develop cancer in the course of their life.

1.1.1 Carcinogenesis

Cancer is a multi-step process in which cells undergo metabolic and behavioral changes, leading to excessive proliferation to escape the surveillance by the immune system and ultimately to distant tissues invasion (metastasis). The initial step of carcinogenesis is a modification in the genomic DNA. Most common in tumor cells are point mutations, gene amplifications, deletions or chromosomal translocations (Croce, 2008). The majority of genetic changes can be divided into two categories: gain-of-function mutations in proto-oncogenes, which stimulate cell growth, division, and survival; and loss-of-function mutations in tumor suppressor genes that normally help prevent unrestrained cellular growth and promote DNA repair and cell cycle checkpoint activation (Lee & Muller, 2010). Further changes during carcinogenesis base on the accumulation of modifications in the genetic programs that for example control cell proliferation and lifespan, relationships with neighboring cells and capacity to escape the immune system. This process results at the end in the formation of a mass of deregulated cells. These acquired capabilities of cancer cells were described by Hanahan and Weinberg in 2000 as hallmarks of cancer (Figure 2). They include sustaining proliferative signaling, evading growth suppressors, resisting cell death, enabling replicative immortality, inducing angiogenesis, and activating invasion and metastasis (Hanahan and Weinberg, 2000). In 2011 they expanded their hallmarks to include the emerging hallmarks: deregulating cellular energetics and avoiding immune destruction as well as the enabling characteristics: genome instability and mutation and tumor-promoting inflammation (Figure 2) (Hanahan and Weinberg, 2011).

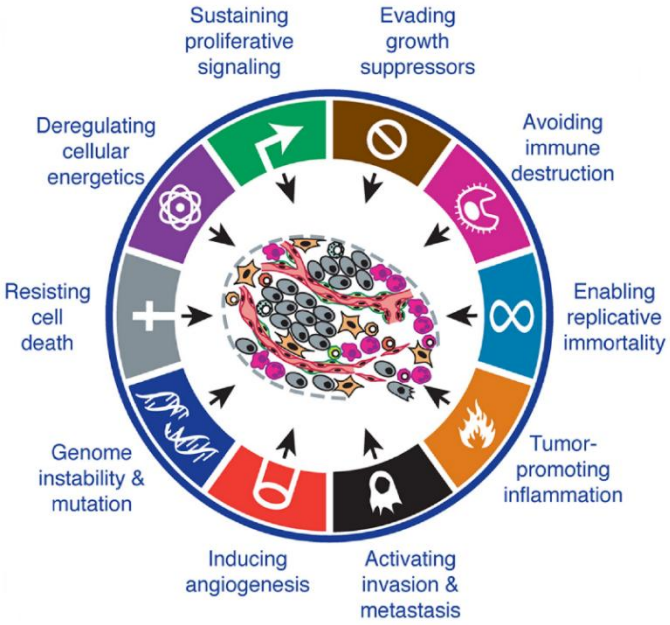

Figure 2: Hallmarks of cancer.

The illustration displays the acquired properties of cancer cells also known as hallmarks of cancer according to Hanahan & Weinberg (2000), as well as enabling characteristics and emerging hallmarks of cancer cells that were added a decade later (Hanahan and Weinberg, 2011).

1.1.2 Cancer treatment

In principle, cancer can develop in every tissue or organ and currently more than 200 cancer types are described (Todd et al., 2018). Although 30–50 % of all human cancer cases are

preventable according to estimations of the WHO by reducing exposure to cancer risk factors, 8.8 million people worldwide died from cancer in 2015. This shows that obviously no universal remedy was developed so far. The main therapies are surgery, chemotherapy and radiotherapy, but also hormone therapy, targeted cancer drugs and immunotherapy are often used. In addition, combinational approaches are very common.

More than 80 % of all cancer cases will need surgery, some several times (Sullivan et al., 2015), where surgery can be diagnostic, preventive, curative, supportive, palliative and reconstructive. For example, surgical biopsies can confirm the diagnosis, preventive surgery is performed to remove tissue that is likely to become cancerous, surgical resection is crucial for palliative care, such as mastectomy for advanced breast cancers to improve the quality of life and reconstructive surgery is used to improve cosmetics for example after mastectomy (Sullivan et al., 2015).

Chemotherapy is a drug treatment involving chemicals that are cytotoxic. So far, there are several different classes of anticancer drugs available based on their mechanisms of action. They include the following: a) alkylating agents which damage DNA; b) anti-metabolites that replace the normal building blocks of RNA and DNA; c) antibiotics that interfere with the enzymes involved in DNA replication; d) topoisomerase inhibitors that inhibit either topoisomerase I or II, which are the enzymes involved in unwinding DNA during replication and transcription; e) mitotic inhibitors that inhibit mitosis and cell division; and f) corticosteroids, which are used for the treatment of cancer and to relieve the side effects from other drugs (Huang et al., 2017). However, chemotherapy works like a two-sided sword, on the one hand annihilating cancerous cells and on the other hand destroying healthy fast-dividing cells like bone-marrow cells, immune cells, hair follicle cells as well as cells from the digestive tract and the reproductive system, leading to a high number of adverse side effects.

Radiotherapy is used in at least two-thirds of cancer treatment regimes in Western countries (Chen and Kuo, 2017). During the last two decades the overall survival rates of cancer patients treated with radiation therapy have improved from about 30 % to about 80 % for some malignancies such as head and neck cancers (Baumann et al., 2016; Le et al., 2015). Radiotherapy destroys cancer by depositing high-energy radiation on the cancer tissue. Radiation can either indirectly or directly damage the genome of the cell. Indirect effects are caused by free radicals, which are derived from the ionization or excitation of the water component of the cells. Radiation acts also directly on the cellular components and induces single strand breaks (SSB) or double strand breaks (DSB), representing the most lethal type of DNA damage, leading to cell death if unrepaired (reviewed in Baskar, Dai, Wenlong, Yeo, & Yeoh, 2014).

Despite advances in cancer treatment, overall survival of cancer patients remains limited and relapses occur frequently, indicating that there are cancer cells that become therapy-resistant (Oei et al., 2017). Therefore, it is necessary to improve existing therapies, to augment radiosensitivity and to obtain a better understanding of resistance mechanism to develop novel therapeutic strategies.

1.2 Chromatin

Chromatin is defined as a complex of macromolecules found in the nucleus of a cell, consisting of DNA and associated proteins. The functions of chromatin comprise packaging of DNA into a more compact and denser shape, reinforcing the DNA macromolecule to allow mitosis, preventing DNA damage as well as controlling gene expression and DNA replication.

1.2.1 Chromatin architecture and modification

The genomic DNA double helix in the eukaryotic nucleus is hierarchically packed by histones into chromatin (Figure 3). Thereby, 147 bp of DNA are wrapped around an octamer of histone proteins, building the nucleosome (Luger et al., 1997; Richmond and Davey, 2003). The octameric protein complex consists of two copies of the core histones H2A, H2B, H3 and H4. The nucleosomal array, a “beads on a string” fiber with a diameter of 11 nm, represents the first level of chromatin organization (Luger et al., 1997). Single nucleosomes are connected by 10–90 bp long DNA linker (Richmond and Davey, 2003).The binding of the linker histone (H1 or H5) organizes the nucleosome arrays into a more condensed 30 nm chromatin fiber (Robinson et al., 2006). Higher order structures are reached finally in mitosis when chromatin is condensed to form chromosomes in metaphase.

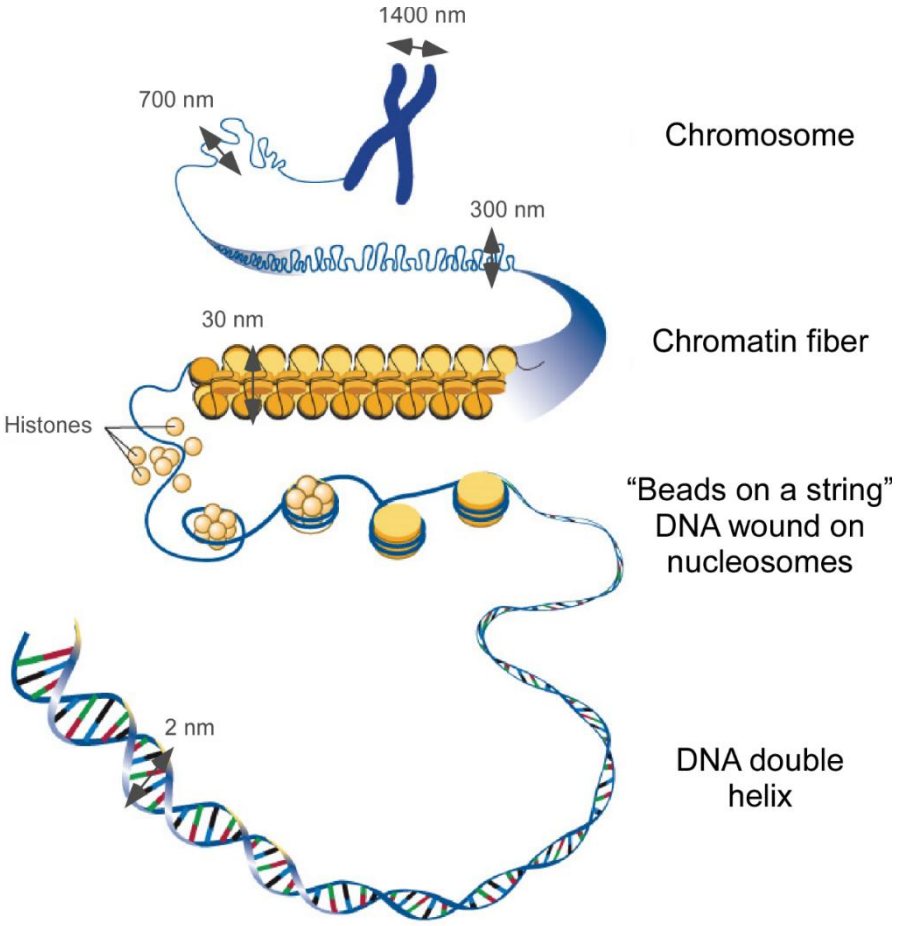

Figure 3: Chromatin architecture.

The DNA double helix is wrapped around a histone octamer forming the primary organizing unit, the nucleosome. Chromatin is further packed in a 30 nm fiber and reaches is maximal condensation as metaphase chromosome. Modified from “NHGRI Image Gallery - National Human Genome Research Institute (NHGRI),” 2018.

Although the core histones form a highly conserved structure, nucleosome stability varies due to the incorporation of non-canonical histone variants and a vast array of post-translational modifications (PTMs). For example, the variant H3.3 replaces the core histones H3.1 and H3.2 predominantly in actively transcribed genes, at the transcription start site of both, active and repressed genes, in regulatory regions such as enhancers, at telomeres and in pericentric heterochromatin (reviewed in Zink & Hake, 2016). Instead of H3 the histone variant CENP-A (also referred to as cenH3) is incorporated into nucleosomes and forms the foundation of centromeric chromatin (Mendiburo et al., 2011). The H2A variants H2A.Z and H2A.B are implicated in transcription initiation thus affecting gene expression (Adam et al., 2001; Soboleva et al., 2012). An astonishing number of PTMs, including the most common like acetylation, methylation, phosphorylation, ubiquitination and sumoylation, occur on histones. While the majority are found in the flexible N- and C-terminal tail domains that protrude from the nucleosome core particle, a significant number also occur in the histone fold or globular domains that regulate histone-histone and histone-DNA interactions (Rothbart and Strahl, 2014). The so-called "histone-code" affects chromatin structure in three ways: either through intrinsic effects on histone–histone interactions, through extrinsic effects on internucleosome contacts, or by providing binding sites for effector molecules. Intrinsic effects alter nucleosome stability by changing histone–histone or histone–DNA interactions, while extrinsic effects tend to influence longer-range contacts between nucleosomes, altering higher-order chromatin organization (Hauer and Gasser, 2017). As an example, the acetylation of histone tails, neutralizes the lysine’s positive charge and this weakens the interaction between histones and DNA resulting in a more relaxed chromatin (Bannister and Kouzarides, 2011; Shogren-Knaak et al., 2006). In contrast, methylation of histone lysines (H3K9me3, H3K27me3 and H4K20me3) causes a more compact DNA restricting the accessibility of regulatory factors to genes which can lead to changes in transcription, replication and DNA repair (Jenuwein and Allis, 2001; Rothbart and Strahl, 2014). Finally, chromatin-modifying proteins that recognize histone PTMs often trigger changes enzymatically (Hauer and Gasser, 2017).

According to its compaction level, chromatin is classified into two categories: less condensed, gene-rich euchromatin and highly condensed, gene-poor heterochromatin. In general, euchromatin tends to reside closer to the nuclear interior, whereas heterochromatin localizes at the nuclear periphery, where specific interactions with the envelope may occur, and often forms blocks surrounding the nucleolus (Bártová et al., 2008; Woodcock and Ghosh, 2010). Heterochromatin can be further categorized into facultative and constitutive heterochromatin. Facultative heterochromatin is developmentally regulated and acts as a key regulator of cellular differentiation and morphogenesis (Nikolov and Taddei, 2016). It can reversibly undergo transitions from a compact, transcriptionally inactive state to become more open and transcriptionally competent (Woodcock and Ghosh, 2010). In contrast, constitutive heterochromatin is always compact and is formed at telomeres, centromeres and repetitive elements, where it plays a major role in genome stability (Nikolov and Taddei, 2016; Woodcock and Ghosh, 2010). But all in all during each cell cycle, there are, inherently, two periods when chromatin organization undergoes global changes: DNA replication in S phase and when chromosomes condense in mitosis (Li and Reinberg, 2011).

1.2.2 Chromatin binding proteins

Histone variants and PTMs can alter the chromatin structure either directly or through recruitment of chromatin-binding proteins that influence the chromatin state and various processes. A key chromatin-binding protein significant for heterochromatin is the heterochromatin protein 1 (HP1). Three isoforms, HP1α, HP1β, and HP1γ, have been characterized in humans (Saunders et al., 1993; Singh et al., 1991; Wreggett et al., 1994), which possess a characteristic domain organization but differ in their functions, expression profiles and its chromosomal localization (Bosch-Presegué et al., 2017; Kwon and Workman, 2011). HP1α and HP1β are predominantly bound within heterochromatic regions, while HP1γ shows an euchromatic distribution (Minc et al., 2000). The enrichment of the HP1α isoform at pericentric domains is critical for centromeric function otherwise leading to mitotic defects in mammals (Gilbert et al., 2003; De Koning et al., 2009; Obuse et al., 2004; Peters et al., 2001). HP1 consist of an N-terminal chromodomain (CD), followed by a hinge domain and a C-terminal chromoshadow domain (CSD) (Maison and Almouzni, 2004). The HP1 chromodomain specifically recognizes methylated H3K9 (Bannister et al., 2001; Jacobs and Khorasanizadeh, 2002) and is important for the recruitment to heterochromatin regions of the genome (Lachner et al., 2001; Peters et al., 2001). The HP1 chromoshadow domain can dimerize (Brasher et al., 2000; Cowieson et al., 2000), which allows interactions with proteins that contain a PxVxL motif (Murzina et al., 1999; Smothers and Henikoff, 2000; Thiru et al., 2004). Initially discovered to be a major constituent of heterochromatin important for gene silencing, HP1 is now known to be a dynamic protein that also functions in transcriptional elongation, centromeric sister chromatid cohesion, telomere maintenance and DNA repair and replication (Ayoub et al., 2008; Goodarzi et al., 2008; Kwon and Workman, 2011; Zeng et al., 2010).

One protein, which is associated with HP1 during DNA replication and repair is the chromatin assembly factor 1 (CAF1) (Kwon and Workman, 2011; Murzina et al., 1999; Quivy et al., 2008). HP1 binds to the PxVxL motif in CAF1 (Thiru et al., 2004). CAF1 mediates histone H3 and H4 deposition onto newly replicated DNA strands during replication and repair (Gaillard et al., 1996; Kaufman et al., 1995). Additionally, an HP1-CAF1-PCNA complex, whereof PCNA is an important replication protein, may function as a platform that contributes to both maintenance and duplication of heterochromatin (Maison and Almouzni, 2004).

1.3 Cell Cycle

The cell cycle is a series of events leading to the production of two daughter cells that have the same chromosomal set as the maternal cell. Chromosome segregation takes place during M phase, also called mitosis (Figure 4). It comprises prophase, metaphase, anaphase, telophase followed by cytokinesis, the cytoplasmic segregation. During Synthesis or S phase, DNA replication occurs and each chromosome is duplicated, resulting in two sister chromatids. Both of these crucial processes are separated by two Gap or Growth phases, G_1 and G_2. These are periods, where cells obtain mass and accumulate components needed for either DNA synthesis or mitosis. G_1, S and G_2 phase together are also called interphase. When cells have left the cell cycle and have stopped dividing, they rest in the G_0 phase, either transiently (quiescent) or permanently (upon terminal differentiation or senescence) (Otto and Sicinski, 2017).

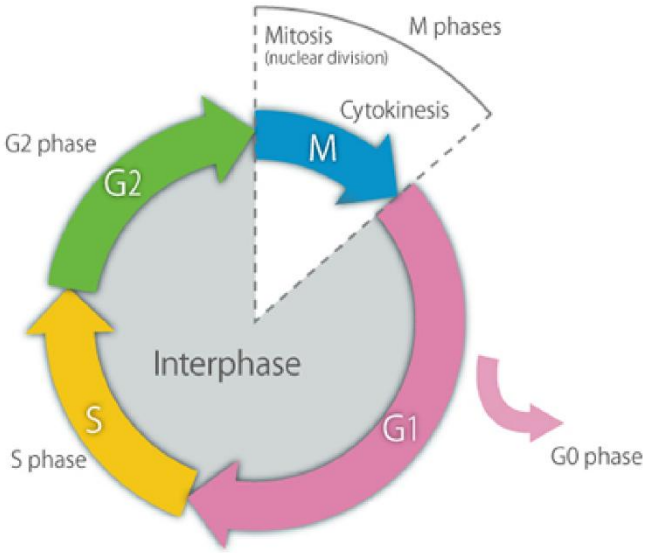

Figure 4: The cell cycle.

The eukaryotic cell cycle is divided into four phases: G_1, S, G_2 and M phase. Cells can leave the cell cycle from G_1 into G_0 phase. Modified from “Overview of the Cell Cycle - University of Tokyo” (2018).

1.3.1 Cell cycle regulation

The cell cycle is a highly organized and regulated process. The central proteins that drive cell cycle progression are cyclins and cyclin-dependent kinases (CDKs) (reviewed in Morgan, 1995). CDKs, serine/threonine protein kinases, are constitutively expressed, whereas cyclins are tightly regulated throughout the cell cycle on two levels, systematic synthesis and ubiquitin-dependent degradation. Once cyclins bind to CDKs, previously inactive CDKs alter their conformation leading to an activated state. Once activated by their cyclins, CDKs can phosphorylate key substrates to promote DNA synthesis or mitotic progression. The kinase activity of CDK/cyclin complexes is tightly regulated by CDK inhibitors (CDKi), which can halt the cell cycle progression under unfavorable conditions (Lim and Kaldis, 2013).

In more detail, cyclin D is produced in response to extracellular signals (e.g. growth factors). Cyclin D binds to existing CDK4 or CDK6, highly homologous kinases that are expressed in a

tissue-specific manner, forming the active cyclin D-CDK4/6 complex (Otto and Sicinski, 2017). The cyclin D-CDK4/6 complex in turn phosphorylates its substrate protein Rb, leading to activation of transcription factor E2F and finally resulting in the transcription of various genes like cyclin E, cyclin A and DNA polymerase. Cyclin E thus produced, binds to CDK2, forming the cyclin E-CDK2 complex, which promotes the progression from G_1 to S phase and phosphorylates its inhibitor p27, thereby inducing its proteasome-dependent degradation. In early S phase, cyclin E is replaced by cyclin A as binding partner of CDK2, which leads to the progression of S phase. Later in S and G_2 phase, cyclin A binds to CDK1 (Otto and Sicinski, 2017; Vermeulen et al., 2003). G_2/M transition is caused by Cyclin B-CDK1 complex activation, resulting in nuclear envelope breakdown and initiation of prophase, while complex inactivation causes mitotic exit (Asghar et al., 2015).

1.3.2 Cell cycle checkpoints

To ensure the proper progression of the cell cycle and to avoid transmission of an altered genome to daughter cells, elaborate control mechanisms known as cell cycle checkpoints have evolved. Cell cycle checkpoints are safeguard mechanisms that cells implement to arrest cell cycle progression in order to either repair damage or eventually commit suicide in case of unrepairable damage (Visconti et al., 2016). The source of DNA damage can be intrinsic, such as intermediates of metabolism, shortening of telomeres, oncogene overexpression and DNA replication errors, or otherwise extrinsic, such as sunlight, carcinogens or ionizing radiation (Barnum and O'Connell, 2014). In response to DNA damage, cell cycle checkpoints can be activated in G_1 and S phase as well as at the G_2/M transition (Figure **5**) (Bartek and Lukas, 2007; Kastan and Bartek, 2004). The main goal is to maintain CDKs in an active state until the lesion is removed. If DNA damage induces DNA double strand breaks (DSB), the recognition by the MRN (Mre11, Rad50 and Nbs1) complex and the subsequent recruitment and activation of the ATM (ataxia telangiectasia mutated) kinase is essential (Lee and Paull, 2004).

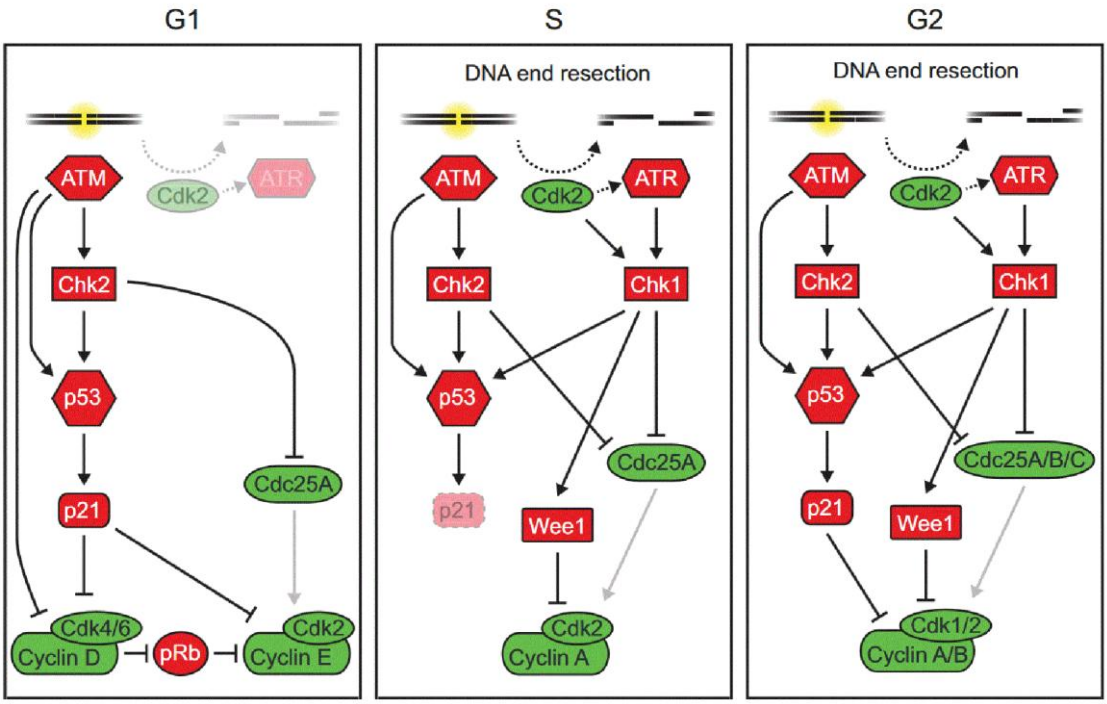

Figure 5**: DNA damage induced cell cycle checkpoint pathways.**
Interplay between the cell cycle machinery and the DNA damage response results in different signaling pathways. For details, see text. Figure adapted from Shaltieì et. al. (2015).

If the G_1 checkpoint is activated, ATM phosphorylates and activates checkpoint kinase 2 (Chk2) (Matsuoka et al., 1998). Both kinases are required for the stabilization of p53, which in turn results in the induction of the CDK inhibitor p21 (Banin et al., 1998; Canman et al., 1998; Kastan et al., 1991). Accumulated p21 binds to and inhibits cyclin-CDK complexes to block cell cycle progression into S phase (Deng et al., 1995; Harper et al., 1995). S phase entry is also prevented by ATM- and Chk2-dependent inhibition of Cdc25A phosphatase that reverses the inhibitory phosphorylation of CDK2 (Agami and Bernards, 2000; Deckbar et al., 2010; Falck et al., 2001; Hirao et al., 2002; Mailand et al., 2000) .

When single or double strand breaks occur in S phase, the intra S phase checkpoint is activated to prevent further replication (Errico and Costanzo, 2012). DNA lesions can be repaired by different repair pathways, whereby the cell cycle influences the choice of the repair system. Homologous recombination (HR) repair only takes place when a sister chromatid as a template is available in S or G_2 phase, whereas non-homologous end-joining (NHEJ) repair is possible during the whole cell cycle (Rothkamm et al., 2003). To repair a DSB through HR, DNA end-resection is necessary at the broken ends to produce sindle stranded DNA (ssDNA) overhangs (Mimitou and Symington, 2011). The ssDNA generated by resection or by the DNA damage itself, activates the ATR (ataxia telangiectasia and Rad3-related) kinase and in turn its effector checkpoint kinase 1 (Chk1) (Zou and Elledge, 2003). Even though ATM, ATR, Chk2 and Chk1 all contribute to the stabilization of p53 (Meek and Anderson, 2009), downstream p21 accumulation is prevented during DNA replication by the PCNA associated CRL4Cdt2 ubiquitin ligase (Abbas et al., 2008; Havens and Walter, 2011) leading to a continuous degradation of p21. The kinase Wee1, which becomes expressed in S phase, inhibits CDK2 through phosphorylation (Chow et al., 2003; Watanabe et al., 1995). In addition, Chk1 and Chk2 target

the counteracting phosphatase Cdc25A for degradation to hamper further CDK activation, thus blocking progression in S phase (Beck et al., 2012; Hughes et al., 2013; O'Connell et al., 1997).

Damages occurring in G_2 phase lead to an activation of the G_2/M checkpoint. Comparable to damages in S phase, ATM, ATR, Chk1 and Chk2 are also important key players, and Wee1-dependent phosphorylation of CDKs remains crucial for checkpoint control in G_2. In contrast to the intra S checkpoint the induction of p21 transcription in G_2 is required for inhibition of CDK-cyclin complexes (Bunz et al., 1998). In addition, ATM- and ATR-dependent activation of p38 contributes to the inhibition of Cdc25A, Cdc25B and Cdc25C (Reinhardt et al., 2007).

In mitosis, another safeguard mechanism grants the correct segregation of the genome independently of DNA damages. If kinetochores are not occupied by mitotic microtubules, or are attached but not under tension, the spindle assembly checkpoint (SAC) delays progression from metaphase to anaphase. The mitotic checkpoint complex (MCC) inhibits the large E3 ubiquitin ligase known as anaphase-promoting complex/cyclosome (APC/C) and delays degradation of cyclin B and of the anaphase inhibitor securin (Musacchio and Salmon, 2007). The degradation of securin normally allows separase to be released and to cleave cohesin complexes at the kinetochore (Barnum and O'Connell, 2014). By inhibiting the APC/C, the MCC stabilizes these substrates, effectively preventing mitotic exit (Musacchio, 2015).

1.4 Replication

To maintain the integrity of the genome, duplication of the genetic information during replication is a highly coordinated interplay of a plethora of proteins in order to preserve the correct function of the cell and its progeny. The process of DNA replication is strictly controlled during the cell cycle to ensure that genome duplication takes place only once per cycle. It begins with a preliminary step already in G_1 phase when origins of replication are licensed, whereas firing of origins starts at the beginning of S phase. After elongating the DNA strands, replication terminates when converging replication forks meet.

1.4.1 Regulation and mechanism of DNA replication

To ensure genomic stability, DNA must be replicated once and only once during each cell cycle. Re-replication of the whole genome or even parts of it would result in gene amplification, polyploidy and other kinds of genome instability, which is a hallmark of cancer (section 1.1.1) (Albertson, 2006; Truong and Wu, 2011). To ensure the complete and faithful transmission of genetic information without re-replication, pre-recognition complexes (pre-RCs) assemble during late mitosis and early G_1 phase at 30,000–50,000 replication origins, the replication start sites (Leonard and Méchali, 2013). A process termed origin licensing (Figure 6 A). The first step of pre-RC assembly is the binding of origin recognition complex (ORC) proteins to replication origins in late mitosis (Bell and Stillman, 1992). Afterwards Cdc6 (cell division cycle 6) and Cdt1 (Cdc10-dependent transcription factor 1) are recruited (Chen et al., 2007; Speck et al., 2005). Furthermore, the ring-shaped head-to-head double hexamer MCM2-7 (minichromosome maintenance complex) is loaded onto DNA (Coster and Diffley, 2017; Evrin et al., 2009; Frigola et al., 2017; Remus et al., 2009).

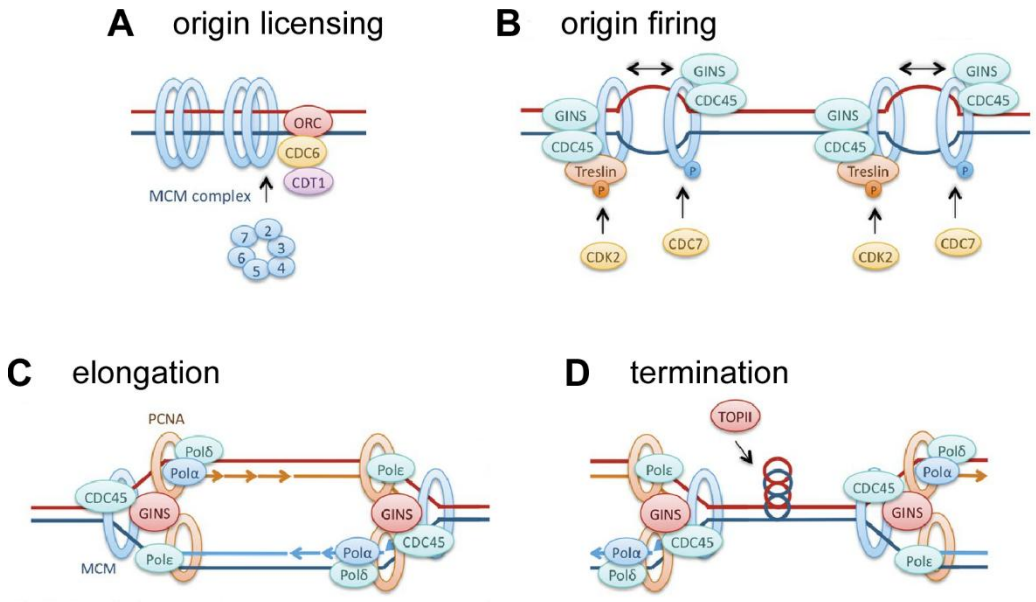

Figure 6: Overview of DNA replication.

A) Origin licensing occurs during the late M or G_1 phase, when ORC, Cdc6 and Cdt1 recruit the MCM2–7 helicase to chromatin. **B)** Origins are activated (origin firing) in S phase by Cdc7 and CDK2. This promotes loading of Cdc45 and the GINS complex. **C)** The GINS complex maintains interactions within

the replisome, containing the MCM2–7 and Cdc45 replicative helicase, the sliding clamp PCNA and DNA polymerases (Pol) α and δ as well as ε, which replicate the lagging and leading strands respectively (elongation). **D)** During termination, sister chromatids become intertwined (catenated), and these structures are resolved by the DNA topoisomerase TOPII. Images modified from (Jones and Petermann, 2012).

After origin licensing, firing of origins (Figure 6 B) at the G_1/S transition is induced by cyclin E-CDK2 and Cdc7-Dbf4 (DDK) activity (Nougarède et al., 2000; Sheu and Stillman, 2010). The CMG complex forms, which is named after its components: Cdc45, the MCM proteins and the GINS complex ("go-ichi-ni-san" means "5, 1, 2, 3" in Japanese and represents abbreviations for proteins Sld5-Psf1-Psf2-Psf3) (Ilves et al., 2010; Moyer et al., 2006). Recruitment of MCM10, Cdc45 and GINS to MCM is required to activate MCM2-7 and promote its DNA helicase activity (Figure 6 C). During this activation process, MCM2-7 double hexamers are separated, each CMG complex moves to the opposite direction and the helicase starts to unwind the DNA moving from 3' to 5' direction. This process guarantees bi-directional DNA replication from the replication origin (Kang et al., 2017). Because of the 5′ to 3′ polarity of DNA synthesis, one strand is continuously synthesized, the leading strand, and the other strand is discontinuously synthesized, the lagging strand. During lagging strand synthesis, replication protein A (RPA) protects generated ssDNA from cellular nucleases and also prevents formation of hairpin structures that might impede the progression of the replication fork (Wold, 1997). For lagging strand synthesis, polymerase α is recruited to the MCM helicase. First, primase subunit of polymerase α starts synthesis by generating short ribonucleotide primers (7–10 nt), where then 20–30 deoxyribonucleotides are incorporated by the DNA polymerase subunit of polymerase α (Kang et al., 2017; Perera et al., 2013). Afterwards, polymerase δ synthesizes the nascent strand extending the primers until reaching the 5′ terminus of the preceding Okazaki fragment. The Okazaki fragments are then processed by flap endonuclease Fen1 and Pol δ and ligated by DNA ligase I to form a continuous replicated DNA strand (Garg et al., 2004; Howes and Tomkinson, 2012; Stodola and Burgers, 2016). DNA polymerase ε is required for DNA synthesis on the leading strand (Ganai and Johansson, 2016). DNA polymerases have a semi-closed hand structure, which allows them to load onto DNA and translocate. This structure permits DNA polymerase to hold the single-stranded template, incorporate dNTPs at the active site, and release the newly formed double strand. However, the conformation of DNA polymerases does not allow for their stable interaction with the template DNA. To strengthen the interaction between template and polymerase, DNA sliding clamps have evolved, promoting the processivity of replicative polymerases. In eukaryotes, this sliding clamp is a homotrimeric, ring-shaped protein known as proliferating cell nuclear antigen (PCNA), which enhances the polymerase processivity up to 1,000-fold (Leman and Noguchi, 2013). PCNA is loaded onto the DNA by the hetero-pentameric Replication Factor C (RFC) complexes (RFC1-RFC and Ctf18-RFC). RFC binds PCNA and opens the PCNA ring in the presence of ATP. The RFC-PCNA complex then binds to the 3´ DNA template which triggers ATP hydrolysis by RFC, resulting in RFC release and PCNA closure, thus finally encircling the DNA (Shiomi and Nishitani, 2017).

After replication elongation converging replication forks meet, a process that is called replication termination (Figure 6 D). DNA synthesis is completed, topological stress must be resolved and replisome proteins have to disassemble or be removed. Unwinding of the parental duplex by the

MCM helicase leads to overwinding of the unreplicated DNA resulting in the formation of positive supercoils ahead of the fork. In addition to relaxation of supercoils by type I or type II DNA topoisomerases, the entire fork can rotate clockwise relative to the direction of fork movement to counteract the overwinding of unreplicated DNA. When termination occurs, parental DNA between converging forks becomes too short to supercoil owing to the inherent stiffness of DNA. At this stage, which occurs when 150 bp or less of parental DNA remains, relief of topological stress becomes dependent on the formation of pre-catenanes, which can be resolved by type II but not by type I topoisomerases (Dewar and Walter, 2017). After genome duplication, replisome proteins dissociate except the two ring-shaped molecules MCM and PCNA, which remain encircling the double stranded DNA (dsDNA). How the CMG complex recognizes that it has fulfilled its duty and can disassemble is still unknown (Kang et al., 2017). MCM7 of the MCM2-7 complex is poly-ubiquitinated, but not degraded by the proteasome. Instead it is extracted from chromatin by a p97/VCP/Cdc48 segregase (Maric et al., 2014; Priego Moreno et al., 2014). The sliding clamp PCNA is removed by the Elg1-RFC complex (Elg1 called ATAD5 in human) in an ATP-dependent manner (Kubota et al., 2013; Lee et al., 2013; Shiomi and Nishitani, 2013).

1.4.2 Replication in the context of chromatin

Given the relatively large sizes of eukaryotic genomes, complete genome duplication requires DNA replication to start at numerous replication origins at once, which results in many discrete chromosomal loci replicating in parallel (Aladjem and Redon, 2017). In contrast to yeast and prokaryotes, mammalian cells have no strong sequence specificity or consensus sequences at origin start sites (Vashee et al., 2003). Furthermore, there are 30,000–50,000 potential origins of replication in the human genome but only 10 % are used within a given adult somatic cell cycle (Ma et al., 2015). The fundamental question of how replication initiation is regulated is still under investigation. Analysis revealed different spatio-temporally regulated replication patterns that are also related to the number of replication origins and to the chromatin state of the genome.

The temporal organization is defined by alterations of the characteristic pattern of replicating protein complexes associated with early, mid and late S phase. (Fox et al., 1991; Leonhardt et al., 2000; Nakamura et al., 1986). For example, the sliding clamp PCNA shows a typical change in its distribution pattern in S phase. It is distributed at replication sites throughout the nucleoplasm during early S phase. As S phase continuous, PCNA foci are concentrated around the nucleoli as well as in peripheral areas of the nucleus. In late S phase foci increase in size but decrease in number and often take on characteristic ring or horseshoe-like structures (Leonhardt et al., 2000; Nakamura et al., 1986; O'Keefe et al., 1992). In addition, origins are not uniformly distributed with respect to replication timing. It has been shown that origin density is significantly lower in late domains compared with early domains (Besnard et al., 2012).

The spatial order of replication reflects the higher organization of the genome. During early S phase euchromatin is replicated, followed by facultative heterochromatin during mid S phase and constitutive heterochromatin duplication mainly during late S phase (O'Keefe et al., 1992). Moreover, transcriptionally active early replicating regions are commonly enriched in histone H4

acetylation. H4 acetylation could promote origin firing by increasing the accessibility of DNA to the helicase complexes needed for replication fork movement, or by facilitating histone octamer eviction for DNA unwinding (Ma et al., 2015). In contrast, to H4 acetylation of early replicating regions, methylation of H4 seems to play a role in late-firing origins. The conversion of H4K20me1 to higher H4K20me states are not sufficient to define a efficient origin *per se*, but rather serve as an enhancer for MCM2-7 loading and replication activation (Brustel et al., 2017). Furthermore, late-firing origins are usually associated with repressive, closed chromatin structures. For example HP1-bound regions at centromeric heterochromatin repeats in *Drosophila* replicate late, and a reduction of HP1 levels leads to earlier replication of these specific DNA regions (Schwaiger et al., 2010).

In general, the chromatin architecture also influences the replication. Efficient replication fork progression requires that the replisome gains access to the DNA. However, the ordered chromatin structure, including dsDNA wrapped around nucleosomes and associated linker histones, represents a barrier itself. Thus, phosphorylation of the C-terminal tail of linker histone H1 by CDK2 leads to a relaxation of the chromatin structure at the G_1/S transition (Alexandrow and Hamlin, 2005; Contreras et al., 2003). DNA wrapped around core histones will still impede replication. This implies that nucleosomes need to be removed in front of the replication fork and to be loaded afterwards again combined with *de novo* deposition of newly synthesized histones (Figure 7). Nucleosome disruption probably requires ATP-dependent chromatin-remodeling enzymes, whereas histone chaperones sequester the released histones to facilitate recycling (Groth et al., 2007). The FACT (facilitates chromatin transcription) complex may disrupt 10–15 nucleosomes per minute ahead of the fork (Abe et al., 2011; Alabert and Groth, 2012) and the histone chaperone ASF1 (anti-silencing function 1) acts as acceptor of parental nucleosomes (Groth et al., 2005). In addition, ASF1 is a donor for the histone loader CAF1 (chromatin assembly factor 1). CAF1 binds to the replication clamp PCNA, travels with the replisome (Shibahara and Stillman, 1999) and deposits parental and newly synthesized histones behind the replication fork (Tagami et al., 2004; Takami et al., 2007).

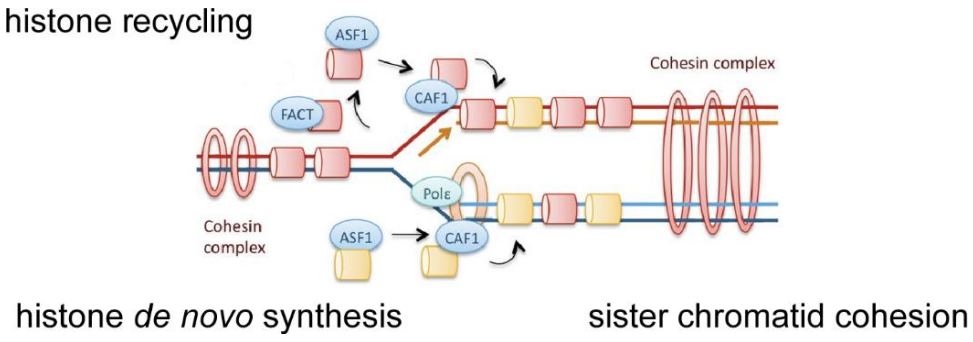

Figure 7: Replication coupled assembly and cohesion of chromatin.
Nucleosomes are removed by FACT ahead of the replication fork and recycled onto daughter strands, together with newly synthesized histones. The histone chaperone ASF1 binds parental and new histones and transfers them to the histone loader CAF1. Sister chromatids are tethered together by cohesin complex proteins. Images modified from Jones & Petermann (2012).

In addition to the replication-coupled process of nucleosome assembly, newly replicated sister chromatids need to be tethered together to promote the proper segregation of chromatids during mitosis. This replication-associated process is called sister chromatid cohesion and requires a ring-shaped protein complex termed cohesin (Figure 7). Cohesin consists of four SMC (Structural maintenance of chromosome) subunits (Losada et al., 1998; Michaelis et al., 1997). The complex is loaded onto chromatin already during G_1 phase in a Cdc7-dependent manner (Takahashi et al., 2008). The replisome slides through this ring and the two daughter strands are embraced by the cohesin complex (Alabert and Groth, 2012). Acetylation of SMC3, a subunit of the SMC complex, by ESCO1/2 (establishment of sister chromatid cohesion 1/2), which is bound to PCNA, is required for replication fork progression (Terret et al., 2009).

1.4.3 Replication stress and its resulting damage response

The faithful duplication and distribution of DNA to daughter cells is a fundamental biological process for maintaining genome stability and suppressing cancer. Presumably, DNA is constantly subjected to 50,000–100,000 DNA lesions per cell per day caused by intrinsic and extrinsic factors (Hübscher and Maga, 2011). Virtually all forms of DNA damage can influence DNA replication (Allen et al., 2011) by slowing or stalling of replication fork progression and/or DNA synthesis, a process defined as replication stress (Zeman and Cimprich, 2014).

Intrinsic factors include reactive oxygen species (ROS) generated as a by-product of cellular metabolism, which can cause oxidative damage to DNA (Burcham, 1999). Replication stress can also be caused by intrinsically difficult to replicate sequences in the genome, such as G-quadruplexes and repeat sequences (Pearson et al., 2005; Valton and Prioleau, 2016). Additionally, collisions between replication and transcription machinery can be a problem for proper DNA synthesis, because it can lead to fork stalling, R-loop formation and topological stress (Bermejo et al., 2012; Helmrich et al., 2013), causing transcription-associated recombination and chromosomal rearrangements (reviewed by Aguilera & Gaillard, 2014). Extrinsic damage sources can be UV-light, ionizing radiation (section 1.1.2) or chemicals (section 2.2.2.3). Also heavy metals and acrylamide may contribute to genomic instability by interfering with DNA replication and repair (Langie et al., 2015).

When the replication machinery encounters DNA replication disturbances at the lagging strand, DNA lesions are well tolerated because of the discontinuous nature of Okazaki-fragment synthesis and maturation (Berti and Vindigni, 2016). Forks can bypass the lesions and reinitiate DNA synthesis at a downstream position, leaving behind a ssDNA gap (Elvers et al., 2011; Lopes et al., 2006). These gaps can then be filled using specialized lesion bypass pathways in which the replicative polymerase is changed by a translesion synthesis (TLS) polymerase, for example PrimPol (Figure 8 A) (Prakash et al., 2005). TLS pols such as Rev1, Pol η, Pol ι, Pol κ and Pol ζ can also directly participate at the replication fork by replacing the replicative polymerases δ and ε (Figure 8 B) (Muñoz and Méndez, 2017), whereby mono-ubiquitination at Lys164 of PCNA is necessary for this so called polymerase switching (Ulrich and Takahashi, 2013; Yang et al., 2013). However, this TLS pathway is error-prone and a major source of mutagenesis (Hoeijmakers, 2001).

In contrast to the error-prone TLS, an error-free mechanism has evolved, which involves a template switch (TS) (Figure 8 C). In TS, a stalled nascent DNA strand invades the sister chromatid in a RAD51-dependent fashion and uses the newly synthesized undamaged strand as a template (reviewed by Muñoz & Méndez, 2017).

If DNA synthesis is impaired at the leading strand, the lesions are a major obstacle. DNA synthesis is uncoupled from DNA unwinding by helicases (Byun et al., 2005), which means that the replicative helicase continues to unwind the DNA duplex but the polymerase stalls. This leads to the generation of stretches of ssDNA that is covered by RPA (Zou and Elledge, 2003), whereby the strength of the cellular response correlates with the amount of RPA-coated ssDNA (MacDougall et al., 2007). Afterwards the ATR-ATRIP complex is recruited and activates the intra S checkpoint as described in section 1.3.2, resulting in an inhibition of the cell cycle progression. In addition, ATR prevents new origin firing by inhibiting replication initiation (Karnani and Dutta, 2011), but it also promotes firing of dormant origins within pre-existing replication factories (Ge and Blow, 2010; McIntosh and Blow, 2012).

In addition to the ATR-Chk1 pathway, the replication fork is also stabilized and protected by another repair-independent mechanism involving HR components. BRCA1/2 and FANCD2 promote the formation of RAD51 nucleofilaments on ssDNA stretches that are present at stalled replication forks, preventing their resection by Mre11 (Hashimoto et al., 2010; Petermann et al., 2010; Schlacher et al., 2011, 2012).

Stalled replication forks can reverse their course to form four-way “chicken foot” structures resembling Holliday junctions (Figure 8 D) (Higgins et al., 1976; Lopes et al., 2001; Sogo et al., 2002). Fork reversal is a physiological response to protect fork integrity (Zellweger et al. 2015) occurring in two steps: first, reversed forks form through coordinated annealing of the two newly synthesized strands, and second, the reversed fork structures restart (Berti and Vindigni, 2016). Here, the ssDNA binding protein RAD51 is also required in the first step, where it stabilizes the reversed fork (Bugreev et al., 2011) or might promote the initial step by invading the complementary parental strand (Berti and Vindigni, 2016). Several factors mediate fork reversal and/or stabilize reversed intermediates, including PARP1, SMARCAL and FBH1 (Muñoz and Méndez, 2017), but the current understanding of the mechanism of reversed fork formation is very limited (Berti and Vindigni, 2016). To resume DNA synthesis in the second step, reversed forks need to be remodeled again into forks that move in the forward direction (Berti and Vindigni, 2016). This remodeling may be mediated by RECQ1 helicase, which is regulated by PARP1 (Berti et al., 2013) or by WRN helicase in cooperation with DNA2 nuclease, catalyzing the nucleolytic degradation of reversed DNA arms (Thangavel et al., 2015). A third protein composition involved in replication fork remodeling consists of BLM helicase and ZRANB3 (Muñoz and Méndez, 2017).

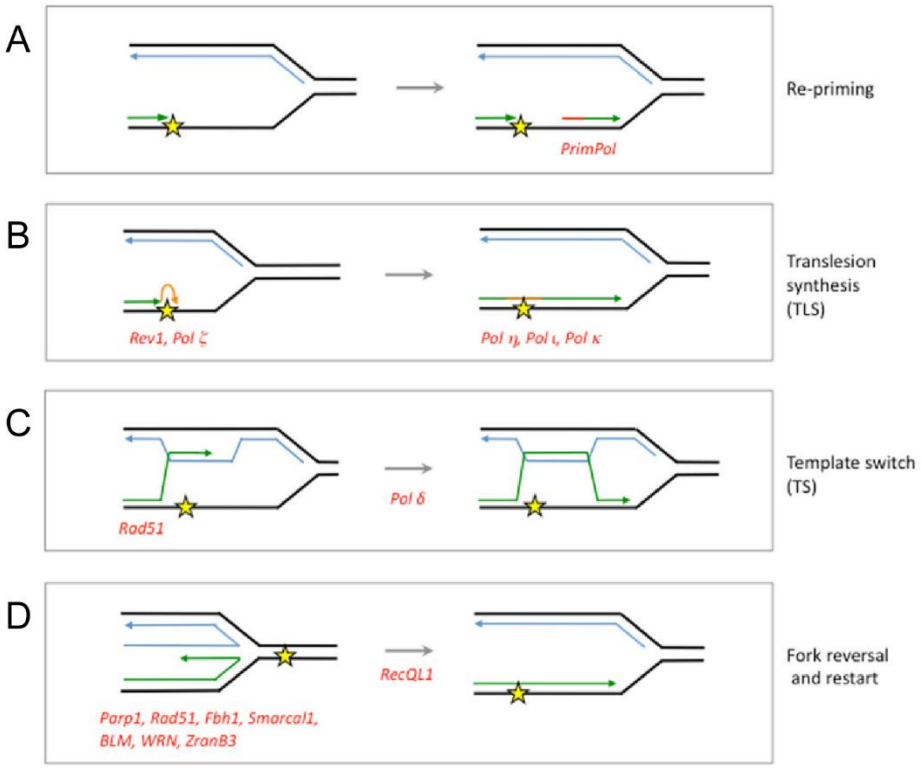

Figure 8: Cellular mechanisms at replication forks in response to DNA damage.
A) Replisomes can bypass damage by re-priming downstream of the stalled fork. **B)** A stalled fork can bypass damage by recruiting translesion polymerases **C)** A stalled fork can bypass DNA damage by template switching, using the lagging strand as a template instead of the damaged parental strand. **D)** Fork reversal in response to damage, wherein the leading strand anneals with the lagging strand to form a four-way structure.

Prolonged fork stalling or failure to resume DNA synthesis by the mechanisms described above lead to fork collapse and formation of one-ended DSBs (Berti and Vindigni, 2016). The replication machinery is no longer stabilized and its components dissociate from the stalled fork or the replisome is still present but not functional or properly positioned (Zeman and Cimprich, 2014). Afterwards other repair mechanism can take place.

Cells have evolved several damage response and repair mechanisms to maintain genomic stability. Double strand breaks (DSB) are repaired by non-homologous end-joining (NHEJ) and HR pathways. Interstrand crosslinks are repaired using interstrand crosslink repair pathway, which involves a combination of repair pathways consisting of NER, homologous recombination (HR), TLS (translesion synthesis), and Fanconi anemia (FA) repair pathways (Iyer and Rhind, 2017; Muñoz and Méndez, 2017). Finally, a repair pathway termed base excision repair (BER) targets modified bases, while pyrimidine dimers are replaced by the nucleotide excision repair (NER) pathway (reviewd in Iyer & Rhind, 2017).

1.5 The chromosomal passenger complex

Genomic instability is a major driving force for carcinogenesis. The two major mechanisms to maintain the cellular integrity are the complete and precise duplication of the genome during replication in S phase and the equal segregation of chromosomes during mitosis. In the latter process, the chromosomal passenger complex (CPC) plays a pivotal role. It regulates key mitotic events, including correction of chromosome-microtubule attachment errors, activation of the spindle assembly checkpoint and construction and regulation of the contractile apparatus that drives cytokinesis (Carmena et al., 2012).

1.5.1 Structural organization of the chromosomal passenger complex

The CPC consists of a catalytic and a localization module (Figure 9 A). The latter comprises the proteins Survivin, Borealin and INCENP and targets the CPC to centromeres, the mitotic spindle and to the midbody during cell division. The C-terminal part of Survivin, Borealin and the N-terminus of INCENP are connected via a three-helix-bundle (Jeyaprakash et al., 2007). INCENP (inner centromere protein) is a rather large protein, connecting both modules. In addition the involvement of its N-terminus in the localization module, it also contains a large disordered region, enriched in phosphorylation sites (Krenn and Musacchio, 2015), followed by a putative coiled-coil domain (Jeyaprakash et al., 2007) or a single alpha helix (SAH) (Figure 9 B) (Samejima et al., 2015). In contrast to the previous assumption, computational analysis have shown that it lacks the regular sequence pattern typical for coiled–coils (Krenn and Musacchio, 2015), favoring recent studies of avian INCENP regarding a SAH fold. Furthermore, this SAH could act as a ”dog leash”, allowing a dynamic function of the catalytic module while at the same time being stably anchored, thereby avoiding the need of CPC dimerization (as required for coiled coil formation), which is necessary for catalytic module activation (Samejima et al., 2015). The C-terminal end of INCENP, the so-called IN-Box, forms the catalytic module with the kinase Aurora B (Adams et al., 2000; Kaitna et al., 2000).

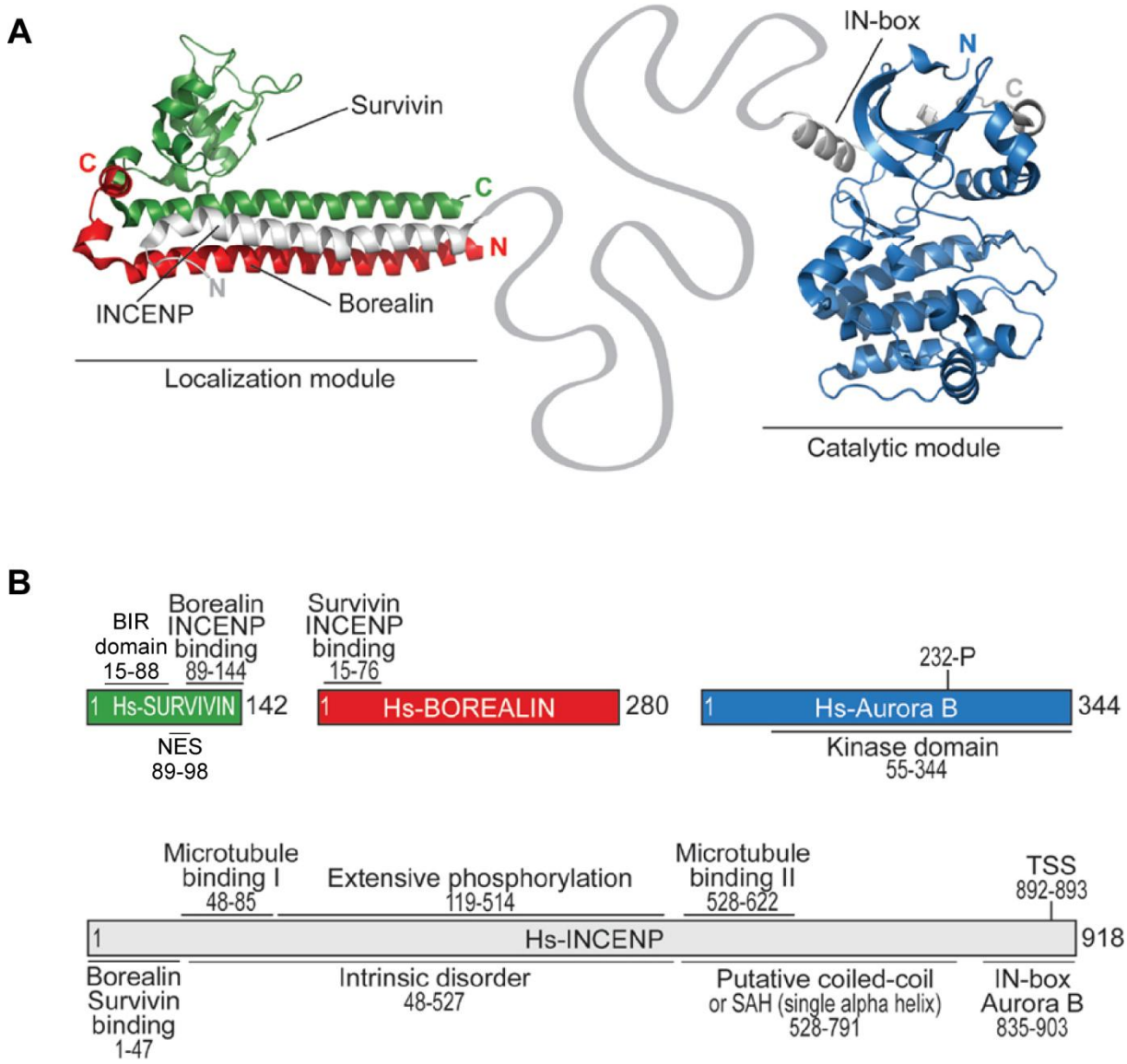

Figure 9: Architecture of the CPC.

A) Structural organization of the localization and catalytic module linked by INCENP. **B)** Schematic representation of human CPC members with main structural features. Figure modified from (Krenn and Musacchio, 2015).

Aurora B belongs to a family of highly conserved serine/threonine kinases together with the other mammalian Aurora kinases A and C. They have a conserved catalytic domain-containing C-terminus and a divergent N-terminus, indicating that latter is important for their spatiotemporal localization and function (Li et al., 2015a). Aurora B is functionally active in different stages of mitosis and described in detail in section 1.5.2.1. Aurora A associates with the spindle poles to regulate entry into mitosis, centrosome maturation and spindle assembly (Carmena et al., 2009). In contrast, Aurora B, in complex with the other CPC members, is mainly located on the centromere in early mitosis, and on the midbody during cytokinesis (Carmena et al., 2012), where it mainly regulates spindle assembly checkpoint, kinetochore attachment and cytokinesis (Carmena et al., 2012; Li et al., 2015a). Whereas recent findings also show that Aurora A and B can assume their respective functions, for example Aurora A can phosphorylate substrates of Aurora B and substitutes its function in spindle checkpoint and *vice versa* centrosome targeting

of Aurora B substitutes the function of Aurora A in mitotic entry (Li et al., 2015a). Aurora C is also able to replace Aurora B's function. Aurora C is primarily active during early embryonic development (Sasai et al., 2004, 2016). Borealin is also called Dasra B or CDCA8 (cell division cycle associated 8) and its phosphorylation by CDK1 is essential for localization to centromeres during mitosis (Tsukahara et al., 2010). Survivin is with 16.5 kDa the smallest member of the CPC. It interacts via its C-terminal α-helical domain with the other CPC members Borealin and INCENP as described above. Survivin is additionally a member of the inhibitor of apoptosis protein (IAP) family, characterized by its N-terminal BIR (baculoviral IAP repeat) domain (section 1.5.2) (Figure 9 B) (Ambrosini et al., 1997). Between both domains, Survivin has a conserved leucine-rich nuclear export sequence (NES) allowing interaction with the export receptor chromosomal region maintenance 1 (Crm1), also known as Exportin-1, which mediates targeting of the CPC to centromeres during early stages of mitosis (Knauer et al., 2006). Besides its interaction with the other CPC members as a monomer, Survivin can also form bow tie-shaped homodimers in solution via a dimer interface (aa 6–10 and 89–102, not depicted) (Chantalat et al., 2000).

1.5.2 Localization and function of chromosomal passenger complex proteins

The periodical expression of the CPC members, for example Survivin, is tightly regulated in a cell cycle-dependent manner (Li et al., 1998). Expression is induced by transcriptional control of the human Survivin gene, named *birc5*. It consists of 4 exons and 3 introns on chromosome 17q25 (Ambrosini et al., 1997). The protein expression peaks in G_2/M phase (Li et al., 1998) and its stability and function depends on PTMs (reviewed by Zhang, Yang, & Li, 2006). After abscission of the two daughter cells, Survivin is proteasomally degraded (Zhao et al., 2000). The cell cycle-regulated expression and localization is related to multiple functions of the CPC.

1.5.2.1 Localization and function of the CPC during mitosis

To fulfill its kinase activity during mitosis, Aurora B needs to be activated. Aurora B is bound to INCENP, which activates Aurora B initially to a minor extent. This enables Aurora B to phosphorylate a TSS (Thr-Ser-Ser)-motif in INCENP (Bishop and Schumacher, 2002; Honda et al., 2003), which in combination with the *trans* autophosphorylation of Thr232 in the kinase domain concludes Aurora B's activation mechanism, thus needing a high local protein concentration (Sessa et al., 2005). Additionally, other kinases such as Chk1, a kinase known for its role in the DNA damage checkpoint (section 1.3.2 and 1.4.3), can phosphorylate Aurora B at Ser311, thus activating it (Petsalaki et al., 2011).

The CPC is located at chromosome arms when cells enter mitosis. Aurora B phosphorylates histone H3S10 (Hsu et al., 2000) and induces the dissociation of HP1 from H3K9me3 (Fischle et al., 2005; Hirota et al., 2005), which facilitates the relocation of the CPC from chromosome arms to centromeres (Nozawa et al., 2010).

In prometa- and metaphase is the complex located at centromeres. Centromeric enrichment of the CPC depends further on two histone modifications overlapping at the centromere. Survivin's

BIR domain binds to by haspin kinase phosphorylated H3T3 (Kelly et al., 2010; Wang et al., 2010) at chromosome arms between paired sister chromatids, but most prominent at the centromere (Dai et al., 2005; Wang et al., 2010). Phosphorylation by haspin is mediated by Plk1 (Polo-like kinase-1) in a CDK1-phosphorylation-dependent manner (Zhou et al., 2014). The second histone mark is pH2AT120 near the kinetochore, introduced by Bub1 kinase. Shugoshins Sgo1 and Sgo2 are recruited to pH2AT120 and they can interact with Survivin (Kawashima et al., 2007) or Borealin, which in turn is phosphorylated by CDK1 (Tsukahara et al., 2010). In addition, an interaction between the export receptor Crm1 and Survivin is important for tethering the CPC to centromeres (Knauer et al., 2006).

The CPC at centromeres is responsible for the control of proper chromosome-microtubule-attachment. Centromeres are enriched in histone variant CENP-A, which acts as a recruitment platform for inner kinetochore proteins, also known as constitutive centromere-associated network (CCAN) (Perpelescu and Fukagawa, 2011). Upon mitotic entry, outer kinetochore proteins, also called KMN (KNL1/Mis12/Ndc80) network (Cheeseman and Desai, 2008), are recruited and interact during metaphase directly with the spindle microtubules emanating from opposite poles of the mitotic spindle.

The CPC is necessary to destabilize and repair erroneous kinetochore-microtubule attachments. Aurora B phosphorylates several KMN network components to weaken the distance of the KMN network to microtubules (Alushin et al., 2010; Cheeseman et al., 2006; DeLuca et al., 2006; Welburn et al., 2010).

If metaphase chromosomes are not correctly attached to microtubules and the lack of tension is sensed, the spindle assembly checkpoint (SAC) is activated by the CPC (Krenn and Musacchio, 2015; Santaguida et al., 2011; Shandilya et al., 2016). The mitotic checkpoint complex (MCC) is recruited to kinetochores, which inhibits the anaphase-promoting complex or cyclosome (APC/C) resulting in a delay of cell cycle progression and sister chromatid separation until all kinetochores are bipolarly attached by microtubules (Alfieri et al., 2016; Krenn and Musacchio, 2015). When all chromosomes have obtained the correct bi-orientation, the SAC is switched off by PP1 or PP2A, counteracting phosphatases that reverse Aurora B-dependent phosphorylations (Foley et al., 2011; Shrestha et al., 2017; Trinkle-Mulcahy et al., 2006). APC/C is activated and ubiquitinates cyclin B and Securin, which further undergo proteasomal degradation. This activates separase, resulting in cohesin cleavage to allow sister chromatid separation, and inactivates CDK1, triggering the progression to anaphase (Hümmer and Mayer, 2009; Krenn and Musacchio, 2015).

During the meta- to anaphase transition, the CPC leaves the inner centromere and localizes to central spindle microtubules. Re-localization is initiated by the decrease in Cdk1 activity and dephosphorylation of INCENP (Hümmer and Mayer, 2009). PP1 dephosphorylates H3T3 (Qian et al., 2011; Vagnarelli et al., 2011), thus regulating CPC binding. In addition, the CPC is actively removed from chromosomes in a p97-dependent manner (Dobrynin et al., 2011; Ramadan et al., 2007).

The new central spindle targeting of the CPC requires Plk1 and Mklp2 (mitotic kinesin-like protein 2), a kinesin 6 family member that binds microtubules at the central spindle (Gruneberg et al., 2004; Hümmer and Mayer, 2009; Kitagawa et al., 2014). Aurora B phosphorylates Mklp1

and Kif2A, promotes centralspindlin clustering at the spindle midzone and controls microtubule length, thereby stabilizing the central spindle (Douglas et al., 2010; Uehara et al., 2013).

Finally, during telophase and cytokineses the CPC can be found at the midbody. The timing of abscission is tightly controlled by Aurora kinase activity, which delays abscission if chromatin persists in the intercellular bridge, whereas declining activity promotes abscission (reviewed by Nähse, Christ, Stenmark, & Campsteijn, 2017). CPC-dependent recruitment of centralspindlin to the spindle midzone at anaphase activates RhoA in telophase and induces contractile ring assembly at the membrane (Basant et al., 2015). In addition, the CPC and centralspindlin coordinate the regulation of a ESCRT-III component for abscission of the two daughter cells (Capalbo et al., 2016).

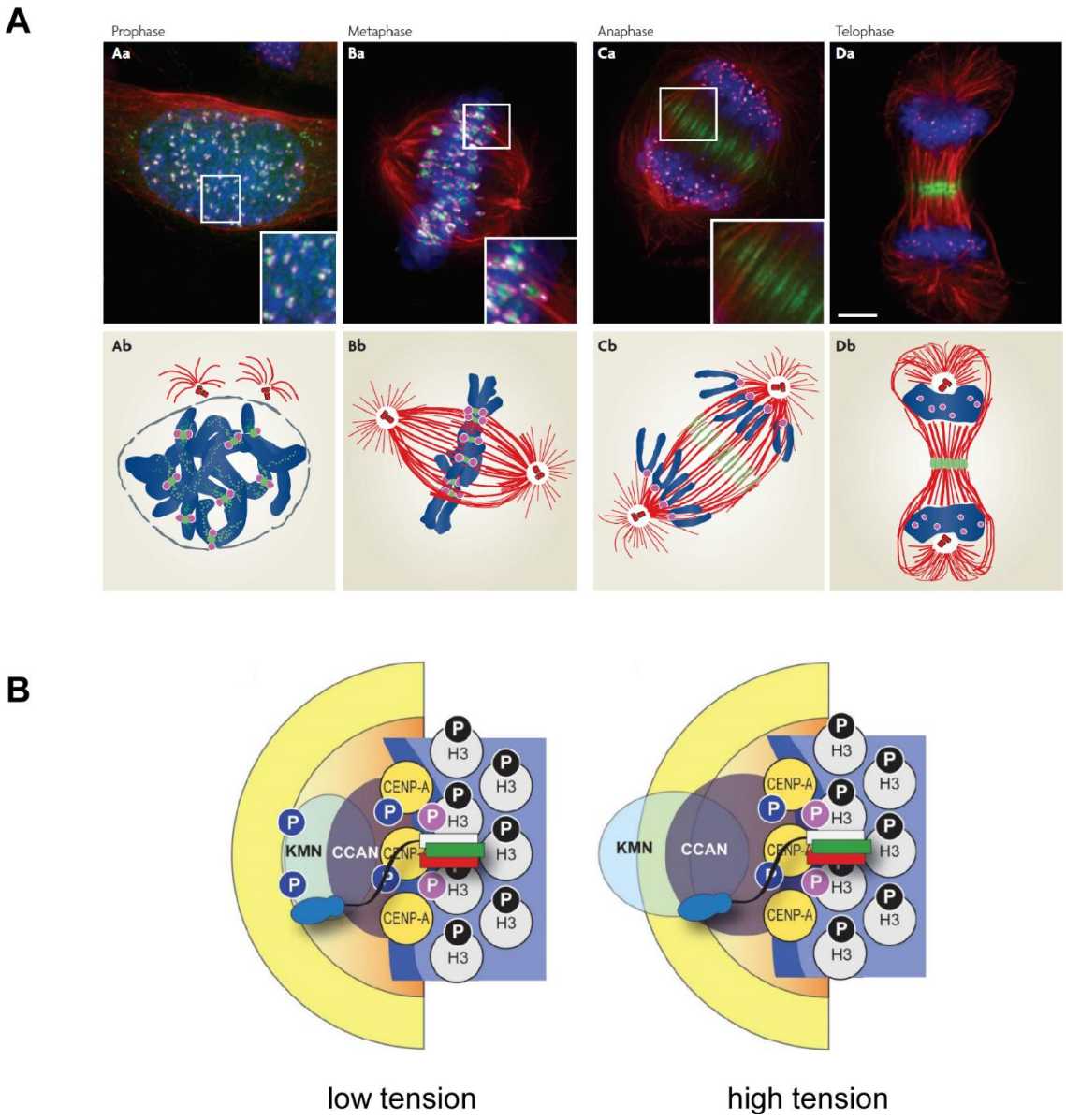

Figure 10**: CPC localization during mitosis.**

A) Immunofluorescence staining (Aa-Da) for Aurora B (green), kinetochores/centromeres (pink), tubulin (red) and DNA (blue) and schematic representations (Ab-Db) of CPC localizations during mitotic stages. The CPC is bound to chromosome arms and at the centromere in prophase. During metaphase, chromosomes align at the metaphase plate and the CPC is located only at centromeres. In anaphase, the

CPC is detectable at the spindle midzone and later in telophase at the midbody. Figure adapted from (Ruchaud et al., 2007). **B)** Model of CPC localization at kinetochores during metaphase. The localization module (red, green and white boxes, representing the three-helix bundle of Survivin, Borealin and part of INCENP) is bound to H3T3p and linked by INCENP (black curved line) to Aurora B (blue head on curved line) that can reach KMT targets for phosphorylation (P) when there is low tension between kinetochore and microtubules. Under high tension, the substrates become unreachable. Figure adapted from Krenn & Musacchio (2015).

1.5.2.2 Localization and function during interphase

In contrast to a large number of publications dealing with the localization and function of the CPC members during mitosis (section 1.5.2.1), the knowledge regarding the subcellular localization and role during interphase is rather limited. Beardmore et al. (2004) could show a localization change of Survivin-GFP from diffusely distributed in the cytosol in G_1 phase, later to centromeres and in G_2 phase to kinetochores. Aurora B was only detectable during mitosis. Cooke et al. (1987) detected INCENP in the midbody in early G_1 phase, which remained from the previous mitosis and a speckled nuclear distribution in interphase cells. Furthermore, Rodriguez et al. (2006) showed that Survivin and Aurora B undergo continuous shuttling between nucleus and cytoplasm in interphase, whereas INCENP resides soleyly in the nucleus and Borealin was detected in the nucleolus and the cytoplasm. They concluded that in contrast to their closely related localization during mitosis, the nucleocytoplasmic localization during interphase is largely unrelated. In contrast, Monier et. al. (2007) detected Aurora B together with Survivin and INCENP at pericentric heterochromatin in late S and G_2 phase. Ainsztein et. al. (1998) detected INCENP first on chromosome arms and only during promethaphase/metaphase at centromeres. Centromeric localization occurs via binding of a PxVxL motif in INCENP to HP1α (Ainsztein et al., 1998; Kang et al., 2011). Ruppert et al. (2018) suggested that HP1 might concentrate and activate the CPC at centromeric heterochromatin in G_2. Afterwards HP1 is released from chromatin by Aurora B-mediated phosphorylation of H3S10, which allows H3T3p and Sgo1 to redirect the CPC to mitotic centromeres (section 1.5.2.1).

The CPC is supposed to interact in its inactive state with nucleophosmin/nucleoplasmin (NPM) family components. These have multiple functions as histone chaperones and they shuttle other proteins from the nucleus to the cytoplasm (Hanley et al., 2017).

Borealin co-localizes during interphase with SENP3, a SUMO specific protease that processes a precursor form to the mature or active SUMO. But SUMOylation of Borealin was only detected during mitosis (Klein et al., 2009).

Aurora B can indirectly bind and phosphorylate p53 (Wu et al., 2011), thus leading to an impaired transcriptional activity. In addition, Aurora B inhibits CDK inhibitor p21, a p53 target, thus preventing delayed replication and premature mitotic exit (González-Loyola et al., 2015; Trakala et al., 2013). A complex consisting of Aurora B, Suvivin and mTOR (mammalian target of rapamycin) promote cell cycle progression from G_1 to S phase in lymphocytes (Song et al., 2007). Aurora B, CDK1 and Plk1 are bound by Tim during G_2 and at the beginning of M phase. Tim is also bound to replication proteins during S phase and is required for the recruitment of Plk1 to centromeric DNA and formation of catenated DNA structures at human centromeres. Plk1 and Tim are both implicated in the DNA damage response after checkpoint activation, thus are two proteins linking mitotic kinase activity with DNA replication termination (Dheekollu et al.,

2011). Additionally, DNA damage sensing by ATR and Chk1 at the intra S checkpoint (section 1.3.2) delays abscission, indicating that Aurora B is not only responsible for genomic stability by coordinating chromosome segregation, but also sensitive of damage resulting from previous events (Mackay and Ullman, 2015). Chk1 phosphorylates Aurora B at Ser331 in unperturbed cells which is essential for Aurora B activity at the entry of mitosis (Petsalaki et al., 2011) and needed to prevent the formation of lagging chromosomes in metaphase (Kabeche et al., 2017). In contrast, Zuazua-Villar et. al. (2014) have shown that activated Chk1 suppresses Aurora B phosphorylation and prevents mitotic entry. Moreover, a member of the GINS complex, which is bound to active replisomes, indirectly affects localization and function of Survivin and INCENP in chromosome segregation, possibly through a task in centromere replication in S phase (Huang et al., 2005). Overall, these findings hint towards an additional role during replication or after replication stress, that linking mitosis and replication to maintain genomic integrity.

1.5.2.3 Other functions of CPC members

CPC member Survivin is a multifunctional protein. Besides its nuclear function during mitosis, in association with the other CPC members, a cytoplasmic fraction of Survivin, without CPC association, is involved in apoptosis. It binds to pro-caspase 9 via the mediator HBXIP (hepatitis B X-interacting protein) to inhibit apoptosis (Marusawa et al., 2003). Recent findings further hint to an involvement of Survivin in immune responses and autoimmune diseases such as rheumatoid arthritis (reviewed by Ebrahimiyan, Aslani, Rezaei, Jamshidi, & Mahmoudi, 2018; Gravina et al., 2017). In addition, Survivin overexpression leads to resistance of tumor cells to both, chemotherapy and ionizing radiation (Capalbo et al., 2007). Reichert et al. (2011) could show an accumulation of Survivin at nuclear damage sites after irradiation and elucidated interactions between Survivin and γH2AX, Ku70, 53BP1 and DNA-PKcs. In contrast, results of our working group point to a nuclear enrichment of Survivin after irradiation in distinct foci not directly at damage sites, where above-mentioned damage response proteins are located, but rather at centromeric heterochromatin in association with the other CPC members (Schröder, 2014, doctoral thesis). These findings might indicate an additional role of all CPC members in DNA damage response. However, this has to be investigated in more detail.

1.5.3 Deregulation of the CPC in cancer

The CPC member Survivin is highly expressed during embryonic and fetal development (Boidot et al., 2014), and deletion of the Survivin gene *birc5* in mouse embryos causes early embryonic lethality (Uren et al., 2000). In contrast, Survivin is weakly expressed in some normal tissues, such as colon basal endothelial cells, thymocytes, CD34+ stem cells and vascular endothelial cells (reviewed by Liu & Mitchell, 2010), or entirely absent in terminally differentiated adult tissues (Ambrosini et al., 1997). Thus, a participation of Survivin in the renewal especially of fast proliferating cells can be suggested (Athanasoula et al., 2014).

In contrast to normal cells, cancer cells undergo metabolic and behavioral changes, leading them to proliferate excessively. All CPC members are overexpressed in a multitude of cancers. For example, Borealin is overexpressed in colorectal (Wang et al., 2014) and lung cancer

(Hayama et al., 2007) and a high expression was related to poor prognosis in gastric cancer (Chang et al., 2006). INCENP was also increased in colorectal cancer (Kabisch et al., 2015), whereas Survivin (Adida et al., 2000; Ambrosini et al., 1997) and Aurora B (Tanaka et al., 1999; Tatsuka et al., 1998) have been found to be overexpressed in various cancer types. Furthermore, Survivin overexpression promotes tumor progression by an upregulated VEGF expression leading to angiogenesis of cancer cells (Fernández et al., 2014; Sanhueza et al., 2015). Protein overexpression of at least one CPC member is associated with high rates of tumor recurrence, abbreviated patient survival and resistance to chemo- and radiotherapy (Athanasoula et al., 2014; Capalbo et al., 2007; Chen et al., 2014). Thus designating the CPC, besides having a function as a molecular marker for malignancies, as a potential target for cancer therapy.

Therapeutic inhibition of Survivin in tumor cells may possibly yield cumulative benefits due to its involvement in cell division, apoptosis as well as chemo- and radioresistance. Several approaches comprising mRNA inhibitors, immunotherapeutic agents and small molecule inhibitor treatments targeting Survivin's functions are under investigation (reviewed in Athanasoula et al., 2014; Garg et al., 2016). In addition, several Aurora B kinase inhibitors are used in clinical trials (reviewed in Tang et al., 2017).

1.6 Aims of this thesis

The faithful duplication and segregation of the entire genome requires close coordination of an elegant network of many different protein factors in the cell. One example of a protein complex,ensuring the proper segregaton of the genome to progeny cells, is the chromosomal passenger complex (CPC). It consists of a catalytic module, the kinase Aurora B and a localization module. The latter comprises the proteins Survivin, Borealin and INCENP and targets the CPC to the respective structures for precise and equal segregation of the genome during mitosis. All CPC members are overexpressed in a multitude of cancers. The protein overexpression of at least one CPC member is associated with high rates of tumor recurrence, abbreviated patient survival and resistance to chemo- and radiotherapy (Athanasoula et al., 2014; Capalbo et al., 2007; Chen et al., 2014). Thus designating the CPC, besides having a function as a molecular marker for malignancies, as a potential target for cancer therapy. While its role in maintaining the genomic stability during mitosis is well characterized, the functional role of the CPC during interphase is still unknown.

To gain further insights into the role of the CPC during interphase, first of all the localization of the CPC should be analyzed in a cell cycle dependent manner as well as with respect to key replication- or chromatin-associated proteins via immunofluorescence. Furthermore, potential interactions of the CPC members with characteristic replisome and chromatin-binding proteins should also be a matter of investigation by iPOND, PLA and co-immunoprecipitations. Further insights into the interaction of the CPC should also be confirmed by defining interaction sites between the respective proteins. In addition, a potential functional involvement of the CPC during replication should be investigated by flow cytometry analysis and a combination of siRNA-mediated depletion of Survivin or inhibition of Aurora B kinase with replication fork velocity analysis. In order to determine whether the CPC could also be implicated in processes after induction of replication stress, the expression of CPC proteins and their localization to different cell compartments should be analyzed either via western blotting or immunofluorescence. In addition, the question what happens with the CPC after helicase-polymerase uncoupling after replication stress induction should be addressed. Finally, it should also be determined by immunofluerescence whether the CPC is involved in DNA synthesis during mitosis.

2 Materials and Methods

2.1 Materials

2.1.1 Chemicals and consumables

Unless stated otherwise, all chemicals used were obtained from the companies AppliChem (Darmstadt), Roth (Karlsruhe) and Sigma-Aldrich (Deisenhofen). For the cultivation of eukaryotic cells, disposables from Sarstedt (Nümbrecht) and Greiner (Frickenhausen) were used. For confocal microscopy µ-Slide 8-well chamber slides were bought from Ibidi GmbH (München) and glass bottom dishes from MatTek (Ashland, MA, USA). Restriction enzymes were purchased from New England Biolabs (Frankfurt am Main), oligo nucleotides (primer) from Eurofins Genomics (Ebersberg) and DNA and protein marker from MBI Fermentas (St. Leon-Rot). Further notes concerning materials used can be found in the corresponding sections dealing with their application.

2.1.2 Buffer and solutions

Frequently used buffers and solutions are listed in Table 1. They were usually prepared with double-distilled water (ddH_2O) and pH values were adjusted at room temperature. Further buffers or solutions, not listed here, can be found in the corresponding section.

Table 1: Composition of buffers and solutions.

buffer or solution	composition
PBS	137 mM NaCl, 2.7 mM KCl, 10 mM Na_2HPO_4, 2 mM KH_2PO_4, pH 7.4
PBST	PBS + 0.1 % (v/v) Tween-20
TBS	50 mM Tris-HCl, 150 mM NaCl, pH 7.4
TBST	TBS + 0.1 % (v/v) Tween-20
4x SDS stacking gel buffer	500 mM Tris-HCl pH 6.8, 0.8 % (w/v) SDS
4x SDS resolving gel buffer	1.5 M Tris-HCl pH 8.8, 0.8 % (w/v) SDS
5x SDS sample buffer	60 mM Tris-HCl pH 6.8, 5 mM EDTA, 30 % (v/v) glycerin, 15 % (w/v) SDS, 7.5 % (v/v) 2-mercaptoethanol, 0.1 % (w/v) bromophenole blue
SDS running buffer	25 mM Tris, 192 mM glycine, 0.1 % (w/v) SDS
Transfer buffer	25 mM Tris pH 8.3, 192 mM glycine, 0.01 % (w/v) SDS, 20 % (v/v) methanol
RIPA buffer	50 mM Tris-HCl, 150 mM NaCl, 5 mM EDTA, 1 % (v/v) NP-40, 1 % (v/v) sodium deoxycholat, 1 mM DTT, 1 × protease inhibitor , 1 mM PMSF
TAE-buffer	40 mM Tris, 20 mM acetic acid, 1 mM EDTA, pH adjusted to 8.3 with acetic acid

buffer or solution	composition
Jiang IP buffer	0.5 % NP-40, 5 mM EDTA, 2 mM EGTA, 20 mM MOPS, 1 mM PMSF, 20 mM $Na_4P_2O_7$, 30 mM NaF, 40 mM b-glycerophosphate, 1 mM Na_3VO_3
IP lysis buffer	50 mM Hepes pH 7.5, 150 mM NaCl, 0.5 % NP-40, 1x protease inhibitor, 1x phosStop
IP wash buffer	50 mM HEPES pH7.5, 150 mM NaCl
PTEMF buffer	20 mM PIPES pH 6.8, 10 mM EGTA, 0.2 % Triton X-100, 1 mM $MgCl_2$, 4 % formaldehyde
CSK buffer	100 mM NaCl, 3 mM $MgCl_2$, 10 mM HEPES pH7.4, 300 mM sucrose, 0.3 % (v/v) Triton X-100, protease inhibitor, phosphatase inhibitor

2.1.3 Laboratory devices

All laboratory devices used are listed in Table 2 or can be found in the correspondent section dealing with the application.

Table 2: Laboratory devices with manufacturer.

device	manufacturer
Allegra X-22 Series Centrifuges	Beckman Coulter GmbH, Krefeld
BioPhotometer Plus	Eppendorf AG, Hamburg
Centrifuge 5417C/R	Eppendorf AG, Hamburg
Centrifuge ROTINA 380/Rotina 380 R	Andreas Hettich GmbH & Co. KG, Tuttlingen
Centrifuge ROTOFIX 32 A	Andreas Hettich GmbH & Co. KG,Tuttlingen
Chemistry pumping unit (model PC 500 LAN NT)	VACUUBRAND GMBH + CO KG, Wertheim
CO_2 incubator	Binder GmbH, Tuttlingen
CO_2 incubator model INC153	Memmert GmbH & Co. KG, Schwabach
Eppendorf Research Plus	Eppendorf AG, Hamburg
Exchangeable Thermoblocks	Eppendorf AG, Hamburg
Film processor CAWOMAT 2000 IR	CAWO GmbH, Schrobenhausen
Forma Orbital Shaker (420 Series)	Thermo Fisher Scientific, Waltham, USA
GrantBio orbital shaking platform POS-300	Grant Instruments (Cambridge) Ltd, Roystock, UK
Heated table	MEDAX GmbH & Co. KG, Neumünster
Heating immersion circulator ED	JULABO GmbH,Seelbach
Heating plate RCT Standard	IKA-Werke GmbH & Co.KG, Staufen
Heating plate RH basic 2 /,KT/C, RH	IKA-Werke GmbH & Co.KG, Staufen

device	manufacturer
Magnetic stirrer, different models	IKA-Werke GmbH & Co.KG, Staufen
Microbiological safety cabinet NU-437-300E/400E/500E/600E	INTEGRA Biosciences GmbH, Fernwald
Microbiological safety cabinet HERAsafe® KS/KSP	Thermo Fisher Scientific, Waltham, USA
Mikroliterrotor 24x2ml und PCR-Rotor	Thermo Electron Corporation, Langenselbold
Mini-Protean Tetra Cell System	Bio-Rad Laboratories GmbH, München
Mini-Transfer-Blot® Electrophoretic Transfer Cell	Bio-Rad Laboratories GmbH, München
Multipipette® Stream	Eppendorf AG, Hamburg
Nalgene "Mr. Frosty" Freezing Container	Thermo Fisher Scientific, USA
neoLab rotor with vortex mixer	neoLab Migge Laborbedarf- Vertriebs GmbH, Heidelberg
PerfectBlue™ horizontal mini gel system	Peqlab Biotechnologie GmbH, Erlangen
PerfectBlue™ Tank Electro Blotter Web S	Peqlab Biotechnologie GmbH, Erlangen
pH/mV/°C meter with microprocessor	HANNA Instruments Deutschland GmbH, Kehl
PIPETMAN® P/Neo	Gilson International B.V., Limburg-Offheim
pipetus®	Hirschmann Laborgeräte GmbH & Co. KG, Eberstadt
power supply peqPOWER 300	Peqlab Biotechnologie GmbH, Erlangen
power supply PowerPac™Basic	Bio-Rad Laboratories GmbH, München
precision balance	Kern & Sohn GmbH, Balingen
Spectrafuge™ Mini Centrifuge	Labnet International Inc, Edison, NJ, USA
thermal printer DPU-414	Seiko Instruments GmbH, Neu-Isenburg
thermocycler TPersonal 48	Biometra GmbH, Göttingen
thermocycler TProfessional standard gradient 96	Biometra GmbH, Göttingen
thermomixer Comfort with exchangeable thermoblocks	Eppendorf AG, Hamburg
tube roller RS-TR 5	Phoenix Instrument GmbH, Garbsen
tube roller SRT9	Stuart Bibby Scientific Ltd, Stone, UK
tube rotator SB2	Stuart Bibby Scientific Ltd, Stone, UK
ultrasonic device Sonopuls mini20	BANDELIN electronic GmbH& Co.KG, Berlin
UV Sterilizing PCR Workstation	Peqlab Biotechnologie GmbH, Erlangen
vortex mixer PV-1	Grant Instruments (Cambridge) Ltd, Royston, UK

device	manufacturer
vortex mixer Vortex-Genie® 2	Scientific Industries, Bohemia, NY, USA
Vortex-Genie 2	Scientific Industries, USA
water bath 1002-1013	Gesellschaft für Labortechnik mbH, Burgwedel

2.1.4 Software and computer-based analysis

The software used in this thesis is listed in Table 3.

Table 3: Used software and manufacturer.

Software	manufacturer
Adobe Photoshop CS5	Adobe Systems GmbH, Munich
BioEdit	Ibis Therapeutics, Carlsbad, CA, USA
Canvas 11	Canvas GFX, Inc., Plantation, FL, USA
CellProfiler 3.0	Carpenter Lab at the Broad Institute of Harvard and MIT, Cambridge, MA, USA
Gene Construction Kit	Textco BioSoftware, Inc, Raleigh, NC, USA
GraphPad Prism 5.04	GraphPad Software, La Jolla, CA, USA
Image Studio Lite 4.0	LI-COR Biosciences Inc., Lincoln, NE, USA
ImageJ, Image Processing and Analysis in Java Fuji	National Institute of Health, Bethesda, MD, USA
Kaluza Analysis 1.3	Beckman Coulter, Brea, CA, USA
Leica Application Suite AF Leica Application Suite X	Leica Microsystems GmbH, Mannheim
PyMOL	Schrödinger LCC, Portland, OR; USA
SnapGene Viewer 3.3.4	GSL Biotech, Chicago, IL, USA

2.1.5 Eukaryotic cell lines

The cell lines used in this thesis are listed in Table 4.

Table 4: Characterization of cell lines.

cell line	tissue/organism/characteristics	ATCC-number/reference	medium
A431	epidermoid carzinoma, *Homo sapiens*	CRL-1555	DMEM
A431 Surv-GFP	A431 cells stably expressing Survivin-GFP		DMEM 800
HeLa	cervical adenocarzinoma, *Homo sapiens*	CCL-2	DMEM
WI-38	lung fibroblasts, *Homo sapiens*	CCL-75	WI-38

cell line	tissue/organism/characteristics	ATCC-number/reference	medium
293T	Embryonic kidney, *Homo sapiens*	CRL-11268	DMEM
U2OS	Bone, osteosarcoma, *Homo sapiens*	HTB-96	DMEM
NIH 3T3	fibroblasts, Mus musculus	CRL-1658	DMEM

2.1.6 Media and additives

Media und additives used for cell culturing are listed in Table 5. Composition of the appropriate culture medium is listed in Table 6.

Table 5: Culture media and additives.

medium, additive	manufacturer
DMEM (1x) Dulbecco's Modified Eagle Medium	Life technologies, Carlsbad, CA USA
FCS	Life technologies, Carlsbad, CA USA
Antibiotic-Antimycotic (100x) (AA)	Life technologies, Carlsbad, CA USA
L-Glutamine 200mM (100x)	Life technologies, Carlsbad, CA USA
MEM Non-Essential Amino Acids Solution (100x) (NEAA)	Life technologies, Carlsbad, CA USA
Sodium bicarbonate, 7.5 % solution	PAA, Pasching, A
Sodium pyruvate	AppliChem, Darmstadt
Geniticin (G418)	Biochrom AG, Berlin

Table 6: Composition of cell culture media.

medium	Additives with final concentration
DMEM	DMEM, 10% (v/v) FCS, AA (1x)
WI-38	MEM, 10% FCS, AA (1x), L-Glutamine (2 mM), NEAA (1x), sodium bicarbonate (1.5 g/l), sodium pyruvate (1 mM)
DMEM 800	DMEM, 800 µg/ml Geniticin

2.1.7 Antibodies

The listed specific primary (Table 7) and secondary antibodies (Table 8) were used for protein detection in western blotting (WB, section 2.2.3.7) and in immunofluorescence (IF, section 2.2.2.8). Secondary antibodies are conjugated either with Alexa Fluor (AF) or horesradisch peroxidase (HRP). Further antibodies can be found in the corresponding section dealing with the application.

Table 7: Primary antibodies.

antigen	origin	dilution		manufacturer
		WB	IF	(order number)
ATR	rabbit	1:1000		GeneTex Inc., Irvine, CA, USA (GTX 128146)
Aurora B	rabbit	1:2000	1:2000	Sigma, Munich (A5102)
Aurora B	mouse		1:500	BD Transduction Laboratories, Heidelberg (611082)
Aurora B pT232		1:500		courtesy of Prof. H. Meyer (University of Duisburg-Essen); Rockland Immunochemicals, Limerick, PA, USA(600-401-677)
Borealin	mouse		1:200	MBL International, Woburn, MA, USA (M147-3)
Borealin	rabbit	1:500		Novus Biologicals, Littleton, CO, USA (NBP1-77330)
CAF1	rabbit		1:200	NEB/ Cell Signalling (5480)
CREST (Centromere, Kinetochore)	human serum		1:200	Antibodies Incorporated, Davis, CA, USA (15-234)
DNA Ligase I	mouse		1:100	MBL International, Woburn, MA, USA (K0190-3)
GFP-tag	rabbit	1:2000		Santa Cruz Biotechnology Inc., Santa Cruz, CA, USA (sc-8334)
HA-tag	mouse	1:1000		Covance (MMS-101R)
histone H3	mouse	1:1000		Abcam, Cambridge, UK (ab195277)
HP1α	rabbit		1:400	NEB/Cell Signaling (2616)
INCENP	mouse		1:150	Life Technologies GmbH, Darmstadt (39-2800)
INCENP	rabbit	1:1000 (5% BSA/TBST)		NEB/Cell Signaling (2807)
Lamin A/C	rabbit	1:1000		NEB/Cell Signaling (2032)
Mcm2	goat		1:100	Santa Cruz Biotechnology Inc., Santa Cruz, CA, USA (Sc-9839)
Myc-tag	mouse	1:1000	1:1500	NEB/Cell Signaling (2276)

antigen	origin	dilution		manufacturer
		WB	IF	(order number)
pATM (pSer1981)	mouse	1:300	1:500	Santa Cruz Biotechnology Inc., Santa Cruz, CA, USA (sc-47739)
PCNA	mouse	1:2000	1:3200 (MetOH)	NEB/Cell Signaling (2586)
PCNA	rabbit		1:200 (MetOH)	Abcam, Cambridge, UK (Ab92552)
pH3S10	mouse		1:100	NEB/Cell Signaling (9706)
pRPA32 Ser33	rabbit	1:500		Novus Biologicals, Littleton, CO, USA (NB100-544)
RPA32	mouse	1:20	1:50	Merck Millipore, Burlington, CA, USA (NA18)
Survivin	rabbit	1:1000	1:400	Novus Biologicals, Littleton, CO, USA (NB500-201)
Survivin	mouse	1:1000		Novus Biologicals, Littleton, CO, USA (NB500-205)
α-Tubulin	mouse	1:8000		Sigma, Munich (T5168)
α-Tubulin	mouse	1:8000		Sigma, Munich (T6074)
γH2AX (pSer139)	mouse	1:5000	1:10,000	BioLegend, San Diego, CA, USA (613402)

Table 8: Secondary antibodies.

antibody	origin	dilution		manufacturer
		WB	IF	(order number)
anti-mouse IgG-AF488	goat		1:1,000	Life Technologies GmbH, Darmstadt (A11001)
anti-mouse IgG-AF568	goat		1:1,000	Life Technologies GmbH, Darmstadt (A11004)
anti-mouse IgG-AF633	goat		1:1,000	Life Technologies GmbH, Darmstadt (A21050)
anti-rabbit IgG-AF488	goat		1:1,000	Life Technologies GmbH, Darmstadt (A11008)
anti-rabbit IgG-AF568	goat		1:1,000	Life Technologies GmbH, Darmstadt (A11011)
anti-rabbit IgG-AF633	goat		1:1,000	Life Technologies GmbH, Darmstadt (A21070)

antibody	origin	dilution WB	dilution IF	manufacturer (order number)
anti-goat IgG-AF488	donkey		1:1,000	Life Technologies GmbH, Darmstadt (A11055)
anti-rat IgG-AF568	goat		1:1,000	Life Technologies GmbH, Darmstadt (A11077)
anti-human IgG-AF568	goat		1:1,000	Life Technologies GmbH, Darmstadt (A21090)
anti-mouse IgG-HRP	sheep	1:10,000		GE Healthcare Life Sciences, Freiburg (NXA931)
anti-rabbit IgG-HRP	donkey	1:10,000		GE Healthcare Life Sciences, Freiburg (NA934)

2.1.8 Oligonucleotides

2.1.8.1 DNA oligonucleotides

DNA oligonucletides used for PCR were purchased from Eurofins Genomics (Ebersberg). DNA nucleotides for sequencing were provided by LGC Genomics (Berlin).

Table 9: DNA oligonucleotides.

name	sequence	application
PIP-substitution_fw	5`-CACCAGGCTGCTCACCCACCGAACCTTCTGGAG-3’	PCR
PIP-substitution_rv	5`-AGCGATAGCAGCGCTGAGCGGGGTGCCTCG-3’	PCR
CMV_fw	5`-GCAAATGGGCGGTAGGCGT-3’	sequencing
pcDNA3.1_rv	5`-TAGAAGGCACAGTCGAGGCT-3’	sequencing

2.1.8.2 siRNA

Synthetically generated siRNAs used for RNA interference (RNAi) were purchased in 20 nM scale scale, resuspended in RNAse-free water and stored as 20 µM stock solutions at -20 °C.

Table 10: Sequences of siRNAs for RNA interference.

name	target/ sense strand	reference/ supplier
siCtr	non human homology 5’-UUCUCCGAACGUGUCACGUdTdT-3’	(Dobrynin et al., 2011), microsynth AG, Balgach, CH
siSurvivin (B02)	Human Survivin (3’-UTR) 5'-AACAAGAGCACAGUUGAAACAUCUA-3'	Invitrogen, Karlsruhe
siSurvivin (BIRC5.5)	5'-GCAUUCGUCCGGUUGCGCUTT-3'	Qiagen, Hilden

2.1.8.3 Plasmids

The plasmids used in this thesis are listed in Table 11. The pCCC plasmid differs from the others, because it encodes not the corresponding protein PCNA itself but rather a so-called chromobody. This chromobody is based on the antigen binding domain (V_HH) of a camelid antibody that specifically recognizes PCNA and which is fused to a RFP-tag. The advantage is that the chromobody does not interfere with endogenous protein function and that the endogenous protein can be visualized via the RFP-tag.

Table 11: Eukaryotic expression plasmids.

plasmid	description	Received from/ supplier/ reference
pc3-Survivin-GFP	Survivin fused C-terminal with GFP	Courtesy of Prof. R. Stauber (University of Mainz)/ (Knauer et al., 2006)
pCCC	PCNA chromobody (V_HH) fused with RFP	ChromoTek GmbH, Planegg-Martinsried
pc3-Survivin-tdTomato	Survivin fused C-terminal with tdTomato	Courtesy of Prof. R. Stauber (University of Mainz)
peGFP-N3-HP1α	HP1α fused N-terminal with GFP	courtesy of Prof. H. Meyer (University of Duisburg-Essen)
pc3-Survivin-HA	Survivin fused C-terminal with HA	Knauer group
pc3-myc-Survivin	Survivin fused N-terminal with myc	Knauer group
pc3-Aurora B-HA	Aurora B fused C-terminal with HA	Knauer group
pc3-Borealin-HA	Borealin fused C-terminal with HA	Knauer group
pcDNA3.1(+)	used as empty vector in transfections	Life Technologies GmbH, Darmstadt
pENeGFP-PCNA	PCNA fused N-terminal with GFP	courtesy of Prof. C. Cardoso (Technical University Darmstadt)
pENenRFP-PCNA	PCNA fused N-terminal with RFP	courtesy of Prof. C. Cardoso (Technical University Darmstadt)
pcDNA3.1-myc-INCENP	INCENP fused N-terminal with myc	courtesy of Prof. H. Meyer (University of Duisburg-Essen)
pcDNA3.1-myc-INCENP-PIPmut	INCENP with aa exchange of Gln853, Ile856, Thr859 and Thr860 to Ala fused N-terminal with myc	this thesis

2.1.9 Bacterial strains

The respective bacteria were grown at 37 °C in LB medium (AppliChem, Darmstadt) or on dishes containing LB agar (AppliChem, Darmstadt), both supplemented with the respective antibiotics (section **Fehler! Verweisquelle konnte nicht gefunden werden.**).

Table 12: Bacterial strains.

strain	genotype	supplier
E. coli XL2-Blue™	*endA1 supE44 thi-1 hsdR17 recA1 gyrA96 relA1 lac [F´ proAB lacI^q ZΔM15 Tn10 (Tet^r) Amy Cam^r]*	Strategene (Heidelberg)
NEB® 5-alpha *E. coli*	*fhuA2 Δ(argF-lacZ)U169 phoA glnV44 Φ80 Δ(lacZ)M15 gyrA96 recA1 relA1 endA1 thi-1 hsdR17*	New England Biolabs (Ipswich, MA, USA)

2.1.10 Kits

All kits used in this work are listed in (Table 13).

Table 13: Used kits, application and manufacturer

kit	application	manufacturer
Nucleo Bond® Xtra Midi	isolation of plasmids from 200ml bacterial culture	Machery-Nagel (Düren)
Nucleo Spin® Multi-8-Plasmid	isolation of plasmids from 5ml bacterial culture	Machery-Nagel (Düren)
NucleoSpin® Gel and PCR Clean- up	purification of DNA (PCR/agarose gel)	Machery-Nagel (Düren)
Q5® Site-directed mutagenesis	site directed mutagenesis of plasmids to make specific DNA alterations (insertions, deletions and substitutions)	New England BioLabs GmbH (Frankfurt am Main)
Subcellular Protein Fractionation Kit for Cultured Cells	segregation and enrichment of proteins from different cellular compartments	Thermo Fisher Scientific (Waltham, MA, USA)
µMACS® isolation kit for tagged proteins	isolation of tagged fusion proteins	Miltenyi Biotec (Bergisch-Gladbach)
Pierce™ ECL Plus Western Blotting Substrate SuperSignal™ West Femto Maximum Sensitivity Substrate	substrate for the horseradish peroxidase (HRP)	Pierce Biotechnology, Inc. (Rockford, IL, USA)

kit	application	manufacturer
Click-iT™ EdU Alexa Fluor™ 488 Imaging Kit Click-iT™ EdU Alexa Fluor™ 594 Imaging Kit	fluorescent labeling of proliferating cells for microscopy	Thermo Fisher Scientific (Waltham, MA, USA)
Duolink® In Situ Detection Reagents Orange	detection of protein-protein-interaction	Sigma-Aldrich, Steinheim

2.2 Methods

2.2.1 Molecular Biology

2.2.1.1 Polymerase chain reaction (PCR)

For mutation of longer plasmid sequences, the Q5® Site-Directed mutagenesis kit (New England BioLabs GmbH, Frankfurt am Main) was used according to the manufacturer's instructions. The PCR reaction was mixed according to Table 14. A plasmid was used as template DNA. Lyophilized primers were dissolved in ddH_2O to a final concentration of 100 µM and diluted in a ration of 1:10 and than added to the eaction mix. Primer sequences and annealing temperature were generated using the NEB online design software, NEBaseChanger™. The plasmid DNA sequence should be mutated to substitute the respective aa to alanine, because it is the smallest aa, has no reactive groups and therefore the secondary structure is not altered due to sterical hindrances.

Table 14: Compositin of a PCR.

name	volume (µl)	final conc.
Q5 Hot start high-fidelity 2x Master Mix	12.5	1x
forward primer (10 µM)	1.25	0.5 µM
reverse primer (10 µM)	1.25	0.5 µM
template DNA (1-25 ng/µl)	1	1-25 ng
nuclease-free water	9	

The mixtures were transferred to a thermocycler and the cycling condition described in Table 15 were performed for PCR.

Table 15: Cycling conditions of a PCR.

step		temperature	time
initial denaturation		98 °C	30 s
25 cycles	denaturation	98 °C	10 s
	annealing	71 °C	30 s
	elongation	72 °C	5 min
final extension		72 °C	2 min
hold		4 °C	

2.2.1.2 KLD treatment

After PCR, the amplified material is subjected to a KLD treatement according to the instructions of the Q5® Site-Directed mutagenesis kit (New England BioLabs GmbH, Frankfurt am Main). It contains a mix of kinase, ligase and DpnI enzymes allowing phosphorylation, intramolecular circularization and template removal. The reaction was mixed as shown in Table 16 and incubated for 5 min at RT.

Table 16: Composition of a KLD reaction.

name	volume (µl)	final conc.
PCR product	1	
2x KLD reaction buffer	5	1x
10x KLD enzyme mix	1	1x
nuclease-free water	3	

2.2.1.3 Transformation of competent bacteria

After KLD treatment (section 2.2.1.2), 5 µl of the KLD mix were mixed with 50 µl of chemically-competent NEB® 5-alpha *E. coli* and incubated on ice for 30 min. Afterwards heat shock was performed at 42 °C for 30 seconds and sampes were further incubated on ice for 5 min. 950 µl SOC medium, included in the Q5® Site-Directed mutagenesis kit (New England BioLabs GmbH, Frankfurt am Main), was added and samples were indubated at 37 °C for 1 h. 80 µl of the dilution of a ratio of 1:40 was spread onto the selection dish, containg LB Agar with carbinicillin (final conc. 100 µg/ml; AppliChem GmbH, Darmstadt), and incubated over night at 37 °C.

Alternatively, if plasmids need to be reproduced, 50 µl of *E. coli* XL2-Blue™ were thawed on ice and a volume containing approximately 10 ng plasmid DNA was added and incubated on ice for 30 min. Afterwards heat shock was performed at 42 °C for 45 seconds and sampes were placed on ice for 1 min. Finally, the mixture was sprad onto the selection dish, containg LB Agar with carbinicillin (final conc. 100 µg/ml; AppliChem GmbH, Darmstadt), and incubated over night at 37 °C*. E.coli* cells transformed with plasmids carrying a kanamycin resistance, were resuspended in 500 µl antibiotic-free LB medium and incubated 1 h at 37 °C before spreaded onto the selection dish, containing LB agar with kanamycin (final conc. 50 µg/ml; AppliChem GmbH, Darmstadt) and incubation over night at 37 °C.

2.2.1.4 Agarose gel electrophoresis

Agarose gel electrophoresis was used to separate nucleic acids according to their size. Gels were used with a concentration ranging from 1 % to 2 % (w/v) agarose depending on the size of the molecules. The agarose was boiled in 1 x TAE buffer and DNA intercalating agents such as ethidium bromide or HDGreen Plus (INTAS Science Imaging Instruments GmbH, Göttingen) were added. Gels were poured and placed in electrophoresis chamber after polymerization. Samples were mixed with 6 x DNA loading dye (Thermo Fisher Scientific, Waltham, USA) and loaded on the gel. Electrophoresis was performed with constant voltage of 100 V for 1 in 1 x TAE. DNA bands were visualized with UV light (E-Box VX2, Vilber Lourmat, Eberhardzell)

and band size was detected in comparison to appropriate size standards (GeneRuler™ 1 kb DNA Ladder and GeneRuler™ 100 bp DNA Ladder; Thermo Fisher Scientific, Waltham, USA).

2.2.1.5 Extraction of DNA fragments from agarose gels and PCR samples

For extraction of DNA fragments from agarose gels or from PCR samples the NucleoSpin® Gel and PCR Clean- up kit (Macherey-Nagel, Düren) was used according to the manufacturer's instructions. Elution was performed with 30 µl of the provided elution buffer.

2.2.1.6 Isolation of plasmids from bacterial cells

Depending on the required amount of DNA the Nucleo Bond® Xtra Midi or the Nucleo Spin® Multi-8-Plasmid kit (section 2.1.10) was used for the isolation of plasmids from *E.coli* cells. For both purposes a single *E.coli* colony from LB agar plates (section 2.2.1.3) or a sample from a bacterial glycerol stock (section 2.2.1.7) is transferred either to 5 ml LB medium for mini preparation or to 200 ml LB medium for midi preparation of plasmids, both containing the respective antibiotic and incubated overnight at 37 °C. For the mini preparation of plasmids, 4 ml of the bacterial culture were centrifuged for 10 min at 1,000 xg and the plasmids were isolated according to the manufacturer's instruction of the Nucleo Spin® Multi-8-Plasmid kit. Plasmid DNA was eluted in 80 µl of the provided elution buffer. For the midi preparation of plasmids, the bacterial culture was centrifuged for 15 min at 3,900 xg and 4 °C and the plasmids were isolated according to the manufacturer's instruction of the Nucleo Bond® Xtra Midi kit. Plasmid DNA was precipitated with isopropanol and washed with ethanol and afterwards dissolved in ddH_2O.

2.2.1.7 Preparation of bacterial glycerol stocks

For long term storage of plasmid DNA-containg *E.coli* cells, bacterial clycerol stocks were obtained by mixing 400 µl of sterile 86 % glycerol with 600 µl of an overnight bacterial culture in a cryovial. Cryovials were shock frozen and stored at -80 °C.

2.2.1.8 Quantification of DNA concentration

The purity and the concentration of a plasmid DNA solution was determined via NanoDrop2000c (Thermo Fisher Scientific Waltham, MA, USA) measurements of the absorption of aromatic purine and pyrimidine bases at 260 nm. A ratio of approximately 1.8 for the absorbance at 260 nm and 280 nm is accepted as 'pure' DNA as well as the range of 2.0 to 2.2 of the A260/A230 values.

2.2.1.9 DNA sequencing and sequence analysis

The concentration was adjusted to approximately 100 ng/µl prior to sending the samples to LGC Genomics GmbH (Berlin), who performed the DNA sequencing. The resulting sequences were analyzed with the BioEdit software (section 2.1.4).

2.2.2 Cell Biology

2.2.2.1 Cultivation of mammalian cell lines

Adherent growing eukaryotic cells were routinely maintained under sterile conditions. They were cultivated in T-75 cell culture flask in 10 ml of the respective medium in the incubator at 37 °C, 5 % CO_2 and approximately 90 % relative humidity. At a confluence level of 70-90 % the growth medium was aspirated and cells were washed with 6 ml sterile DPBS (Life Technologies, Carlsbad, CA, USA) to remove the remaining culture medium and cells were detached from cell culture flask bottom by adding 2 ml TrypsinLE Express (Life Technologies, Carlsbad, CA, USA). Cell culture flask were placed on a heating plate preheated to 37 °C. To stop the enzymatic activity, 8 ml of the respective medium was added. Afterwards, cells were diluted depending on their confluence in a ratio of 1:5 to 1:20 into a new cell culture flask.

2.2.2.2 Freezing and thawing of cell lines

Storage of cells over a prolonged period was carried out in 10 % (v/v) DMSO/FCS. Cells were trypsinized and proteolytic activity was stopped as describe in section 2.2.2.1. Cells were transferred to 15 ml reaction tubes and centrifuged for 5 min at 300 xg. After aspirating the medium, the cell pellet was first resuspended in 5 ml FCS and afterwards 5 ml 20% (v/v) DMSO/FCS was added. 1 ml each of the cell suspension was transferred into cryotubes (Thermo Fisher Scientific, Waltham, MA, USA), placed in the Mr. Frosty freezing container (Thermo Fisher Scientific, Waltham, MA USA) and chilled stepwise (1 C/min) to -80 °C and stored afterwards in a liquid nitrogen tank (-130 °C).

For thawing, cells were heated in a water bath at 37 °C. 1 ml of the respective growth medium was added and the solution was transferred into a 15 ml reaction tube containing additional 8 ml growth medium. Cells were centrifuged for 5 min at 300 xg and the supernatant was aspirated to remove the DMSO. Cells were resuspended in 10 ml of fresh growth medium and transferred into the T-75 cell culture flask. After 24 h growth medium was replaced by new medium and cells were further cultivated as described in section 2.2.2.1.

After one week of cultivation, an assay was performed for visual detection of potential mycoplasma contamination. Mycoplasmas are the smallest bacteria and not visible in the microscope. They can attach to the eukaryotic cells and can also entry the cell by fusing with the cell membrane. Mycoplasmas compete with the eukaryotic host cells for nutrients, alter DNA, RNA and protein synthesis and introduce chromosomal aberrations (Drexler and Uphoff, 2002). To detect mycoplasma contaminations, the Plasmo Test™ Mycoplasma Detection kit (Invivogen, San Diego, CA USA) was performed according to the instructions of the manufacturer. Only mycoplasma-free cell lines were subjected to any experimental procedure.

2.2.2.3 Inhibitor treatment of eukaryotic cells

To specifically inhibit the kinase activity of Aurora B, the inhibitor Hesperadin was used in a final concentration of 100 nM (stock solution 1 mM in DMSO). Hesperadin is an indolinone compound that interacts with both the ATP- and the adjacent hydrophobic binding pocket of Aurora B (Hauf et al., 2003; Sessa et al., 2005).

PIP box inhibitor T2AA was used in a final concentration of 40 µM (stock: 100mM in DMSO) (Sigma-Aldrich, Steinheim). T2AA is a T2 amino alcohol, a T3 derivate that lacks thyroid hormone activity. It is a non-petide small molecule (Punchihewa et al., 2012) that binds to PCNA at the PIP box cavity thus abolishing interaction of PCNA with PIP box-containing proteins (Inoue et al., 2014).

RO-3306 (Sigma-Aldrich, Steinheim), a selective ATP-competetive inhibitor of CDK1, was used in a final concentration of 0.9 µM to arrest cells in G_2/M phase.

For the induction of replication stress several inhibitors were used. For example, camptothecin (CPT) targets topoisomerase I (TopoI). TopoI binds under normal conditions to DNA and generates a SSB to reduce the torsional stress of supercoiled DNA at replication forks (Champoux, 1978; Hsiang et al., 1989). CPT binds to the TopoI-DNA complex and inhibits the re-ligation of the DNA, thereby sustaining the SSB. The collision with the subsequent replication fork generates DSBs (Pommier, 2006). In contrast to the described mechanism caused by the treatment with high CPT concentrations (1 µM), lower concentrations of CPT (25 nM) induce replication fork slowing and fork reversal to prevent chromosomal breakage. CPT activates both, the ATR-Chk1 and the ATM-Chk2 signaling (Ray Chaudhuri et al., 2012).

Aphidicolin (APH; Santa Cruz Biotechnology Inc., Santa Cruz, CA, USA) binds to the active site of DNA polymerases α, β and ε and block the incorporation of nucleotides into the DNA strand, leading to replication fork stalling (Cheng and Kuchta, 1993). While the polymerase is inhibited, the helicase is still able to unwind the DNA (Sogo et al., 2002). This so-called uncoupling, leads to long stretches of ssDNA and checkpoint activation by ATR-Chk1 (Byun et al., 2005). Hydroxyurea (HU) inhibits the ribonucleotide reductase so that the dNTP pool is depleted. This results in stalled forks and uncoupling of helicase and polymerase function similar to APH treatment (Jossen and Bermejo, 2013). After prolonged treatment it can further result in collapsed forks and in DSBs (Petermann et al., 2010).

Cisplatin mainly forms intrastrand crosslinks. These structural DNA modifications block uncoiling and separation of the DNA double helix (Fichtinger-Schepman et al., 1985). Damage response is triggered by ATM-Chk2 and ATR-Chk1 pathway, similar to TopoI treatment. Cisplatin was used in a final concentration of 0.2 µM.

The DNA topoisomerase inhibitor camptothecin is of great interest because it helpt to maintain strand breaks generated by topoisomerases during replication.

2.2.2.4 X-ray irradiation

Cells were irradiated with the Philips Constant Potential X-ray System MG160. The device operated at 130 kV and 16 mA and a dose rate of approximately 1.2 Gy/min. Cells were irradiated with 6 Gy which leads to SSB or DSB and induces stress response via ATM-Chk2 and ATR-Chk1 signaling pathways (Maréchal and Zou, 2013). After the irradiation, the cells were returned to the incubator for 1 h and afterwards processes as described in the respective section.

2.2.2.5 Transient transfection of eucaryotic cells

Transient transfection of eukraryotic cells with plasmid DNA was performed either with cationic polymers as polyethylenimine (PEI; Sigma, Taufkirchen) for 293T cells or with Lipofectamine 2000 (Life technologies, Carlsbad, CA USA) used for all other cell lines. Thereby Lipofectamine 2000 forms cationic liposomes complexing with the negatively charged nucleic acid molecules. These can then overcome the electrostatic repulsion of the cell membrane and liposomes can fuse with the cell membrane effecting the entry of the nucleic acidl (Dalby et al., 2004). PEI binds the nucleic acids and these enter the cell via endocytosis. Endosomes swell due to an influx of ions and further burst and the polymer-DNA complex are released into the cytoplasm.

Cells were seeded in 10 cm dishes 24 h prior to transfection. For PEI transfection 240 µl DPBS were mixed with 44 µl 10 mM PEI for each well. Additionally 240 µl DPBS were mixed with 8 µg plasmid DNA. Both solutions were mixed together, vortexed and incubated at RT for 5 min. Lipofectamine 2000 was used for transfections for microscopic analysis which were perfomed in µ-Slide 8-well chamber slides. Cells were seeded in avolume of 300 µl growth medium and transfected after 24 h. Therefore, 12.5 µl OptiMEM and 150 ng plasmid DNA as well as 12.5 µl OptiMEM with 1 µl Lipofectamine 2000 were mixed and both pooled and incubated for 5 min at RT. In both cases, the mixed transfection agent was added dropwise to the cells and incubated for 24 h. If cells were seeded in another item, volumes were adjusted accordingly.

2.2.2.6 RNA interference (RNAi)

For the RNA interference (RNAi) approach, siRNAs (small interfering RNAs) were complexed to cationic and neutral lipids and added to the cells, where they could fuse with the cell membrane and the siRNAs were released into the cytoplasm. The siRNAs bind complementary to the corresponding mRNA. The formation of the RNA-induced silencing complex (RISC) destroys the mRNA-siRNA strand and prevents translation, thus reducing the protein amount of the respective target. The cells were transfected fast-forward with HiPerFect (Quiagen, Hilden), which means that the cells were seeded in a 6-well plate in 2 ml growth medium shortly before transfection and in the meantime incubated at standard growth conditions. The appropriate amount of the respective siRNA was pipetted to 100 µl OptiMEM,(resulting in a final concentration of 20 nM in the medium). Furthermore, 10 µl of HiPerFect transfection reagent was added and after brief vortexing, the entire solution was incubated at RT for 5-10 min. The transfection mixture was added dropwise to the cells and incubated for 72 h incubation at standard growth conditions.

2.2.2.7 Cell cycle analysis via flow cytometry

Flow cytometry is a laser-based technology for cell counting by suspending cells in a stream of fluid and passing them through an electronic detection apparatus. A flow cytometer allows simultaneous analysis of physical and chemical characteristics of up to thousands of particles per second. To monitor the cell cycle phase distribution of the cell population with or without RNA interference, cells were labeled and stained with BrdU, combined with PI staining. This is the most accurate measure of cells in the various stages of the cell cycle. It is the preferred method because it combines the detection of active DNA synthesis, through antibody based

staining of incorporated BrdU in the newly synthesized DNA strand, with total DNA content from propidium iodide, a fluorescent DNA intercalating dye.

Exponentially growing cells were pulse labeled with 10 µM BrdU (courtesy of H. Meyer, University Duisburg-Essen) for 30 min under standard growth conditions. Cells were then collected by trypsinisation and centrifugation at 400 xg for 5 min at 4 °C and washed with PBS. After centrifugation with 1000 xg for 5 min at 4 °C, pellet was resuspended in 30 µl PBS and 500 µl ico-cold methanol was added dropwise while vortexing very slowly. The samples were incubated overnight at -20 °C. Next, cells were centrifuged at 900 xg for 1 min, reaction tube was turned around and centrifuged again. These centrifugation steps were repeated between the following steps. Cells were washed with 500 µl 0.1% (v/v) Triton X-100 in PBS, centrifuged and resuspended in 500 µl 2 M HCl containing 0.5% (v/v) Triton X-100 for 30 min at RT to denature the labeled, dsDNA. After centrifugation, the cells were washed twice with 0.01% (v/v) Triton X-100 in PBS till pH was neutral (pH indication paper, Macherey Nagel, Göttingen). Cells were centrifuged and resuspended in 50 µl of FITC-conjugated anti-BrdU Antibody (Cat. 556028, BD Pharmingen, San Diego, CA, USA), which was diluted 1:5 with 1% BSA/0.01% Triton X-100/PBS. After centrifugation and washing with 500 µl 0.01% (v/v) Triton X-100 in PBS, cells were incubated for 1 h at 37°C with 250 µl of 25 µg/ml Propidium Iodide (PI) (Abcam, Cambridge, UK) in 0.01% (v/v) Triton X-100/PBS with 10 µg/µl RNaseA (Qiagen, Hilden). Sample was centrifuged again and stained cells were resuspended in 500 µl 0.01% (v/v) Triton X-100 in PBS. Flow cytometry analysis was then performed with FACS Calibur (BD, Franklin Lakes, NJ, USA). 10.000 cells per sample were counted analyzed via Kaluza Analysis 1.3.

2.2.2.8 Immunofluorescence staining

Cellular proteins were visualized via indirect immunofluorescence staining by using a specific primary antibody, recognizing the appropriate antigen, and a secondary antibody conjugated to a fluorophore, which detects the primary antibody.

Therefore, cells were seeded and optionally transfected and/or treated and at appropriate time points fixed with Roti®-Histofix (4 % phosphate buffered formaldehyde solution; Roth, Karlsruhe) for 20 minutes at RT. After washing the cells 3x with PBS, the cellular membrane was permeabilized with 0.3 % (v/v) Triton X-100/PBS for 10 min at RT to allow antibodies access to intracellular antigens. For PCNA staining, permeabilization was performed with methanol for 10 min at -20 °C. After washing 3x with PBS, unspecific binding sites were blocked with 5 % (w/v) BSA/0.15 % (v/v) Triton X-100 in PBS for 30 min at RT. Afterwards, cells were incubated with the appropriate primary antibody (Table 7) diluted in blocking buffer for 1 h at RT or overnight at 4 °C. Cells were washed again 3x with PBS and the fluorophore-conjugated secondary antibody (Table 8) diluted in blocking buffer containing 0.5 µg/ml of the DNA staining dye Hoechst 33342 (Sigma-Aldrich, Steinheim) was added and incubated for 1 h at RT in the dark. After washing 3x with PBS, the cells were stored in 0.1 % (w/v) sodium azide/PBS at 4 °C until they were analyzed microscopically (section 2.2.2.12).

Optionally, an *in situ* protein extraction step prior to protein fixation can be conducted to remove excess non-chromatin-bound protein. Therefore, cells were treated for 5 min at 4 °C with CSK buffer (Table 1), washed with PBS and afterwards fixation was performed as mentioned above.

2.2.2.9 EdU incorporation and staining

To identify cells actively engaged in DNA replication, the Click-iT™ EdU Alexa Fluor™ Imaging Kits (section 2.1.10) were used according to the manufacturer's instructions. In this assay the thymidine analogue EdU (5-ethynyl-2'-deoxyuridine) is incorporated into the newly synthesized DNA strand and fluorescently labeled with an Alexa Fluor dye via a click chemistry reaction. Furthermore, the EdU labeling is compatible with antibody co-stainings or dyes that allows single cell immunofluorescene analysis of defined cell cycle phases. In brief, the cells were incubated with 10 µM EdU for 20 min before fixation and permeabilization (section 2.2.2.8). Afterwards cells were washed twice with 3 %(w/v) BSA/PBS and the Click-iT reaction cocktail was prepared, added and incubated for 30 min at RT, protected from light. The reaction cocktail was removed and the samples were washed once with 3 %(w/v) BSA/PBS. For co-staining the samples were incubated with primary antibodies and further processed as described in section 2.2.2.8.

2.2.2.10 DNA fiber assay

The DNA fiber assay can be employed to study the *in vivo* function of proteins in DNA replication at a single molecule level. This approach directly visualizes the progression of individual replication forks within living cells and hence provides quantitative information on various aspects of DNA synthesis, such as replication fork speed by elongating/ongoing forks, fork stalling or collapsing, new initiation events by origin firing and fork termination (Figure 11 A).

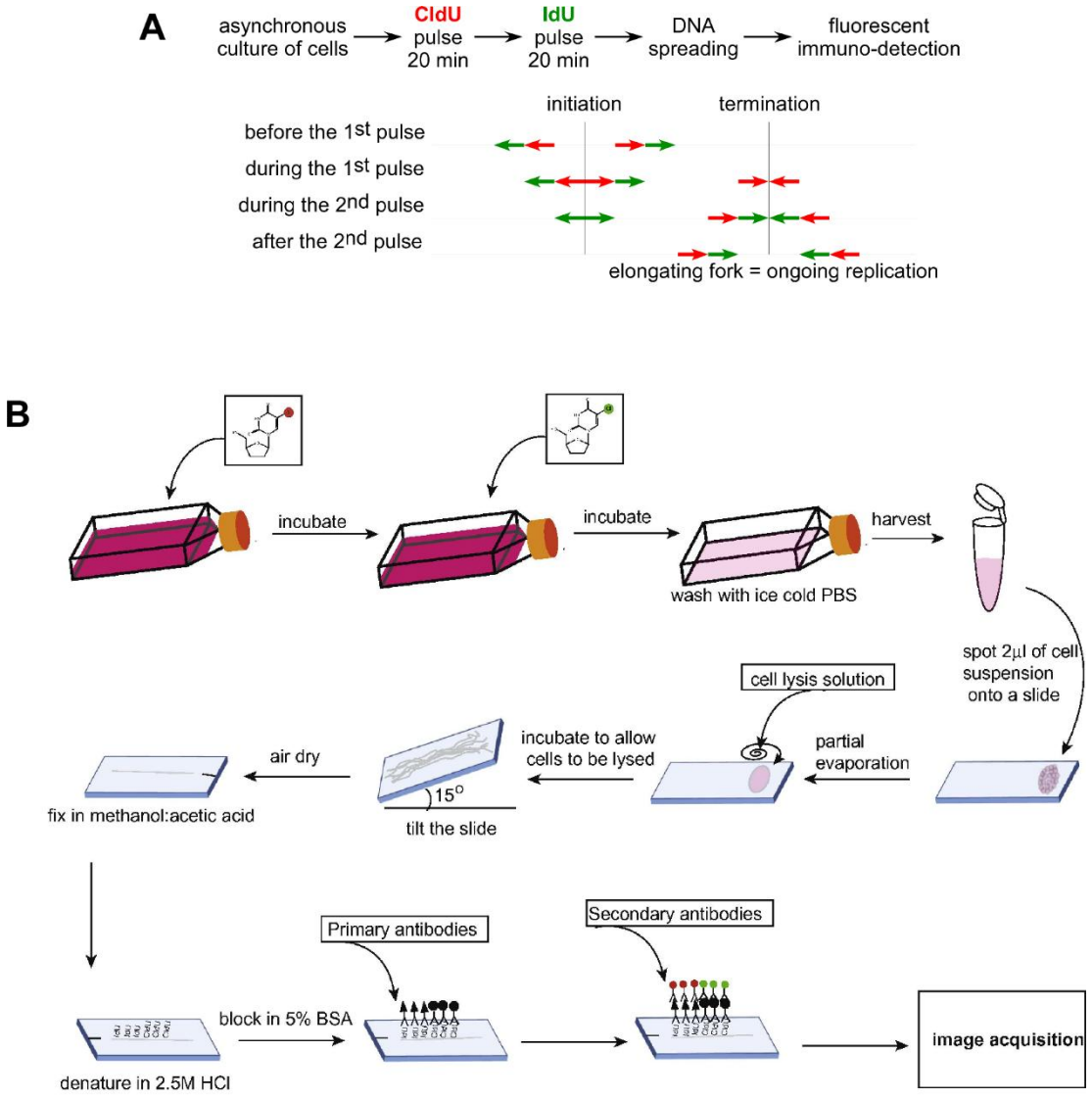

Figure 11: The DNA fiber assay.

A) Asynchronously growing cell cultures are sequentially labeled by two consecutive pulses of CldU and IdU. This allows recognition of elongating forks, initiation and termination events. Red and green arrows represent newly synthesized DNA labeled with CldU or IdU, respectively. The labeling pattern differs depending on when during the consecutive pulses the respective event occurs.(Schröder, 2014; doctoral thesis) **B)** Schematic showing DNA fiber assay technique protocol (see text for details) (Nieminuszczy et al., 2016).

Exponentially growing cells, seeded in a well of a 6-well plate were initially pulse-labeled with the first thymidine analogue. Chlorodeoxyuridine (CldU) was added to the cell culture in a final concentration of 25 µM and the cells were incubated 20 min under normal growth conditions. Thereafter, iododeoxyuridine (IdU) was added in a final concentration of 250 µM (excess of IdU makes removal of CldU needless), and the cells were again incubated for 20 min under normal growth conditions. After double labeling, cells were trypsinized, pelleted (300 xg, 5 min, 4 °C) and washed twice with ice-cold PBS. The cell pellet was resuspended in a small volume of cold PBS (0.25–0.5 ml), the cells were counted and diluted to a final concentration of 5x 10^5 cells/ml in cold PBS and kept on ice. 2 µl of the cell suspension were spotted on the top of 5 uncoated microscope slides and air–dried for 5-7 min until the drop was sticky but not completely dry. Subsequently, 7 µl of spreading buffer (200 mM Tris-HCl pH 7.4, 50 mM EDTA, 0.5 % (w/v)

SDS) are applied on top of the cell suspension, then mixed by gently stirring with a pipette tip and incubated for 2 min. Following cell lysis, slides were tilted slightly (approximately to 15°) and the drops were allowed to run down the length of the glass slide and to spread the DNA fibers along the slide. Once dried, the DNA spreads were fixed by incubating the slides for 10 min in a 3:1 solution of methanol/acetic acid in a glass staining jar. The slides were dried and stored at 4 °C. For the immunostaining of the incorporated halogenated thymidine analogs, the slides were initially washed twice with H_2O for 5 min in a glass staining jar. The dsDNA was denatured by covering the glass slides with 2.5 M HCl for 75 min in a staining tray. Afterwards, the slides were rinsed twice with PBS, washed twice with blocking solution (PBS, 1 % BSA, 0.1 % Tween 20) for 5–10 min each and then incubated in blocking solution for 30–60 min. Excess blocking solution was removed with a paper towel and slides placed horizontally in a humidified chamber. Subsequently, 115 µl of an antibody mix of a rat α-BrDU (dilution: 1:1000; Clone BU1/75 (ICR1); AbD Serotec, MCA2060GA) and a mouse α-BrdU (dilution: 1:500; Clone B44; BD Bioscience, Franklin Lakes, NJ, USA (347580)) in blocking solution was added, covered with a large coverslip and incubated for 1 h at RT. After coverslips are removed by gently moving down the slide without applying force, slides were rinsed 3x with PBS and fixed for 10 min in 4 % paraformaldehyde (PFA). Slides were rinsed again 3x with PBS and then washed 3x with blocking solution for 1, 5 and 25 min. 115 µl of a mix of secondary antibodies (α-rat coupled with AF568 and α-mouse with AF488) in blocking solution were added, covered with large coverslip and incubated for 1.5–2 h protected from light. After removing the coverslips, slides were rinsed twice with PBS, washed 3x with blocking solution for 1, 5 and 25 min and again rinsed twice with PBS. Finally, they were mounted by using FluorSave™ reagent (Calbiochem/Merck, Schwalbach) and stored at -20 °C. The stained DNA fibers were visualized microscopically with a Leica SP5 confocal laser scanning microscope or a Nikon Ti Eclipse Epi (section 2.2.2.12). The length of stained fibers was measured using ImageJ software and with the help of the conversion factor of 2.59 kb/µm of DNA fiber the replication fork speed (kb/min) was determined.

2.2.2.11 Proximity ligation assay

The Duolink proximity ligation assay is an antibody-based assay that detects protein–protein interactions occurring within 40 nm of each other (Figure 12). Protein targets in fixed cells were recognized by primary antibodies. Secondary antibodies, called PLA probes PLUS and MINUS, bind to the primary antibodies. Each of the PLA probes has a short DNA strand attached to it. If the two target proteins are in close proximity, which means under 40 nm, or in a protein-protein complex, the DNA strands are ligated with hybridized connector oligos to form a complete DNA circle. Next, the oligonucleotide arm of the PLA probes acts as a primer for a rolling circle amplification using the ligated circle as template. Fluorescent-labeled oligonucleotides hybridize to the amplification product and the resulting fluorescent spot is visible in the fluorescence microscope.

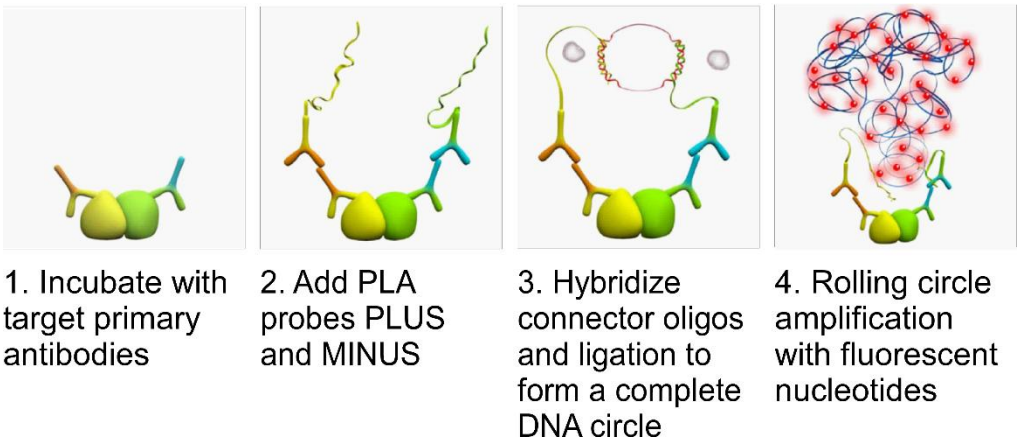

Figure 12: Principle of the Proximity Ligation Assay.
Primary antibodies bind to specific protein targets. Secondary antibodies have nucleotide tails. Connector oligos only hybridize if both proteins are closer than 40 nm. Ligation of the complex forms a circular template. After rolling circle amplification, added fluorophore-coupled oligonucleotides are incorporated resulting in a microscopically point-shaped signal. Modified from (Duolink In Situ-Fluorescence User Manual 2018)

Proximity ligation assay was carried out using a Duolink *in situ* PLA kit (section Kits2.1.10), following the manufacturers protocol. Briefly, cells were seeded in 3 cm microscopic glass bottom dishes (MatTek Corporation, Ashland, MA, USA) and incubated for 24 hours in the corresponding medium. Cells were washed 3 times with PBS, fixed with Roti®-Histofix (4 % phosphate buffered formaldehyde solution; Roth, Karlsruhe) for 20 minutes at RT, washed again 3x with PBS and permeabilized with ice-cold methanol for 20 min at -20 °C. After washing 3x with PBS, dishes were then blocked with 5 % (w/v) BSA/0.15 % (v/v) Triton X-100 in PBS for 30 min at 37 °C and incubated for 1 h in a humidified chamber at RT with primary antibodies diluted in blocking buffer. Same dilutions of primary antibodies were used as in immunofluorescence stainings (see section 2.1.7). Duolink® In Situ PLA probes Anti-Rabbit PLUS and Anti-Mouse MINUS (Sigma-Aldrich, Steinheim) were added after 3x washing with PBS and incubated for 1 hour at 37°C. Cells were washed again 3x with PBS and Ligation solution was added, followed by incubation for 30 minutes at 37°C. Amplification was carried out after washing 3x with PBS for 100 minutes at 37°C. DNA was stained with 10 µg/ml Hoechst33342 dye in PBS for 10 min at RT. After washing with PBS, dishes were stored with 0.1 % (w/v) sodium azide/PBS at 4 °C over night. Cells were observed with a confocal laser scanning microscope (section 2.2.2.12).

2.2.2.12 Fluorescence microscopy

For immunofluorescence imaging cellular proteins were visualized either indirectly by labeled fluorophore-coupled secondary antibodies or directly by overexpressed proteins via their fluorescence-tag. Imaging was performed either with an epifluorescence or a confocal microscope. The former detects the overall fluorescence emitted by the specimen while the latter uses point illumination by focused laser beams to excite the sample and out-of-focus light is eliminated by a pinhole in front of the detector thereby increasing the optical resolution. The epifluorescence microscope, Nikon Ti Eclipse Epi microscope (Nikon GmbH, Düsseldorf) was

only used for DNA fiber assay analysis after hesperadin treatment. In all other cases, the Leica TCS SP5 or SP8 confocal laser scanning microscopes (Leica Mikrosysteme Vertrieb GmbH, Wetzlar) were used.

2.2.3 Biochemistry

2.2.3.1 Preparation of whole cell lysates from eukaryotic cells

Whole cell extracts were prepared with a RIPA buffer (Table 1) to lyse eukaryotic cells. Detachment of cells from cell culture dish or flask were achieved by scraping the cells off or trypsinizing. The cell suspension was centrifuged with 500 xg for 5 min at 4 °C and the cell pellet was washed with ice-cold PBS and resuspendend in the appropriate amount of RIPA lysis buffer (100-150 µl for 10 cm cell culture dish) and incubated for 30 min on ice. After incubation, the cells lysate was sonicated (15 s at 95 % amplitude) using Sonoplus mini20 device. Cell debris was removed by centrifugation 15000 xg for 20 min at 4 °C and the supernatant was transferred into a new reaction tube. The protein concentration was determined as described in section 2.2.3.3. Lysates were mixed with 5x SDS sample buffer (Table 1), denatured for 5min at 95 °C and stored at -20 °C before they were used in SDS-PAGE (section 2.2.3.6) and western blotting (section 2.2.3.7).

2.2.3.2 Subcellular fractionation

For stepwise separation and preparation of cytoplasmic, membrane, nuclear soluble, chromatin-bound and cytoskeletal protein extracts from mammalian cultured cells the Subcellular Protein Fractionation Kit for Cultured Cell (Table 13) was used. It was conducted according to the manufacturer's protocol. The first reagent added to a cell pellet causes selective cell membrane permeablization, releasing soluble cytoplasmic contents. The second reagent dissolves plasma, mitochondria and ER/golgi membranes but does not solubilize nuclear membranes. After recovering the intact nuclei by centrifugation, a third reagent yields the soluble nuclear extract. A second nuclear extraction with micrococcal nuclease is performed to release chromatin-bound nuclear proteins. The recovered insoluble pellet is then extracted with the final reagent to isolate cytoskeletal proteins. The subcellular extracts can be further analyzed via SDS-PAGE (section 2.2.3.6) and western blotting (section 2.2.3.7).

2.2.3.3 Determination of protein concentration

The protein concentration was determined using the colorimetric Bradford assay, a rapid and sensitive method for the quantification of microgram quantities of protein (Bradford, 1976). It is based on the binding of Coomassie brilliant blue dye to arginine, tryptophan, tyrosine, histidine and phenylalanine residues of proteins. 800 µl PBS are mixed with 200 µl of the 5x concentrated Bio-Rad protein assay dye reagent (Bio-Rad, Munich) and 1-2 µl sample lysate in a disposable cuvette by vortexing. After incubation of 5-60 min at RT, the absorption at a wavelength of 595 nm was measured with a BioPhotometer Plus and compared to a standard curve defined by concentrations of bovine serum albumin (BSA).

2.2.3.4 Co-immunoprecipitation with µMACS magnetic beads

The co-immunoprecipitation (co-IP) was used to investigate protein-protein-complexes. Therefore, 293T cells were plated on a 10 cm culture dish and transfected one day later with two plasmids coding for two differently tagged proteins. 16-24 h after transfection, the cells were lysed in 1 ml Jiang IP buffer (section 2.1.2) on ice for 30 min and additionally sonificated 3x 15 s. Afterwards the lysate was centrifuged for 20 min at 4 °C with 14.000 rpm. 50 µl supernatant was mixed with 15 µl 5x SDS sample buffer and heated to 95 °C for 5 min and serve as input sample. The remaining supernatant was mixed with 50 µl of antibody-coupled magnetic beads from the µMACS isolation kit (section2.1.10) and incubated on ice for 30 min. The mix was transferred to a µ column, which was prior to this placed in a magnetic µMACS separator and equilibrated with 200 µl Jiang IP buffer. After the sample flow through, the µ column was washed with 100 µl Jiang IP buffer, 300 µl wash buffer 1, 2x with 200 µl wash buffer 1 and 100 µl wash buffer 2 (wash buffer 1 and 2 from the kit). For elution of proteins, first 20 µl, and after a 5 min incubation, further 50 µl of elution buffer heated to 95 °C were applied. The eluted samples were collected and as well as the input samples subjected to SDS-PAGE (section 2.2.3.6) and western blotting (section 2.2.3.7).

2.2.3.5 Co-immunoprecipitation with Protein A magnetic beads

The co-immunoprecipitation (co-IP) was used to investigate protein-protein-complexes. Therefore, 293T cells were plated on a 10 cm culture dish and transfected one day later with two plasmids coding for two differently tagged proteins. 16-24 h after transfection, the cells were lysed in 500 µl IP lysis buffer (section 2.1.2) on ice for 10 min. Afterwards the lysate was centrifuged for 15 min at 4 °C with 16.000 xg. 25 µl supernatant was mixed with 6.5 µl 5x SDS sample buffer and heated to 95 °C for 5 min and serves as input sample. The remaining supernatant was mixed with antibody-coupled magnetic beads and incubated for 1 h at 4 °C. Prior to mixing the magnetic beads with the sample, 50 µl of Protein A magnetic Sure Beads™ (BioRad Laboratories Inc., Hercules CA, USA) were washed with 300 µl IP lysis buffer and placed in the SureBeads™ magnetic rack (BioRad Laboratories Inc., Hercules CA, USA) and the buffer was removed from magnetic beads. The washed magnetic beads were incubated with 2.5 µl anti-GFP antibody (GTX 113617, GeneTex Inc., Irvine, CA, USA) in 300 µl IP lysis buffer for 1.5 h at 4 °C followed by 2 washing steps with 300 µl IP lysis buffer. The antibody-loaded beads, incubated with supernatant of the sample, were washed with 500 µl ice-cold IP lysis buffer, for 3 min at 4 °C at 650 rpm. Afterwards beads were washed 2x with 500 µl ice-cold IP wash buffer (section 2.1.2). Supernatant was removed and 45 µl of 2x SDS sample buffer was added to the magnetic beads and heated to 95 °C for 5 min and subjected to SDS-PAGE (section 2.2.3.6) and western blotting (section 2.2.3.7).

2.2.3.6 SDS-polyacrylamide gel electrophoresis

For analytical separation of proteins based on their molecular weight, SDS-PAGE (sodium dodecylsulphate-polyacrylamide gel electrophoresis) was performed according to the standard method of Laemmli (1970). The polyacrylamid gel was prepared as summmerized in Table 17. First the resolving gel was cast and coated with isopropanol and after polymerization,

isopropanol was removed and the stacking gel was poured over the resolving gel. A comb was inserted to generate wells. Subsequently, 20-50 µg total protein of protein lysates (section 2.2.3.1) was loaded into a well. The SDS-PAGE was carried out in SDS running buffer first at 100 V and when samples had passed the stacking gel at 140 V. For molecular mass determination, the Spectra Multicolor Broad Range Protein Ladder (Thermo Fisher Scientific, Waltham, MA, USA) was used as the size standard.

Table 17: Composition of polyacrylamide gels of 1.5 mm thickness.

	resolving gel				2 stacking gels (4 %)
	7.5 %	**10 %**	**12.5 %**	**15 %**	
ddH_2O	4.3 ml	3.6 ml	2.9 ml	2.0 ml	2.5 ml
4x SDS resolving gel buffer	2.4 ml	2.4 ml	2.4 ml	2.4 ml	-
4x SDS stacking gel buffer	-	-	-	-	1.35 ml
30 % (v/v) acrylamide	2.3 ml	1.6 ml	2.1 ml	2.5 ml	650 µl
10 % (w/v) APS	96 µl	96 µl	96 µl	96 µl	50 µl
TEMED	10 µl	10 µl l	10 µl	10 µl	5 µl

In contrast to single-concentration gels, gradient gels can resolve a much wider size range of proteins on a single gel but are mostly more difficult to cast with a gradient forming apparatus. Here, a simpler method was used based on pipetting and mixing of two concentrations of resolving gels. Thus, gradient gels were cast with a higher concentration of acrylamide at the bottom than the top. Therefore, the low concentrated (4 %) stacking gel solution (Table 18) was soaked up into a pipette and afterwards the high concentrated (20 %) stacking gel solution (Table 18) was absorbed. Then the pipette was hold in a 45° angle and the solutions were mixed by inserting a single bubble into the pipette. The bubble went up in the pipette and then the gel was poured very slowly.

Table 18: Composition of 4-20 % polyacrylamide gradient gels of 1.5 mm thickness.

	resolving gel		2 stacking gels (4 %)
	4 %	**20 %**	
ddH_2O	3.0 ml	345 µl	2.5 ml
4x SDS resolving gel buffer	1.3 ml	1.3 ml	-
4x SDS stacking gel buffer	-	-	1.35 ml
30 % (v/v) acrylamide	0.7 ml	3.3 ml	650 µl
10 % (w/v) APS	50 µl	50 µl	50 µl
TEMED	5 µl	5 µl	5 µl

2.2.3.7 Western blotting

After separation of protein mixtures by SDS-PAGE (section 2.2.3.6), the proteins were transferred to a polyvinylidene difluoride (PVDF) membrane. Before transfer, the Amersham Hybond PVDF membrane (GE Healthcare Life Sciences, Freiburg) was briefly activated in 100% methanol and then equilibrated together with the gels and six slightly larger pieces of Rotilabo®-blotting paper (Roth, Karlsruhe) in transfer buffer (section 2.1.2). All equilibrated components were stacked in a semidry apparatus or in a wet-blot chamber. Electrophoresis was run for 18 h at 120 mA and 4 °C or for 1,5 h at 400 mA at RT. Afterwards, the membrane was placed into a blocking solution of 5 % (w/v) milk powder/TBST or 5 % (w/v) BSA/TBST for 30 min to block unspecific binding sites. Furthermore, the membrane was incubation with primary antibodies (section 2.1.7) overnight at 4 °C or for 1 h at RT. After incubation with the primaryantibodies, the membrane was washed three times with TBST for 5 minutes and then incubated for 1 h at RT with HRP (horseradish peroxidase)-coupled secondary antibodies (section 2.1.7). This was followed by washing the membrane twice for 5 min each with TBST and once with TBS for additional 5 min. Detection of HRP activity was performed via chemiluminescence with Pierce™ ECL Plus Western Blotting Substrate and SuperSignal™ West Femto Maximum Sensitivity Substrate (section 2.1.10) according to the manufacturer's instructions. Signals were caught on X-ray film and developed using the film processor CAWOMAT 2000 IR (section 2.1.3). For quantification of signal intensities the software ImageJ (section 2.1.4) was used. To remove bound antibodies from membranes and allow further immunodetection, ReBlot Plus strong antibody stripping solution from Millipore (Schwalbach) was used according to the instructions of the manufacturer.

2.2.3.8 iPOND

To understand the process of replication, chromatin assembly and replication stress response requires the ability to monitor protein dynamics at active replication forks. Here a procedure to isolate proteins on nascent DNA (iPOND) that permits a spatiotemporal analysis of proteins at replication forks or on chromatin following DNA replication in cultured cells was used.

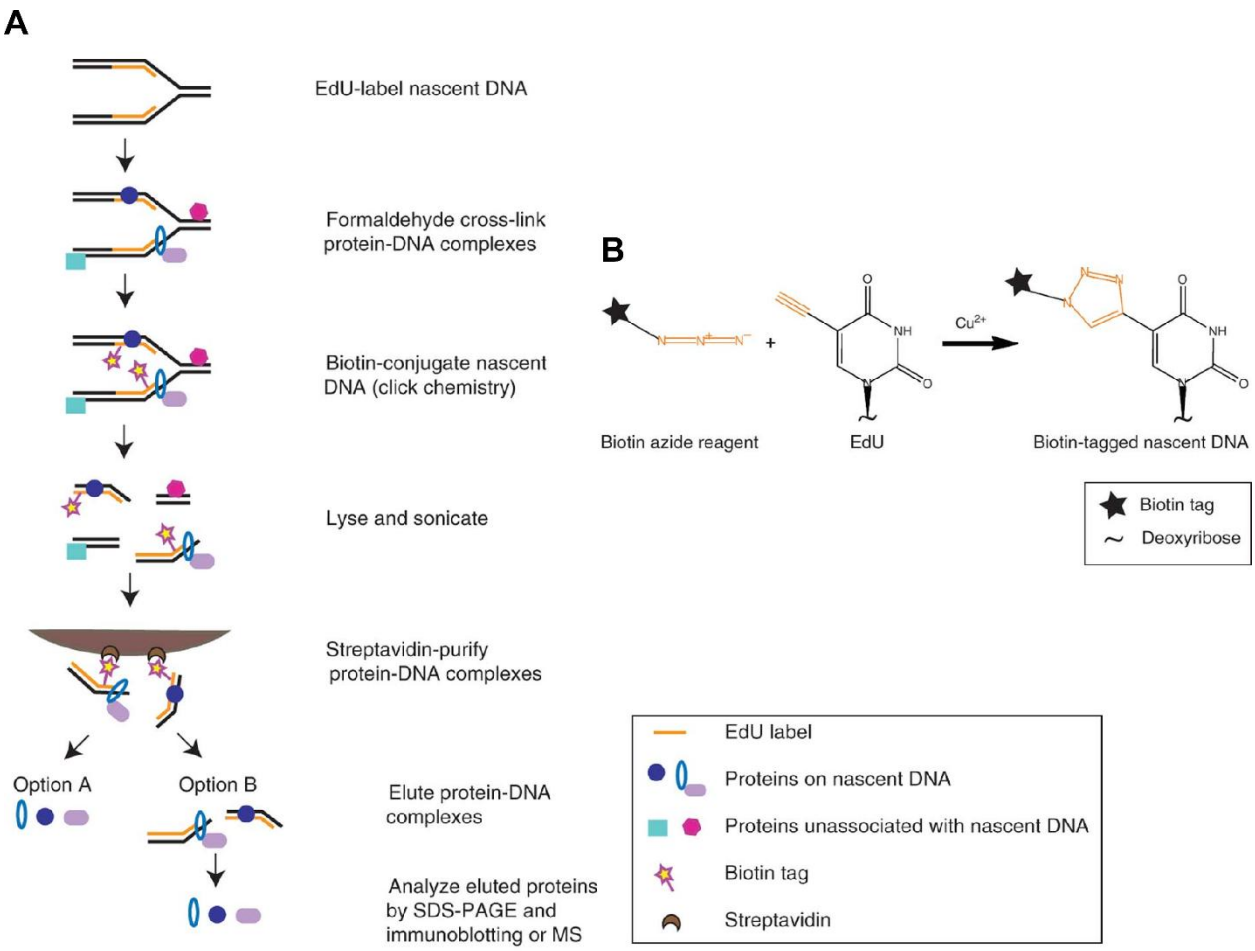

Figure 13: The iPOND.

A) Schematic overview of the iPOND procedure. Cells were pulse labeled with EdU, a nucleoside analog of thymidine, to label nascent DNA *in vivo*. The cells are then fixed with formaldehyde, which stops DNA replication and crosslinks protein-DNA complexes. A click reaction in the presence of copper to conjugate biotin to EdU is completed in detergent permeabilized cells. Cells are then lysed in denaturing conditions and sonication completes the DNA fragmentation producing solubilized DNA-protein complexes. Streptavidin-coated beads purify the nascent, EdU-labeled DNA-protein complexes. Finally, the proteins are eluted from the complexes for analysis by SDS-PAGE and immunoblotting or mass spectrometry. **B)** Click chemistry addition of biotin tags to nascent DNA. EdU contains an alkyne functional group that permits copper-catalyzed cycloaddition (click chemistry) to a biotin azide to yield a stable covalent linkage. Orange color represents the functional groups involved in the click chemistry reaction. Figures A and B adapted from Sirbu et al. (2012).

The iPOND was performed as described in Sirbu et. al. (Sirbu et al., 2012). 293T cells were labeled with 10 µM EdU (Thermo Fisher Scientific, Waltham, MA, USA) for 20 min. Next, the cells were crosslinked with 1 % formaldehyde for 20 min, permeabilized for 30 min in permeabilization buffer and then incubated for 2 h in click reaction buffer. Cells were resuspended in lysis buffer and sonicated for 45 min consisting of 20 s pulse time with an amplitude of 90 % and a pause duration of 30 s. Samples were centrifuged for 10 min at 16,000x g and an aliquot of supernatant was kept as loading control. Afterwards supernatants were incubated 16 h at 4 °C with streptavidin coupled agarose beads (Merck Millipore, Darmstadt)). The beads were washed in lysis buffer and 1 M NaCl and then incubated in 2x SDS sample buffer for 25 min at 95 °C. Alternatively, cells were incubated with thymidine for 20 or 40 min after EdU pulse labeling and the iPOND was performed as described above.

2.2.4 Quantitative data analysis

2.2.4.1 Analysis of the Proximity Ligation Assay with ImageJ

For interaction analysis performed with Proximity Ligation Assays, images were processed with ImageJ. PLA was performed as described in section 2.2.2.11 and images were taken with a Leica TCS SP5 Confocal laser scanning microscope**.** Cell nuclei were identified with ImageJ as described in Figure 14 using images of Hoechst-stained cells. Afterwards images of cells with PLA signals were used to determine the number of PLA signals per nucleus (Figure 14) by dividing the “raw integrated density” values by the “max grey value”.

macro: nuclei

```
run(“8-bit”);
run(“Smooth”);
run(“Gamma...”, “value=0.40");
run(”Median...“, “radius=4");
run(”Gaussian Blur...“, “sigma=4");
setOption(”BlackBackground“, false);
run(”Make Binary“);
run(”Watershed“);
run(”Analyze Particles...“, “size=0.2-Infinity circularity=0.30-1.00 show=Nothing display exclude clear add”);
```

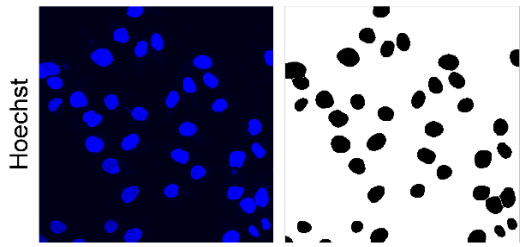

macro: foci

```
run(“8-bit”);
run(“Invert”);
run(“Smooth”);
run(“Subtract Background...”, “rolling=50 light”);
run(“Gamma...”, “value=1.30");
run(”Convolve...“, “text1=[-1 -1 -1 -1 -1\n-1 -1 -1 -1 -1\n-1 -1 30 -1 -1\n-1 -1 -1 -1 -1\n-1 -1 -1 -1 -1\n] normalize”);
setOption(“BlackBackground”, false);
run(“Make Binary”);
run(“Find Maxima...”, “noise=0 output=[Single Points] light”);
roiManager(“Show None”);
roiManager(“Show All”);
roiManager(“measure”);
```

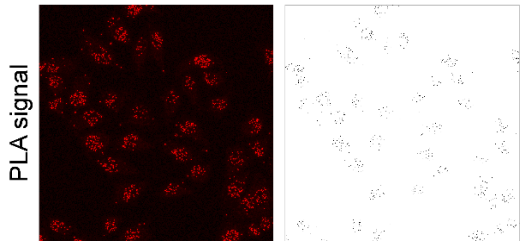

Figure 14: Analysis of the PLA with ImageJ.

ImageJ was used to define nuclei with macro nuclei based on cells stained with Hoechst. PLA signals were identified with the macro foci. The number of foci per nucleus was determined. Images were taken with a Leica TCS SP5 Confocal laser scanning microscope.

2.2.4.2 Analysis of the Proximity Ligation Assay with CellProfiler

Alternativley, PLA intensities were not only evaluated with ImageJ (section 2.2.4.1) but als with CellProfiler. Microscopic images were taken with a Leica TCS SP8 Confocal laser scanning microscope. Image evaluation was performed by Dr. Nina Schulze from the Imaging Centre Campus Essen using CellProfiler. Nuclei visualized by Hoechst staining were defined as primary objects and mean intensities of PLA signals for each EdU positive nuclei was evaluated.

2.2.4.3 Analysis of other immunofluorescence images with CellProfiler

The cells were stained according to section 2.2.2.8 and microscopic images were taken with a Leica TCS SP8 Confocal laser scanning microscope. Image evaluation was performed by Dr. Nina Schulze from the Imaging Centre Campus Essen using CellProfiler. Nuclei visualized by Hoechst staining were defined as primary objects and the standard deviation of mean intensities was evaluated.

3 Results

Cancer is one of the leading causes of death and emerges from genomic instabilities. Mitosis and replication are the two major processes to maintain the genomic integrity by faithful duplication of the genome followed by dividing the chromosomes equally to the progeny cells. So far, a plethora of functions for the chromosomal passenger complex (CPC) has been identified in mitosis (section 1.5.2.1). In contrast to the localization and according functions of the CPC during mitosis, the function of the CPC during interphase is still poorly understood (section 1.5.2.2). Thus, it is of utmost importance to understand the underlying mechanisms to improve cancer therapies.

3.1 Characterization of CPC localization during the cell cycle

3.1.1 Co-localization of CPC members with PCNA throughout S phase

To analyse the localization of Survivin during interphase, exponentially growing WI-38 cells were immunostained using antibodies specific for Survivin and PCNA. PCNA, a central component of the replication machinery, shows a typical distribution pattern in S phase (Leonhardt et al., 2000; Nakamura et al., 1986; O'Keefe et al., 1992). PCNA is distributed at replication sites throughout the nucleoplasm during early S phase (Figure 15). As S phase continues, PCNA foci are concentrated around the nucleoli as well as in peripheral areas of the nucleus. In late S phase, these foci increase in size but decrease in number and often resemble characteristic ring or horseshoe-like structures. In accordance with the typical distribution pattern of PCNA, cells could be assigned to the specific cell cycle stage. Survivin was already expressed in early S phase and formed nuclear foci. While some of these Survivin foci were in close proximity or co-localized with PCNA, most of them seem not to be related to PCNA. Only in late S phase, the majority of Survivin foci co-localized with PCNA, but there were still some separate foci of either Survivin or PCNA. At the subsequent G_2 phase, Survivin expression and localization was similar to the pattern observed in late S phase.

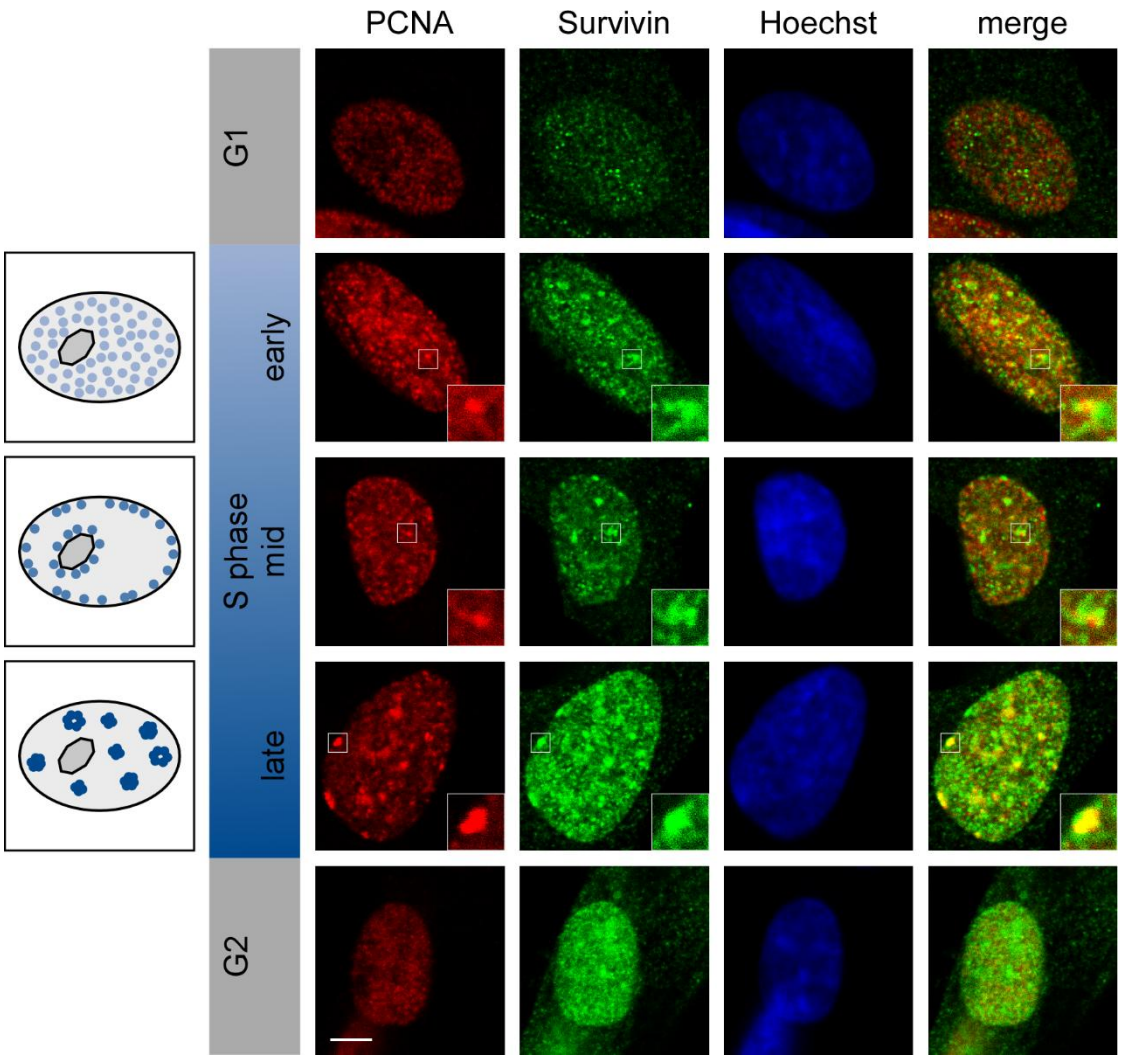

Figure 15: Survivin is expressed during interphase and co-localizes with PCNA.
WI-38 cells were fixed, permeabilized and immunostained with Survivin- (AF488, green) and PCNA- (AF568, red) specific antibodies. DNA was stained with Hoechst (blue). Images were taken with a Leica SP5 confocal laser scanning microscope. Scale bar: 5 µm. The insets show higher magnifications of the areas outlined in the main panels. Left: Schematic representation of replication sites during S phase.

Survivin plays an essential role in apoptosis regulation as a monomer (Pavlyukov et al., 2011), although it is known that Survivin monomers homodimerize in solution (Chantalat et al., 2000; Muchmore et al., 2000). However, to fulfill its mitotic function Survivin acts in a complex with Borealin, INCENP and Aurora B (Ruchaud et al., 2007). Thus, it should be investigated if other CPC members, e.g. the kinase Aurora B, are also present in distinct replication foci like Survivin.

WI-38, HeLa and A431 cells were immunostained with specific antibodies against Aurora B and PCNA (Figure 16). In all tested cell types, Aurora B was located in the nucleus during S phase and formed foci also mostly co-localized or in close proximity to PCNA. Since both, Survivin and Aurora B co-localized with PCNA, it can be assumed that they indeed act as a complex.

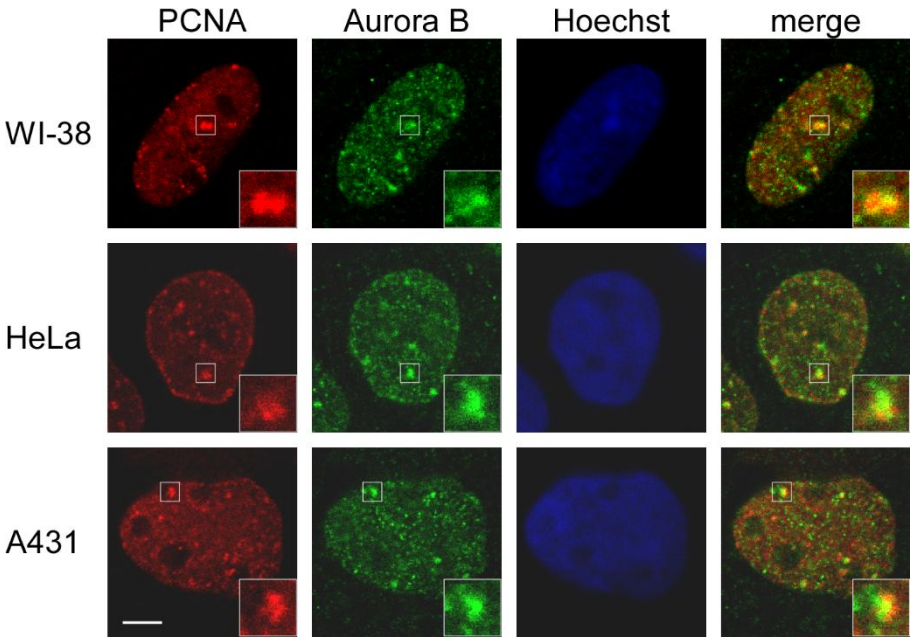

Figure 16: Aurora B also co-localizes with PCNA.
WI-38, HeLa and A431 cells were fixed, permeabilized and immunostained with Aurora B- (AF488, green) and PCNA- (AF568, red) specific antibodies. DNA was stained with Hoechst (blue). Images were taken with a Leica SP5 confocal laser scanning microscope. Scale bar: 5 µm. The insets show higher magnifications of the areas outlined in the main panels.

Although it was demonstrated, that Survivin formed foci throughout S phase (Figure 15), mechanistic insights on the spatio-temporal process of foci formation was still lacking. Therefore, time-lapse studies should reveal if Survivin is firmly anchored in the nucleus and persists throughout S phase or if its distribution changes by assembly and disassembly. In order to track the formation of Survivin foci throughout the cell cycle and compare it to PCNA expression and localization, a particular fluorescent chromobody, specifically recognizing PCNA, was used. The advantage of this technique is that endogenous PCNA can be fluorescently visualized without causing artificial effects in replication, as it can occur after overexpression of proteins.

A431 cells stably expressing Survivin-GFP were transfected with a plasmid coding for the PCNA chromobody (pCCC) and time-lapse microscopy was performed. Cells were imaged at 35 different positions every 9 min during a 20 h period. Images of one position spanning a period of 9.5 h are depicted in Figure 17.

PCNA, visualized by the RFP-tagged chromobody, displayed the characteristic distribution pattern throughout S phase and was otherwise diffusely distributed in the nucleus of G_1 and G_2 phase cells or the cytoplasm during mitosis. In contrast, Survivin was only detectable during mitosis and not during interphase. In all other positions examined, the cells either migrated too fast to visualize the whole cell cycle, were not transfected with pCCC or died during the examination (data not shown). Therefore, the experiment needs to be improved to obtain further evidence regarding the spatial and temporal regulation of Survivin foci formation throughout the cell cycle.

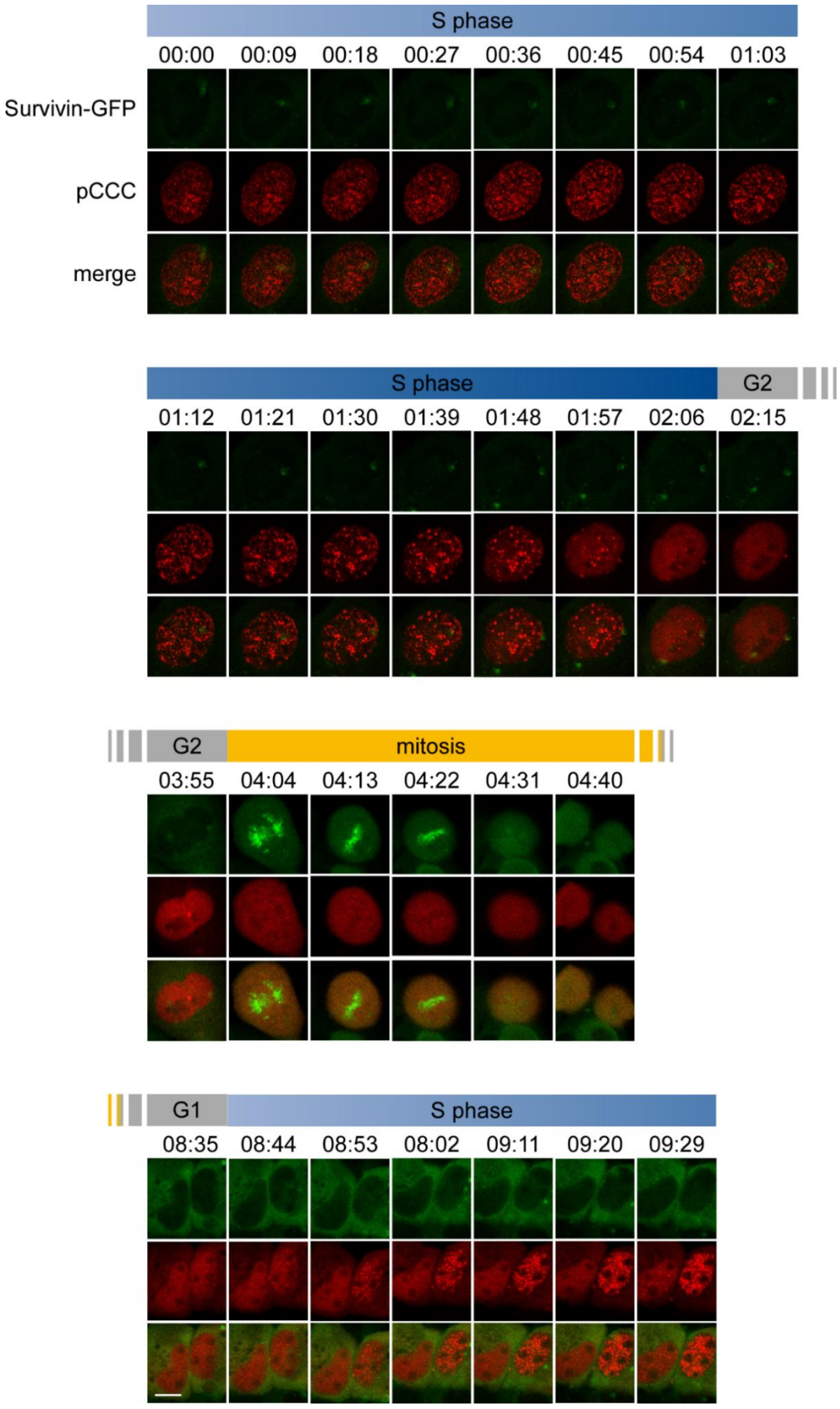

Figure 17: Visualization of Survivin-GFP localization during the cell cycle.

A431 cells stably expressing Survivin-GFP (green) were transfected with pCCC (red). Time-lapse live cell imaging was performed 24 h after transfection with a Leica TCS SP5 confocal laser scanning microscope. Cells were imaged every 9 min during a period of 20 h. Scale bar: 10 µm.

3.1.2 CPC localization during replication at heterochromatic regions

The replication of the genome is a spatio-temporally highly organized process. The temporal organization is defined by the alteration of the characteristic pattern of replicating protein complexes associated with early, mid and late S phase as described above for PCNA (Fox et al., 1991; Leonhardt et al., 2000; Nakamura et al., 1986). The spatial order of replication reflects the higher organization of the genome. During early S phase, euchromatin is replicated followed by facultative heterochromatin during mid S phase, while constitutive heterochromatin is replicated mainly during late S phase (O'Keefe et al., 1992). Especially during late S phase, when the constitutive heterochromatin is replicated, Survivin co-localized with PCNA. Thus, the CPC should be analyzed relative to the chromatin status. A key property of heterochromatin is its association with heterochromatin protein 1 (HP1). HP1 consists of two domains. The N-terminal chromo domain (CD) binds to H3K9me2/3 and a C-terminal chromo shadow domain (CSD) interacts with PxVxL motifs in a diverse set of proteins (Maison and Almouzni, 2004; Nozawa et al., 2010; Smothers and Henikoff, 2000; Thiru et al., 2004). In interphase, HP1 CD binds to H3K9me2/3, which mediates the binding of HP1α to centromeres (Hayakawa et al., 2003). This interaction is disrupted during mitosis by Aurora B-mediated phosphorylation of H3S10, which releases most HP1 from chromatin (Fischle et al., 2005; Hirota et al., 2005). However, HP1α CSD can bind to a PxVxL motif in INCENP, maintaining a small pool of HP1α at centromeres in mitosis (Ainsztein et al., 1998; Kang et al., 2011; Nozawa et al., 2010). In addition, HP1 CSD binds to CAF1 (chromatin assembly factor 1), a factor that is implicated in histone deposition during DNA replication, which in turn interacts with PCNA (Murzina et al., 1999; Quivy et al., 2004).

In brief, the co-localization of PCNA and CPC members in late S phase, when heterochromatin is replicated might suggest a possible link between HP1, PCNA and the CPC during replication. To corroborate this hypothesis, A431 and HeLa cells were co-transfected with plasmids coding for GFP-HP1α and Survivin-tdTomato and fixed 24 h later (Figure 18 A). Survivin-tdTomato was located in the cytoplasm and formed nuclear foci. These Survivin foci co-localized with GFP-HP1α foci in interphase. As overexpression of exogenous proteins can be responsible for alterations in protein localization and cell physiology, and to exclude that the protein tags had an effect on protein localization and function, endogenous INCENP and HP1α were immunostained in parallel (Figure 18 B). Both proteins accumulated in nuclear foci in WI-38, HeLa and U2OS cells. In addition, INCENP foci also co-localized with HP1α-positive chromatin regions.

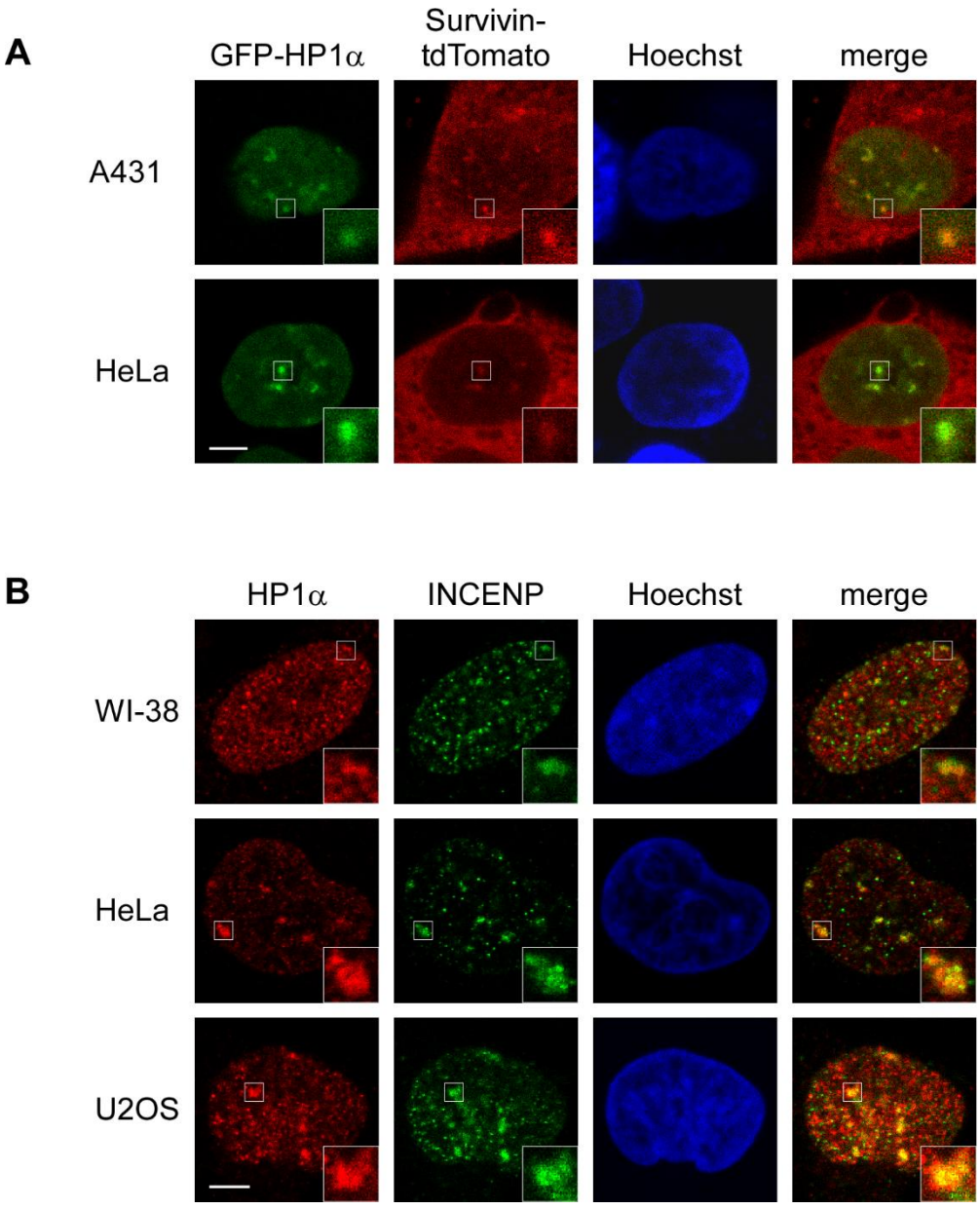

Figure 18: CPC members co-localize with HP1α.

A) A431 and HeLa cells were co-transfected with plasmids coding for eGFP-HP1α (green) and Survivin-tdTomato (red). The cells were fixed 24 h after transfection and DNA was stained with Hoechst (blue). **B)** WI-38, HeLa and U2OS cells were fixed, permeabilized and immunostained with HP1α- (AF568, red) and INCENP- (AF488, green) specific antibodies. DNA was stained with Hoechst (blue). **A, B)** Images were taken with a Leica TCS SP5 confocal laser scanning microscope. Scale bar: 5 µm. The insets show higher magnifications of the areas outlined in the main panels.

Both overexpressed and endogenous CPC proteins co-localized with heterochromatin in interphase cells. To identify whether this also holds true specifically for S phase cells, U2OS cells were transfected with GFP-HP1α and 24 h later immunostained for Aurora B and the replication protein PCNA (Figure 19).

PCNA accumulated at replication sites, surrounding one nucleolus (magnifications in Figure 19), and several foci were distributed throughout the nucleus indicating that the cells resided in mid S phase. GFP-HP1α and Aurora B were similarly localized surrounding the nucleolus like PCNA

but both proteins accumulated in additional foci in the nucleus that did not coincide with PCNA foci.

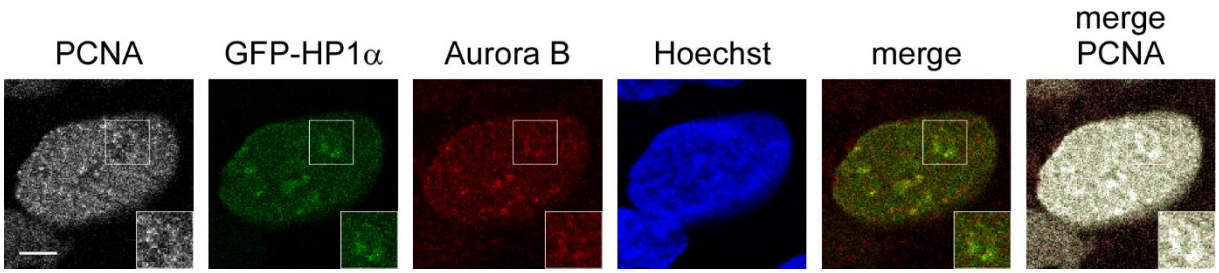

Figure 19: Aurora B and HP1α co-localize in S phase cells.

U2OS cells were transfected with plasmids coding for eGFP-HP1α (green). The cells were fixed 24 h after transfection, permeabilized and immunostained with PCNA- (AF633, white) and Aurora B- (AF568, red) specific antibodies. DNA was stained with Hoechst (blue). Images were taken with a Leica TCS SP5 confocal laser scanning microscope. Scale bar: 5 µm. The insets show higher magnifications of the areas outlined in the main panels.

As mentioned above, the different subtypes of heterochromatin, constitutive and facultative heterochromatin, are replicated at different stages throughout S phase. Although both are replicated in the second half of S phase, the facultative heterochromatin is replicated earlier than the constitutive. The latter is formed at telomeres, centromeres and repetitive elements. In order to gain more insight whether the CPC accumulates in distinct heterochromatic regions, the CREST anti-centromere autoimmune serum was used to visualize specifically centromeric regions (Figure 20).

Immunofluorescence staining of A431, HeLa and U2OS cells revealed that Aurora B accumulated in foci where CREST-positive signals were present. Particularly for HeLa and U2OS cells Aurora B foci not only co-localized with CREST signals but also protruded from CREST signals.

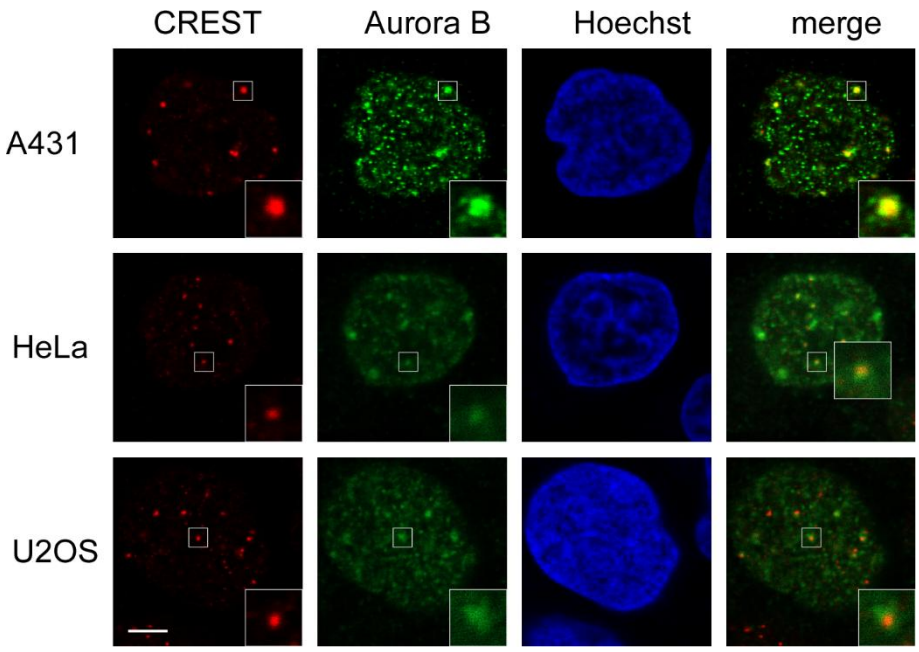

Figure 20: Aurora B foci are located at centromeric heterochromatin.

A431, HeLa and U2OS cells were fixed, permeabilized and immunostained with CREST immunserum (AF568, red) specific for centromeres and Aurora B- (AF488 or AF633, green) specific antibody. DNA was stained with Hoechst (blue). Images were taken with a Leica TCS SP8 confocal laser scanning microscope. Scale bar: 5 µm. The insets show higher magnifications of the areas outlined in the main panels.

To confirm the localization of Aurora B at centromeres during replication, cells were co-stained with replication markers. A431 cells incorporated EdU for 20 min into nascent DNA, which was later visualized by EdU-specific staining combined with CREST and Aurora B staining (Figure 21 A). Replication sites were detected at the nuclear periphery and some larger accumulations distributed through the nucleus, corresponding to a cell in transition from mid to late S phase. Aurora B was detectable in three types of nuclear localizations, first at each CREST signal, second, at some replication sites and third in solitary foci without EdU or CREST staining.

Additionally, mouse NIH3T3 cells were immunostained for PCNA, CREST and Aurora B (Figure 21 B). Characteristic for this cell type are clusters of chromatin, called chromocenters, which can be identified as Hoechst-dense domains. Centromeres comprise two adjacent chromatin domains. The centric domain serves as the site of kinetochore formation and the surrounding pericentric heterochromatin (PHC) domain contributes to the cohesion of sister chromatids (Alonso et al., 2010; Bernard et al., 2001; Guenatri et al., 2004). In NIH3T3 interphase cells, pericentric heterochromatin forms large spots, which co-localize with the Hoechst-dense clusters and the centric chromatin appears at the periphery of the clusters as several individual spots (Guenatri et al., 2004). CREST immunserum detects centromere proteins (CENP), which are mainly located at the kinetochore thus the centric domain.

As expected, Hoechst staining allowed to detect chromocenters as large spots and CREST signals appeared at their periphery. Replication sites, visualized by PCNA staining, were determined at the chromocenters. Aurora B was also located at the chromocenters. On closer inspection of the magnifications, PCNA, CREST and Aurora B could be detected in close proximity to each other, and mostly PCNA and Aurora B co-localized at chromocenters. Taken

together, these observations reinforce the hypothesis that the CPC is located at centromeric heterochromatin during replication.

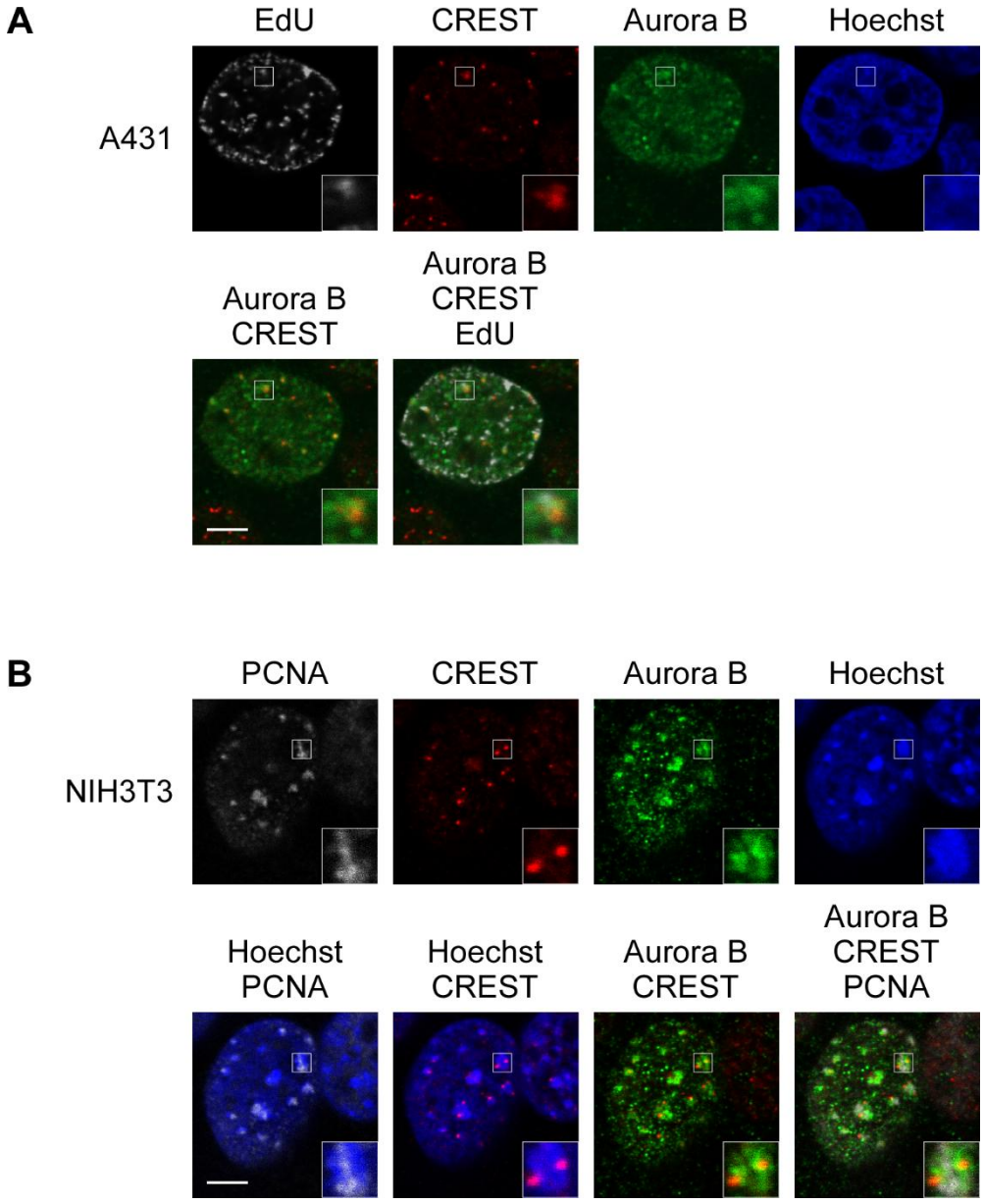

Figure 21: Aurora B foci are located at centromeric heterochromatin during replication.
A) 10 µM EdU was incorporated for 20 min before fixation to visualize replicating A431 cells via Click-iT™ Kit (AF-488, white) and cells were co-stained for Aurora B (AF633, green) and centromeres (CREST, AF568, red). DNA was stained with Hoechst (blue). **B)** NIH3T3 cells were co-stained with PCNA (AF633, white)-, Aurora B (AF488, green)- and centromere (CREST, AF568, red)-specific antibodies. Images were taken with a Leica TCS SP8 Confocal laser scanning microscope. Scale bar: 5 µm. The insets show higher magnifications of the areas outlined in the main panels.

3.2 Interactions of CPC proteins

So far, it was demonstrated here, that the chromosomal passenger complex is already expressed in S phase and accumulates in foci, which partially co-localize with replication protein PCNA. This co-localization takes place preferentially during late S phase when constitutive heterochromatin is replicated. The CPC could also be located to heterochromatic structures during replication, more precisely to centromeres via HP1α and centromeric co-localization.

3.2.1 Isolation of CPC on nascent DNA

In order to address the question if the CPC is bound to the replisome via PCNA or to heterochromatin, an iPOND assay (section 2.2.3.8) was established in collaboration with the bachelor student Sarah Maurer. This method permits a high-resolution spatiotemporal analysis of proteins at replication forks or on chromatin following DNA replication in cultured cells (Sirbu et al., 2012). The spatial and temporal resolution achieved with iPOND depends on EdU incubation time, the rate of DNA synthesis, and chromatin fragment size. Therefore, the DNA fragment size before and after sonication was determined (section 2.2.3.8). 293T cells were resuspended in lysis buffer, sonicated and the DNA was separated via agarose gel electrophoresis (Figure 22 B).

The DNA of the non-sonicated sample was nearly completely retained in the loading pocket of the agarose gel, only little amounts of DNA were separated by gel electrophoresis as a smear. In contrast, sonication lead to a DNA fragment size smaller than 300 bp.

To perform the iPOND, 293T cells were incubated with EdU for 20 min (Figure 22 A). After cross-linking and labelling of EdU with Biotin using click chemistry, the samples were lysed and sonicated. Samples of 293T cells were taken before incubation with (Input) and after elution from (Eluate) streptavidin coated beads and were run on a 4–20 % gradient gel and immunoblotted. Membranes were probed with antibodies specific for histone H3, PCNA, Survivin and Aurora B (Figure 22 C).

To exclude unspecific protein binding to streptavidin beads, a control sample was treated with DMSO instead of Biotin-Azide (Click). Histone H3 serves as control for chromatin proteins and was indeed detected only in the Click eluate, but not in the DMSO control. PCNA, as a control for replication-associated proteins bound to the DNA, was observed similarly although it was not detectable in both input samples. Survivin appeared to be bound to nascent DNA, apparent by a faint band in the Click eluate. The other CPC member Aurora B was detected as faint bands in both input samples but could not be detected in the eluate. This could stem from an insufficient protein amount, as in comparison to the input-eluate ratio of Survivin, the amount of Aurora B in the input samples was considerably lower.

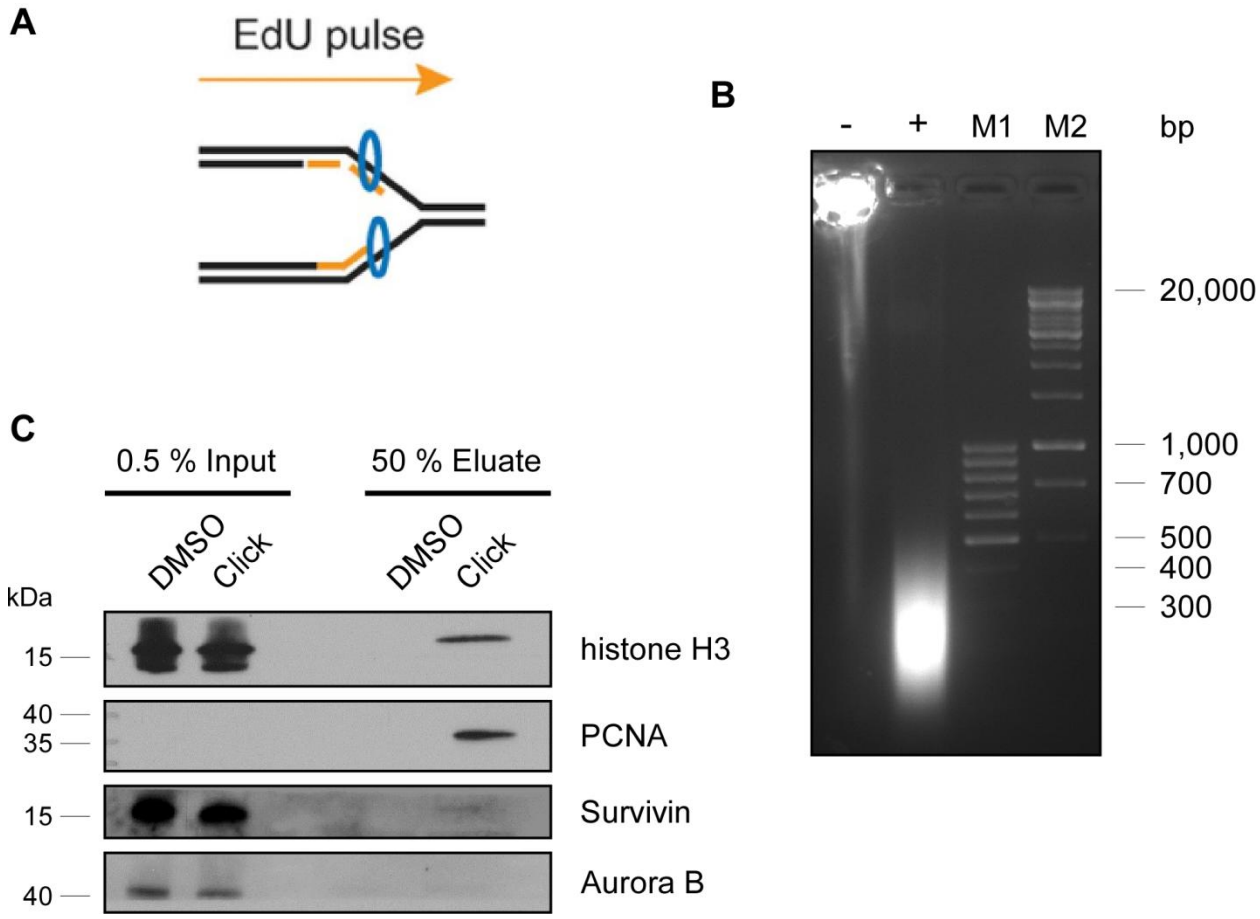

Figure 22: Survivin is bound to nascent DNA.

A) Schematic overview of the experimental procedure of the iPOND. 293T cells were treated with EdU for 20 min (yellow tracks), to label the nascent DNA *in vivo* prior to performing iPOND. After cross-linking and labelling of EdU with Biotin using click chemistry, the samples were lysed and sonicated. Figure adapted from (Sirbu et al., 2012). **B)** The DNA fragment size of 293T cells before and after sonication with an amplitude of 90% for 45 min, alternating between 20 s pulse time and no pulse for 40 s was detected via agarose geleletrophoresis. The Fragment size can be determined based on the sizes of the DNA ladder (M1: 100 bp gene ruler and M2: 1 kb plus gene ruler). **C)** iPOND samples of 293T cells were taken before incubation with (Input) and after elution from (Eluate) streptavidin coated beads and were run on a 4–20% gradient gel and immunoblotted. Membranes were probed with antibodies specific for histone H3, PCNA, Survivin and Aurora B. Histone H3 serves as control for chromatin- and PCNA as control for replication-associated proteins. To exclude unspecific protein binding to streptavidin beads a control sample was treated with DMSO instead of Biotin-Azide (Click)

With this, it could be shown, that Survivin is bound to the newly synthesized DNA strand in the vicinity of the replisome, but whether this link is provided through an interaction with the chromatin or with replication proteins remains to be elucidated. To address this, the iPOND was performed in combination with a subsequent thymidine chase (Figure 23 A). The continuous presence of EdU labels the fork itself and a growing area behind the fork as incubation time continues. The following thymidine pulse chase initially labels only the fork, but with continuing chase time the EdU labeled region will be located at further away from the fork as it progresses on the DNA helix. The advantage of this additional pulse-chase technique is that the changing patterns of proteins present during replication itself, and then later as chromatin is reconstructed around the newly synthesized DNA can be examined. The iPOND was performed in 293T cells

as described previously but with an additional pulse chase of thymidine for 20 or 40 min after EdU labelling (Figure 23 B).

In the absence of click chemistry (DMSO), no proteins were isolated from nascent DNA. Chromatin bound histone H3 was detectable in all eluate samples similarly, independent of the duration of the thymidine chase. PCNA was enriched specifically at the replication fork (0 min chase), but not on nascent DNA further away from the replication fork (20 min or 40 min chase), representative for a replisome associated protein. However, none of the CPC members could be detected in any of the eluate samples. In consequence, this experiment so far allows no definite conclusion whether the CPC members are associated with chromatin or replication proteins.

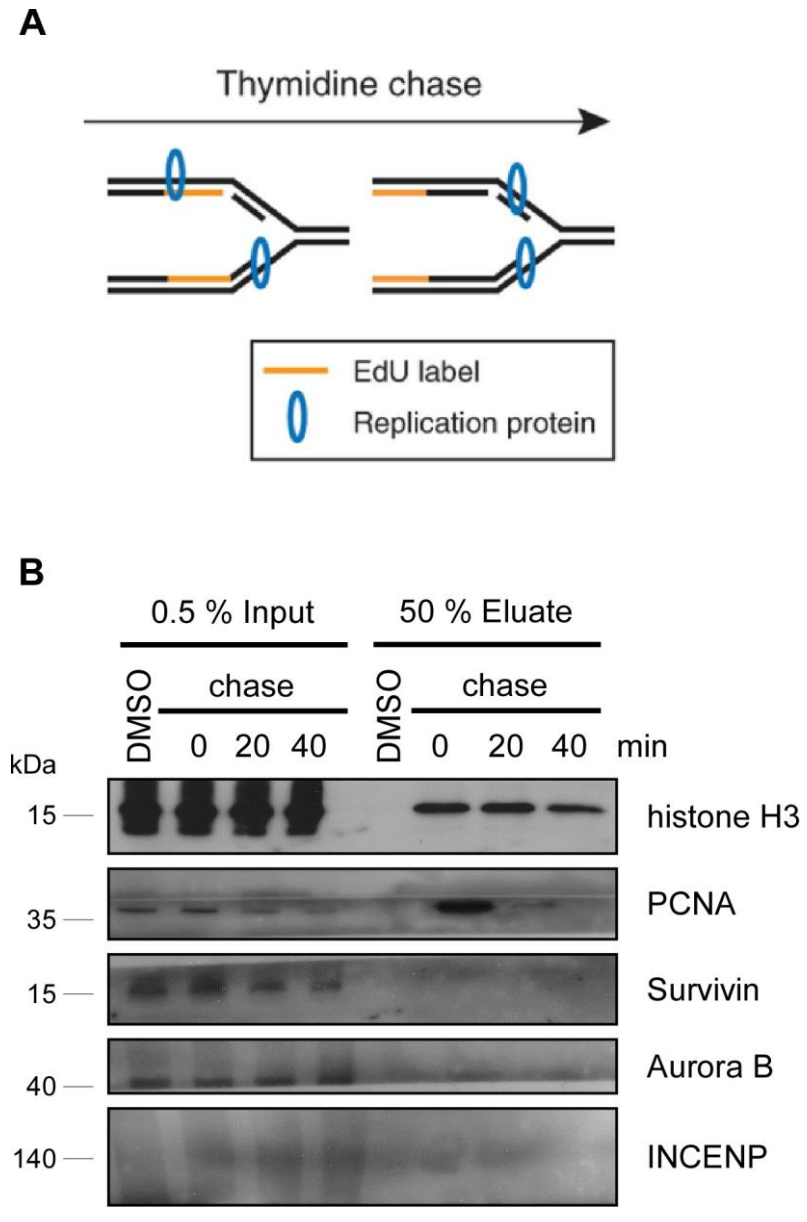

Figure 23: Analysis of CPC members by iPOND with thymidine chase.

A) Schematic overview of the experimental procedure of the iPOND followed by a subsequent thymidine chase. 293T cells were treated with EdU for 20 min (yellow tracks), to label the nascent DNA *in vivo* prior to performing iPOND followed by thymidine chase with different durations. Figure adapted from (Sirbu et al., 2012). **B)** 293T cells were treated with EdU for 20 min followed by a thymidine chase for 20 or 40 min. iPOND samples were taken before incubation with (Input) and after elution from (Eluate) streptavidin coated beads and were run on a 4–20% gradient gel and immunoblotted. Membranes were probed with

antibodies specific for histone H3, PCNA, Survivin, Aurora B and INCENP. Histone H3 served as control for chromatin- and PCNA as control for replication-associated proteins. To exclude unspecific protein binding to streptavidin beads, a control sample was treated with DMSO instead of Biotin-Azide.

3.2.2 Interactions of the CPC with PCNA

The iPOND revealed that the CPC is bound to replication sites, supporting the data from the localization studies, but whether the CPC is bound to the replisome member PCNA or to heterochromatin proteins still needs to be clarified. In initial experiments to determine the potential interaction of CPC proteins with PCNA, the *in situ* PLA technology was applied (section 2.2.2.11). Initially, HeLa cells were fixed, permeabilized and unspecific binding sites were blocked. Incubation with primary antibodies was carried out under the same conditions as usual immunofluorescence staining. Secondary antibodies, which have a nucleotide tail, were incubated with the samples. During a ligation step, two circle-forming DNA oligonucleotides and the nucleotide tails were ligated, and the DNA circle was amplified. Fluorescently labeled complementary oligonucleotide probes bound to the DNA can then be visualized microscopically as fluorescent dots. The number of PLA signals per nucleus was determined using ImageJ as detailed in section 2.2.2.11 (Figure 24).

The number of PLA signals per nucleus of PCNA together with DNA Ligase I, a known interaction partner of PCNA, served as positive control (dark blue bars). Here, significantly more PLA signals were detected than in the negative control samples (light blue bars), which were only incubated with a single primary antibody and both PLA probes. In each interaction analysis of the respective CPC member together with PCNA, a significant number of PLA signals per nucleus was detected (yellow bars), indicating an interaction.

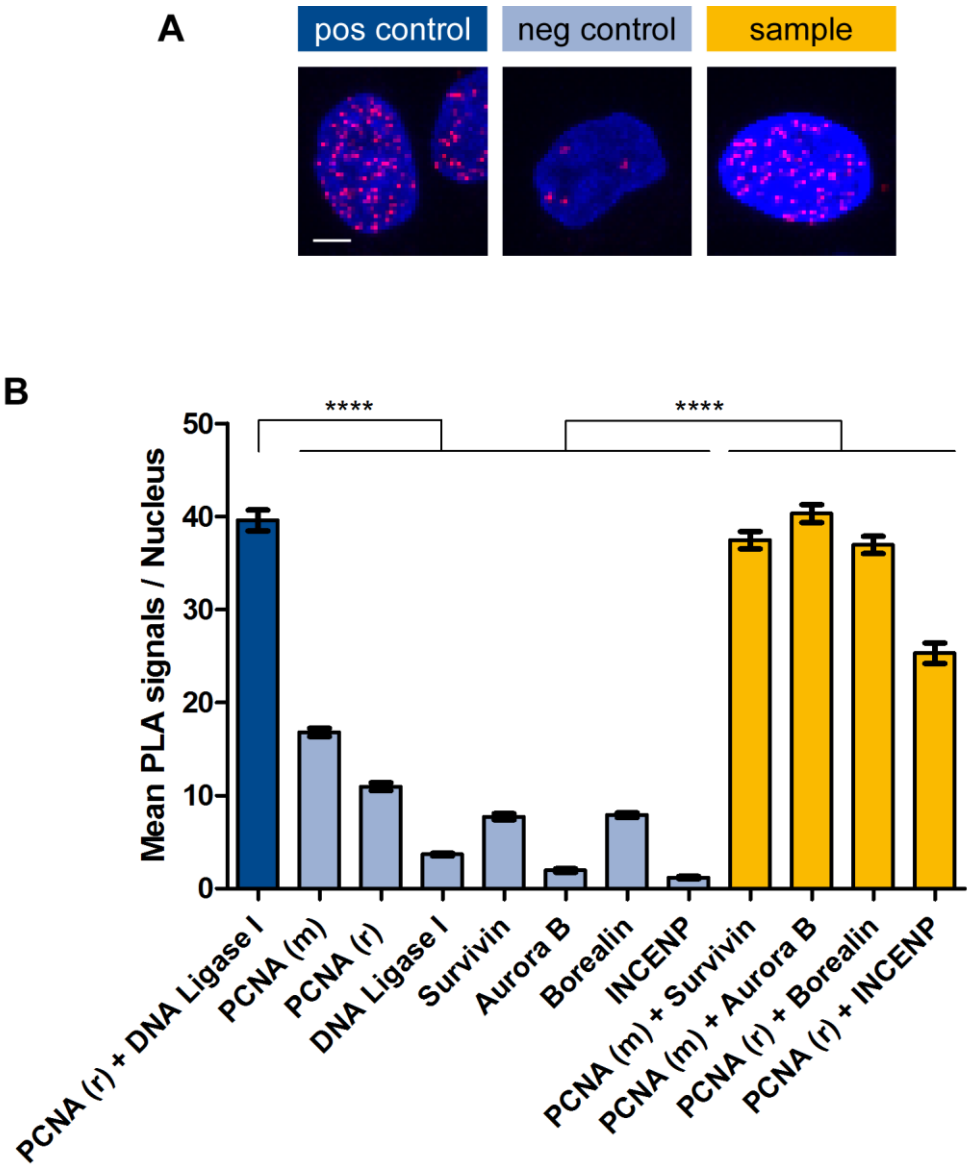

Figure 24: CPC proteins interact with PCNA analyzed by Proximity Ligation Assay.

A) HeLa cells were fixed, and a Proximity Ligation Assay was performed as described in section 2.2.2.11. Images were taken with a Leica TCS SP5 confocal laser scanning microscope. Scale bar: 5 µm. Representative images are shown. Each red spot represents a single PLA interaction signal. DNA was stained with Hoechst (blue). **B)** Number of PLA signals per nucleus from 165 cells were quantified with ImageJ. Bar graphs represent means ± SEM of a positive control (dark blue), negative controls (light blue) and interaction samples (yellow). Two-tailed unpaired t-test was performed, **** $p < 0.0001$.

Next, the interaction between PCNA and the CPC should be confirmed by co-immunoprecipitation. 293T cells were co-transfected with GFP-PCNA or an empty vector, together with Survivin-HA, Aurora B-HA, Borealin-HA or myc-INCENP, respectively (Figure 25). Lysates were immunoprecipitated (section 2.2.3.4) with µMACS magnetic beads coupled to a GFP-specific antibody and immunoblotted. Membranes were probed with antibodies specific for HA-, GFP- or myc-tag (Figure 25).

Indeed, binding of Aurora B-HA, Borealin-HA and myc-INCENP to GFP-PCNA could be detected. Of note, a faint unspecific binding of myc-INCENP to GFP-coupled µMACS beads could also be detected. However, it was less intense than the interaction signal between myc-

INCENP and GFP-PCNA. In contrast, no binding between GFP-PCNA and Survivin-HA was observed although the amount of Survivin-HA in the input sample was higher than for the other CPC members.

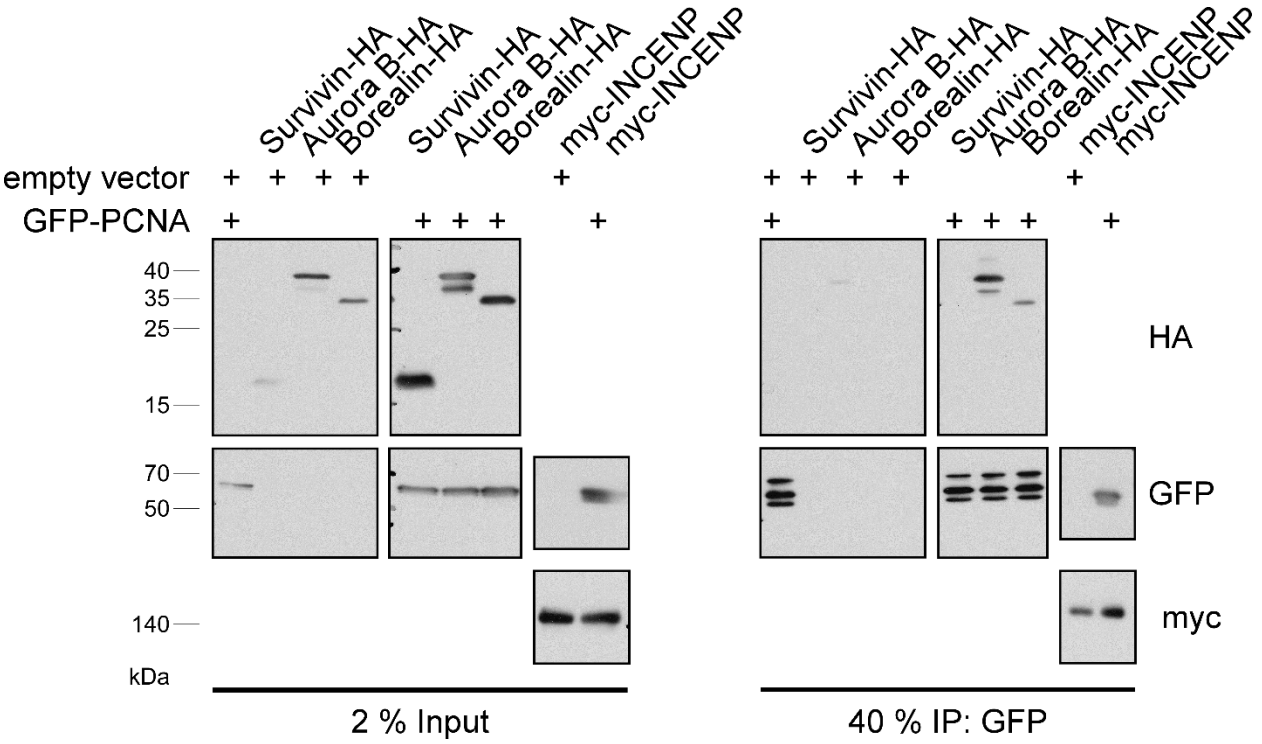

Figure 25: CPC proteins interact with PCNA analyzed by co-immunoprecipitation.

293T cells were co-transfected with GFP-PCNA or an empty vector, together with Survivin-HA, Aurora B-HA, Borealin-HA or myc-INCENP. Lysates were immunoprecipitated (IP) with magnetic beads coupled to a GFP-specific antibody and immunoblotted. Membranes were probed with antibodies specific for HA, GFP or myc.

These results show that PCNA interacts with members of the CPC, but it still needs to be elucidated which CPC protein is directly bound to PCNA. Most interactions with PCNA are mediated by an APIM (AlkB homolog 2 PCNA-interacting motif) or a PIP (PCNA-interacting protein) box motif in the interacting protein (Figure 26 A) (Gilljam et al., 2009; Warbrick, 2000). To investigate which CPC member mediates the direct interaction with PCNA, the amino acid sequences of each CPC member were searched for the consensus sequence of the APIM or the PIP box motif, respectively. A putative PIP box motif was found in the human protein INCENP, reaching from aa 853 to aa 860 (Figure 26 B) and thus located at its C-terminal part known to interact with Aurora B (Figure 26 D). This binding motif is also conserved in several INCENP homologs including chimpanzee (*P. troglodytes*), mouse (*M. musculus*) chicken (*G. gallus*) and frog (*X. tropicalis* and *X. laevis*) (Figure 26 C). This suggests that the recruitment of the CPC to replication sites might be mediated by direct interaction of INCENP with PCNA.

A

APIM motif: (K/R)-(F/Y/W)-(L/I/V/A)-(L/I/V/A)-(K/R)

PIP box motif: Q-x-x-(L/I/M)-x-x-(F/Y)-(F-Y)

B

```
   1 MGTTAPGPIH LLELCDQKLM EFLCNMDNKD LVWLEEIQEE AERMFTREFS  50
  51 KEPELMPKTP SQKNRRKKRR ISYVQDENRD PIRRRLSRRK SRSSQLSSRR 100
 101 LRSKDSVEKL ATVVGENGSV LRRVTRAAAA AAAATMALAA PSSPTPESPT 150
 151 MLTKKPEDNH TQCQLVPVVE IGISERQNAE QHVTQLMSTE PLPRTLSPTP 200
 201 ASATAPTSQG IPTSDEESTP KKSKARILES ITVSSLMATP QDPKGQGVGT 250
 251 GRSASKLRIA QVSPGPRDSP AFPDSPWRER VLAPILPDNF STPTGSRTDS 300
 301 QSVRHSPIAP SSPSPQVLAQ KYSLVAKQES VVRRASRRLA KKTAEEPAAS 350
 351 GRIICHSYLE RLLNVEVPQK VGSEQKEPPE EAEPVAAAEP EVPENNGNNS 400
 401 WPHNDTEIAN STPNPKPAAS SPETPSAGQQ EAKTDQADGP REPPQSARRK 450
 451 RSYKQAVSEL DEEQHLEDEE LQPPRSKTPS SPCPASKVVR PLRTFLHTVQ 500
 501 RNQMLMTPTS APRSVMKSFI KRNTPLRMDP KCSFVEKERQ RLENLRRKEE 550
 551 AEQLRRQKVE EDKRRRLEEV KLKREERLRK VLQARERVEQ MKEEKKKQIE 600
 601 QKFAQIDEKT EKAKEERLAE EKAKKKAAAK KMEEVEARRK QEEEARRLRW 650
 651 LQQEEEERRH QELLQKKKEE EQERLRKAAE AKRLAEQREQ ERREQERREQ 700
 701 ERREQERREQ ERREQERQLA EQERRREQER LQAERELQER EKALRLQKEQ 750
 751 LQRELEEKKK KEEQQRLAER QLQEEQEKKA KEAAGASKAL NVTVDVQSPA 800
 801 CTSYQMTPQG HRAPPKINPD NYGMDLNSDD STDDEAHPRK PIPTWARGTP 850
 851 LSQAIIHQYY HPPNLLELFG TILPLDLEDI FKKSKPRYHK RTSSAVWNSP 900
 901 PLQGARVPSS LAYSLKKH                                  918
```

C

```
                        PIP box
H. sapiens          853 QAIIHQYY 860
P. troglodytes      848 QAIIHQYY 855
M. musculus         817 QAIVHQYY 824
G. gallus           774 QAVIHQYY 781
X. tropicalis       834 QAIRQQYY 841
X. laevis           809 QAIRQQYY 816
```

D

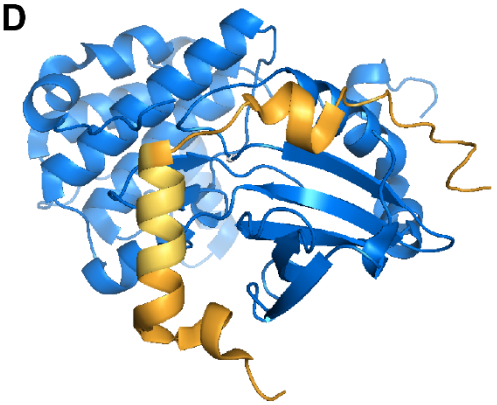

Figure 26: Sequence analysis revealed a conserved PIP box motif in INCENP.

A) Consensus sequences of APIM (AlkB homolog 2 PCNA-bind)- and PIP (PCNA-interacting protein)-binding motif. **B)** Amino acid sequence of human INCENP with the putative PIP box motif highlighted in yellow. **C)** Sequence alignments of the PIP box motif in INCENP homologs. Highly conserved residues are marked in yellow. Protein Accesssion numbers: Homo sapiens: NP_001035784.1; Pan troglodytes: XP_001151913.1; Mus musculus: NP_057901.2; Gallus gallus: NP_990661.1; Xenopus tropicalis: NP_001121150.1; Xenopus laevis: NP_001081890.1. **D)** Crystal structure of Aurora B (aa 55–344; blue) in complex with INCENP (aa 835–903; dark yellow) and its PIP box motif (aa 853–860; highlighted in light yellow). Protein Data Bank (PDB) code: 4AF3.

To verify the binding of INCENP to PCNA via its putative PIP box motif, the interaction should be inhibited by treatment with T2AA. T2AA is a small molecule that binds to a deep cavity of PCNA, which usually interacts with the PIP box in binding partners thereby inhibiting the interaction (Inoue et al., 2014; Punchihewa et al., 2012). A PLA was conducted as described in section 2.2.2.11, in combination with EdU incorporation into newly synthesized DNA visualized by the Click-iT^{TM} Kit (section 2.1.10) to detect replicating cells. HeLa cells were treated with 40 µM of PIP box inhibitor T2AA or as a control with DMSO for 4 h. During the last 30 min of inhibitor treatment, 10 µM EdU was added (Figure 27 A). Cells were fixed and permeabilized, EdU visualization was performed as well as PLA staining, using primary antibodies specific for INCENP and PCNA. Following secondary antibody incubation and amplification of ligated oligonucleotide templates, punctate fluorescent signals were detected by confocal microscopy and counted using CellProfiler only in EdU positive cells (Figure 27 B, C).

In negative controls, using single primary antibodies for PCNA or INCENP, fluorescent foci were rarely observed and the mean PLA signal intensity was low in replicating HeLa cells (Figure 27 B, C). When cells were incubated with both antibodies, mean PLA signal intensities per nuclei were 1.5-fold higher than in negative control samples. The decreased mean PLA signal intensities correlate also with lower EdU intensities (Figure 27 B) resulting from less EdU incorporation due to replication inhibition.

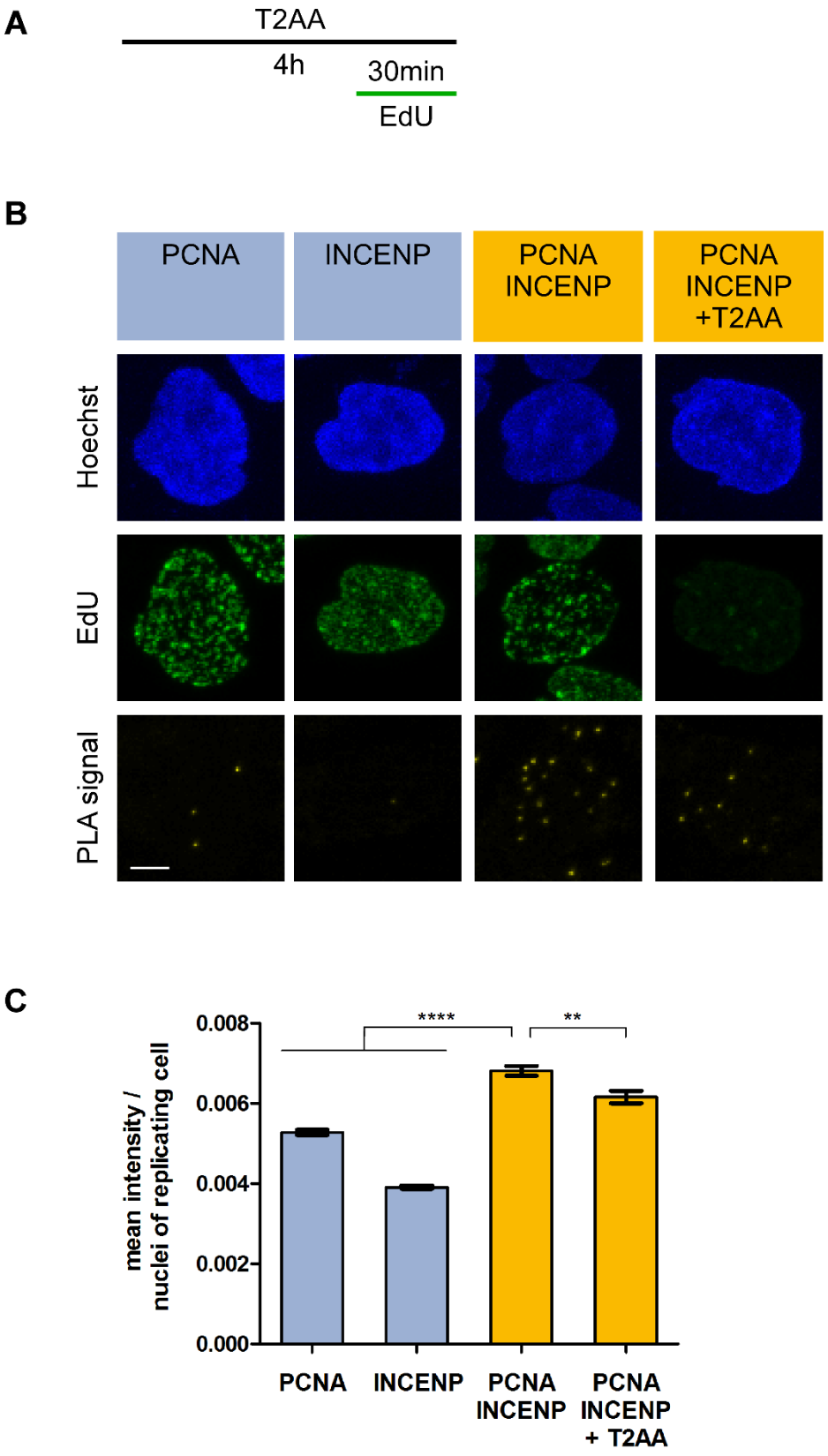

Figure 27: PIP box inhibitor T2AA inhibits interaction between PCNA and INCENP.

A) Schematic overview of cell treatment. HeLa cells were treated with 40 µM T2AA for 4 h. During the last 30 min of inhibitor treatment, EdU (10 µM) was to be incorporated in nascent DNA of replicating cells. **B)** After treatment as described in A, EdU (AF 488, green) was visualized via Click-iT™ Kit and PLA was performed using primary antibodies against PCNA and INCENP. For negative controls, only a single primary antibody was used, together with both PLA probes. Each yellow spot represents a single PLA interaction signal. DNA was stained with Hoechst (blue). Images were taken with a Leica TCS SP8

confocal laser scanning microscope. Scale bar: 5 µm. **C)** Mean intensity per nuclei of replicating cell was determined via Cell Profiler. Bar graphs represent means ± SEM of negative controls (light blue) and interaction samples (yellow).

To confirm the PIP box motif in INCENP as interaction site for PCNA binding, an INCENP-PIP mutant was designed and used in co-immunoprecipitation experiments. To generate the INCENP-PIP mutant, the pcDNA3.1-myc-INCENP plasmid was used as a template for site directed mutagenesis (section 2.2.1.1) with PCR primers bearing the mutations of glutamine 853, isoleucine 856, tyrosine 859 and tyrosine 860 to alanine (Figure 28 A). 293T cells were co-transfected with plasmids coding for GFP-PCNA and myc-INCENP wt or myc-INCENP PIPmut, as indicated. Lysates were immunoprecipitated (section 2.2.3.5) with Protein A magnetic beads coupled to a GFP-specific antibody (+ Ab) or with uncoupled beads (- Ab) and immunoblotted. Membranes were probed with antibodies specific for myc or PCNA (Figure 28 B).

Single transfection of GFP-PCNA, myc-INCENP wt or myc-INCENP PIPmut served as controls. As expected, GFP-PCNA was immunoprecipitated by GFP-coupled magnetic beads but not the two myc-INCENP variants. Co-transfection of GFP-PCNA either with myc-INCENP wt or with myc-INCENP PIPmut and precipitation with non-antibody coupled magnetic beads also served as negative controls. The negative controls showed unspecific binding of both INCENP variants to the beads. In the actual samples with anti-GFP coupled beads, myc-INCENP wt but not myc-INCENP PIPmut was detected in the GFP-PCNA immunoprecipitate.

The decrease of binding between GFP-PCNA and myc-INCENP due to the mutation of the PIP box motif is more prominent for the actual samples with GFP-coupled beads (6.6-fold) compared to the non-coupled beads (1.7-fold decrease), indicating a loss of the interaction due to the mutation of the PIP box motif.

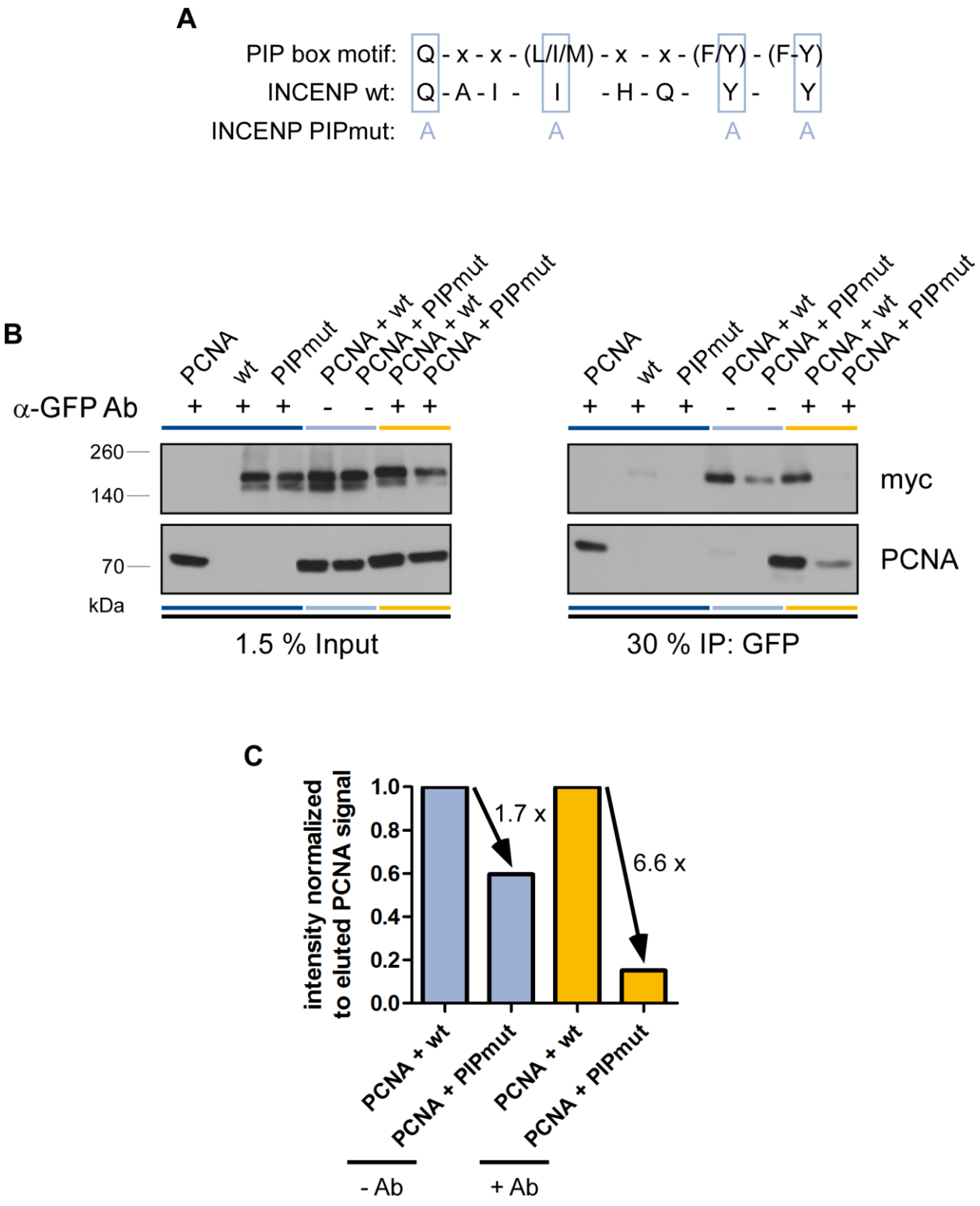

Figure 28: INCENP binds to PCNA via a PIP box motif.

A) Overview of the consensus sequence of a PIP box motif, the same motif in INCENP wildtype (wt) and the mutated (PIPmut) PIP box motif. The amino acids of the PIP box that have been mutated to Alanine (A in blue) are indicated in blue boxes. **B)** 293T cells were co-transfected with GFP-PCNA, myc-INCENP wt or myc-INCENP PIPmut as indicated. Single transfections are highlighted in dark blue. Lysates were immunoprecipitated (IP) with magnetic beads coupled to a GFP-specific antibody (yellow) or with uncoupled beads (light blue) and immunoblotted. Membranes were probed with antibodies specific for myc and PCNA. **C)** Quantification of relative band intensities of the immunoblot shown in B normalized to eluted PCNA signals.

Next, it should be elucidated staining if the interaction of PCNA is disrupted when the PIP box motif is mutated as depicted in Figure 28 A. U2OS cells were transfected with myc-INCENP wt or myc-INCENP PIPmut plasmids. After 24 h cells were fixed, permeabilized and immunostained with anti-PCNA and anti-myc specific antibodies.

As shown in Figure 29, PCNA formed typical replication foci as described in section 3.1.1. INCENP, visualized by its N-terminal myc tag, located in foci that mostly still co-localized with PCNA. A disruption of the interaction by mutating the interaction site did not lead to localization changes of INCENP. This suggests that the PIP box motif in INCENP does not play a role in foci formation.

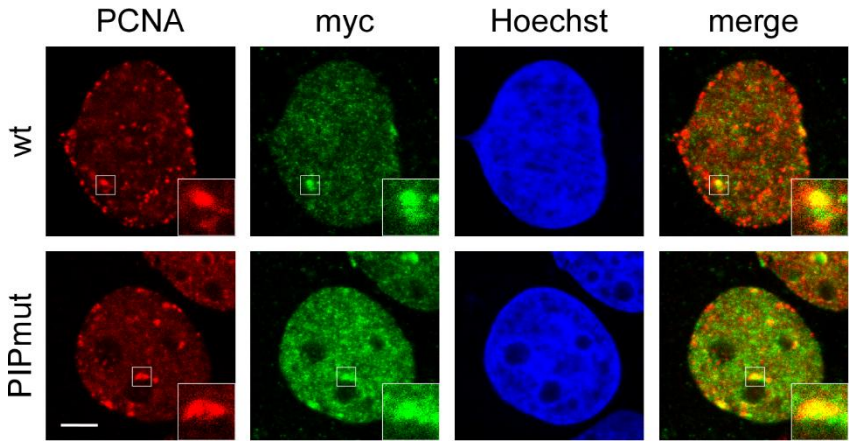

Figure 29: Mutation of the PIP box motif in INCENP does not disrupt its co-localization with PCNA. U2OS cells were immunostained with myc (AF488, green)- as well as PCNA (AF 568, red)-specific antibodies. DNA was stained with Hoechst (blue). Images were taken with a Leica TCS SP8 confocal laser scanning microscope. Scale bar: 5 µm. The insets show higher magnifications of the areas outlined in the main panels.

3.2.3 Interactions of the CPC with heterochromatin during replication

Heterochromatin protein 1 (HP1) and the epigenetic histone mark histone H3 Lys9 trimethylation (H3K9me3) are highly conserved hallmarks of heterochromatin. The chromodomain (CD) of HP1 binds to chromatin via di- or tri-methylated histone H3 (H3K9me2/3), whereas the chromoshadow domain (CSD) mediates HP1 dimerization and binds ligands that contain PxVxL motifs (Nielsen et al., 2002; Smothers and Henikoff, 2000; Thiru et al., 2004). It was shown that INCENP contains a PxVxL motif, interacting with the CSD of HP1 during late G_2 and mitosis (Kang et al., 2011; Mackay et al., 1998). Borealin is also able to bind to HP1α, mediated by a PxVxL motif in the C-terminal part of Borealin (Liu et al., 2014). Likewise, we could detect a co-localization between HP1α and CPC members already during replication (Figure 18 and Figure 19), but so far it is unknown if the proteins directly interact with each other. To address this question, a co-immunoprecipitation was conducted. 293T cells were co-transfected with eGFP-HP1α together with Survivin-HA, Borealin-HA, Aurora B-HA or myc-INCENP, respectively, or one plasmid was replaced by an empty vector. 24 h after transfection cells were lysed with Jiang IP buffer, and immunoprecipitation with HA- and myc-specific beads or anti-GFP coupled beads was performed as described in section 2.2.3.4. Lysates were immunoblotted and Membranes were probed with antibodies specific for GFP-, myc- and HA-tags (Figure 30).

As controls, Survivin-HA, Aurora B-HA, Borealin-HA and myc-INCENP were immunoprecipitated, and no unspecific binding occured when CPC members were co-transfected with empty vectors (Figure 30 A). The same holds true for GFP-HP1α when co-transfected with an empty vector and immunoprecipitated with anti-HA coupled beads. Western blot analysis with anti-GFP antibodies showed no co-immunoprecipitation when CPC members were immunoprecipitated with anti-myc or anti-HA coupled beads.

In a reciprocal setting (Figure 30 B), GFP-HP1α was immunoprecipitated via magnetic beads coupled with a GFP-specific antibody. Although Survivin-HA and Aurora B-HA were immunoprecipitated, this might be due to unspecific binding of these proteins to antibody-coupled beads, as indicated by the negative controls. Myc-INCENP also unspecifically bound to antibody-coupled beads, while it was not detectable after immunoprecipitation of GFP-HP1α. However, Borealin-HA was indeed co-immunoprecipitated, suggesting that Borealin may interact with HP1α. Here, no unspecific binding of Borealin-HA to the anti-GFP beads was detected.

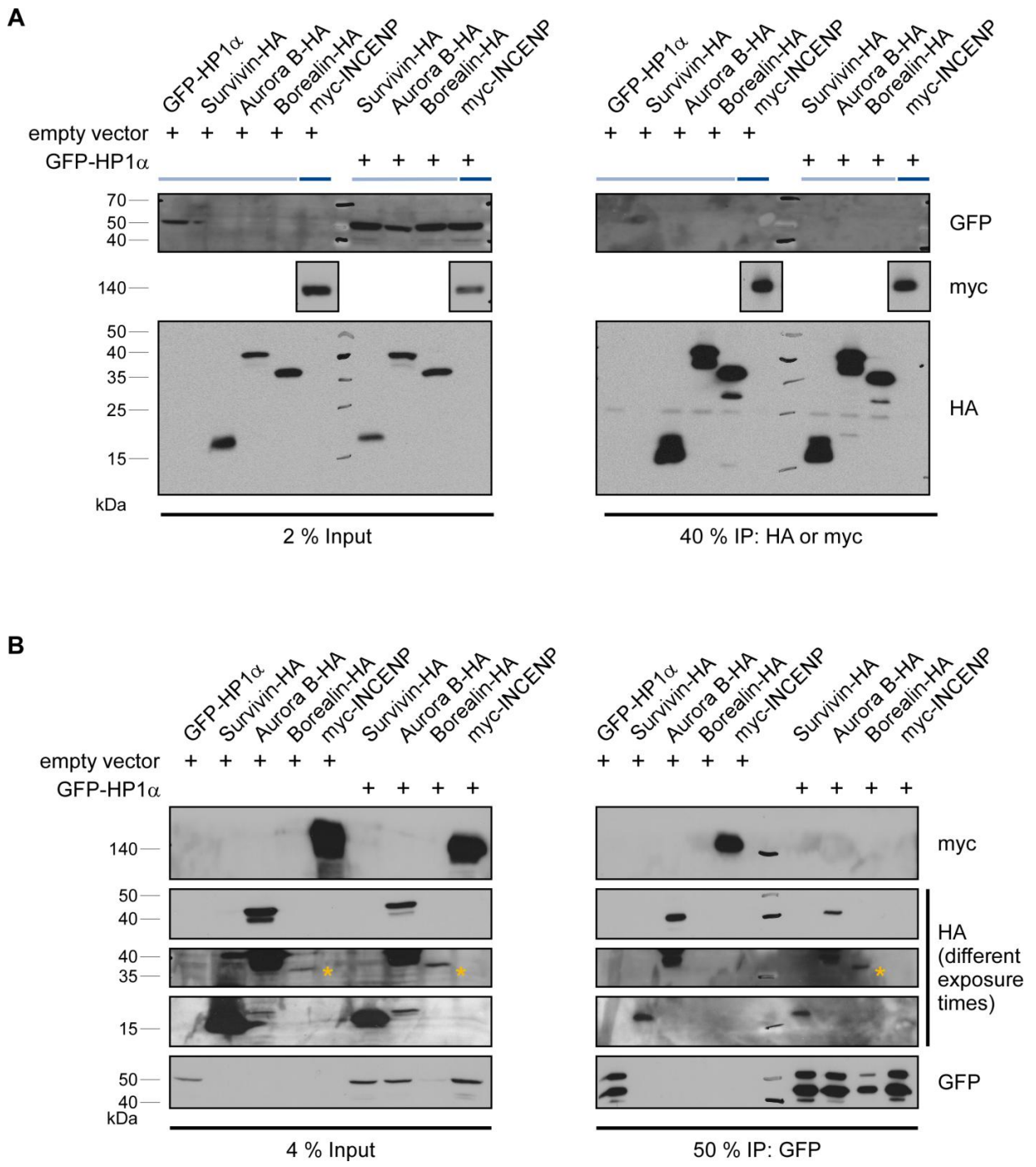

Figure 30: Co-immunoprecipitation analyses of CPC members and HP1α.

293T cells were co-transfected with eGFP-HP1α together with Survivin-HA, Aurora B-HA, Borealin-HA or myc-INCENP, respectivel, or one replaced by an empty vector. **A)** Lysates were immunoprecipitated (IP) with magnetic beads coupled to a HA- (light blue) or myc- (dark blue) specific antibodies and immunoblotted. Membranes were probed with antibodies specific for GFP, myc and HA. **B)** Lysates were immunoprecipitated (IP) with magnetic beads coupled to an anti-GFP antibody and immunoblotted. Membranes were probed with antibodies specific for GFP, myc and HA. Protein signal of Borealin was marked with a yellow asterisk.

Of note, supporting experiments, using different magnetic or sepharose beads, several IP lysis buffers or additional treatment with micrococcal nuclease for chromosomal DNA fragmentation, were not successful in abolishing unspecific protein binding (data not shown).

3.3 Function of the CPC during S phase

The expression of Survivin is cell cycle-regulated and peaks in G_2/M phase. During mitosis and cytokinesis changes the localization of the CPC dynamically accompanied by its various functions. In this work, a centromeric localization of the chromosomal passenger proteins could be observed during S phase, leading to the assumption that the CPC might have an additional, so far unknown, functional role during replication.

3.3.1 Effect of Survivin depletion on cell cycle distribution

In initial experiments to determine whether the CPC could be functionally implicated in processes during replication, the cell cycle distribution of Survivin-depleted cells was analyzed and compared to control cells. U2OS cells were transfected with Survivin-specific and non-targeting siRNA as a control, and 48 h later partly transfected with myc-Survivin. 48 h after transfection, cells were pulse-labeled with BrdU. Cells were harvested and used for western blot analysis (Figure 31 B) and flow cytometric analysis. Flow cytometry was conducted as described in section 2.2.2.7. 10.000 cells were counted and further gated and analyzed with Kaluza Analysis (Figure 31 C, D).

Immunoblot analysis of extracts from the cells used for flow cytometric analysis revealed a decrease of Survivin expression in lysates from Survivin-depleted cells (Figure 31 B). Survivin protein levels were increased after transfection with myc-Survivin compared to cells which were treated with siRNA. Quantification of the cell cycle distribution in U2OS cells measured by flow cytometry revealed a reduced amount of S and G_1 phase cells while the percentage of G_2/M phase cells increased after Survivin depletion compared to siCtrl treated cells (Figure 31 C, D). In addition to the cell cycle arrest in G_2/M phase, an additional 8N population could be observed in Survivin knockdown cells. This was potentially caused by finished mitosis in the absence of cytokinesis, which leads to one cell with 4N and not two daughter cells with each 2N, and a further re-replication resulting in an 8N population. Transfection of myc-Survivin in Survivin-depleted cells could not completely rescue the observed effect. The amount of S phase cells in the rescue experiment was the same as in Survivin-depleted cells, and with 16 % only half of the amount of S phase cells in the control sample. The amount of G_1 phase cells in the sample where Survivin depletion was rescued by ectopic expression of myc-Survivin increased from 12 % to 21 % but was still decreases compares to the siControl (around 40 %). Percentage of G_2/M phase cells increased to 47 % after Survivin depletion in comparison to siControl-treated cells (19 %) and further increased to 63 % in Survivin-depleted cells after Survivin rescue. The 8N peak was no longer detectable in Survivin-depleted cells after ectopic Survivin expression.

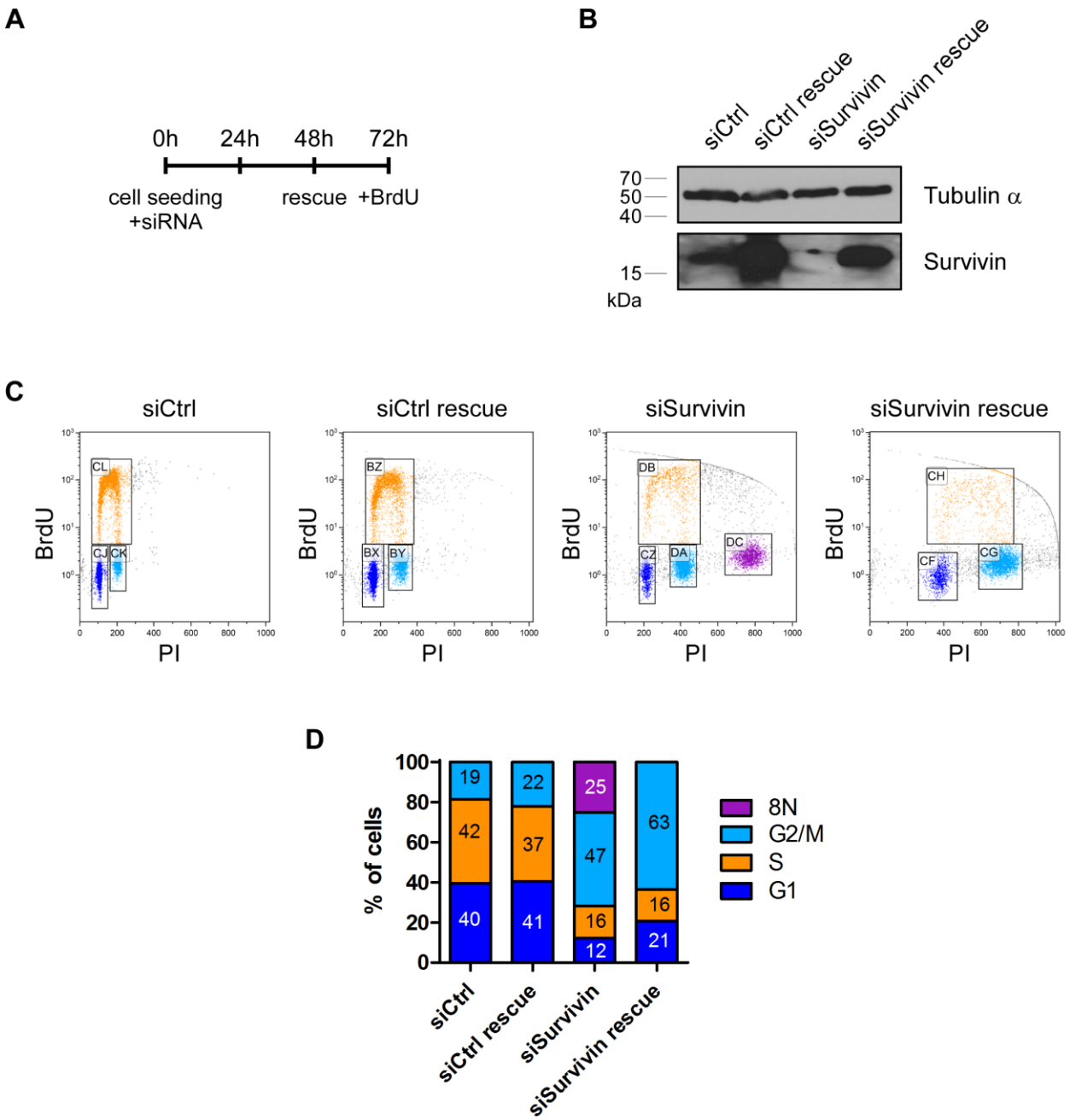

Figure 31: Survivin depletion alters cell cycle distribution.

A) Schematic overview of cell treatment. U2OS cells were seeded and transfected with siRNAs, targeting Survivin or with a non-targeting control. 48 h after transfection of siRNA the cells were additionally transfected with myc-Survivin (rescue). After 72 h cells were pulse labeled with 10 µM BrdU for 30 min and stained for flow cytometry analysis. **B)** Immunoblotting was used to assess the expression of Survivin after knockdown. Membranes were probed with antibodies specific for Survivin and Tubulin α as a loading control. **C)** Cell cycle profiles of U2OS cells treated as described in A. The dot plot represents BrdU incorporation versus DNA content, as determined by PI staining. Cell cycle phases are gated; G_1: dark blue, S: orange, G_2/M: light blue, 8N peak: purple. **D)** Numerical analysis of the percentage of cells in the different cell cycle phases as analyzed by flow cytometry and shown in C.

3.3.2 Effect of Survivin depletion on replication fork speed

To understand the impact of the chromosomal passenger complex on DNA replication, the DNA fiber assay technique was used to visualize fork velocities at the single molecule level. A431 cells were transfected with Survivin-specific and non-targeting siRNA as well a mock control. 72 h after transfection, cells were sequentially pulse-labeled with thymidine analogues CldU and IdU for 20 min each. Cells were harvested, and DNA was spreaded as described in section 2.2.2.10. Following fixation and denaturation of dsDNA, fibers were stainend with two different antibodies, specific for either CldU or IdU. DNA fibers were visualized microscopically, and fiber lengths from elongating forks (red-green tracks) were measured with ImageJ. Linear measures in µm were converted into kb to calculate fork velocities.

Microscopic images revealed a shorter tract length for Survivin-depleted cells compared to mock-or siControl-transfected cells (Figure 32 B). Quantification of the replication fork speed revealed a distribution between 0.2–4 kb/min, with the majority of forks exhibiting a fork velocity of 0.6–1.2 kb/min (Figure 32 C). The mean incorporation rate was significantly decreased in Survivin-depleted cells (0.70 ± 0.01 kb/min) compared to mock- (0.92 ± 0.02 kb/min) or siControl-treated (0.88 ± 0.02 kb/min) cells (Figure 32 D).

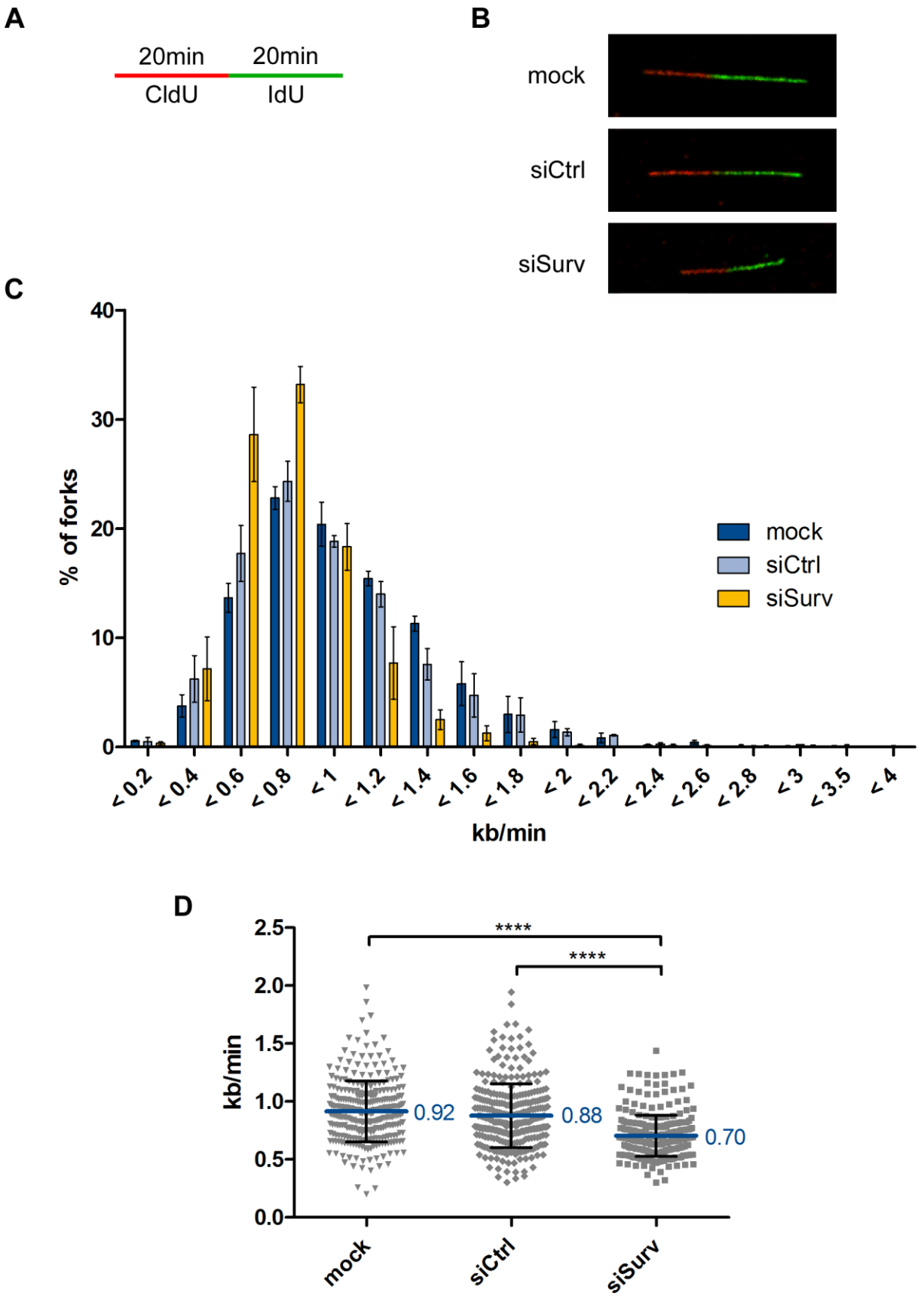

Figure 32: Survivin knockdown leads to a reduced replication fork speed.

A) Schematic overview of cell treatment. A431 cells were transfected with siRNA specific for Survivin and non-targeting siRNA or without siRNA (mock) as a control, respectively. 72 h after transfection, cells were sequentially pulse-labeled with CldU and IdU for 20 min each. Cells were harvested, and the DNA fiber assay was performed. **B)** Representative images of replication tracks in mock-, non-targeting siRNA

(siCtrl)- and siSurvivin (siSurv)-transfected cells are shown. Images were taken with a Leica TCS SP5 confocal laser scanning microscope. Scale bar: 5 µm. **C)** Length of stained fibers from elongating forks (red-green tracks) were measured with ImageJ and µm values were converted into kb to calculate the replication fork speed in kb/min. Data derived from three independent experiments with 300 fibers analyzed per experiment. Results are depicted as a frequency distribution. Means ± SD are shown. **D)** Dot plot of the mean replication fork speed of one representative data set out of three independent experiments as shown in C. Bar graphs represent means ± SD (n=300 fibers of each group); ****p<0.0001; t test.

3.3.3 Effect of Aurora B inhibition on replication fork velocities

The results presented above demonstrated that the absence of CPC members results in a reduced replication fork speed. To elucidate if the DNA replication depends on the kinase activity of Aurora B, a DNA fiber assay was performed, where Aurora B's ability to phosphorylate target proteins was inhibited. Therefore, cells were treated with the specific Aurora B inhibitor Hesperadin for in a final concentration of 100 nM. During the last 40 min, cells were sequentially pulse-labeled with thymidine analogues CldU and IdU for 20 min each. Cells were harvested and DNA was spreaded as described in section 2.2.2.10. After fixation and denaturation of dsDNA, fibers were stained with two different antibodies, specific for either CldU or IdU. DNA fibers were visualized microscopically, and fiber lengths from elongating forks (red-green tracks) were measured with ImageJ. Linear measures in µm were converted into kb to calculate fork velocities. Efficiency of Aurora B inhibition via Hesperadin treatment was monitored by western blotting.

Western blot analysis revealed a phosphorylation of H3S10 in DMSO-treated and untreated cells, whereas no phosphorylation could be detected in cells treated with Hesperadin for 2 h or 4 h, while histone H3 levels remained constant (Figure 33 B). For Aurora B pT232, faint bands were visible in each sample regardless of cell treatment with Hesperadin or DMSO. Microscopic images indicated a similar tract length for Hesperadin-treated cells compared to negative control cells, treated with DMSO (Figure 33 C). Quantification of the replication fork speed again revealed a distribution between 0.2–4 kb/min, with the majority of forks exhibiting a fork velocity of 0.6–1.4 kb/min (Figure 33 D). The mean incorporation rate in Hesperadin-treated cells (0.88 ± 0.02 kb/min) is similar to DMSO-treated control cells (0.91 ± 0.02 kb/min) (Figure 33 E).

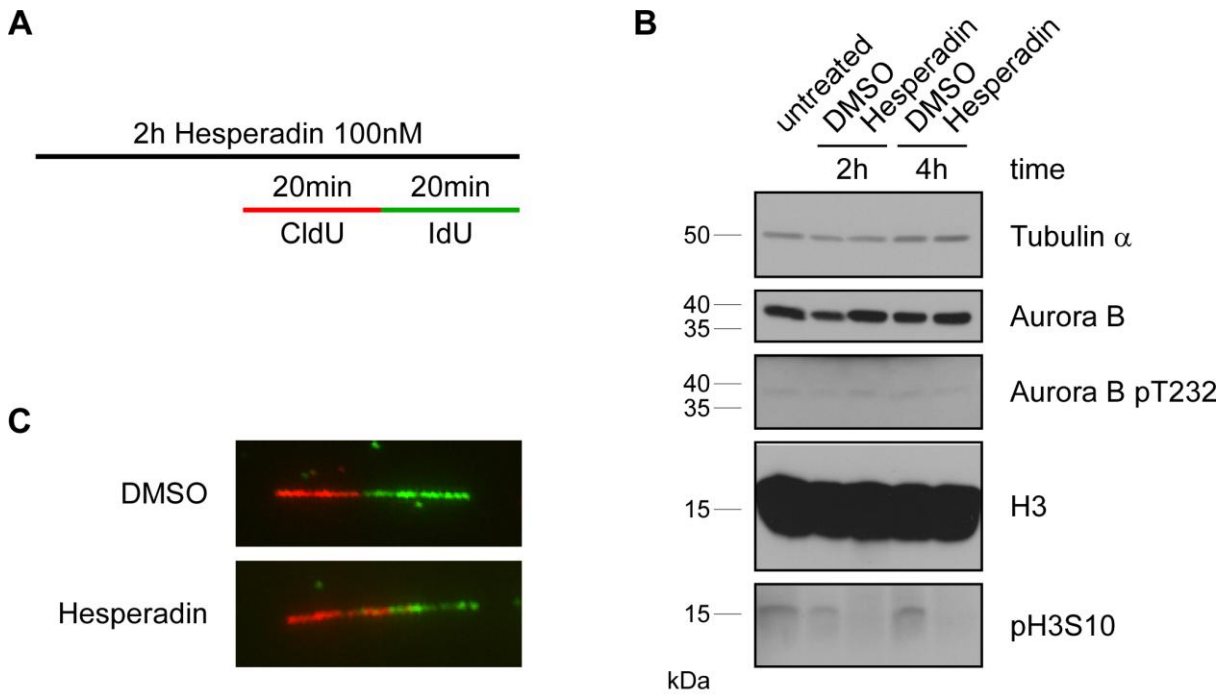
A
2h Hesperadin 100nM
20min
20min
CldU
IdU
B
untreated
DMSO
Hesperadin
DMSO
Hesperadin
2h
4h
time
50
Tubulin α
40
35
Aurora B
40
35
Aurora B pT232
15
H3
15
pH3S10
kDa
C
DMSO
Hesperadin

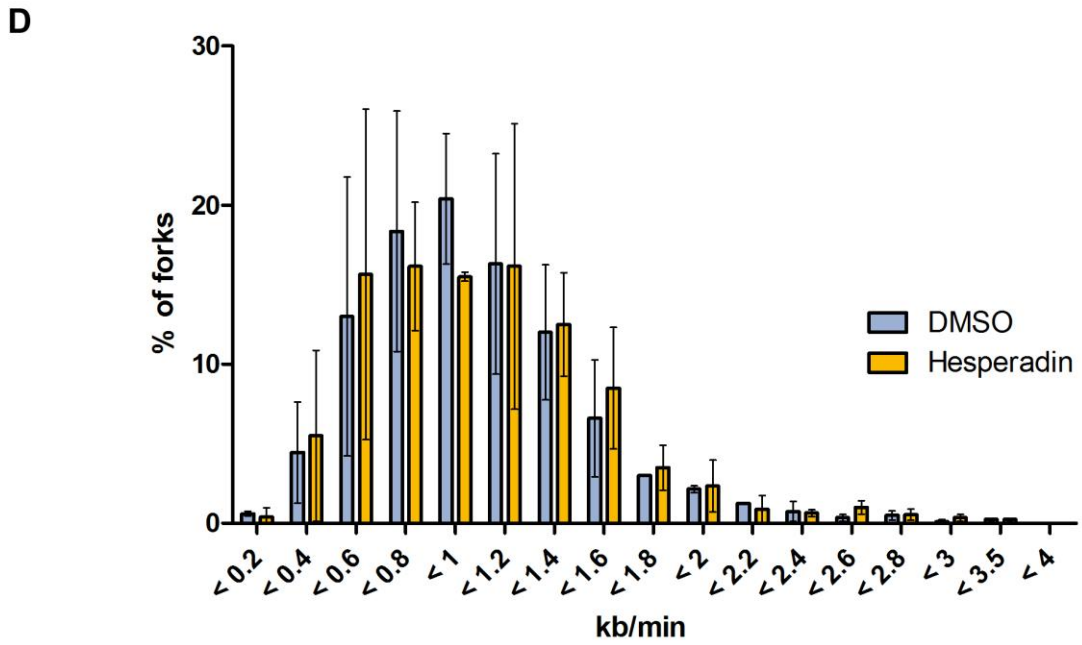
D
30
20
10
0
% of forks
DMSO
Hesperadin
< 0.2
< 0.4
< 0.6
< 0.8
< 1
< 1.2
< 1.4
< 1.6
< 1.8
< 2
< 2.2
< 2.4
< 2.6
< 2.8
< 3
< 3.5
< 4
kb/min

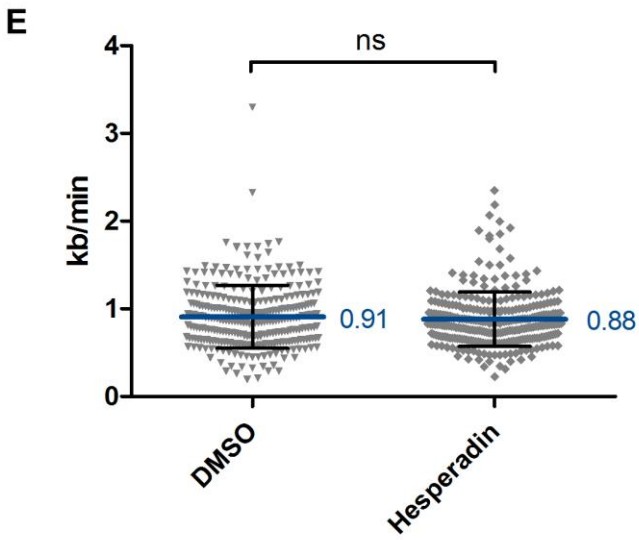
E
ns
4
3
2
1
0
kb/min
0.91
0.88
DMSO
Hesperadin

Figure 33: Aurora B inhibition does not influence replication fork speed.

A) Schematic overview of cell treatment. A431 cells were treated with 100 nM Hesperadin for 2 h or with DMSO as a control. During the last 40 min, cells were sequentially pulse-labeled with CldU and IdU for 20 min each. Cells were harvested, and the DNA fiber assay was performed.**B)** Phosphorylation status of Aurora B and histone H3 following Hesperadin treatment was assess by immunoblotting with antibodies specific for Aurora B and histone H3 and their phosphorylated forms (Aurora B Thr 323, H3 Ser 10). Tubulin α served as loading control. **C)** Representative images of replication tracks in Hesperadin- or DMSO-treated cells are shown. Images were taken with Nikon Ti Eclipse Epi microscope. **D)** Length of stained fibers from elongating forks (red-green tracks) were measured with ImageJ. Linear measures in µm were converted into kb to calculate the replication fork speed in kb/min. Data were derived from two independent experiments with 300 fibers analyzed per experiment. Results are depicted as a frequency distribution. Means ± SD are shown. **E)** Dot plot of the mean replication fork speed of one representative data set out of two independent experiments as shown in C. Bar graphs represent means ± SD (n = 300 fibers of each group); ns: non-significant; t test.

3.4 Impact of replication stress on the CPC

DNA replication forks are frequently challenged and arrested by DNA lesions induced by endogenous or exogenous agents. The replication fork might thus stall at damaged regions, leading to ssDNA stretches or DSBs that could trigger genome instability. Both events result in the activation of the checkpoint kinases and start the subsequent activation of the respective signaling cascade.

3.4.1 Protein expression and localization of the CPC after induction of replication stress

In initial experiments to determine whether Survivin and the CPC could also be implicated in processes initiated by replication stress, the expression of CPC proteins and their localization to different cell compartments was analyzed.

In exponentially growing U2OS cells, replication stress was induced by treatment with 1 µM and 25 nM camptothecin (CPT), 100 mM aphidicolin (APH), 0.5 mM hydroxyurea (HU) and 0.2 µM cisplatin or cells were irradiated with X-rays (6 Gy). 1 µM CPT treatment was used to induce a complete DNA damage response activation as a control. After 1 h of treatment or 1 h after irradiation, one quarter of the cells was used to prepare whole cell lysates (section 2.2.3.1), while the rest was subjected to subcellular fractionation (section 2.2.3.2). All lysates were analyzed via SDS-PAGE on a gradient gel and immunoblotting.

Lamin A/C, a protein of the nuclear membrane, was used to confirm the purity of the nuclear fractions and as a loading control for whole cell lysates. Indeed, all whole cell lysates contained similar amounts of Lamin A/C. A Lamin A/C was also detectable in the cytoplasmic fraction of the irradiated sample, indicating that this sample was contaminated with nuclei. Soluble nuclear fractions contained similar amounts of Lamin A/C in all samples, whereas chromatin-bound fractions showed only the upper band detected by the Lamin A/C-specific antibody. The markers for DSB recognition and repair, γH2AX and pATM, were increased in whole cell lysates after treatment with 1 µM CPT, 0.5 mM HU and irradiation with 6 Gy in comparison to the untreated sample. H2AX was equally phosphorylated in the chromatin-bound fraction, Additionally low amounts could also be detected in the irradiated sample in the cytoplasmic fraction, maybe due to low purity of the fractionation, similar to Lamin A/C. In the cytoplasmic as well as the chromatin-bound fractions, comparable levels of ATM phosphorylation (pATM) were detectable, while in the soluble nuclear fractions pATM was only increased in cells treated with 1 µM as well as 25 nM CPT and 6 Gy but not in 0.5 mM HU-treated cells. In all whole cell lysates, unspecific bands at a molecular weight of 40 kDa were visible when the antibody specific for RPA32 phosphorylated at Ser33 (pRPA32) was used. However, specific pRPA32 signals were detectable in whole cell lysates from cells treated with 1 µM CPT as well as reduced signals for cells treated with 0.5 mM HU and after irradiation with 6 Gy. In samples treated with 1 µM CPT, phosphorylation was increased in all subcellular fractions. ATR protein levels were constant or decreased in whole cell lysates of treated cells compared to the untreated control samples. In the cytoplasmic and the soluble nuclear fraction, CPT- (1 µM and 25 nM) and APH-treated cells revealed higher amounts of ATR than the untreated control samples. In contrast, in chromatin-bound fractions only CPT- (1 µM) and HU-treated (0.5 mM)

samples, protein levels of ATR were increased. All CPC proteins were similar expressed in each sample of whole cell lysates. Only in the subcellular fractions some CPC protein levels were altered, for example, protein levels of Aurora B and Survivin were increased in the cytoplasm after CPT and APH treatment as wells as after irradiation.

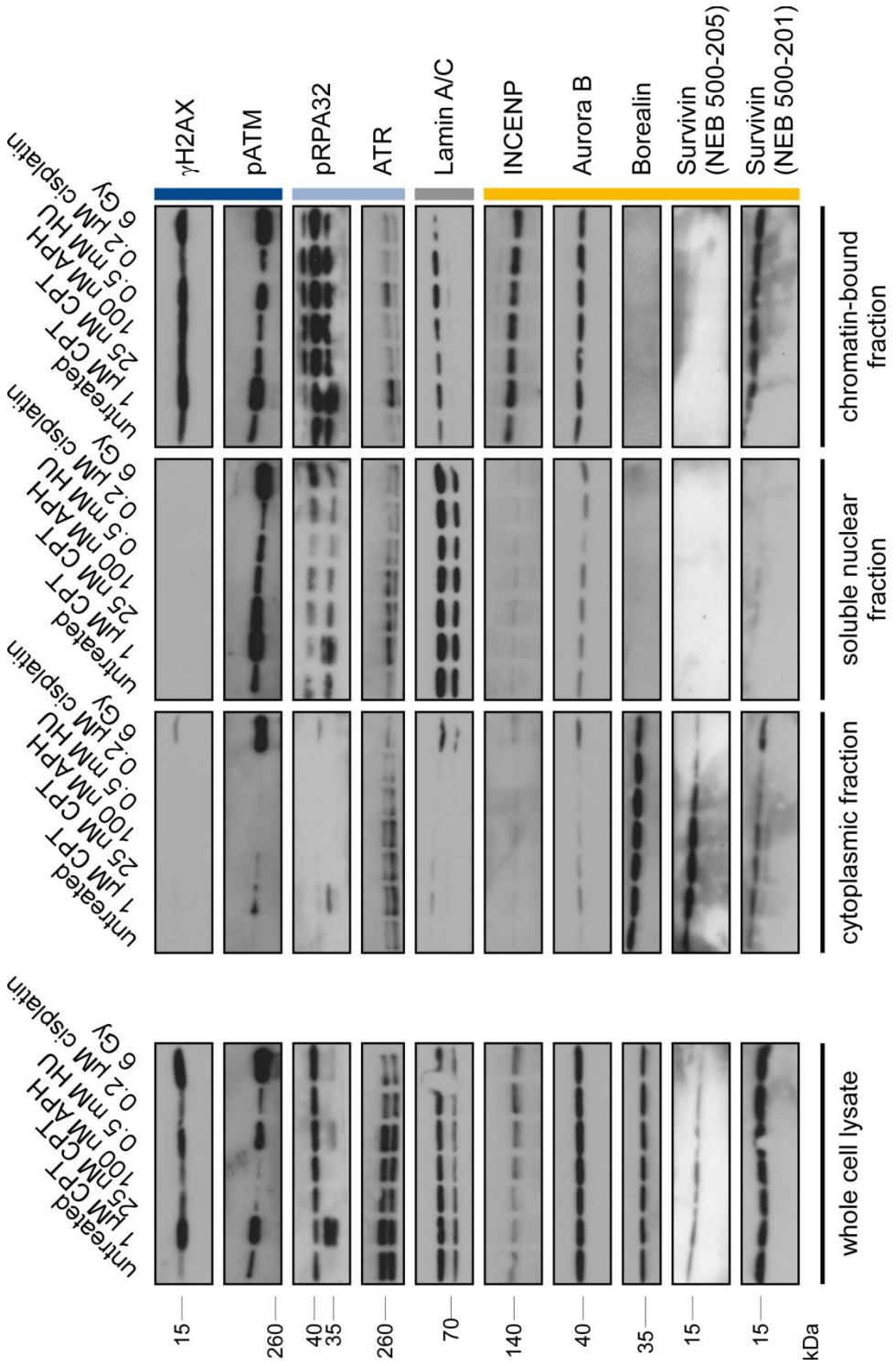

Figure 34: Expression and phosphorylation levels of different relevant proteins after induction of replication stress.

U2OS cells were treated with different types of replication stress inducers, including low and high concentrations of camptothecin (CPT, 1 µM and 25 nM), 100 mM aphidicolin (APH), 0.5 mM hydroxyurea (HU), 0.2 µM Cisplatin and irradiation with 6 Gy. Whole cell lysates and subcellular fractions (cytoplasmic, soluble nuclear and chromatin-bound) were immunoblotted with antibodies specific for γH2AX (Ser139),

pATM (Ser1981), pRPA32 (Ser33), ATR, Lamin A/C, and INCENP, Aurora B, Borealin and Survivin. γH2AX and pATM served as marker proteins for double strand break recognition and repair (dark blue), pRPA and ATR for single strand stretches and recognition thereof (light blue), Lamin A/C as loading control (grey) and CPC proteins INCENP, Aurora B, Borealin and Survivin are highlighted in yellow.

To confirm protein levels as analyzed by immunoblot and to investigate their localization, immunofluorescence analyses were performed by the bachelor student Sarah Maurer. Exponentially growing U2OS cells were treated for 1 h with 1 µM camptothecin (CPT) and either fixed directly or pre-extracted with CSK buffer for 5 min at 4 °C and fixed afterwards. The advantage of pre-extraction is that the excess of proteins, which do not form detectable foci, are washed away and only chromatin bound proteins remain. Cells were immunostained, and microscopic images were analyzed via CellProfiler (Figure 35).

Likewise, an increased phosphorylation of the DNA damage response proteins γH2AX and pATM after induction of replication stress by CPT treatment independent of pre-extraction or direct fixation of samples was detected (Figure 35 A-C). This indicated successful induction of replication stress. Immunostaining of Survivin revealed a significantly decreased standard deviation of mean intensity in directly fixed samples after CPT-treatment, whereas the values increased non-significantly when cells were pre-extracted and excessive non-chromatin bound proteins were removed (Figure 35 A, D). In contrast, Aurora B was non-significantly increased in CPT-treated fixed samples while it remained completely unchanged in pre-extracted samples after CPT treatment (Figure 35 A, E).

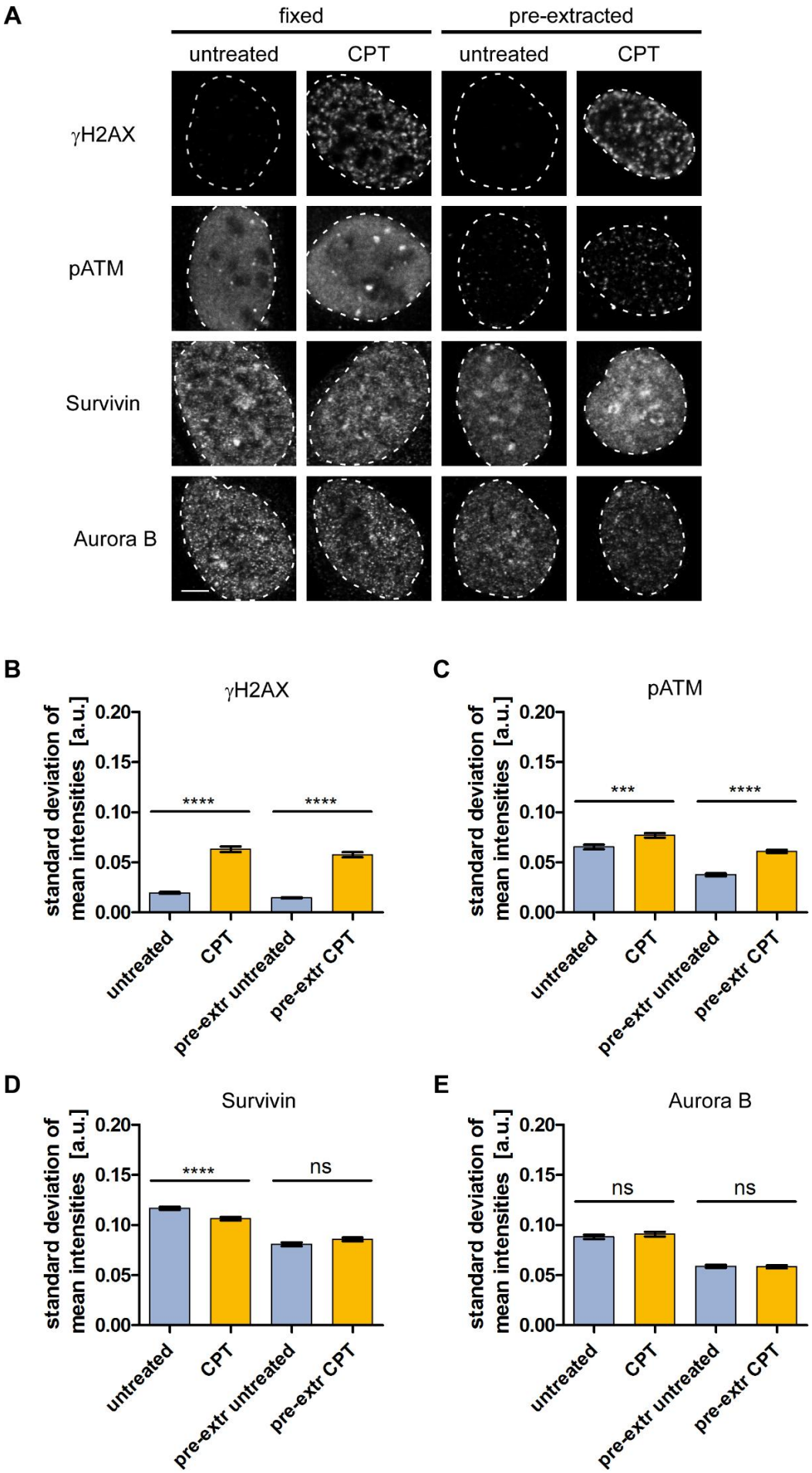
A
fixed
pre-extracted
untreated
CPT
untreated
CPT
γH2AX
pATM
Survivin
Aurora B
B
γH2AX
standard deviation of mean intensities [a.u.]
0.20
0.15
0.10
0.05
0.00
****
****
untreated
CPT
pre-extr untreated
pre-extr CPT
C
pATM
***
****
D
Survivin
****
ns
E
Aurora B
ns
ns

Figure 35: Analysis of protein localization and expression after induction of replication stress.
A) U2OS cells were treated with 1 µM camptothecin (CPT) for 1 h and either directly fixed or pre-extracted and fixed. All samples were permeabilized and stained with specific antibodies for γH2AX, pATM, Survivin and Aurora B. DNA was stained with Hoechst (not shown), and nuclei contour is indicated with dashed lines. Images were taken with a Leica TCS SP8 confocal laser scanning microscope. Scale bar: 5 µm. **B-E)** Bar plots of standard deviation of mean intensities of γH2AX **(B)**, pATM **(C)**, Survivin **(D)** and Aurora B **(E)** of untreated (light blue) and CPT-treated samples (yellow). Mean ± SEM. 200-700 cells per condition were analyzed via CellProfiler. t-test ns: non-significant, *** $p \leq 0.001$ and **** $p \leq 0.0001$.

3.4.2 Effect of replication fork uncoupling on CPC proteins

Replication stress can result in a functional uncoupling of the helicase complex from the replicative polymerase (Byun et al., 2005). When the replication fork progression continues in the absence of processive DNA synthesis, long patches of ssDNA covered with the single strand binding protein RPA (Replication protein A) emerge. Proteins involved in the elongation step of DNA synthesis (e.g. PCNA, polymerase δ, DNA ligase 1 and Fen1) dissociate from replication sites (Görisch et al., 2008). An important process coupled to DNA synthesis and also influenced by replication stress is chromatin assembly linked by the interaction of the sliding clamp PCNA with the chromatin assembly factor 1 (CAF1) (Shibahara and Stillman, 1999). Not only CAF1 binds to PCNA but also to the heterochromatin protein HP1α (Murzina et al., 1999).

Based on the co-localization and interaction of the CPC with PCNA and HP1α and the fact that these proteins play important roles during replication itself or replication-associated processes, the question arises what happens with the CPC after helicase-polymerase uncoupling. To address this question, U2OS cells were incubated with EdU for a total duration of 30 min, and aphidicolin (50 µg/ml) was added after the first 10 min. Following treatment, EdU was detected and replication- and heterochromatin-associated proteins as well as CPC members were immunostained. Following treatment with either DMSO or aphidicolin, the localization pattern of several proteins in S phase cells (EdU-positive cells, not shown) was examined (Figure 36). As expected, Mcm2 did not change its localization after induction of polymerase stalling by aphidicolin treatment compared to the DMSO control. However, RPA32, a subunit of the single strand binding protein was enriched in nuclear foci after aphidicolin treatment. In contrast, PCNA and DNA Ligase I were no longer present in discrete foci, but instead diffusely distributed throughout the nucleus. CPC proteins were still accumulated after polymerase stalling and uncoupling of the replication machinery by aphidicolin treatment. The histone chaperone CAF1 changed its localization from bright nuclear foci to a diffuse distribution, whereas the localization of HP1 was not altered in response to aphidicolin treatment compared to the DMSO control.

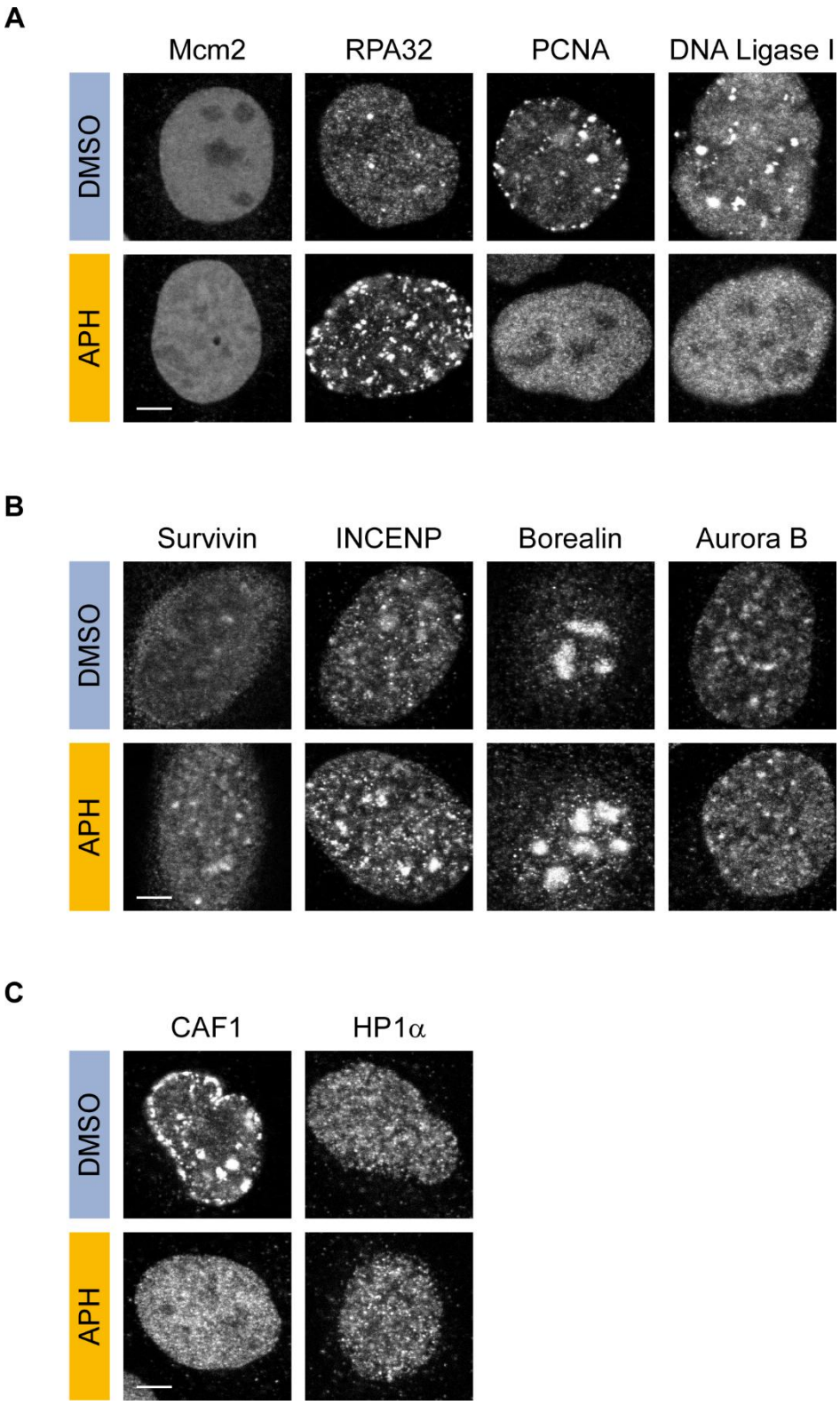

Figure 36: CPC still accumulats in foci after polymerase stalling by aphidicolin treatment.
U2OS cells were treated with 50 µg/ml aphidicolin (APH) for 20 min. Representative images of nuclei of S phase cells (detected via EdU labeling and staining, not shown) are presented. Cells were immunostained with the appropriate antibodies specific for the replication proteins Mcm2, RPA32, PCNA and DNA Ligase I **(A)**, the CPC members Survivin, INCENP, Borealin and Aurora B **(B)** as well as chromatin-associated proteins CAF1 and HP1α **(C)**. DNA was stained with Hoechst (not shown). Images were acquired with a Leica TCS SP8 confocal laser scanning microscope. Scale bar: 5 µm.

3.4.3 Replication during mitosis does not depend on CPC localization

Replication stress generates stretches of ssDNA at stalled or damaged forks, thereby activating the replication checkpoint by phosphorylation of ATR and Chk1 (reviewed in Zeman & Cimprich, 2014). This damage response pathway delays cell cycle progression so that stalled replication forks can be recovered, damaged DNA can be repaired, and replication can be completed before entry into mitosis (Lossaint et al., 2013; Magiera et al., 2014). In some cases of endogenous or low levels of exogenous (e.g. low doses of aphidicolin) replication stress, or other types of DNA damage, the damage checkpoint is not activated (Koundrioukoff et al., 2013). Here, cells are not arrested in S phase and proceed into mitosis with under-replicated DNA or unresolved DNA structures (Chan et al., 2009; Naim and Rosselli, 2009). Moreover, this can initially lead to chromosomal and later to genomic instability and cancer (Burrell et al., 2013). Recent studies have shown that in cases of replication stress without checkpoint activation, for example induced by low levels of aphidicolin, DNA synthesis takes place even during mitosis (Bergoglio et al., 2013; Bhowmick et al., 2016; Minocherhomji et al., 2015).

To define if the CPC is involved in DNA synthesis during mitosis, asynchronously growing U2OS cells were synchronized by inhibition of CDK1 with RO-3306 (0.9 µM) for 16 h to arrest cells in G_2 phase. Simultaneously, cells were treated with low dose aphidicolin (0.4 µM) to induce replication stress or with DMSO as a control. Cells were released for 35 min from the G_2 arrest to allow progression into prometaphase of mitosis. Additionally, 10 µM EdU was added to visualize new DNA synthesis (Figure 37 A). Afterwards, cells were fixed and permeabilized simultaneously for 20 min with PTEMF buffer. EdU detection and immunofluorescence staining was performed (Figure 37 B) as described in section 2.2.2.9 and 2.2.2.8.

In contrast to EdU incorporation during DNA replication in S phase, in mitotic cells EdU incorporation was only detectable when cells were treated with APH. INCENP was associated with chromatin irrespective of APH exposure. However, a co-localization between INCENP and nascent DNA was not detectable, indicating that CPC members promote their mitotic function without a relocation to replication sites.

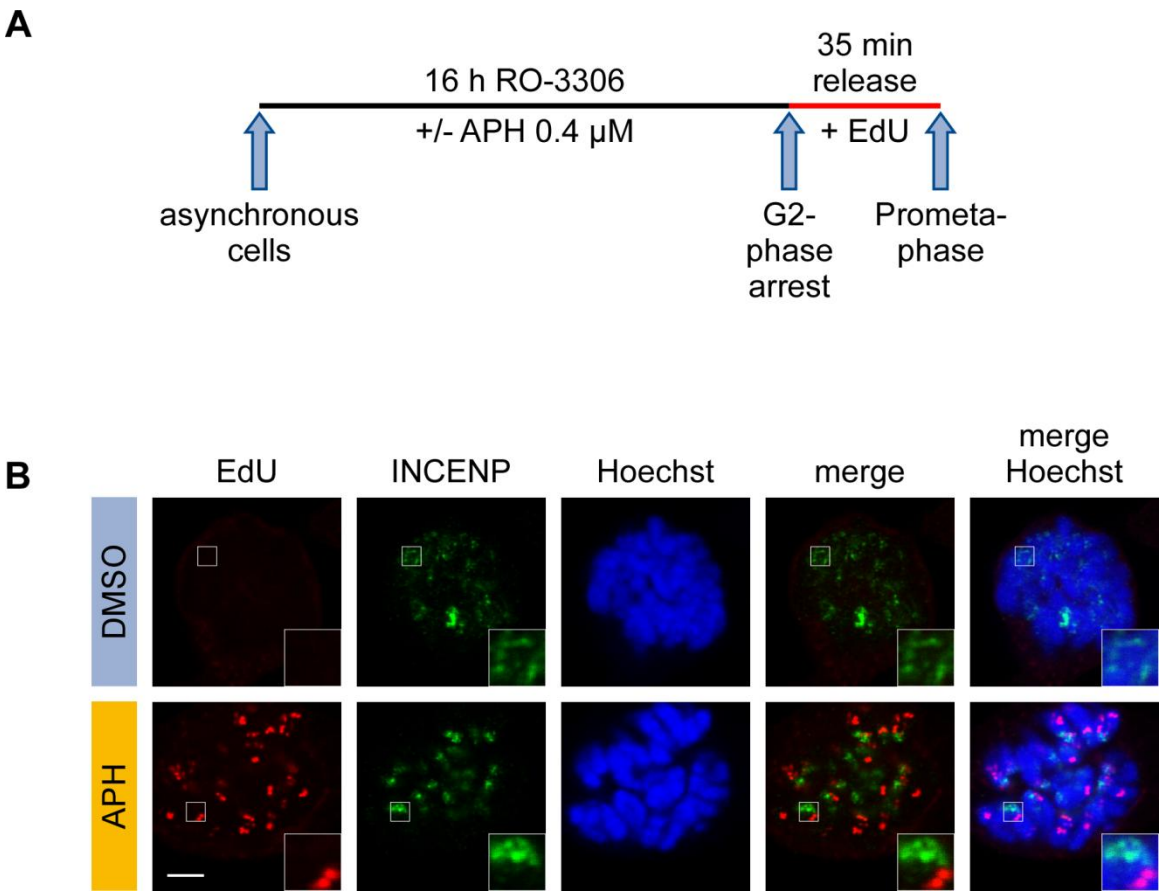

Figure 37: INCENP does not localize to replication sites during mitosis in response to replication stress.

A) Schematic overview of cell treatment. Cells were synchronized with RO-3306 and simultaneously treated for 16 h with low dose aphidicolin (0.4 µM) or DMSO, respectively. Cells were released in fresh medium containing EdU. **B)** U2OS cells were fixed and permeabilized simultaneously with PTEMF buffer and immunostained with an INCENP (AF488, green)- specific antibody. DNA was stained with Hoechst (blue). EdU (AF594, red) was visualized via Click-iT^{TM} Kit. Images were taken with a Leica TCS SP8 confocal laser scanning microscope. Scale bar: 5 µm. The insets show higher magnifications of the areas outlined in the main panels.

4 Discussion

Cancer is one of the leading causes of death. Cancer cells acquire properties to grow and proliferate abnormally and to invade or spread to other parts of the body. These alterations frequently result in genomic instabilities. Mitosis and replication are the two major processes pivotal for maintenance of the genomic integrity by faithful duplication of the genome and by dividing the chromosomes equally to the progeny cells. Both processes are monitored or influenced by surveillance mechanisms, for instance cell cycle checkpoints, damage recognition and response pathways.

One of the most crucial orchestrators of mitosis is the CPC. So far, a plethora of functions for the CPC has been identified in mitosis, ranging from correction of chromosome-microtubule attachment errors and activation of the spindle assembly checkpoint to construction and regulation of the contractile apparatus that drives cytokinesis (Carmena et al., 2012). The CPC member Survivin further acts as an inhibitor of apoptosis (Ambrosini et al., 1997). In addition, an involvement of Survivin (and the other CPC members) in the DNA damage response and repair pathway was suggested (Capalbo et al., 2010; Reichert et al., 2011; Schröder, doctoral thesis, 2014). Recent studies linked these mitotic and damage response functions of the CPC with a novel role in response to replication stress (Dheekollu et al., 2011; Mackay and Ullman, 2015; Zuazua-Villar et al., 2014). In contrast to the well-studied regulation and function of the CPC during mitosis, its role during interphase needs to be elucidated in more detail.

4.1 Formation of CPC foci during S phase and their characterization

4.1.1 CPC accumulates in nuclear foci at replication sites

Previous publications reveal different localizations for the CPC and its individual components, ranging from being absent, located in the cytoplasm, in the nucleus or at centromeric regions (section 1.5.2.2). Furthermore, the CPC and especially Survivin were described to be cell cycle regulated, and their expression should peak in G_2/M (Li et al., 1998). To gain deeper insights into the localization of the CPC throughout the cell cycle, immunostaining should visualize Survivin especially during interphase (Figure 15). Due to its typical distribution pattern in S phase, PCNA was used to assign the localization of Survivin to different cell cyle phases. Survivin indeed showed a cell cycle-dependent expression, but was already expressed in early S phase, accumulating in nuclear foci. Most of these did not seem to be directly correlated to PCNA, although some Survivin foci co-localized with PCNA or were at least in close proximity. Surprisingly, in late S phase the majority of Survivin foci co-localized with PCNA, indicating a potential binding of both proteins. Nevertheless, there were still some separate foci of either Survivin or PCNA during late S phase. At the subsequent G_2 phase, Survivin localization was similar to the foci pattern observed in late S phase. This distinct subbcellular localization of Survivin without an association with PCNA points to an additional binding to chromatin or chromatin-associated proteins.

Due to the fact that in mitosis Survivin acts in conjunction with the other CPC members Borealin, INCENP and Aurora B (reviewed by Ruchaud, Carmena, & Earnshaw, 2007) while it fulfills its anti-apoptotic function as a monomer (Pavlyukov et al., 2011), the localization of Aurora B was also investigated (Figure 16). Aurora B also co-localized with PCNA in WI-38 (lung fibroblasts), HeLa (cervical adenocarzinoma) and A431 (epidermoid carcinoma) cells, suggesting that this co-localization is cell line-independent, and that Survivin might act as part of the CPC and not as monomer or homodimer.

To elucidate the aforementioned CPC foci regarding their spatio-temporal dynamics throughout S phase, A431 cells stably expressing Survivin-GFP were transfected with a plasmid coding for the PCNA chromobody (pCCC) to perform time-lapse microscopy (Figure 17). Here, Survivin-GFP was only detectable during mitosis and not during interphase. Compared to the low molecular weight of Survivin of 16.5 kDa, the GFP tag with its 27 kDa might compromise Survivin's localization and function. Despite its correct localization in mitosis, a sterical hindrance due to the large GFP tag could abolish the localization and the function during replication. The experimental setup could be improved by using an N-terminal GFP tag instead of the C-terminal tag, as the GFP tag could bury binding sites or domains at one terminus of the fused protein of interest. A second and more favorable possibility is to a use a smaller tag. For example the tetracysteine-biarsenical system, which is the smallest (< 0.7 kDa) available tag system (Albert Griffin et al., 2000; Crivat and Taraska, 2012). For this, a short peptide sequence enriched in cysteines is cloned into the plasmid coding for the target protein. The tag is not autofluorescent like GFP, thus it needs to be visualized by the green membrane-permeable biarsenical dye FlAsH-EDT_2 (fluorescein arsenical hairpin binder) for live cell microscopy. Another problem in this lime-lapse microscopy experiment was that in all other positions examined, the cells either migrated too fast to visualize the whole cell cycle, were not transfected with pCCC or died during the examination. By using a stable cell line expressing both, PCNA chromobody and tagged-Survivin, in combination with cell tracking of single cells, a highly variable transfection efficiency could be avoided, and the efficiency of long-term microscopic inspection conditions could be enhanced.

4.1.2 CPC accumulates at centromeric heterochromatin in S phase

Co-localization of CPC members and PCNA was predominantly observed during late S phase when constitutive heterochromatin is replicated. Constitutive heterochromatin is defined epigenetically by methylation of histone H3 at Lys 9 and recruitment of its binding partner HP1 (Bannister et al., 2001; Jacobs and Khorasanizadeh, 2002). To elucidate if the CPC foci are associated with heterochromatin during S phase, several fluorescence analyses were performed. Indeed, overexpressed GFP-HP1α and Survivin-tdTomato (Figure 18 A), as well as the respective endogenous proteins (Figure 18 B), clearly co-localized in the tested cell lines. In addition, this co-localization was related to replication sites as visualized by association with PCNA (Figure 19), thus suggesting that the CPC is located at heterochromatic regions during replication.

Constitutive heterochromatin is formed at telomeres, centromeres and repetitive elements (Elgin and Grewal, 2003; Grewal and Jia, 2007). To investigate the specific heterochromatic site, the

anti-centromere immunserum CREST was used. In human cells, Aurora B accumulated in specific CREST-positive foci and even protruded from CREST signals (Figure 20), suggesting a centromeric and surrounding pericentric localization. In combination with detection of replication sites, Aurora B was detectable in three types of nuclear localizations, namely at centromeres detected by CREST staining, at some EdU-positive replication sites and in solitary foci without EdU or CREST staining (Figure 21 A). This suggests that the CPC is localized at (peri-)centromeric heterochromatin during S phase, but that it can also be found at some other heterochromatic regions at actively replicated DNA or at DNA which was already or which still needs to be replicated. The localization was confirmed in mouse NIH3T3 cells at replication sites in Hoechst-dense chromocenters, consisting of pericentric heterochromatin and CREST-positive centromeric chromatin spots at their periphery (Guenatri et al., 2004). Aurora B could be detected in close proximity to these regions and mostly, PCNA and Aurora B co-localized at chromocenters (Figure 21 B). Taken together, this reinforces the hypothesis that the CPC is located at centromeric and pericentric heterochromatin during replication. Accumulation of Aurora B at chromocenters in NIH3T3 cells during G_2 phase was also demonstrated by Crosio et al. (2002), whereby Aurora B co-localized with phosphorylated H3 at centromeric regions.

Similar to the localization of the CPC during S phase observed in this thesis, CPC members also accumulate in nuclear foci, and more precisely, at centromeric heterochromatin after irradiation (Schröder, doctoral thesis, 2014). Irradiation-induced accumulation seems to depend on a Crm1-Survivin interaction (Schröder, doctoral thesis, 2014), which is also necessary for centromeric targeting of the CPC during early stages of mitosis (Knauer et al., 2006, 2007a). However, whether the CPC accumulation at heterochromatin domains during replication also depends on an interaction with the export receptor Crm1, requires further evaluation.

4.1.3 CPC interactions during replication

Until now, interactions of the CPC with chromatin where detected during G_2/M transition and mitosis. During G_2/M transition, INCENP (Ainsztein et al., 1998; Kang et al., 2011) or Borealin (Liu et al., 2014) bind to HP1, which in turn associates with H3K9me3. This interaction is abolished via phosphorylation of H3S10 by Aurora B (Hsu et al., 2000), leading to the dissociation of HP1 from chromatin (Fischle et al., 2005; Hirota et al., 2005). The centromeric localization during mitosis depends on two overlapping histone modifications. On the one hand, Survivin's BIR domain directly binds to H3T3p (Kelly et al., 2010), and on the other hand Survivin (Kawashima et al., 2007) or Borealin (Tsukahara et al., 2010) can indirectly associate with histone H2A phosphorylated at T120 via binding to Shugoshins Sgo1 and Sgo2. So far, an interaction between CPC members and replication proteins was not described in literature. In order to address the question, if the CPC is bound to the replisome or to heterochromatin, an iPOND assay was performed. This assay allows a high-resolution spatiotemporal analysis of proteins at replication forks or on chromatin following DNA replication in cultured cells, whereby the spatial and temporal resolution depends amongst others on chromatin fragment size (Sirbu et al., 2012). Sonication of the samples led to a DNA fragment size smaller than 300 bp (Figure 22 B), perfectly consistent with the optimal range as postulated by Sirbu et al. (2012). In contrast to Aurora B, Survivin appeared to be bound to nascent DNA, as detected in the Click eluate (Figure 22 C). Wether Aurora B is not bound to nascent DNA or whether the lack of

interaction was due to an insufficient protein amount needs to be further evaluated. Nevertheless, the latter is a pertinent explanation as in comparison to the input-eluate ratio of Survivin, the amount of Aurora B in the input samples was considerably decreased and thus potentially under detection level. While Survivin seems to be bound to the newly synthesized DNA strand in the vicinity of the replisome, it is still unknown whether this link is provided through an interaction with chromatin or with replication proteins, respectively. Unfortunately, this question could not be answered so far, because in the iPOND performed in combination with a subsequent thymidine chase, the CPC members could be designated neither as replisome-associated nor chromatin-associated proteins due to their absence in the eluate samples (Figure 23). Due to the low levels of the CPC proteins detectable by immunoblot, the iPOND should be coupled to mass spectrometry analysis instead to improve the detection of low abundant proteins bound to nascent DNA.

To further characterize the interactions of the CPC and to evaluate if its binding to nascent DNA is mediated via the replisome or the chromatin, we focused on proteins co-localizing with the CPC during replication. CPC members co-localized with the sliding clamp PCNA (Figure 15, Figure 16, Figure 19, Figure 21), and Survivin was detected on newly synthesized DNA (Figure 22). PLA analysis demonstrated a close proximity (< 40 nm) of all CPC members to PCNA (Figure 24), indicating an interaction of the CPC with PCNA. Decreased signals for the INCENP-PCNA interaction are maybe due to spatial arrangements of antibody epitopes or the size of the antibodies (IgG size approximately 10 nm; Yeo et al., 2015), so that connector oligos are not always able to connect the antibody nucleotide tails. The data obtained by immunofluorescence and PLA suggest an interaction between PCNA and the CPC proteins and was further confirmed by co-immunoprecipitation (Figure 25). In contrast to Survivin-HA, Aurora B-HA as well as Borealin-HA and myc-INCENP were detected in immunoprecipitates of PCNA, although a high amount of Survivin-HA was detected in the input samples. This is not in agreement with the aforementioned results of the PLA analysis, which revealed an interaction of all CPC members with PCNA. Complex formation without Survivin is highly unlikely as previous studies have demonstrated that depletion of one CPC member leads to reduced levels of the other CPC members, indicating that the protein interactions within the complex stabilize the individual CPC members (Honda et al., 2003; Vader et al., 2006).

To clarify which CPC member binds to PCNA directly, the sequences of the respective CPC members were screened for typical PCNA binding motifs. Most interactions with PCNA are mediated by an APIM (AlkB homolog 2 PCNA-interacting motif) or a PIP (PCNA-interacting protein) box motif in the interacting protein (Gilljam et al., 2009; Warbrick, 2000). Indeed, a putative PIP box motif was found in the human protein INCENP (aa 853 to aa 860; Figure 26 B), located at its C-terminus, which also interacts with Aurora B (Figure 26 D). This binding motif is also conserved in several INCENP homologs ranging from chimpanzee (*P. troglodytes*), mouse (*M. musculus*) and chicken (*G. gallus*) to frogs (*X. tropicalis* and *X. laevis*) (Figure 26 C). The motif was verified by PLA analysis in T2AA-treated cells. T2AA is a small molecule binding to a deep cavity of PCNA, which usually interacts with the PIP box in binding partners, thereby inhibiting the interaction (Inoue et al., 2014; Punchihewa et al., 2012). As expected, T2AA treatment reduced the mean PLA signal intensity compared to non-inhibited S phase cells (Figure 27). The PIP box motif could additionally be confirmed by co-immunoprecipitation,

where an INCENP variant bearing a mutated PIP box motif was not able to bind to PCNA. Here, the signals for the INCENP variant with a mutated PIP box motif decreased more than those of INCENP wt. However, an unspecific binding to beads was detected, similar to the co-IPs with other CPC members. DNA or RNA, which adhere to basic surfaces on proteins, can cause unspecific binding to beads. This can be especially problematic with proteins such as PCNA that naturally bind DNA (Nguyen and Goodrich, 2006). Supporting experiments, using different magnetic or sepharose beads, various IP lysis buffer receipts or additional treatment with micrococcal nuclease for chromosomal DNA fragmentation were not successful in abolishing unspecific protein binding (data not shown). Furthermore, also benzonase or ethidium bromid could be tested instead of micrococcal nuclease. Additional improvements might include pre-clearing of lysates by incubating the lysates with beads alone before using the supernatant for the IP. Despite the unspecific bindings observed in co-IPs, our results hint towards a direct interaction between PCNA and INCENP via its PIP box motif. However, immunofluorescence stainings revealed PCNA co-localization with both INCENP variants (wt and PIPmut) (Figure 29). This in turn suggests that the CPC interacts with PCNA, but foci formation might be independent of PCNA interaction. The recruitment of the CPC to replication sites is potentially mediated by another binding partner or by direct binding to chromatin.

Because previous studies revealed an interaction between either INCENP or Borealin with a HP1 dimer during G_2/M transition (Ainsztein et al., 1998; Kang et al., 2011; Liu et al., 2014), co-immunoprecipitation studies including HP1α and the CPC proteins were performed. While HP1α was not detected when differently tagged CPC members where immunoprecipitated (Figure 30 A), the reciprocal experiment showed that Borealin-HA bound to HP1α (Figure 30 B). Furthermore, it should be mentioned that Survivin and Aurora B bound unspecifically to the beads. In further experiments, this unspecific binding needs to be eliminated, for example by implementing the above-mentioned procedures such as DNA fragmentation by benzonase or ethidium bromide treatment or pre-clearing of lysates. In addition, the interaction should be confirmed in synchronized S phase cells to exclude interactions between HP1α and the CPC proteins that occur during other cell cycle phases and are not associated with the process of replication. Finally, the potential binding sites responsible for these interactions specifically during replication need to be identified. One potential interaction domain is a PxVxL motif, which was shown to be crucial for Borealin and INCENP binding to the CSD domain in HP1 during G_2/M transition (Ainsztein et al., 1998; Kang et al., 2011; Liu et al., 2014).

Previous studies by Trembecka-Lucas et al. (2012, 2013) revealed an interaction between a HP1β homodimer and PCNA. The complex forms when cells exit G_1 phase, which correlates with the changes in localization of PCNA during S phase. The complex was also detected at DNA damage sites caused by laser-induced microirradiation. They however did not evaluate, if other HP1 isoforms, namely HP1α and HP1γ might also be able to interact with PCNA. While a HP1β monomer was also able to form a complex with PCNA, cells failed to complete S phase when dimerization of HP1 was prohibited, indicating that a complex of monomeric HP1 together with PCNA is functionally impaired. The C-terminal CSD domain of HP1 can dimerize forming both homo- and heterodimers with a nonpolar groove that acts as a docking site for proteins containing the consensus sequence PxVxL. As a result, HP1 can bind several other PxVxL motif containing proteins, e.g. chromatin-modifying proteins (SUV39H1,SETDB1), DNA

replication and repair proteins (CAF1, Ku70, BRCA1, ORC1-6) (Lomberk et al., 2006) and the CPC members Borealin and INCENP (this study; Kang et al., 2011; Liu et al., 2014). The interaction between HP1β and PCNA was analysed with FRET experiments by Trembecka-Lucas et al. (2013), however a direct interaction or binding sequence was not shown. As due to physical properties of the FRET technique, only protein binding proximities of approx. 10 nm are accessible, an indirect binding mediated by a small linking protein is still possible. One concept (Figure 38) combining all the above discussed proteins would include the binding of PCNA to the PIP box motif in INCENP, which in turn binds Aurora B at its C-terminus, while the N-terminus interacts with Survivin and Borealin's N-terminus via the three-helix bundle. The C-terminal part of Borealin, which is not involved in complex formation and contains a PxVxL motif, could bind to HP1, thereby bringing it in close proximity to PCNA.

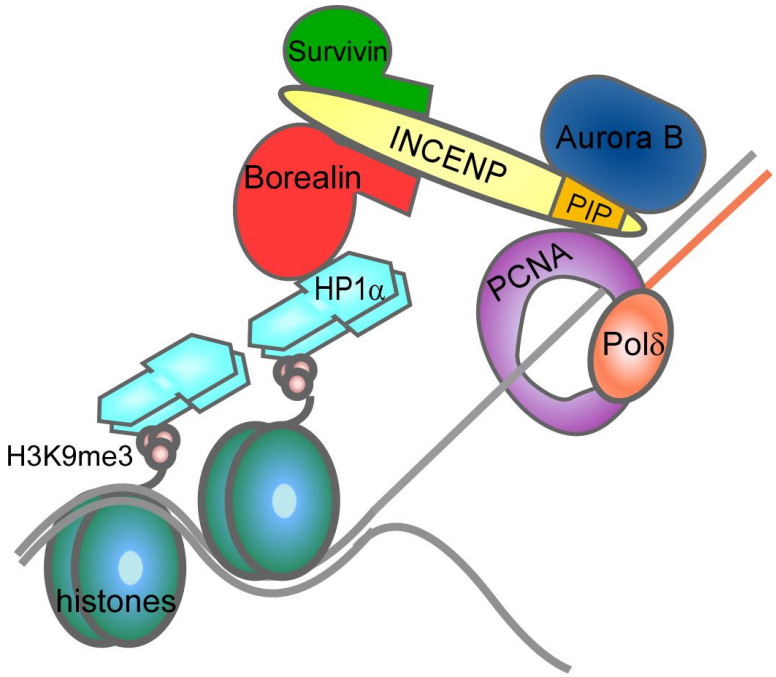

Figure 38: Modell of CPC interactions to PCNA and HP1α.
PCNA can interact with the PIP box motif in INCENP, which in turn binds Aurora B at its C-terminus. INCENP's N-terminus interacts with Survivin and Borealin's N-terminus via the three-helix bundle while the C-terminal part of INCENP could bind to HP1 and thereby bringing it in close proximity to PCNA.

4.2 Participation of the CPC in replication

During mitosis and also cytokinesis, the localization of the CPC changes dynamically in accordance with its various functions. In this thesis, a centromeric localization of the CPC during S phase and an interaction with HP1α at replication sites could be substantiated. Furthermore, the co-localization and interaction of the CPC with PCNA suggests that the CPC might have an additional, so far unknown, functional role during replication. To evaluate whether the CPC could be functionally implicated in replication processes, flow cytometry was performed to analyze the cell cycle-dependent distribution of Survivin-depleted cells. The percentage of cells in G_2/M phase increased dramatically while the amount of S and G_1 phase cells decreased when depleted of Survivin (Figure 31). In contrast to these results, other studies revealed an additional S phase arrest, suggesting a role of Survivin in promoting S phase entry (Dai et al., 2011; Suzuki et al., 2000). Furthermore, depletion or inhibition of Aurora B can result in a delayed G_1/S transition (Trakala et al., 2013). So far, there was no evidence for a direct involvement of Aurora B or Survivin in replication, but rather for a participation in cell cycle regulation. Recent data suggest that Aurora B directly phosphorylates p53 to accelerate its proteasomal degradation, thus suppressing the expression of cell cycle inhibiting targets, e.g. p21 (Gully et al., 2012). Indeed, p21 is upregulated after Aurora B inhibition (Trakala et al., 2013), which in turn inhibits cyclin E/CDK2 and thereby initiates G_1/S transition (reviewed by Karimian, Ahmadi, & Yousefi, 2016). While the N-terminal domain of p21 is responsible for CDK-cyclin inhibition, the C-terminus harbours a PIP box motif and can bind to PCNA (Chen et al., 1995; Luo et al., 1995; Warbrick et al., 1995), thus additionally inhibiting S phase (Cayrol et al., 1998). Phosphorylation of p21 on Thr145 by Akt inhibits its PCNA binding, thus promoting cell cycle progression by interaction of DNA polymerases with PCNA and other replication proteins to assure proper DNA synthesis (Rössig et al., 2001). Whether binding of p21 to PCNA also competes with the INCENP-PCNA interaction analyzed in this thesis, requires further elucidation. In addition to the above-mentioned regulation of the G_1/S transition, p21 might also inhibit CDK1 and arrest G_2/M transition (reviewed by Karimian, Ahmadi, & Yousefi, 2016). A G_2/M arrest was also observed by flow cytometry as shown in this thesis. Similar results could be also obtained through Survivin depletion via modified siRNAs (Li et al., 2015b) or micro RNAs (Chen et al., 2016). The accumulation of cells in G_2/M could depend on the blockage of the G_2/M transition and mitotic arrest by checkpoint activation and failure of chromosome segregation or cytokinesis. Indeed, mitotic defects were visualized in previous studies, including lagging chromosomes that were sister chromatids left near the spindle equator in anaphase as well as an absent spindle midzone and lacking midbody microtubules (Yang et al., 2004). Survivin-depleted cells fail to complete cytokinesis and further duplicate their genome in S phase, resulting in polyploid cells (Li et al., 1999; O'Connor et al., 2000). This could also be observed in the flow cytometry data shown here by an additional 8 N peak. Impaired DNA replication normally activates the intra S checkpoint, resulting in an S phase arrest. However, the amount of S phase cells was decreased following Survivin depletion. This does not exclude a functional role of the CPC during replication. It is possible that Survivin depletion might not lead to an activation of the S phase checkpoint. Instead, replication occur but might be incomplete. This would activate the G_2/M checkpoint, which in turn results in an accumulation of cells in G_2. Furthermore, an impaired replication can also be caused by chromosomal defects induced by interfering with Survivin's mitotic function. Consequently, the mitotic and a potential

replicative dysfunction can not be distinguished from each other. One possibility to overcome this problem is to synchronize cells in G_1 phase, deplete Survivin during the arrest, and analyze the following S phase after the release. However, with cell synchronization the cell cycle is already affected, so that thus obtained data could be flawed by the cell cycle arrest or due to Survivin depletion. Another more favorable but also more laborious solution would be to adopt the novel auxin-inducible degron (AID) technology (Figure 39), which allows rapid protein depletion within minutes up to only a few hours, instead of the days needed for a conventional silencing technique utilizing siRNAs. The mAID system, developed by Natsume et al. (2016), uses a plant degradation system controlled by the phythormone auxin. The target gene is modified via CRISPR/Cas, so that the respective protein is fused with a mAID-tag, derived from the IAA17 protein of *Arabidopsis thaliana*. These AID mutants are generated in cell lines expressing OsTIR1. OsTIR1 is an auxin perceptive F-box protein, which forms a functional SCF (Skp1-Cullin-F-box) ubiquitin ligase. Auxin, added to the cell culture medium, binds to OsTIR1, promoting mAID-TIR1-SCF interaction. This leads to polyubiquitination and proteasomal degradation of the target protein, typically with a half-life of 10-20 min. As revealed by flow cytometric analyses, the knockdown phenotype could not be rescued completely (Figure 31), maybe due to suboptimal expression levels of the ectopic Survivin or off-target effects of the siRNA.The latter are negligible when using the AID system because OsTIR1 and AID-substrate orthologues do not exists in human cells (Wood et al., 2016).

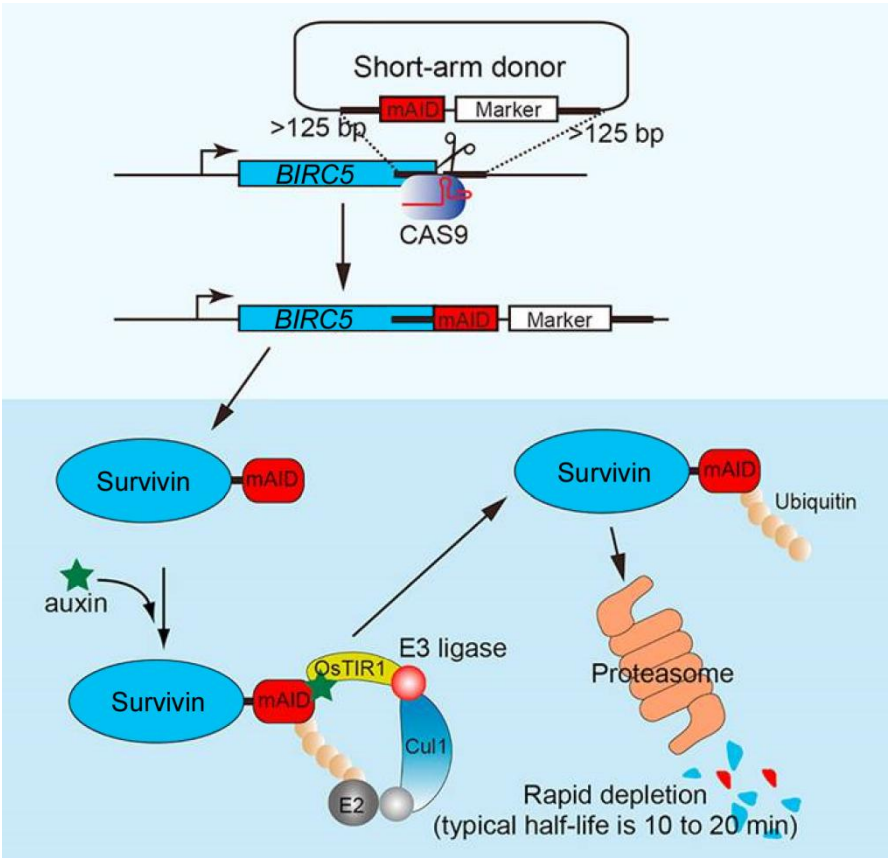

Figure 39: Overview of prospective protein depletion by the auxin-inducible degron system.
The target gene *BIRC5* will be modified via CRISPR/Cas, thus the protein Survivin is fused with a mAID-tag. Auxin addition will promote mAID-TIR1-SCF interaction, leading to polyubiquitination and rapid proteasomal degradation of Survivin. Modified from Natsume et al. (2016).

So far, analyses presented in this thesis revealed an accumulation of CPC proteins in the nucleus during S phase, co-localizing with the replicative sliding clamp and processivity factor PCNA, interacting via a PIP box motif in INCENP. All these results suggested a functional role of the CPC in replication. While flow cytometry only relies on measuring the overall rates of DNA synthesis to determine the complex replication program, fiber assay analyses allow investigating the replication fork dynamics on a single molecule level. Different aspects of replication can be observed, including new initiation events, termination events and stalled, collapsed as well as elongating forks. In this thesis, only elongating forks were covered by the investigation. Forks travel at a speed of 0.88 kb/min in mock-treated cells and 0.92 kb/min in siCtrl-transfected cells, whereas forks in Survivin-depleted cells are significantly slower (0.70 kb/min) (Figure 32). In addition, the distribution of fork velocities in the histogram plot revealed an increased number of slower forks after Survivin depletion.

Slowing of replication forks can be caused by several events. First, a slower polymerase results in a decelerated incorporation of nucleotides. Although average rates of leading and lagging strand DNA synthesis are similar, the incorporation rate of individual DNA polymerases can vary 10-fold and might also pause (Graham et al., 2017). Furthermore, core polymerases can be replaced when the replisome encounters obstacles at forks (Muñoz and Méndez, 2017; Prakash et al., 2005). The TLS polymerase PrimPol additionally assists in fork progression in unperturbed S phase (Mourón et al., 2013). Whether Survivin might influence the processivity of polymerases or polymerase switching could be analyzed by evaluating if TLS polymerases are bound to PCNA after Survivin depletion. It could also be investigated indirectly by assessing the PTM status of PCNA, as TLS polymerases are bound by PCNA, mono-ubiquitinated at Lys164 (Ulrich and Takahashi, 2013; Yang et al., 2013). In addition, replication fork speed can also be influenced by inhibition of origin firing or increased termination of forks. Therefore, initiation and termination rates as well as inter-origin-distances could be determined in dependence of Survivin expression. The inter-origin distance and thereby the origin density, correlate in general with fork velocities. At a lower origin density, the inter-origin distance is increased and the replication fork progresses faster, and *vice versa*, at a high origin density, the inter-origin decreases and forks progress slower (Conti et al., 2010; Takebayashi et al., 2005). Under normal circumstances, only 10 % of the licensed origins actually fire, all others are so-called dormant origins and are passively replicated by forks emanating from flanking origins (Ma et al., 2015). If replication is impaired, for example after fork stalling or fork collapse, neighboring dormant origins are allowed to fire (Kawabata et al., 2011). Although replication initiation sites share common characteristics, no consensus sequence has been identified in the human genome (reviewed by Alver, Chadha, & Blow, 2014). It is still unknown how origins are selected for the accumulation of licensing proteins, and how licensed origins are selected to fire. To study dormant origin firing, the replication events at the human *beta-globin* locus (HBB) could be observed. The locus consists of two regions, Rep-P and RepI, that are actively replicated either in early or in late S phase, as well as a locus control region (LCR), which is replicated passively under normal conditions (Conti et al., 2010; Zhang et al., 2016). Thus, origin activation within the LCR analyzed by RT-PCR on nascent strand DNA (Conti et al., 2010) could give valuable insights into Survivin's function in regulation of dormant origins.

The fact that the CPC was located at heterochromatic regions during S phase, indicates a possible involvement in the regulation of the replication of centromeric heterochromatin. As a pivotal determinant of replication fork velocity, the compaction status of chromatin should be evaluated upon depletion of the CPC members. Heterochromatin is characterized by a highly compacted structure, which relies on trimethylation of histone H3 at Lys9, the docking site for HP1. Here, a co-localization between HP1α and the CPC was observed and moreover, an interaction between HP1α and Borealin could be demonstrated. CPC localization could be further investigated after the disruption of pericentric heterochromatin by 5-AzaC (5-azacytidine) treatment, which causes decreased DNA methylation. Another common characteristic of heterochromatin is that it is usually hypoacetylated. Behind the replication fork, repressive chromatin must be re-established, which is mediated by histone deacetylases (HDACs). HDACs are recruited to the replication fork by binding directly or indirectly to PCNA. (Milutinovic et al., 2002; Rowbotham et al., 2011). Inhibition or depletion of HDACs also slows down replication forks (Conti et al., 2010; Peixoto et al., 2012) and disturbs centromeric localization of the CPC during mitosis, leading to severe mitotic defects (Stevens et al., 2008; Taddei et al., 2001; Unruhe-Knauf and Knauer, 2017). Whether HDAC inhibition, for example via TSA (Trichostatin A) or SAHA (suberoylanilide hydroxamic acid), also disrupts centromeric localization of the CPC during replication needs to be further investigated. If the normal compaction pathway is defective, histone H4K12 is acetylated at pericetric heterochromatin by Tip60 (tat-interacting protein 60). A loss of Tip60 leads to decompaction of heterochromatin and defects in chromosome segregation in mitosis (Grézy et al., 2016). Tip60 acetylates Aurora B on Lys125 in mitotic cells to prevent PP2A-dependent dephosphorylation of Aurora B at Thr232, a phosphorylation event that is required for optimal catalytic activity at kinetochores (Mo et al., 2016). If Tip60 regulates Aurora B activity analogously during replication is unknown. Whether Aurora B kinase activity influences the replication fork speed was also evaluated by fiber assay analyses (Figure 33). Here, cells were treated with the Aurora B specific inhibitor Hesperadin. This indolinone compound interacts with both the ATP- and the adjacent hydrophobic binding pocket of Aurora B (Hauf et al., 2003; Sessa et al., 2005). In untreated cells, Aurora B's autophoshorylation at Thr232 leads to full kinase activity, and thereby to phosphorylation of histone H3 at Ser10 at the transition from G_2 to M phase. While Aurora B phosphorylation was also detectable in samples where Aurora B was inhibited, phosphorylation of H3S10 was absent after treatment (Figure 33 B). This was maybe caused by unspecific binding of the antibody to non-phosphorylated Aurora B, as the latter implies a successful inhibition of the kinase activity during G_2/M phase. In contrast to Survivin-depletion, replication fork speed was not significantly reduced after inhibiton of Aurora B (Figure 33 C), thus implying that kinase activity is not necessary for proper replication. The CPC could for example act as a recruitment or binding platform for other interaction partners involved in replication.

In addition, also nucleosome assembly is coupled to the replication fork progression. Mejlvang et al. (2014) showed that replication fork velocity depends on the supply of new histones and efficient nucleosome assembly, which in turn regulate PCNA unloading. The histone chaperone CAF1 links nucleosome assembly to DNA synthesis by binding to PCNA (Shibahara and Stillman, 1999). In addition, CAF1 forms a complex with HP1α and SETDB1, which monomethylates histones so that CAF1 can deposit them into chromatin (Loyola et al., 2009;

Sarraf and Stancheva, 2004). Further, H3K9me1 is trimethylated by SUV39H1/H2, allowing HP1α to bind via its chromodomain and re-establish the heterochromatin state (Lachner et al., 2001; Loyola et al., 2009). Because the CPC accumulated on the chromatin during late S phase when the heterochromatin is replicated and re-established, and HP1 is directly or indirectly bound to PCNA via the CAF1 complex, the question arises whether the CPC is somehow involved in the maintenance of heterochromatin on nascent DNA. That the CPC localizes and/or interacts with some of these proteins also corroborates this potential function. Recent studies could further show that for the re-establisment of the heterochromatin state during replication also non-coding RNAs (ncRNAs) are required. One example are centromere repeat-associated small interacting RNAs (crasiRNAs). CrasiRNAs are only 34–42 nt in length, and they are important for centromere establishment and chromosome segregation. They have been identified in CENP-A-rich regions. The mechanism by which they regulate centromere function is still unknown, but it is assumed that crasiRNAs trigger H3K9 methylation and HP1 binding (reviewed by Sadakierska-Chudy & Filip, 2015). Blower (2016) could show in *Xenopus egg* extracts that these crasiRNAs bind to the CPC via Aurora B during mitosis and regulate localization and activation of the CPC. Whether crasiRNAs also link CPC localization to centromeres still needs to be investigated.

In addition, chromatid cohesion can have an impact on replication fork speed. Cohesin consists of four SMC (Structural maintenance of chromosome) subunits (Losada et al., 1998; Michaelis et al., 1997). The complex is loaded onto chromatin already during G_1 phase (Takahashi et al., 2008). During replication, the replisome slides through this ring and the two daughter strands are embraced by the cohesin complex (Alabert and Groth, 2012). PCNA binds ESCO1/2 (Establishment of sister chromatid cohesion 1/2), which acetylates SMC3, a subunit of the SMC complex and thereby accelerates the replication fork (Terret et al., 2009). Sister-chromatid cohesion is established in S phase and it persists until mitosis when sister chromatids are captured by microtubules from opposite poles. As mentioned before, the CPC is necessary for correct kinetochore-microtubule attachments by ensuring their bi-orientation. Recent findings have shown that stable bi-orientation requires CPC localization via the CEN-box in the N-terminal domain of INCENP and its loss weakens centromeric cohesion, so that the CPC prevents premature sister chromatid separation (Hengeveld et al., 2017). When all chromosomes are correctly attached, PP2A counteracts Aurora B-mediated phosphorylation events by dephosphorylating respective targets, thereby resulting in cohesin cleavage and chromatid separation (Foley et al., 2011; Shrestha et al., 2017; Trinkle-Mulcahy et al., 2006). Both, PP2A and the CPC can bind to Sgo1, which in turn binds to HP1 (Kang et al., 2011). Whether the CPC plays a role in promoting sister chromatid cohesion during S phase, or whether a subset of CPC proteins is necessary for maintaining cohesion from S phase to mitosis is still unknown.

Although, we could show that the CPC accelerates the replication fork, the detailed molecular mechanism is still under investigation. Potentially, binding of the CPC to centromeric heterochromatin and/or to the sliding clamp PCNA influences the replication itself or replication-associated processes. Further studies should also focus on the PIP box motif in INCENP. One question that should be addressed here is whether mutation of the PIP box also affects replication fork speed and subsequent cell divisions.

4.3 CPC expression and localization after induction of replication stress

As demonstrated here by fiber assay analysis, the depletion of Survivin resulted in a decreased replication fork velocity. The slowing or stalling of replication fork progression and/or DNA synthesis is defined as 'replication stress' (Zeman and Cimprich, 2014). Since Survivin depletion causes replication stress, the question arises whether induced replication stress reversely affects the CPC. Replication stress is caused by intrinsic and extrinsic factors. Challenging intrinsic obstacles are for example genomic sequences, which are difficult to replicate such as repeated sequences of centromeres (Pearson et al., 2005). Here, it was also shown that the CPC is located at centromeric regions during late S phase, when these sequences are replicated. Extrinsic damage sources can be UV-light, ionizing radiation or chemicals. The endogenous or exogenous agents challenge DNA replication forks and cause DNA lesions. Replication forks can stall or collapse at these damaged regions, leading to ssDNA stretches or DSBs that could trigger genome instability. Both events result in the activation of checkpoint kinases and initiate the subsequent activation of the signaling cascade (section 151.3.2). To determine whether the CPC could also be implicated in processes after induction of replication stress, expression of CPC proteins and their localization to different cell compartments were analyzed (Figure 34).

Therefore, cells were treated with different chemicals or ionizing radiation. Camptothecin (CPT, 1 µM) binds to the TopoI-DNA complex and inhibits the re-ligation of the DNA, thereby sustaining the SSB. The collision with the subsequent replication fork generates DSBs (Pommier, 2006). Lower concentrations of CPT (25 nM) induce replication fork slowing and fork reversal to prevent chromosomal breakage. CPT activates both, ATR-Chk1 and ATM-Chk2 signaling (Ray Chaudhuri et al., 2012). Aphidicolin (APH) binds to DNA polymerases and thereby blocks the incorporation of nucleotides into the DNA strand, leading to replication fork stalling (Cheng and Kuchta, 1993). While the polymerase is inhibited, the helicase is still able to unwind the DNA (Sogo et al., 2002). This so-called uncoupling leads to long stretches of ssDNA and checkpoint activation by ATR-Chk1 (Byun et al., 2005). Hydroxyurea (HU) inhibits the ribonucleotide reductase so that the dNTP pool is depleted. This results in stalled forks and uncoupling of helicase and polymerase function similar to APH treatment (Jossen and Bermejo, 2013). After prolonged incubation, this might further result in collapsed forks and in DSBs (Petermann et al., 2010). Cisplatin mainly forms intrastrand crosslinks, which block uncoiling and separation of the DNA double helix (Fichtinger-Schepman et al., 1985). Damage response is triggered by ATM-Chk2 and ATR-Chk1 pathway, similar to TopoI treatment. Treatment with X-rays leads to SSB or DSB and induces stress response also via both signaling pathways (Maréchal and Zou, 2013).

Upon treatment or 1 h after irradiation, whole cell lysates and subcellular fractions were analyzed by immunoblotting (Figure 34). All treatments activated either one or both stress response pathways, except treatment with 25 nM CPT and cisplatin. Low CPT concentrations might have indeed induced replication fork slowing and fork reversal so that DNA damage could be prohibited as expected. However, cisplatin induced no damage response, suggesting that the treatment was unsuccesful. All CPC proteins showed similar expression levels in all

samples of whole cell lysates, indicating that the total protein quantity remains the same. Aurora B and Survivin were slightly increased only in the cytoplasmic fraction after CPT and APH treatment as well as after irradiation. Both nuclear chromatin fractions showed similar levels independent of the type of treatment.

The observation that irradiation did not enhance nuclear CPC proteins is contradictory to previous results, where it was shown that for example Survivin forms irradiation-induced nuclear foci at damage sites and further interacts with several proteins (γH2AX, Ku70, 53BP1 and DNA-PK_{CS}) involved in repair pathways (Reichert et al., 2011). In contrast, previous results of our working group also point to a nuclear enrichment of Survivin after irradiation in distinct foci but not directly at damage sites, where above-mentioned damage response proteins are located, but rather at centromeric heterochromatin in association with the other CPC members (Schröder, 2014, doctoral thesis).

An increased protein amount of Aurora B and Survivin in the cytoplasm after CPT and APH treatment as well as irradiation could be induced via upregulation of protein expression, but then the total protein amount would have increased as well. Previous studies have shown that for example Chk2 phosphorylates the transcription factor FoxM1 (forkhead box M1) after irradiation. This stabilizes the transcription factor and leads to a corresponding increased transcription of DNA repair genes and also to an increased transcription of cell cycle regulated genes such as those of Survivin and Aurora B (Grant et al., 2013; Tan et al., 2007). Additional analysis of CPC mRNA could indicate if transcription is enhanced after replication stress. Another possibility that might lead to increased levels of Aurora B and Survivin in cytplasmic fractions after replication stress is that both proteins could be exported from the nucleus into the cytoplasm, but then the content in the nuclear fraction would have decreased. Previous results have shown that Survivin has a conserved nuclear export signal (NES) that interacts with Crm1. In dividing cells, this NES is essential for tethering the CPC to the mitotic machinery and thus for proper cell division (Knauer et al., 2006, 2007a, 2007b). In addition, the Crm1-Survivin interaction is also required for the cytoprotective activity of Survivin. Export-deficient cells fail to protect tumor cells against chemo- and radiotherapy-induced apoptosis (Knauer et al., 2007b). Thus, Survivin might also be exported via Crm1 interaction after replication stress and could inhibit apoptosis so that the replication fork can be protected and restart or damage can be repaired. Thus, the impact of replication stress on the induction of apoptosis should be investigated in Survivin-depleted cells. Furthermore, it would also be of interest to identify whether prolonged replication stress that leads to apoptosis is negatively correlated with potential Survivin export processes. In addition, Aurora B's non-catalytic N-terminal domain was also suggested to bind to Crm1, thus accessing the Crm1-dependent nuclear export pathway similar to Survivin (Rannou et al., 2008; Rodriguez et al., 2006). Further experiments are necessary to evaluate for example whether general export inhibiton mediated for example by leptomycin B treatment could interfere with the potential Crm1-mediated export of Survivin and Aurora B after replication stress induction.

To confirm that the nuclear localization of the CPC is not alteres by induction of replication stress, immunofluorescence analyses were performed. Replication stress was again induced by treatment with 1 µM CPT for 1 h, and cells were either fixed directly or pre-extracted and fixed afterwards. Pre-extraction was used to remove the excess of proteins, which do not form

detectable foci, so that only chromatin bound proteins remain. CPT treatment successfully induced replication stress, as detected by an increased phosphorylation of the DNA damage response proteins γH2AX and pATM independent of pre-extraction or direct fixation (Figure 35 A-C). The standard deviation of the mean intensity of Survivin was significantly decreased in samples directly fixed after CPT treatment, whereas the values increased non-significantly when cells were pre-extracted (Figure 35 A, D). This indicates that while chromatin-bound Survivin is slightly enriched after replication stress induction, the overall and thereby the soluble nuclear fraction is reduced, maybe either by proteasomal degradation or by being exported into the cytoplasm as revealed by immunoblot. To clarify this, cell stainings should be combined with quantitative analyses of subcellular CPC localization. Whether the slightly increased nuclear fraction of Survivin is located at stalled replication forks or damage sites after replication stress induction still needs to be elucidated. In contrast, Aurora B expression was non-significantly increased in CPT-treated fixed samples, while it was not altered in pre-extracted samples after CPT treatment (Figure 35 A, E). Taken together, only marginal or no alterations were detected in nuclear protein expression of Survivin and Aurora B after induction of replication stress, corresponding to western blot analyses. So far, only nuclear protein levels were analyzed, but cytoplasmic levels should also be confirmed. Furthermore, in both experiments, western blot and immunofluorescence staining, only total protein amountsof Aurora B were analyzed. The amount of the active, phosphorylated form of Aurora B should also be determined, in order to evaluate if Aurora B's kinase activity is important for the damage response after induction of replication stress. Studies on ATM mainly focus on its function during DNA damage response, although an additional mitotic function was suggested by Yang et al. (2011). ATM is recruited to centromeres during mitosis and then activated by Aurora B-mediated phopshorylation, interestingly even in the absence of DNA damage. pATM in turn phosphorylates the kinetochore component Bub1 to activate the spindle assembly checkpoint (Yang et al., 2011). Whether Aurora B is active after replication stress and could also phosphorylate ATM still needs to be elucidated.

Until now, replication fork velocity alterations upon Survivin depletion indicate a functional role in replication or replication-associated processes. Not only comprehensive fiber assay analyses concerning initiation and termination could allow deeper mechanistic insights into its functional role, but these assays should also include induction of replication stress. It would be of interest to determine whether the depletion of CPC members affects for example the amount of stalled forks after replication stress, the ability of stalled forks to restart again, or replication fork collapses.

Replication stress can lead to replication fork stalling, whereby dedicated factors can stabilize the fork while other factors resolve the replication block and facilitate the resumption of elongation. If the replication fork cannot be protected, the replisome dissociates and the fork collapses (Rowlands et al., 2017). In this case, replication stress leads to a functional uncoupling of the helicase complex from the replicative polymerase (Byun et al., 2005). When the replication fork progression continues in the absence of processive DNA synthesis, long patches of ssDNA covered with the single strand binding protein RPA are created. Proteins involved in the elongation step of DNA synthesis (e.g. PCNA, polymerase δ, DNA ligase 1 and Fen1) dissociate from replication sites (Görisch et al., 2008) and the fork collapses. Chromatin

assembly is also coupled to DNA synthesis by the interaction of the sliding clamp PCNA with CAF1 (Shibahara and Stillman, 1999). CAF1 not only binds to PCNA but also to the heterochromatin protein HP1α (Murzina et al., 1999). Since it was demsonstratzed here that the CPC can interact with PCNA and HP1 and its expression does not change within the nucleus after induction of replication stress, the question arises what happens with the CPC after helicase-polymerase-uncoupling. To address this, cells were incubated with EdU, first alone to visualize active DNA synthesis and afterwards additionally with high-dose APH to induce uncoupling of the helicase from the polymerase. Following treatment, the localization pattern of several proteins in S phase cells (EdU positive cells) was examined (Figure 36). As expected, Mcm2, a member of the heterohexameric helicase complex, did not alter its localization after APH treatment. RPA32, a subunit of the single strand binding protein revealed an increased focal accumulation after APH treatment, which indicates that longer ssDNA sequences are present and covered within minutes by RPA. In contrast, PCNA and DNA Ligase I were no longer present in discrete foci but instead diffusely distributed throughout the nucleus. So far, these results agree with Görisch et al. (2008). If replication forks stall, PCNA can be mono-ubiquitinated on Lys164, a modification that plays an important role in translesion synthesis, while poly-ubiquitin chains also attached to Lys164 are required for the damage bypass mechanism (reviewed by Shiomi & Nishitani, 2017). In addition, PCNA SUMOylation on the same lysine residue can either inhibit DSB repair by HR or prevent the formation of DSB at stalled forks (Gali et al., 2012). In contrast, high-dose APH treatment induced fork collapse and replisome dissociation. In this case, PCNA is removed by the Elg1-RFC complex (Elg1 called ATAD5 in human) in an ATP-dependent manner (Kubota et al., 2013; Lee et al., 2013; Shiomi and Nishitani, 2013), which should also lead to removal of DNA ligase I (Dewar and Walter, 2017). Checkpoint activation is induced by long stretches of RPA generated by polymerase-helicase uncoupling. Instead of PCNA, the checkpoint clamp Rad9-Rad1-Hus1 (9-1-1 complex) is loaded by clamp loader Rad17-RFC (Bermudez et al., 2003). Rad9 contains an unstructured C-terminal tail, which is required for interaction with TopBP1 and stimulates ATR-mediated Chk1 phosphorylation (Delacroix et al., 2007; Yan and Michael, 2009). The above-mentioned experiments revealed that the histone chaperone CAF1 changed its localization from bright nuclear foci to a diffuse distribution, whereas HP1 did not alter its localization pattern after APH treatment compared to the DMSO control. This indicates that although CAF1 can bind to both PCNA and HP1, the interaction to PCNA might have a greater influence on replication than that to HP1.

The CPC proteins still accumulated after treatment with APH, which induced polymerase stalling and uncoupling of the replication machinery, similar to above-mentioned results of replication fork stalling detected by immunoblot and subcellular fractionation as well as by immunofluorescence staining upon CPT treatment. This suggests that even if the CPC can bind to PCNA, this interaction seems not to be sufficient for targeting to replication sites. Either the CPC could also be uncoupled from the polymerase and move further along the DNA together with the helicase, or it might be coupled to chromatin or other remaining chromatin-bound proteins. One other possibility is that the CPC could bind to the checkpoint clamp 9-1-1. Although 9-1-1 is structurally similar to the homotrimeric ring-shaped PCNA, it alsoreveals substantial differences as it is built up from different subunits reflecting a specialization of function and binding partners. The subunits are arranged in a defined order, and binding

partners are consequently bound in an ordered arrangement, whereas PCNA can bind either the same or different proteins at each subunit in a stochastic manner. The majority of PCNA binding partners possess a PIP box motif, whichinteracts with a hydrophobic pocket at the interdomain connecting loop that bridges two domains of a single PCNA subunit. In contrast to PCNA, the mode of interaction of proteins to 9-1-1 is not completely understood. It appears that the binding to the 9-1-1 clamp is subunit-specific. While Rad9 could bind to a PIP box motif, Rad1 lacks a hydrophobic pocket and is therefore unlikely to interact with a PIP box containing protein, and for Hus1 the situation is even less clear (reviewed by Eichinger & Jentsch, 2011). Interestingly, Fen1, which binds to PCNA via the PIP box motif, can bind to 9-1-1 in a PIP box-independent as well as -dependent manner (Xu et al., 2009). In this thesis, it could be shown that INCENP also harbors a PIP box motif and mutation of essential amino acid residues indeed abolishes the interaction with PCNA. Whether INCENP is also able to bind to 9-1-1 should be further elucidated.

In response to DNA damage, alterations in chromatin organization facilitate the access of repair proteins to DNA (Adam et al., 2015). Similar to the arguments mentioned above regarding the capacity of CPC proteins to modulate replication fork speed, the CPCmight also be involved in the response to fork collapsing and the subsequent repair.

In general, replication stress leads to fork stalling or damaged forks, which in turn activates the replication checkpoint by phosphorylation of ATR and Chk1 (reviewed in Zeman & Cimprich, 2014). This damage or stress response pathway delays cell cycle progression so that stalled replication forks can be recovered, damaged DNA can be repaired, and replication can be completed before entry into mitosis (Lossaint et al., 2013; Magiera et al., 2014). In some cases of endogenous or low levels of exogenous replication stress or other types of DNA damage, the damage checkpoint is not activated (Koundrioukoff et al., 2013). Here, cells are not arrested in S phase and proceed into mitosis with under-replicated DNA or unresolved DNA structures (Chan et al., 2009; Naim and Rosselli, 2009). Moreover, this can initially lead to chromosomal and later to genomic instability and cancer (Burrell et al., 2013). Recent studies have shown that in cases of replication stress without checkpoint activation, for example induced by low levels of APH, DNA synthesis takes place even during mitosis (Bergoglio et al., 2013; Bhowmick et al., 2016; Minocherhomji et al., 2015). To determine whether the CPC is involved in DNA synthesis during mitosis, cells were synchronized in G_2 phase and simultaneously treated with a low dose of APH to induce replication stress. Cells were released to allow progression into prometaphase of mitosis in presence of EdU to visualize new DNA synthesis (Figure 37). In contrast to scheduled EdU incorporation during DNA replication in S phase, EdU incorporation into mitotic cells was only detectable when cells were treated with APH, indicating that DNA synthesis still occurs during mitosis. INCENP was associated with chromatin irrespective of whether or not the cells were exposed to APH. However, INCENP was not detected on newly synthesized DNA in mitotic cells, indicating that CPC members conduct their mitotic function without a relocation to replication sites.

Interestingly, previous studies by Minocherhomji et al. (2015) have shown that Plk1 inhibition impedes mitotic EdU incorporation, implying that DNA synthesis in mitosis occurs after or simultaneously with the release of cohesin from sister chromatid arms. In prophase, most cohesin is removed from chromosome arms in a process, which requires three kinases. Plk1

phosphorylates the SA2 subunit of cohesin (Hauf et al., 2005), and Aurora B as well as CDK1 phosphorylate Sororin (Nishiyama et al., 2013), a protein that stabilizes the cohesin complex, leading to release of cohesin from chromosome arms. Accordingly, inhibition of Aurora B for example by Hesperadin could also abolish the DNA synthesis during mitosis. To investigate this in more detail, an experiment resembling the one mentioned above could be performed under additional inhibition of Aurora B and a quantitative analysis of mitotic cells, which are able to replicate during M phase. As a last resort to repair or synthesize the remaining parts of DNA, resolving replication intermediates before sister chromatid separation and distribution to the daughter cells might ensure a stable propagation of the genome. Even unperturbed cells sometimes enter mitosis with under-replicated DNA, especially if replication stalls late during S phase. Centromeres are replicated during late S phase and due to their repetitive sequences and their molecular architecture prone to chromosome breakage and rearrangements (Mankouri et al., 2013). In addition, ultrafine DNA bridges originate from centromeres. These differ from anaphase bridges and lagging chromosomes because they do not contain histones and cannot be stained with conventional DNA intercalating dyes but can only be visualized by proteins that bind to them (Mankouri et al., 2013). Very recently, Hong et al. (2018) have shown in yeast that the nuclease LEM-3 (mammalian orthologue: Ankle1) is located to the midbody and can process these ultrafine bridges, while its localization is regulated by the Aurora B homolog AIR-2. Thus, resolution of replication intermediates could not only be influenced by Aurora B-dependent cohesin dissociation but also via Aurora B-dependent resolution of chromatin bridges. To further evaluate this aspect, a combination of Aurora B inhibition and induction of replication stress would be indispensable. Here, not only the above-mentioned amount of EdU-positive mitotic cells but also the number of cells with ultrafine bridges in mitosis can give valuable insights into the interplay between under-replicated DNA and its resolution to finally allow proper cell division.

4.4 Future prospective

In sum, the results on the CPC's novel role in replication and replication stress emphasize the concept of its multifunctional nature. The relationship between its mitotic function to successfully complete cell division and Survivin's additional anti-apoptotic function, in combination with the potential new tasks in replication and after replication stress, designate the CPC as promising target for cancer therapy. All targeted aspects might counteract its safeguard mechanism for genome integrity. Thus, targeting the CPC could lead to reduced proliferation and an enhanced apoptotic rate of cancer cells. The proposed functional involvement in replication and damage response after replication stress induction require further in-depth studies to finally end up with a mechanistic understanding of these elaborate processes on a molecular level. In order to separate the CPC's mitotic function from its replicative tasks, the above-mentioned auxin-inducible degron system should be established to allow a temporally defined depletion of CPC members. Thereby, it could be clarified whether both processes include independent functions or if one process might subsequently promote the other. Future comprehensive studies are undoubtedly needed to fully elucidate the replicative function of the CPC. For example, it would be utmost importance to understand how the interaction of the CPC members with HP1 and PCNA is regulated, which process associated with the depletion of CPC proteins actually leads to replication fork slowing and how the CPC is affected by replication stress. In sum, the above-mentioned and further studies can support the understanding of the CPC's functions and represent an important contribution to the improvement of cancer therapy.

References

Abbas, T., Sivaprasad, U., Terai, K., Amador, V., Pagano, M., and Dutta, A. (2008). PCNA-dependent regulation of p21 ubiquitylation and degradation via the CRL4Cdt2 ubiquitin ligase complex. Genes Dev. *22*, 2496–2506.

Abe, T., Sugimura, K., Hosono, Y., Takami, Y., Akita, M., Yoshimura, A., Tada, S., Nakayama, T., Murofushi, H., Okumura, K., et al. (2011). The histone chaperone facilitates chromatin transcription (FACT) protein maintains normal replication fork rates. J. Biol. Chem. *286*, 30504–30512.

Adam, M., Robert, F., Larochelle, M., and Gaudreau, L. (2001). H2A.Z is required for global chromatin integrity and for recruitment of RNA polymerase II under specific conditions. Mol. Cell. Biol. *21*, 6270–6279.

Adam, S., Dabin, J., and Polo, S.E. (2015). Chromatin plasticity in response to DNA damage: The shape of things to come. DNA Repair (Amst). *32*, 120–126.

Adams, R.R., Wheatleya, S.P., Gouldsworthy, A.M., Kandels-Lewis, S.E., Carmena, M., Smythe, C., Gerloff, D.L., and Earnshaw, W.C. (2000). INCENP binds the Aurora-related kinase AIRK2 and is required to target it to chromosomes, the central spindle and cleavage furrow. Curr. Biol. *10*, 1075–1078.

Adida, C., Haioun, C., Gaulard, P., Lepage, E., Morel, P., Briere, J., Dombret, H., Reyes, F., Diebold, J., Gisselbrecht, C., et al. (2000). Prognostic significance of survivin expression in diffuse large B-cell lymphomas. Blood *96*, 1921–1925.

Agami, R., and Bernards, R. (2000). Distinct initiation and maintenance mechanisms cooperate to induce G1 cell cycle arrest in response to DNA damage. Cell *102*, 55–66.

Aguilera, A., and Gaillard, H. (2014). Transcription and recombination: when RNA meets DNA. Cold Spring Harb. Perspect. Biol. *6*, a016543.

Ainsztein, A.M., Kandels-Lewis, S.E., Mackay, A.M., and Earnshaw, W.C. (1998). INCENP centromere and spindle targeting: Identification of essential conserved motifs and involvement of heterochromatin protein HP1. J. Cell Biol. *143*, 1763–1774.

Alabert, C., and Groth, A. (2012). Chromatin replication and epigenome maintenance. Nat. Rev. Mol. Cell Biol. *13*, 153–167.

Aladjem, M.I., and Redon, C.E. (2017). Order from clutter: selective interactions at mammalian replication origins. Nat. Rev. Genet. *18*, 101–116.

Albert Griffin, B., Adams, S.R., Jones, J., and Tsien, R.Y. (2000). Fluorescent labeling of recombinant proteins in living cells with FlAsH. Methods Enzymol. *327*, 565–578.

Albertson, D.G. (2006). Gene amplification in cancer. Trends Genet. *22*, 447–455.

Alexandrow, M.G., and Hamlin, J.L. (2005). Chromatin decondensation in S-phase involves recruitment of Cdk2 by Cdc45 and histone H1 phosphorylation. J. Cell Biol. *168*, 875–886.

Alfieri, C., Chang, L., Zhang, Z., Yang, J., Maslen, S., Skehel, M., and Barford, D. (2016). Molecular basis of APC/C regulation by the spindle assembly checkpoint. Nature *536*, 431–436.

Allen, C., Ashley, A.K., Hromas, R., and Nickoloff, J.A. (2011). More forks on the road to replication stress recovery. J. Mol. Cell Biol. *3*, 4–12.

Alonso, A., Hasson, D., Cheung, F., and Warburton, P.E. (2010). A paucity of heterochromatin at functional human neocentromeres. Epigenetics Chromatin *3*, 6.

Alushin, G.M., Ramey, V.H., Pasqualato, S., Ball, D.A., Grigorieff, N., Musacchio, A., and Nogales, E. (2010). The Ndc80 kinetochore complex forms oligomeric arrays along microtubules. Nature *467*, 805–810.

Alver, R.C., Chadha, G.S., and Blow, J.J. (2014). The contribution of dormant origins to genome stability: From cell biology to human genetics. DNA Repair (Amst). *19*, 182–189.

Ambrosini, G., Adida, C., and Altieri, D.C. (1997). A novel anti-apoptosis gene, survivin, expressed in cancer and lymphoma. Nat. Med. *3*, 917–921.

Asghar, U., Witkiewicz, A.K., Turner, N.C., and Knudsen, E.S. (2015). The history and future of targeting cyclin-dependent kinases in cancer therapy. Nat. Rev. Drug Discov. *14*, 130–146.

Athanasoula, K.C., Gogas, H., Polonifi, K., Vaiopoulos, A.G., Polyzos, A., and Mantzourani, M. (2014). Survivin beyond physiology: Orchestration of multistep carcinogenesis and therapeutic potentials. Cancer Lett. *347*, 175–182.

Ayoub, N., Jeyasekharan, A.D., Bernal, J.A., and Venkitaraman, A.R. (2008). HP1-β mobilization promotes chromatin changes that initiate the DNA damage response. Nature *453*, 682–686.

Banin, S., Moyal, L., Shieh, S., Taya, Y., Anderson, C.W., Chessa, L., Smorodinsky, N.I., Prives, C., Reiss, Y., Shiloh, Y., et al. (1998). Enhanced phosphorylation of p53 by ATM in response to DNA damage. Science *281*, 1674–1677.

Bannister, A.J., and Kouzarides, T. (2011). Regulation of chromatin by histone modifications. Cell Res. *21*, 381–395.

Bannister, A.J., Zegerman, P., Partridge, J.F., Miska, E.A., Thomas, J.O., Allshire, R.C., and Kouzarides, T. (2001). Selective recognition of methylated lysine 9 on histone H3 by the HP1 chromo domain. Nature *410*, 120–124.

Barnum, K.J., and O'Connell, M.J. (2014). Cell cycle regulation by checkpoints. Methods Mol. Biol. *1170*, 29–40.

Bartek, J., and Lukas, J. (2007). DNA damage checkpoints: from initiation to recovery or adaptation. Curr. Opin. Cell Biol. *19*, 238–245.

Bártová, E., Krejcí, J., Harnicarová, A., Galiová, G., and Kozubek, S. (2008). Histone modifications and nuclear architecture: a review. J. Histochem. Cytochem. *56*, 711–721.

Basant, A., Lekomtsev, S., Tse, Y.C., Zhang, D., Longhini, K.M., Petronczki, M., and Glotzer, M. (2015). Aurora B kinase promotes cytokinesis by inducing centralspindlin oligomers that associate with the plasma membrane. Dev. Cell *33*, 204–215.

Baskar, R., Dai, J., Wenlong, N., Yeo, R., and Yeoh, K.-W. (2014). Biological response of cancer cells to radiation treatment. Front. Mol. Biosci. *1*, 24.

Baumann, M., Krause, M., Overgaard, J., Debus, J., Bentzen, S.M., Daartz, J., Richter, C., Zips, D., and Bortfeld, T. (2016). Radiation oncology in the era of precision medicine. Nat. Rev. Cancer *16*, 234–249.

Beardmore, V.A., Ahonen, L.J., Gorbsky, G.J., Kallio, M.J., Plescia, J., Padgett, K.M., Tognin, S., Marchisio, P.C., and Altieri, D.C. (2004). Survivin dynamics increases at centromeres during G2/M phase transition and is regulated by microtubule-attachment and Aurora B kinase activity. J. Cell Sci. *117*, 4033–4042.

Beck, H., Nähse-Kumpf, V., Larsen, M.S.Y., O'Hanlon, K. a., Patzke, S., Holmberg, C., Mejlvang, J., Groth, A., Nielsen, O., Syljuåsen, R.G., et al. (2012). Cyclin-Dependent Kinase Suppression by WEE1 Kinase Protects the Genome through Control of Replication Initiation and Nucleotide Consumption. Mol. Cell. Biol. *32*, 4226–4236.

Bell, S.P., and Stillman, B. (1992). ATP-dependent recognition of eukaryotic origins of DNA replication by a multiprotein complex. Nature *357*, 128–134.

Bergoglio, V., Boyer, A.S., Walsh, E., Naim, V., Legube, G., Lee, M.Y.W.T., Rey, L., Rosselli, F., Cazaux, C., Eckert, K.A., et al. (2013). DNA synthesis by pol η promotes fragile site stability by preventing under-replicated DNA in mitosis. J. Cell Biol. *201*, 395–408.

Bermejo, R., Lai, M.S., and Foiani, M. (2012). Preventing Replication Stress to Maintain Genome Stability: Resolving Conflicts between Replication and Transcription. Mol. Cell *45*, 710–718.

Bermudez, V.P., Lindsey-Boltz, L.A., Cesare, A.J., Maniwa, Y., Griffith, J.D., Hurwitz, J., and

Sancar, A. (2003). Loading of the human 9-1-1 checkpoint complex onto DNA by the checkpoint clamp loader hRad17-replication factor C complex in vitro. Proc. Natl. Acad. Sci. U. S. A. *100*, 1633–1638.

Bernard, P., Maure, J.F., Partridge, J.F., Genier, S., Javerzat, J.P., and Allshire, R.C. (2001). Requirement of Heterochromatin for Cohesion at Centromeres. Science (80-.). *294*, 2539–2542.

Berti, M., and Vindigni, A. (2016). Replication stress: getting back on track. Nat. Struct. Mol. Biol. *23*, 103–109.

Berti, M., Ray Chaudhuri, A., Thangavel, S., Gomathinayagam, S., Kenig, S., Vujanovic, M., Odreman, F., Glatter, T., Graziano, S., Mendoza-Maldonado, R., et al. (2013). Human RECQ1 promotes restart of replication forks reversed by DNA topoisomerase I inhibition. Nat. Struct. Mol. Biol. *20*, 347–354.

Besnard, E., Babled, A., Lapasset, L., Milhavet, O., Parrinello, H., Dantec, C., Marin, J.-M., and Lemaitre, J.-M. (2012). Unraveling cell type–specific and reprogrammable human replication origin signatures associated with G-quadruplex consensus motifs. Nat. Struct. Mol. Biol. *19*, 837–844.

Bhowmick, R., Minocherhomji, S., and Hickson, I.D. (2016). RAD52 Facilitates Mitotic DNA Synthesis Following Replication Stress. Mol. Cell *64*, 1117–1126.

Bishop, J.D., and Schumacher, J.M. (2002). Phosphorylation of the carboxyl terminus of inner centromere protein (INCENP) by the Aurora B Kinase stimulates Aurora B kinase activity. J. Biol. Chem. *277*, 27577–27580.

Blower, M.D. (2016). Centromeric Transcription Regulates Aurora-B Localization and Activation. Cell Rep. *15*, 1624–1633.

Boidot, R., Végran, F., and Lizard-Nacol, S. (2014). Transcriptional regulation of the survivin gene. Mol. Biol. Rep. *41*, 233–240.

Bosch-Presegué, L., Raurell-Vila, H., Thackray, J.K., González, J., Casal, C., Kane-Goldsmith, N., Vizoso, M., Brown, J.P., Gómez, A., Ausió, J., et al. (2017). Mammalian HP1 Isoforms Have Specific Roles in Heterochromatin Structure and Organization. Cell Rep. *21*, 2048–2057.

Bradford, M.M. (1976). A rapid and sensitive method for the quantitation of microgram quantities of protein utilizing the principle of protein-dye binding. Anal. Biochem. *72*, 248–254.

Brasher, S. V, Smith, B.O., Fogh, R.H., Nietlispach, D., Thiru, A., Nielsen, P.R., Broadhurst, R.W., Ball, L.J., Murzina, N. V, and Laue, E.D. (2000). The structure of mouse HP1 suggests a unique mode of single peptide recognition by the shadow chromo domain dimer. EMBO J. *19*, 1587–1597.

Brustel, J., Kirstein, N., Izard, F., Grimaud, C., Prorok, P., Cayrou, C., Schotta, G., Abdelsamie, A.F., Déjardin, J., Méchali, M., et al. (2017). Histone H4K20 tri- methylation at late- firing origins ensures timely heterochromatin replication. EMBO J. *36*, 2726–2741.

Bugreev, D. V., Rossi, M.J., and Mazin, A. V. (2011). Cooperation of RAD51 and RAD54 in regression of a model replication fork. Nucleic Acids Res. *39*, 2153–2164.

Bunz, F., Dutriaux, A., Lengauer, C., Waldman, T., Zhou, S., Brown, J.P., Sedivy, J.M., Kinzler, K.W., and Vogelstein, B. (1998). Requirement for p53 and p21 to sustain G2 arrest after DNA damage. Science *282*, 1497–1501.

Burcham, P.C. (1999). Internal hazards: baseline DNA damage by endogenous products of normal metabolism. Mutat. Res. Toxicol. Environ. Mutagen. *443*, 11–36.

Burrell, R.A., McClelland, S.E., Endesfelder, D., Groth, P., Weller, M.-C., Shaikh, N., Domingo, E., Kanu, N., Dewhurst, S.M., Gronroos, E., et al. (2013). Replication stress links structural and numerical cancer chromosomal instability. Nature *494*, 492–496.

Byun, T.S., Pacek, M., Yee, M.C., Walter, J.C., and Cimprich, K.A. (2005). Functional uncoupling of MCM helicase and DNA polymerase activities activates the ATR-dependent

checkpoint. Genes Dev. *19*, 1040–1052.

Canman, C.E., Lim, D.S., Cimprich, K.A., Taya, Y., Tamai, K., Sakaguchi, K., Appella, E., Kastan, M.B., and Siliciano, J.D. (1998). Activation of the ATM kinase by ionizing radiation and phosphorylation of p53. Science *281*, 1677–1679.

Capalbo, G., Rödel, C., Stauber, R.H., Knauer, S.K., Bache, M., Kappler, M., and Rödel, F. (2007). The Role of Survivin for Radiation Therapy. Strahlentherapie Und Onkol. *183*, 593–599.

Capalbo, G., Dittmann, K., Weiss, C., Reichert, S., Hausmann, E., Rödel, C., and Rödel, F. (2010). Radiation-Induced Survivin Nuclear Accumulation is Linked to DNA Damage Repair. Int. J. Radiat. Oncol. Biol. Phys. *77*, 226–234.

Capalbo, L., Mela, I., Abad, M.A., Jeyaprakash, A.A., Edwardson, J.M., and D'Avino, P.P. (2016). Coordinated regulation of the ESCRT-III component CHMP4C by the chromosomal passenger complex and centralspindlin during cytokinesis. Open Biol. *6*, 160248.

Carmena, M., Ruchaud, S., and Earnshaw, W.C. (2009). Making the Auroras glow: regulation of Aurora A and B kinase function by interacting proteins. Curr. Opin. Cell Biol. *21*, 796–805.

Carmena, M., Wheelock, M., Funabiki, H., and Earnshaw, W.C. (2012). The chromosomal passenger complex (CPC): from easy rider to the godfather of mitosis. Nat. Rev. Mol. Cell Biol. *13*, 789–803.

Cayrol, C., Knibiehler, M., and Ducommun, B. (1998). p21 binding to PCNA causes G1 and G2 cell cycle arrest in p53-deficient cells. Oncogene *16*, 311–320.

Champoux, J.J. (1978). Mechanism of the reaction catalyzed by the DNA untwisting enzyme: Attachment of the enzyme to 3′-terminus of the nicked DNA. J. Mol. Biol. *118*, 441–446.

Chan, K.L., Palmai-Pallag, T., Ying, S., and Hickson, I.D. (2009). Replication stress induces sister-chromatid bridging at fragile site loci in mitosis. Nat. Cell Biol. *11*, 753–760.

Chang, J.-L., Chen, T.-H., Wang, C.-F., Chiang, Y.-H., Huang, Y.-L., Wong, F.-H., Chou, C.-K., and Chen, C.-M. (2006). Borealin/Dasra B is a cell cycle-regulated chromosomal passenger protein and its nuclear accumulation is linked to poor prognosis for human gastric cancer. Exp. Cell Res. *312*, 962–973.

Chantalat, L., Skoufias, D.A., Kleman, J.-P., Jung, B., Dideberg, O., and Margolis, R.L. (2000). Crystal Structure of Human Survivin Reveals a Bow Tie–Shaped Dimer with Two Unusual α-Helical Extensions. Mol. Cell *6*, 183–189.

Cheeseman, I.M., and Desai, A. (2008). Molecular architecture of the kinetochore–microtubule interface. Nat. Rev. Mol. Cell Biol. *9*, 33–46.

Cheeseman, I.M., Chappie, J.S., Wilson-Kubalek, E.M., and Desai, A. (2006). The conserved KMN network constitutes the core microtubule-binding site of the kinetochore. Cell *127*, 983–997.

Chen, H.H.W., and Kuo, M.T. (2017). Improving radiotherapy in cancer treatment: Promises and challenges.

Chen, J., Jackson, P.K., Kirschner, M.W., and Dutta, A. (1995). Separate domains of p21 involved in the inhibition of Cdk kinase and PCNA. Nature *374*, 386–388.

Chen, P., Zhu, J., Liu, D., Li, H., Xu, N., and Hou, M. (2014). Over-expression of survivin and VEGF in small-cell lung cancer may predict the poorer prognosis. Med. Oncol. *31*, 775.

Chen, S., de Vries, M.A., and Bell, S.P. (2007). Orc6 is required for dynamic recruitment of Cdt1 during repeated Mcm2-7 loading. Genes Dev. *21*, 2897–2907.

Chen, X., Chen, X.-G., Hu, X., Song, T., Ou, X., Zhang, C., Zhang, W., and Zhang, C. (2016). MiR-34a and miR-203 Inhibit Survivin Expression to Control Cell Proliferation and Survival in Human Osteosarcoma Cells. J. Cancer *7*, 1057–1065.

Cheng, C.H., and Kuchta, R.D. (1993). DNA polymerase .epsilon.: Aphidicolin inhibition and the relationship between polymerase and exonuclease activity. Biochemistry *32*, 8568–8574.

Chow, J.P.H., Siu, W.Y., Ho, H.T.B., Ma, K.H.T., Ho, C.C., and Poon, R.Y.C. (2003). Differential contribution of inhibitory phosphorylation of CDC2 and CDK2 for unperturbed cell cycle control and DNA integrity checkpoints. J. Biol. Chem. *278*, 40815–40828.

Conti, C., Leo, E., Eichler, G.S., Sordet, O., Martin, M.M., Fan, A., Aladjem, M.I., and Pommier, Y. (2010). Inhibition of histone deacetylase in cancer cells slows down replication forks, activates dormant origins, and induces DNA damage. Cancer Res. *70*, 4470–4480.

Contreras, A., Hale, T.K., Stenoien, D.L., Rosen, J.M., Mancini, M.A., and Herrera, R.E. (2003). The dynamic mobility of histone H1 is regulated by cyclin/CDK phosphorylation. Mol. Cell. Biol. *23*, 8626–8636.

Cooke, C.A., Heck, M.M., and Earnshaw, W.C. (1987). The inner centromere protein (INCENP) antigens: movement from inner centromere to midbody during mitosis. J. Cell Biol. *105*, 2053–2067.

Coster, G., and Diffley, J.F.X. (2017). Bidirectional eukaryotic DNA replication is established by quasi-symmetrical helicase loading. Science *357*, 314–318.

Cowieson, N.P., Partridge, J.F., Allshire, R.C., and McLaughlin, P.J. (2000). Dimerisation of a chromo shadow domain and distinctions from the chromodomain as revealed by structural analysis. Curr. Biol. *10*, 517–525.

Crivat, G., and Taraska, J.W. (2012). Imaging proteins inside cells with fluorescent tags. Trends Biotechnol. *30*, 8–16.

Croce, C.M. (2008). Oncogenes and Cancer. N. Engl. J. Med. *358*, 502–511.

Crosio, C., Fimia, G.M., Loury, R., Kimura, M., Okano, Y., Zhou, H., Sen, S., Allis, C.D., and Sassone-Corsi, P. (2002). Mitotic phosphorylation of histone H3: spatio-temporal regulation by mammalian Aurora kinases. Mol. Cell. Biol. *22*, 874–885.

Dai, D., Liang, Y., Xie, Z., Fu, J., Zhang, Y., and Zhang, Z. (2011). Survivin deficiency induces apoptosis and cell cycle arrest in HepG2 hepatocellular carcinoma cells. Oncol. Rep. *27*, 621–627.

Dai, J., Sultan, S., Taylor, S.S., and Higgins, J.M.G. (2005). The kinase haspin is required for mitotic histone H3 Thr 3 phosphorylation and normal metaphase chromosome alignment. Genes Dev. *19*, 472–488.

Dalby, B., Cates, S., Harris, A., Ohki, E.C., Tilkins, M.L., Price, P.J., and Ciccarone, V.C. (2004). Advanced transfection with Lipofectamine 2000 reagent: primary neurons, siRNA, and high-throughput applications. Methods *33*, 95–103.

Deckbar, D., Stiff, T., Koch, B., Reis, C., Löbrich, M., and Jeggo, P.A. (2010). The limitations of the G1-S checkpoint. Cancer Res. *70*, 4412–4421.

Delacroix, S., Wagner, J.M., Kobayashi, M., Yamamoto, K., and Karnitz, L.M. (2007). The Rad9-Hus1-Rad1 (9-1-1) clamp activates checkpoint signaling via TopBP1. Genes Dev. *21*, 1472–1477.

DeLuca, J.G., Gall, W.E., Ciferri, C., Cimini, D., Musacchio, A., and Salmon, E.D. (2006). Kinetochore Microtubule Dynamics and Attachment Stability Are Regulated by Hec1. Cell *127*, 969–982.

Deng, C., Pumin Zhang, tS, Wade Harper, J., Elledge, S.J., and Leder, P. (1995). Mice Lacking p21 c~P7/wAF7 Undergo Normal Development, but Are Defective in Gl Checkpoint Control. Cell *82*, 875–884.

Dewar, J.M., and Walter, J.C. (2017). Mechanisms of DNA replication termination. Nat. Rev. Mol. Cell Biol. *18*, 507–516.

Dheekollu, J., Wiedmer, A., Hayden, J., Speicher, D., Gotter, A.L., Yen, T., and Lieberman, P.M. (2011). Timeless links replication termination to mitotic kinase activation. PLoS One *6*.

Dobrynin, G., Popp, O., Romer, T., Bremer, S., Schmitz, M.H.A., Gerlich, D.W., and Meyer, H. (2011). Cdc48/p97-Ufd1-Npl4 antagonizes Aurora B during chromosome segregation in HeLa

cells. J. Cell. Biochem. *124*, 1571–1580.

Douglas, M.E., Davies, T., Joseph, N., and Mishima, M. (2010). Aurora B and 14-3-3 coordinately regulate clustering of centralspindlin during cytokinesis. Curr. Biol. *20*, 927–933.

Drexler, H.G., and Uphoff, C.C. (2002). Mycoplasma contamination of cell cultures: Incidence, sources, effects, detection, elimination, prevention. Cytotechnology *39*, 75–90.

Ebrahimiyan, H., Aslani, S., Rezaei, N., Jamshidi, A., and Mahmoudi, M. (2018). Survivin and autoimmunity; the ins and outs. Immunol. Lett. *193*, 14–24.

Eichinger, C.S., and Jentsch, S. (2011). 9-1-1: PCNA's specialized cousin. Trends Biochem. Sci. *36*, 563–568.

Elgin, S.C.R., and Grewal, S.I.S. (2003). Heterochromatin: silence is golden. Curr. Biol. *13*, R895–R898.

Elvers, I., Johansson, F., Groth, P., Erixon, K., and Helleday, T. (2011). UV stalled replication forks restart by re-priming in human fibroblasts. Nucleic Acids Res. *39*, 7049–7057.

Errico, A., and Costanzo, V. (2012). Mechanisms of replication fork protection: a safeguard for genome stability. Crit. Rev. Biochem. Mol. Biol. *47*, 222–235.

Evrin, C., Clarke, P., Zech, J., Lurz, R., Sun, J., Uhle, S., Li, H., Stillman, B., and Speck, C. (2009). A double-hexameric MCM2-7 complex is loaded onto origin DNA during licensing of eukaryotic DNA replication. Proc. Natl. Acad. Sci. U. S. A. *106*, 20240–20245.

Falck, J., Mailand, N., Syljuåsen, R.G., Bartek, J., and Lukas, J. (2001). The ATM–Chk2–Cdc25A checkpoint pathway guards against radioresistant DNA synthesis. Nature *410*, 842–847.

Ferlay, J., Soerjomataram, I., Dikshit, R., Eser, S., Mathers, C., Rebelo, M., Parkin, D.M., Forman, D., and Bray, F. (2015). Cancer incidence and mortality worldwide: Sources, methods and major patterns in GLOBOCAN 2012. Int. J. Cancer *136*, E359–E386.

Fernández, J.G., Rodríguez, D.A., Valenzuela, M., Calderon, C., Urzúa, U., Munroe, D., Rosas, C., Lemus, D., Díaz, N., Wright, M.C., et al. (2014). Survivin expression promotes VEGF-induced tumor angiogenesis via PI3K/Akt enhanced β-catenin/Tcf-Lef dependent transcription. Mol. Cancer *13*, 209.

Fichtinger-Schepman, A.M.J., Van der Veer, J.L., Den Hartog, J.H.J., Lohman, P.H.M., and Reedijk, J. (1985). Adducts of the antitumor drug cis-diamminedichloroplatinum(II) with DNA: formation, identification, and quantitation. Biochemistry *24*, 707–713.

Fischle, W., Tseng, B.S., Dormann, H.L., Ueberheide, B.M., Garcia, B.A., Shabanowitz, J., Hunt, D.F., Funabiki, H., and Allis, C.D. (2005). Regulation of HP1–chromatin binding by histone H3 methylation and phosphorylation. Nature *438*, 1116–1122.

Foley, E.A., Maldonado, M., and Kapoor, T.M. (2011). Formation of stable attachments between kinetochores and microtubules depends on the B56-PP2A phosphatase. Nat. Cell Biol. *13*, 1265–1271.

Fox, M.H., Arndt-Jovin, D.J., Jovin, T.M., Baumann, P.H., and Robert-Nicoud, M. (1991). Spatial and temporal distribution of DNA replication sites localized by immunofluorescence and confocal microscopy in mouse fibroblasts. J. Cell Sci. *99 (Pt 2)*, 247–253.

Frigola, J., He, J., Kinkelin, K., Pye, V.E., Renault, L., Douglas, M.E., Remus, D., Cherepanov, P., Costa, A., and Diffley, J.F.X. (2017). Cdt1 stabilizes an open MCM ring for helicase loading. Nat. Commun. *8*, 15720.

Gaillard, P.H., Martini, E.M., Kaufman, P.D., Stillman, B., Moustacchi, E., and Almouzni, G. (1996). Chromatin assembly coupled to DNA repair: a new role for chromatin assembly factor I. Cell *86*, 887–896.

Gali, H., Juhasz, S., Morocz, M., Hajdu, I., Fatyol, K., Szukacsov, V., Burkovics, P., and Haracska, L. (2012). Role of SUMO modification of human PCNA at stalled replication fork. Nucleic Acids Res. *40*, 6049–6059.

Ganai, R.A., and Johansson, E. (2016). DNA Replication—A Matter of Fidelity. Mol. Cell *62*, 745–755.

Garg, H., Suri, P., Gupta, J.C., Talwar, G.P., and Dubey, S. (2016). Survivin: A unique target for tumor therapy. Cancer Cell Int. *16*.

Garg, P., Stith, C.M., Sabouri, N., Johansson, E., and Burgers, P.M. (2004). Idling by DNA polymerase maintains a ligatable nick during lagging-strand DNA replication. Genes Dev. *18*, 2764–2773.

Ge, X.Q., and Blow, J.J. (2010). Chk1 inhibits replication factory activation but allows dormant origin firing in existing factories. J. Cell Biol. *191*, 1285–1297.

Gilbert, N., Boyle, S., Sutherland, H., de Las Heras, J., Allan, J., Jenuwein, T., and Bickmore, W.A. (2003). Formation of facultative heterochromatin in the absence of HP1. EMBO J. *22*, 5540–5550.

Gilljam, K.M., Feyzi, E., Aas, P.A., Sousa, M.M.L., Müller, R., Vågbø, C.B., Catterall, T.C., Liabakk, N.B., Slupphaug, G., Drabløs, F., et al. (2009). Identification of a novel, widespread, and functionally important PCNA-binding motif. J. Cell Biol. *186*, 645–654.

González-Loyola, A., Fernández-Miranda, G., Trakala, M., Partida, D., Samejima, K., Ogawa, H., Cañamero, M., de Martino, A., Martínez-Ramírez, Á., de Cárcer, G., et al. (2015). Aurora B Overexpression Causes Aneuploidy and p21Cip1 Repression during Tumor Development. Mol. Cell. Biol. *35*, 3566–3578.

Goodarzi, A.A., Noon, A.T., Deckbar, D., Ziv, Y., Shiloh, Y., Löbrich, M., and Jeggo, P.A. (2008). ATM signaling facilitates repair of DNA double-strand breaks associated with heterochromatin. Mol. Cell *31*, 167–177.

Görisch, S.M., Sporbert, A., Stear, J.H., Grunewald, I., Nowak, D., Warbrick, E., and Cardoso, M.C. (2008). Replication fork progression in the absence of processive DNA synthesis SC RIB ND ES SC RIB. 1983–1990.

Graham, J.E., Marians, K.J., and Kowalczykowski, S.C. (2017). Independent and Stochastic Action of DNA Polymerases in the Replisome. Cell *169*, 1201–1213.e17.

Grant, G.D., Brooks, L., Zhang, X., Mahoney, J.M., Martyanov, V., Wood, T.A., Sherlock, G., Cheng, C., Whitfield, M.L., and Whitfield, M.L. (2013). Identification of cell cycle-regulated genes periodically expressed in U2OS cells and their regulation by FOXM1 and E2F transcription factors. Mol. Biol. Cell *24*, 3634–3650.

Gravina, G., Wasén, C., Garcia-Bonete, M.J., Turkkila, M., Erlandsson, M.C., Töyrä Silfverswärd, S., Brisslert, M., Pullerits, R., Andersson, K.M., Katona, G., et al. (2017). Survivin in autoimmune diseases. Autoimmun. Rev. *16*, 845–855.

Grewal, S.I.S., and Jia, S. (2007). Heterochromatin revisited. Nat. Rev. Genet. *8*, 35–46.

Grézy, A., Chevillard-Briet, M., Trouche, D., and Escaffit, F. (2016). Control of genetic stability by a new heterochromatin compaction pathway involving the Tip60 histone acetyltransferase. Mol. Biol. Cell *27*, 599–607.

Groth, A., Ray-Gallet, D., Quivy, J.-P., Lukas, J., Bartek, J., and Almouzni, G. (2005). Human Asf1 Regulates the Flow of S Phase Histones during Replicational Stress. Mol. Cell *17*, 301–311.

Groth, A., Rocha, W., Verreault, A., and Almouzni, G. (2007). Chromatin Challenges during DNA Replication and Repair. Cell *128*, 721–733.

Gruneberg, U., Neef, R., Honda, R., Nigg, E.A., and Barr, F.A. (2004). Relocation of Aurora B from centromeres to the central spindle at the metaphase to anaphase transition requires MKlp2. J. Cell Biol. *166*, 167–172.

Guenatri, M., Bailly, D., Maison, C., and Almouzni, G. (2004). Mouse centric and pericentric satellite repeats form distinct functional heterochromatin. J. Cell Biol. *166*, 493–505.

Gully, C.P., Velazquez-Torres, G., Shin, J.-H., Fuentes-Mattei, E., Wang, E., Carlock, C., Chen,

J., Rothenberg, D., Adams, H.P., Choi, H.H., et al. (2012). Aurora B kinase phosphorylates and instigates degradation of p53. Proc. Natl. Acad. Sci. U. S. A. *109*, E1513-22.

Hanahan, D., and Weinberg, R.A. (2000). The Hallmarks of Cancer. Cell *100*, 57–70.

Hanahan, D., and Weinberg, R.A. (2011). Hallmarks of Cancer: The Next Generation. Cell *144*, 646–674.

Hanley, M.L., Yoo, T.Y., Sonnett, M., Needleman, D.J., and Mitchison, T.J. (2017). Chromosomal passenger complex hydrodynamics suggests chaperoning of the inactive state by nucleoplasmin/nucleophosmin. Mol. Biol. Cell *28*, 1444–1456.

Harper, J.W., Elledge, S.J., Keyomarsi, K., Dynlacht, B., Tsai, L.H., Zhang, P., Dobrowolski, S., Bai, C., Connell-Crowley, L., and Swindell, E. (1995). Inhibition of cyclin-dependent kinases by p21. Mol. Biol. Cell *6*, 387–400.

Hashimoto, Y., Ray Chaudhuri, A., Lopes, M., and Costanzo, V. (2010). Rad51 protects nascent DNA from Mre11-dependent degradation and promotes continuous DNA synthesis. Nat. Struct. Mol. Biol. *17*, 1305–1311.

Hauer, M.H., and Gasser, S.M. (2017). Chromatin and nucleosome dynamics in DNA damage and repair. Genes Dev. *31*, 2204–2221.

Hauf, S., Cole, R.W., LaTerra, S., Zimmer, C., Schnapp, G., Walter, R., Heckel, A., Van Meel, J., Rieder, C.L., and Peters, J.M. (2003). The small molecule Hesperadin reveals a role for Aurora B in correcting kinetochore-microtubule attachment and in maintaining the spindle assembly checkpoint. J. Cell Biol. *161*, 281–294.

Hauf, S., Roitinger, E., Koch, B., Dittrich, C.M., Mechtler, K., and Peters, J.-M. (2005). Dissociation of cohesin from chromosome arms and loss of arm cohesion during early mitosis depends on phosphorylation of SA2. PLoS Biol. *3*, e69.

Havens, C.G., and Walter, J.C. (2011). Mechanism of CRL4(Cdt2), a PCNA-dependent E3 ubiquitin ligase. Genes Dev. *25*, 1568–1582.

Hayakawa, T., Haraguchi, T., Masumoto, H., Hiraoka, Y., Clark, R.F., Powers, J.A., Eissenberg, J.C., Elgin, S.C., Rothfield, N.F., and Earnshaw, W.C. (2003). Cell cycle behavior of human HP1 subtypes: distinct molecular domains of HP1 are required for their centromeric localization during interphase and metaphase. J. Cell Sci. *116*, 3327–3338.

Hayama, S., Daigo, Y., Yamabuki, T., Hirata, D., Kato, T., Miyamoto, M., Ito, T., Tsuchiya, E., Kondo, S., and Nakamura, Y. (2007). Phosphorylation and activation of cell division cycle associated 8 by aurora kinase B plays a significant role in human lung carcinogenesis. Cancer Res. *67*, 4113–4122.

Helmrich, A., Ballarino, M., Nudler, E., and Tora, L. (2013). Transcription-replication encounters, consequences and genomic instability. Nat. Struct. Mol. Biol. *20*, 412–418.

Hengeveld, R.C.C., Vromans, M.J.M., Vleugel, M., Hadders, M.A., and Lens, S.M.A. (2017). Inner centromere localization of the CPC maintains centromere cohesion and allows mitotic checkpoint silencing. Nat. Commun. *8*, 15542.

Higgins, N.P., Kato, K., and Strauss, B. (1976). A model for replication repair in mammalian cells. J. Mol. Biol. *101*, 417–425.

Hirao, A., Cheung, A., Duncan, G., Girard, P.-M., Elia, A.J., Wakeham, A., Okada, H., Sarkissian, T., Wong, J.A., Sakai, T., et al. (2002). Chk2 is a tumor suppressor that regulates apoptosis in both an ataxia telangiectasia mutated (ATM)-dependent and an ATM-independent manner. Mol. Cell. Biol. *22*, 6521–6532.

Hirota, T., Lipp, J.J., Toh, B.H., and Peters, J.M. (2005). Histone H3 serine 10 phosphorylation by Aurora B causes HP1 dissociation from heterochromatin. Nature *438*, 1176–1180.

Hoeijmakers, J.H.J. (2001). Genome maintenance mechanisms for preventing cancer. Nature *411*, 366–374.

Honda, R., Körner, R., and Nigg, E.A. (2003). Exploring the functional interactions between

Aurora B, INCENP, and survivin in mitosis. Mol. Biol. Cell *14*, 3325–3341.

Hong, Y., Sonneville, R., Wang, B., Scheidt, V., Meier, B., Woglar, A., Demetriou, S., Labib, K., Jantsch, V., and Gartner, A. (2018). LEM-3 is a midbody-tethered DNA nuclease that resolves chromatin bridges during late mitosis. Nat. Commun. *9*, 728.

Howes, T.R.L., and Tomkinson, A.E. (2012). DNA ligase I, the replicative DNA ligase. Subcell. Biochem. *62*, 327–341.

Hsiang, Y.H., Lihou, M.G., and Liu, L.F. (1989). Arrest of replication forks by drug-stabilized topoisomerase I-DNA cleavable complexes as a mechanism of cell killing by camptothecin. Cancer Res. *49*, 5077–5082.

Hsu, J.-Y., Sun, Z.-W., Li, X., Reuben, M., Tatchell, K., Bishop, D.K., Grushcow, J.M., Brame, C.J., Caldwell, J.A., Hunt, D.F., et al. (2000). Mitotic Phosphorylation of Histone H3 Is Governed by Ipl1/aurora Kinase and Glc7/PP1 Phosphatase in Budding Yeast and Nematodes. Cell *102*, 279–291.

Huang, C.-Y., Ju, D.-T., Chang, C.-F., Muralidhar Reddy, P., and Velmurugan, B.K. (2017). A review on the effects of current chemotherapy drugs and natural agents in treating non-small cell lung cancer. BioMedicine *7*, 23.

Huang, H.-K., Bailis, J.M., Leverson, J.D., Gómez, E.B., Forsburg, S.L., and Hunter, T. (2005). Suppressors of Bir1p (Survivin) identify roles for the chromosomal passenger protein Pic1p (INCENP) and the replication initiation factor Psf2p in chromosome segregation. Mol. Cell. Biol. *25*, 9000–9015.

Hübscher, U., and Maga, G. (2011). DNA replication and repair bypass machines. Curr. Opin. Chem. Biol. *15*, 627–635.

Hughes, B.T., Sidorova, J., Swanger, J., Monnat, R.J., and Clurman, B.E. (2013). Essential role for Cdk2 inhibitory phosphorylation during replication stress revealed by a human Cdk2 knockin mutation. Proc. Natl. Acad. Sci. U. S. A. *110*, 8954–8959.

Hümmer, S., and Mayer, T.U. (2009). Cdk1 negatively regulates midzone localization of the mitotic kinesin Mklp2 and the chromosomal passenger complex. Curr. Biol. *19*, 607–612.

Ilves, I., Petojevic, T., Pesavento, J.J., and Botchan, M.R. (2010). Activation of the MCM2-7 Helicase by Association with Cdc45 and GINS Proteins. Mol. Cell *37*, 247–258.

Inoue, A., Kikuchi, S., Hishiki, A., Shao, Y., Heath, R., Evison, B.J., Actis, M., Canman, C.E., Hashimoto, H., and Fujii, N. (2014). A small molecule inhibitor of monoubiquitinated proliferating cell nuclear antigen (PCNA) inhibits repair of interstrand DNA cross-link, enhances DNA double strand break, and sensitizes cancer cells to cisplatin. J. Biol. Chem. *289*, 7109–7120.

Iyer, D., and Rhind, N. (2017). The Intra-S Checkpoint Responses to DNA Damage. Genes (Basel). *8*, 74.

Jacobs, S.A., and Khorasanizadeh, S. (2002). Structure of HP1 chromodomain bound to a lysine 9-methylated histone H3 tail. Science *295*, 2080–2083.

Jenuwein, T., and Allis, C.D. (2001). Translating the histone code. Science *293*, 1074–1080.

Jeyaprakash, A.A., Klein, U.R., Lindner, D., Ebert, J., Nigg, E.A., and Conti, E. (2007). Structure of a Survivin–Borealin–INCENP Core Complex Reveals How Chromosomal Passengers Travel Together. Cell *131*, 271–285.

Jones, R.M., and Petermann, E. (2012). Replication fork dynamics and the DNA damage response. Biochem. J. *443*, 13–26.

Jossen, R., and Bermejo, R. (2013). The DNA damage checkpoint response to replication stress: A game of forks. Front. Genet. *4*, 1–14.

Kabeche, L., Nguyen, H.D., Buisson, R., and Zou, L. (2017). A mitosis-specific and R loop-driven ATR pathway promotes faithful chromosome segregation. Science eaan6490.

Kabisch, M., Lorenzo Bermejo, J., Dünnebier, T., Ying, S., Michailidou, K., Bolla, M.K., Wang,

Q., Dennis, J., Shah, M., Perkins, B.J., et al. (2015). Inherited variants in the inner centromere protein (INCENP) gene of the chromosomal passenger complex contribute to the susceptibility of ER-negative breast cancer. Carcinogenesis *36*, 256–271.

Kaitna, S., Mendoza, M., Jantsch-Plunger, V., and Glotzer, M. (2000). Incenp and an Aurora-like kinase form a complex essential for chromosome segregation and efficient completion of cytokinesis. Curr. Biol. *10*, 1172–1181.

Kang, J., Chaudhary, J., Dong, H., Kim, S., Brautigam, C.A., and Yu, H. (2011). Mitotic centromeric targeting of HP1 and its binding to Sgo1 are dispensable for sister-chromatid cohesion in human cells. Mol. Biol. Cell *22*, 1181–1190.

Kang, S., Kang, M.-S., Ryu, E., and Myung, K. (2017). Eukaryotic DNA replication: Orchestrated action of multi-subunit protein complexes. Mutat. Res. Mol. Mech. Mutagen.

Karimian, A., Ahmadi, Y., and Yousefi, B. (2016). Multiple functions of p21 in cell cycle, apoptosis and transcriptional regulation after DNA damage. DNA Repair (Amst). *42*, 63–71.

Karnani, N., and Dutta, A. (2011). The effect of the intra-S-phase checkpoint on origins of replication in human cells. Genes Dev. *25*, 621–633.

Kastan, M.B., and Bartek, J. (2004). Cell-cycle checkpoints and cancer. Nat. 2004 4327015.

Kastan, M.B., Onyekwere, O., Sidransky, D., Vogelstein, B., and Craig, R.W. (1991). Participation of p53 protein in the cellular response to DNA damage. Cancer Res. *51*, 6304–6311.

Kaufman, P.D., Kobayashi, R., Kessler, N., and Stillman, B. (1995). The p150 and p60 Subunits of Chromatin Assembly Factor I: A Molecular Link between Newly Synthesized Histones and DNA Replication. Cell *81*, 1105–1114.

Kawabata, T., Luebben, S.W., Yamaguchi, S., Ilves, I., Matise, I., Buske, T., Botchan, M.R., and Shima, N. (2011). Stalled fork rescue via dormant replication origins in unchallenged S phase promotes proper chromosome segregation and tumor suppression. Mol. Cell *41*, 543–553.

Kawashima, S.A., Tsukahara, T., Langegger, M., Hauf, S., Kitajima, T.S., and Watanabe, Y. (2007). Shugoshin enables tension-generating attachment of kinetochores by loading Aurora to centromeres. Genes Dev. *21*, 420–435.

Kelly, A.E., Ghenoiu, C., Xue, J.Z., Zierhut, C., Kimura, H., and Funabiki, H. (2010). Survivin reads phosphorylated histone H3 threonine 3 to activate the mitotic kinase Aurora B. Science *330*, 235–239.

Kitagawa, M., Fung, S.Y.S., Hameed, U.F.S., Goto, H., Inagaki, M., and Lee, S.H. (2014). Cdk1 coordinates timely activation of MKlp2 kinesin with relocation of the chromosome passenger complex for cytokinesis. Cell Rep. *7*, 166–179.

Klein, U.R., Haindl, M., Nigg, E.A., and Muller, S. (2009). RanBP2 and SENP3 function in a mitotic SUMO2/3 conjugation-deconjugation cycle on Borealin. Mol. Biol. Cell *20*, 410–418.

Knauer, S.K., Bier, C., Habtemichael, N., and Stauber, R.H. (2006). The Survivin-Crm1 interaction is essential for chromosomal passenger complex localization and function. EMBO Rep. *7*, 1259–1265.

Knauer, S.K., Mann, W., and Stauber, R.H. (2007a). Survivin's Dual Role: An Export's View. Cell Cycle *6*, 518–521.

Knauer, S.K., Krämer, O.H., Knösel, T., Engels, K., Rödel, F., Kovács, A.F., Dietmaier, W., Klein-Hitpass, L., Habtemichael, N., Schweitzer, A., et al. (2007b). Nuclear export is essential for the tumor-promoting activity of survivin. FASEB J. *21*, 207–216.

De Koning, L., Savignoni, A., Boumendil, C., Rehman, H., Asselain, B., Sastre-Garau, X., and Almouzni, G. (2009). Heterochromatin protein 1alpha: a hallmark of cell proliferation relevant to clinical oncology. EMBO Mol. Med. *1*, 178–191.

Koundrioukoff, S., Carignon, S., Técher, H., Letessier, A., Brison, O., and Debatisse, M. (2013). Stepwise Activation of the ATR Signaling Pathway upon Increasing Replication Stress Impacts

Fragile Site Integrity. PLoS Genet. *9*.

Krenn, V., and Musacchio, A. (2015). The Aurora B Kinase in Chromosome Bi-Orientation and Spindle Checkpoint Signaling. Front. Oncol. *5*, 225.

Kubota, T., Nishimura, K., Kanemaki, M.T., and Donaldson, A.D. (2013). The Elg1 Replication Factor C-like Complex Functions in PCNA Unloading during DNA Replication. Mol. Cell *50*, 273–280.

Kwon, S.H., and Workman, J.L. (2011). The changing faces of HP1: From heterochromatin formation and gene silencing to euchromatic gene expression: HP1 acts as a positive regulator of transcription. BioEssays *33*, 280–289.

Lachner, M., O'Carroll, D., Rea, S., Mechtler, K., and Jenuwein, T. (2001). Methylation of histone H3 lysine 9 creates a binding site for HP1 proteins. Nature *410*, 116–120.

Langie, S.A.S., Koppen, G., Desaulniers, D., Al-Mulla, F., Al-Temaimi, R., Amedei, A., Azqueta, A., Bisson, W.H., Brown, D.G., Brunborg, G., et al. (2015). Causes of genome instability: the effect of low dose chemical exposures in modern society. Carcinogenesis *36 Suppl 1*, S61-88.

Le, Q.-T., Shirato, H., Giaccia, A.J., and Koong, A.C. (2015). Emerging Treatment Paradigms in Radiation Oncology.

Lee, E.Y.H.P., and Muller, W.J. (2010). Oncogenes and tumor suppressor genes. Cold Spring Harb. Perspect. Biol. *2*, a003236.

Lee, J.-H., and Paull, T.T. (2004). Direct activation of the ATM protein kinase by the Mre11/Rad50/Nbs1 complex. Science *304*, 93–96.

Lee, K., Fu, H., Aladjem, M.I., and Myung, K. (2013). ATAD5 regulates the lifespan of DNA replication factories by modulating PCNA level on the chromatin. J. Cell Biol. *200*, 31–44.

Leman, A.R., and Noguchi, E. (2013). The replication fork: Understanding the eukaryotic replication machinery and the challenges to genome duplication.

Leonard, A.C., and Méchali, M. (2013). DNA replication origins. Cold Spring Harb. Perspect. Biol. *5*, a010116.

Leonhardt, H., Rahn, H.P., Weinzierf, P., Sporbert, A., Cremer, T., Zink, D., and Cardoso, M.C. (2000). Dynamics of DNA replication factories in living cells. J Cell Biol *149*, 271–279.

Li, G., and Reinberg, D. (2011). Chromatin higher-order structures and gene regulation. Curr. Opin. Genet. Dev. *21*, 175–186.

Li, F., Ambrosini, G., Chu, E.Y., Plescia, J., Tognin, S., Marchisio, P.C., and Altieri, D.C. (1998). Control of apoptosis and mitotic spindle checkpoint by survivin. Nature *396*, 580–584.

Li, F., Ackermann, E.J., Bennett, C.F., Rothermel, A.L., Plescia, J., Tognin, S., Villa, A., Marchisio, P.C., and Altieri, D.C. (1999). Pleiotropic cell-division defects and apoptosis induced by interference with survivin function. Nat. Cell Biol. *1*, 461–466.

Li, S., Deng, Z., Fu, J., Xu, C., Xin, G., Wu, Z., Luo, J., Wang, G., Zhang, S., Zhang, B., et al. (2015a). Spatial Compartmentalization Specializes the Function of Aurora A and Aurora B. J. Biol. Chem. *290*, 17546–17558.

Li, Y., Liu, D., Zhou, Y., Li, Y., Xie, J., Lee, R.J., Cai, Y., and Teng, L. (2015b). Silencing of Survivin Expression Leads to Reduced Proliferation and Cell Cycle Arrest in Cancer Cells. J. Cancer *6*, 1187–1194.

Lim, S., and Kaldis, P. (2013). Cdks, cyclins and CKIs: roles beyond cell cycle regulation. Development *140*, 3079–3093.

Liu, R., and Mitchell, D.A. (2010). Survivin as an immunotherapeutic target for adult and pediatric malignant brain tumors. Cancer Immunol. Immunother. *59*, 183–193.

Liu, X., Song, Z., Huo, Y., Zhang, J., Zhu, T., Wang, J., Zhao, X., Aikhionbare, F., Zhang, J., Duan, H., et al. (2014). Chromatin protein HP1a interacts with the mitotic regulator borealin protein and specifies the centromere localization of the chromosomal passenger complex. J.

Biol. Chem. *289*, 20638–20649.

Lomberk, G., Wallrath, L., and Urrutia, R. (2006). The Heterochromatin Protein 1 family. Genome Biol. *7*, 228.

Lopes, M., Cotta-Ramusino, C., Pellicioli, A., Liberi, G., Plevani, P., Muzi-Falconi, M., Newlon, C.S., and Foiani, M. (2001). The DNA replication checkpoint response stabilizes stalled replication forks. Nature *412*, 557–561.

Lopes, M., Foiani, M., and Sogo, J.M. (2006). Multiple Mechanisms Control Chromosome Integrity after Replication Fork Uncoupling and Restart at Irreparable UV Lesions. Mol. Cell *21*, 15–27.

Losada, A., Hirano, M., and Hirano, T. (1998). Identification of Xenopus SMC protein complexes required for sister chromatid cohesion. Genes Dev. *12*, 1986–1997.

Lossaint, G., Larroque, M., Ribeyre, C., Bec, N., Larroque, C., Décaillet, C., Gari, K., and Constantinou, A. (2013). FANCD2 Binds MCM Proteins and Controls Replisome Function upon Activation of S Phase Checkpoint Signaling. Mol. Cell *51*, 678–690.

Loyola, A., Tagami, H., Bonaldi, T., Roche, D., Quivy, J.P., Imhof, A., Nakatani, Y., Dent, S.Y.R., and Almouzni, G. (2009). The HP1alpha-CAF1-SetDB1-containing complex provides H3K9me1 for Suv39-mediated K9me3 in pericentric heterochromatin. EMBO Rep. *10*, 769–775.

Luger, K., Mäder, A.W., Richmond, R.K., Sargent, D.F., and Richmond, T.J. (1997). Crystal structure of the nucleosome core particle at 2.8 Å resolution. Nature *389*, 251–260.

Luo, Y., Hurwitz, J., and Massagué, J. (1995). Cell-cycle inhibition by independent CDK and PCNA binding domains in p21Cip1. Nature *375*, 159–161.

Ma, Y., Kanakousaki, K., and Buttitta, L. (2015). How the cell cycle impacts chromatin architecture and influences cell fate. Front. Genet. *6*, 19.

MacDougall, C.A., Byun, T.S., Van, C., Yee, M., and Cimprich, K.A. (2007). The structural determinants of checkpoint activation. Genes Dev. *21*, 898–903.

Mackay, D.R., and Ullman, K.S. (2015). ATR and a Chk1-Aurora B pathway coordinate postmitotic genome surveillance with cytokinetic abscission. Mol. Biol. Cell *26*, 2217–2226.

Mackay, A.M., Ainsztein, A.M., Eckley, D.M., and Earnshaw, W.C. (1998). A dominant mutant of inner centromere protein (INCENP), a chromosomal protein, disrupts prometaphase congression and cytokinesis. J. Cell Biol. *140*, 991–1002.

Magiera, M.M., Gueydon, E., and Schwob, E. (2014). DNA replication and spindle checkpoints cooperate during S phase to delay mitosis and preserve genome integrity. J. Cell Biol. *204*, 165–175.

Mailand, N., Falck, J., Lukas, C., Syljuâsen, R.G., Welcker, M., Bartek, J., and Lukas, J. (2000). Rapid destruction of human Cdc25A in response to DNA damage. Science *288*, 1425–1429.

Maison, C., and Almouzni, G. (2004). HP1 and the dynamics of heterochromatin maintenance. Nat. Rev. Mol. Cell Biol. *5*, 296–305.

Mankouri, H.W., Huttner, D., and Hickson, I.D. (2013). How unfinished business from S-phase affects mitosis and beyond. EMBO J. *32*, 2661–2671.

Maréchal, A., and Zou, L. (2013). DNA damage sensing by the ATM and ATR kinases. Cold Spring Harb. Perspect. Biol. *5*.

Maric, M., Maculins, T., De Piccoli, G., and Labib, K. (2014). Cdc48 and a ubiquitin ligase drive disassembly of the CMG helicase at the end of DNA replication. Science *346*, 1253596.

Marusawa, H., Matsuzawa, S.-I., Welsh, K., Zou, H., Armstrong, R., Tamm, I., and Reed, J.C. (2003). HBXIP functions as a cofactor of survivin in apoptosis suppression. EMBO J. *22*, 2729–2740.

Matsuoka, S., Huang, M., and Elledge, S.J. (1998). Linkage of ATM to cell cycle regulation by the Chk2 protein kinase. Science *282*, 1893–1897.

McIntosh, D., and Blow, J.J. (2012). Dormant origins, the licensing checkpoint, and the response to replicative stresses. Cold Spring Harb. Perspect. Biol. *4*.

Meek, D.W., and Anderson, C.W. (2009). Posttranslational Modification of p53: Cooperative Integrators of Function. Cold Spring Harb. Perspect. Biol. *1*, a000950–a000950.

Mejlvang, J., Feng, Y., Alabert, C., Neelsen, K.J., Jasencakova, Z., Zhao, X., Lees, M., Sandelin, A., Pasero, P., Lopes, M., et al. (2014). New histone supply regulates replication fork speed and PCNA unloading. J. Cell Biol. *204*, 29–43.

Mendiburo, M.J., Padeken, J., Fulop, S., Schepers, A., and Heun, P. (2011). Drosophila CENH3 Is Sufficient for Centromere Formation. Science (80-.). *334*, 686–690.

Michaelis, C., Ciosk, R., and Nasmyth, K. (1997). Cohesins: chromosomal proteins that prevent premature separation of sister chromatids. Cell *91*, 35–45.

Milutinovic, S., Zhuang, Q., and Szyf, M. (2002). Proliferating cell nuclear antigen associates with histone deacetylase activity, integrating DNA replication and chromatin modification. J. Biol. Chem. *277*, 20974–20978.

Mimitou, E.P., and Symington, L.S. (2011). DNA end resection--unraveling the tail. DNA Repair (Amst). *10*, 344–348.

Minc, E., Courvalin, J.-C., and Buendia, B. (2000). HP1γ associates with euchromatin and heterochromatin in mammalian nuclei and chromosomes. Cytogenet. Genome Res. *90*, 279–284.

Minocherhomji, S., Ying, S., Bjerregaard, V.A., Bursomanno, S., Aleliunaite, A., Wu, W., Mankouri, H.W., Shen, H., Liu, Y., and Hickson, I.D. (2015). Replication stress activates DNA repair synthesis in mitosis. Nature *528*, 286–290.

Mo, F., Zhuang, X., Liu, X., Yao, P.Y., Qin, B., Su, Z., Zang, J., Wang, Z., Zhang, J., Dou, Z., et al. (2016). Acetylation of Aurora B by TIP60 ensures accurate chromosomal segregation. Nat. Chem. Biol. *12*, 226–232.

Monier, K., Mouradian, S., and Sullivan, K.F. (2007). DNA methylation promotes Aurora-B-driven phosphorylation of histone H3 in chromosomal subdomains. J. Cell Sci. *120*, 101–114.

Morgan, D.O. (1995). Principles of CDK regulation. Nature *374*, 131–134.

Mourón, S., Rodriguez-Acebes, S., Martínez-Jiménez, M.I., García-Gómez, S., Chocrón, S., Blanco, L., and Méndez, J. (2013). Repriming of DNA synthesis at stalled replication forks by human PrimPol. Nat. Struct. Mol. Biol. *20*, 1383–1389.

Moyer, S.E., Lewis, P.W., and Botchan, M.R. (2006). Isolation of the Cdc45/Mcm2-7/GINS (CMG) complex, a candidate for the eukaryotic DNA replication fork helicase. Proc. Natl. Acad. Sci. U. S. A. *103*, 10236–10241.

Muchmore, S.W., Chen, J., Jakob, C., Zakula, D., Matayoshi, E.D., Wu, W., Zhang, H., Li, F., Ng, S.-C., and Altieri, D.C. (2000). Crystal Structure and Mutagenic Analysis of the Inhibitor-of-Apoptosis Protein Survivin. Mol. Cell *6*, 173–182.

Muñoz, S., and Méndez, J. (2017). DNA replication stress: from molecular mechanisms to human disease. Chromosoma *126*, 1–15.

Murzina, N., Verreault, A., Laue, E., and Stillman, B. (1999). Heterochromatin Dynamics in Mouse Cells: Interaction between Chromatin Assembly Factor 1 and HP1 Proteins. Mol. Cell *4*, 529–540.

Musacchio, A. (2015). The Molecular Biology of Spindle Assembly Checkpoint Signaling Dynamics. Curr. Biol. *25*, R1002-18.

Musacchio, A., and Salmon, E.D. (2007). The spindle-assembly checkpoint in space and time. Nat. Rev. Mol. Cell Biol. *8*, 379–393.

Nähse, V., Christ, L., Stenmark, H., and Campsteijn, C. (2017). The Abscission Checkpoint: Making It to the Final Cut. Trends Cell Biol. *27*, 1–11.

Naim, V., and Rosselli, F. (2009). The FANC pathway and mitosis: A replication legacy. Cell Cycle *8*, 2907–2912.

Nakamura, H., Morita, T., and Sato, C. (1986). Structural organizations of replicon domains during DNA synthetic phase in the mammalian nucleus. Exp. Cell Res. *165*, 291–297.

Natsume, T., Kiyomitsu, T., Saga, Y., and Kanemaki, M.T. (2016). Rapid Protein Depletion in Human Cells by Auxin-Inducible Degron Tagging with Short Homology Donors. Cell Rep. *15*, 210–218.

Nguyen, T.N., and Goodrich, J.A. (2006). Protein-protein interaction assays: eliminating false positive interactions. Nat. Methods *3*, 135–139.

Nielsen, P.R., Nietlispach, D., Mott, H.R., Callaghan, J., Bannister, A., Kouzarides, T., Murzin, A.G., Murzina, N. V., and Laue, E.D. (2002). Structure of the HP1 chromodomain bound to histone H3 methylated at lysine 9. Nature *416*, 103–107.

Nieminuszczy, J., Schwab, R.A., and Niedzwiedz, W. (2016). The DNA fibre technique ??? tracking helicases at work. Methods *108*, 92–98.

Nikolov, I., and Taddei, A. (2016). Linking replication stress with heterochromatin formation. Chromosoma *125*, 523–533.

Nishiyama, T., Sykora, M.M., Huis in 't Veld, P.J., Mechtler, K., and Peters, J.-M. (2013). Aurora B and Cdk1 mediate Wapl activation and release of acetylated cohesin from chromosomes by phosphorylating Sororin. Proc. Natl. Acad. Sci. U. S. A. *110*, 13404–13409.

NJU-China (2018). igem.org. *2018-02–13*, http://2016.igem.org/Team:NJU-China/test.

Nougarède, R., Della Seta, F., Zarzov, P., and Schwob, E. (2000). Hierarchy of S-phase-promoting factors: yeast Dbf4-Cdc7 kinase requires prior S-phase cyclin-dependent kinase activation. Mol. Cell. Biol. *20*, 3795–3806.

Nozawa, R.-S., Nagao, K., Masuda, H.-T., Iwasaki, O., Hirota, T., Nozaki, N., Kimura, H., and Obuse, C. (2010). Human POGZ modulates dissociation of HP1α from mitotic chromosome arms through Aurora B activation. Nat. Cell Biol. *12*, 719–727.

O'Connell, M.J., Raleigh, J.M., Verkade, H.M., and Nurse, P. (1997). Chk1 is a wee1 kinase in the G2 DNA damage checkpoint inhibiting cdc2 by Y15 phosphorylation. EMBO J. *16*, 545–554.

O'Connor, D.S., Grossman, D., Plescia, J., Li, F., Zhang, H., Villa, A., Tognin, S., Marchisio, P.C., and Altieri, D.C. (2000). Regulation of apoptosis at cell division by p34cdc2 phosphorylation of survivin. Proc. Natl. Acad. Sci. U. S. A. *97*, 13103–13107.

O'Keefe, R.T., Henderson, S.C., and Spector, D.L. (1992). Dynamic organization of DNA replication in mammalian cell nuclei: spatially and temporally defined replication of chromosome-specific alpha-satellite DNA sequences. J. Cell Biol. *116*, 1095–1110.

Obuse, C., Iwasaki, O., Kiyomitsu, T., Goshima, G., Toyoda, Y., and Yanagida, M. (2004). A conserved Mis12 centromere complex is linked to heterochromatic HP1 and outer kinetochore protein Zwint-1. Nat. Cell Biol. *6*, 1135–1141.

Oei, A.L., Vriend, L.E.M., Krawczyk, P.M., Horsman, M.R., Franken, N.A.P., and Crezee, J. (2017). Targeting therapy-resistant cancer stem cells by hyperthermia. Int. J. Hyperth. *33*, 419–427.

Otto, T., and Sicinski, P. (2017). Cell cycle proteins as promising targets in cancer therapy. Nat. Rev. Cancer *17*, 93–115.

Pavlyukov, M.S., Antipova, N. V, Balashova, M. V, Vinogradova, T. V, Kopantzev, E.P., and Shakhparonov, M.I. (2011). Survivin monomer plays an essential role in apoptosis regulation. J. Biol. Chem. *286*, 23296–23307.

Pearson, C.E., Edamura, K.N., and Cleary, J.D. (2005). Repeat instability: mechanisms of dynamic mutations. Nat. Rev. Genet. *6*, 729–742.

Peixoto, P., Castronovo, V., Matheus, N., Polese, C., Peulen, O., Gonzalez, a, Boxus, M.,

Verdin, E., Thiry, M., Dequiedt, F., et al. (2012). HDAC5 is required for maintenance of pericentric heterochromatin, and controls cell-cycle progression and survival of human cancer cells. Cell Death Differ. *19*, 1239–1252.

Perera, R.L., Torella, R., Klinge, S., Kilkenny, M.L., Maman, J.D., and Pellegrini, L. (2013). Mechanism for priming DNA synthesis by yeast DNA Polymerase α. Elife *2*, e00482.

Perpelescu, M., and Fukagawa, T. (2011). The ABCs of CENPs. Chromosoma *120*, 425–446.

Petermann, E., Orta, M.L., Issaeva, N., Schultz, N., and Helleday, T. (2010). Hydroxyurea-Stalled Replication Forks Become Progressively Inactivated and Require Two Different RAD51-Mediated Pathways for Restart and Repair. Mol. Cell *37*, 492–502.

Peters, A.H., O'Carroll, D., Scherthan, H., Mechtler, K., Sauer, S., Schöfer, C., Weipoltshammer, K., Pagani, M., Lachner, M., Kohlmaier, A., et al. (2001). Loss of the Suv39h histone methyltransferases impairs mammalian heterochromatin and genome stability. Cell *107*, 323–337.

Petsalaki, E., Akoumianaki, T., Black, E.J., Gillespie, D.A.F., and Zachos, G. (2011). Phosphorylation at serine 331 is required for Aurora B activation. J. Cell Biol. *195*, 449–466.

Pommier, Y. (2006). Topoisomerase I inhibitors: camptothecins and beyond. Nat. Rev. Cancer *6*, 789–802.

Prakash, S., Johnson, R.E., and Prakash, L. (2005). EUKARYOTIC TRANSLESION SYNTHESIS DNA POLYMERASES: Specificity of Structure and Function. Annu. Rev. Biochem. *74*, 317–353.

Priego Moreno, S., Bailey, R., Campion, N., Herron, S., and Gambus, A. (2014). Polyubiquitylation drives replisome disassembly at the termination of DNA replication. Science (80-.). *346*, 477–481.

Punchihewa, C., Inoue, A., Hishiki, A., Fujikawa, Y., Connelly, M., Evison, B., Shao, Y., Heath, R., Kuraoka, I., Rodrigues, P., et al. (2012). Identification of Small Molecule Proliferating Cell Nuclear Antigen (PCNA) Inhibitor That Disrupts Interactions with PIP-box Proteins and Inhibits DNA Replication. J. Biol. Chem. *287*, 14289–14300.

Qian, J., Lesage, B., Beullens, M., Van Eynde, A., and Bollen, M. (2011). PP1/Repo-man dephosphorylates mitotic histone H3 at T3 and regulates chromosomal aurora B targeting. Curr. Biol. *21*, 766–773.

Quivy, J.-P., Roche, D., Kirschner, D., Tagami, H., Nakatani, Y., and Almouzni, G. (2004). A CAF-1 dependent pool of HP1 during heterochromatin duplication. EMBO J. *23*, 3516–3526.

Quivy, J.-P., Gérard, A., Cook, A.J.L., Roche, D., and Almouzni, G. (2008). The HP1-p150/CAF-1 interaction is required for pericentric heterochromatin replication and S-phase progression in mouse cells. Nat. Struct. Mol. Biol. *15*, 972–979.

Ramadan, K., Bruderer, R., Spiga, F.M., Popp, O., Baur, T., Gotta, M., and Meyer, H.H. (2007). Cdc48/p97 promotes reformation of the nucleus by extracting the kinase Aurora B from chromatin. Nature *450*, 1258–1262.

Rannou, Y., Troadec, M.-B., Petretti, C., Hans, F., Dutertre, S., Dimitrov, S., and Prigent, C. (2008). Localization of aurora A and aurora B kinases during interphase: role of the N-terminal domain. Cell Cycle *7*, 3012–3020.

Ray Chaudhuri, A., Hashimoto, Y., Herrador, R., Neelsen, K.J., Fachinetti, D., Bermejo, R., Cocito, A., Costanzo, V., and Lopes, M. (2012). Topoisomerase I poisoning results in PARP-mediated replication fork reversal. Nat. Struct. Mol. Biol. *19*, 417–423.

Reichert, S., Rödel, C., Mirsch, J., Harter, P.N., Tomicic, M.T., Mittelbronn, M., Kaina, B., and Rödel, F. (2011). Survivin inhibition and DNA double-strand break repair: A molecular mechanism to overcome radioresistance in glioblastoma. Radiother. Oncol. *101*, 51–58.

Reinhardt, H.C., Aslanian, A.S., Lees, J.A., and Yaffe, M.B. (2007). p53-deficient cells rely on ATM- and ATR-mediated checkpoint signaling through the p38MAPK/MK2 pathway for survival

after DNA damage. Cancer Cell *11*, 175–189.

Remus, D., Beuron, F., Tolun, G., Griffith, J.D., Morris, E.P., and Diffley, J.F.X. (2009). Concerted loading of Mcm2-7 double hexamers around DNA during DNA replication origin licensing. Cell *139*, 719–730.

Richmond, T.J., and Davey, C.A. (2003). The structure of DNA in the nucleosome core. Nature *423*, 145–150.

Robinson, P.J.J., Fairall, L., Huynh, V.A.T., and Rhodes, D. (2006). EM measurements define the dimensions of the "30-nm" chromatin fiber: evidence for a compact, interdigitated structure. Proc. Natl. Acad. Sci. U. S. A. *103*, 6506–6511.

Rodriguez, J.A., Lens, S.M.A., Span, S.W., Vader, G., Medema, R.H., Kruyt, F.A.E., and Giaccone, G. (2006). Subcellular localization and nucleocytoplasmic transport of the chromosomal passenger proteins before nuclear envelope breakdown. Oncogene *25*, 4867–4879.

Rössig, L., Jadidi, A.S., Urbich, C., Badorff, C., Zeiher, A.M., and Dimmeler, S. (2001). Akt-dependent phosphorylation of p21(Cip1) regulates PCNA binding and proliferation of endothelial cells. Mol. Cell. Biol. *21*, 5644–5657.

Rothbart, S.B., and Strahl, B.D. (2014). Interpreting the language of histone and DNA modifications. Biochim. Biophys. Acta *1839*, 627–643.

Rothkamm, K., Krüger, I., Thompson, L.H., and Löbrich, M. (2003). Pathways of DNA double-strand break repair during the mammalian cell cycle. Mol. Cell. Biol. *23*, 5706–5715.

Rowbotham, S.P., Barki, L., Neves-Costa, A., Santos, F., Dean, W., Hawkes, N., Choudhary, P., Will, W.R., Webster, J., Oxley, D., et al. (2011). Maintenance of silent chromatin through replication requires SWI/SNF-like chromatin remodeler SMARCAD1. Mol. Cell *42*, 285–296.

Rowlands, H., Dhavarasa, P., Cheng, A., and Yankulov, K. (2017). Forks on the Run: Can the Stalling of DNA Replication Promote Epigenetic Changes? Front. Genet. *8*, 86.

Ruchaud, S., Carmena, M., and Earnshaw, W.C. (2007). Chromosomal passengers: conducting cell division. Nat. Rev. Mol. Cell Biol. *8*, 798–812.

Ruppert, J.G., Samejima, K., Platani, M., Molina, O., Kimura, H., Jeyaprakash, A.A., Ohta, S., and Earnshaw, W.C. (2018). HP1α targets the chromosomal passenger complex for activation at heterochromatin before mitotic entry. EMBO J. e97677.

Sadakierska-Chudy, A., and Filip, M. (2015). A comprehensive view of the epigenetic landscape. Part II: Histone post-translational modification, nucleosome level, and chromatin regulation by ncRNAs. Neurotox. Res. *27*, 172–197.

Samejima, K., Platani, M., Wolny, M., Ogawa, H., Vargiu, G., Knight, P.J., Peckham, M., and Earnshaw, W.C. (2015). The Inner Centromere Protein (INCENP) Coil Is a Single α-Helix (SAH) Domain That Binds Directly to Microtubules and Is Important for Chromosome Passenger Complex (CPC) Localization and Function in Mitosis. J. Biol. Chem. *290*, 21460–21472.

Sanhueza, C., Wehinger, S., Castillo Bennett, J., Valenzuela, M., Owen, G.I., and Quest, A.F.G. (2015). The twisted survivin connection to angiogenesis. Mol. Cancer *14*.

Santaguida, S., Vernieri, C., Villa, F., Ciliberto, A., and Musacchio, A. (2011). Evidence that Aurora B is implicated in spindle checkpoint signalling independently of error correction. EMBO J. *30*, 1508–1519.

Sarraf, S.A., and Stancheva, I. (2004). Methyl-CpG binding protein MBD1 couples histone H3 methylation at lysine 9 by SETDB1 to DNA replication and chromatin assembly. Mol. Cell *15*, 595–605.

Sasai, K., Katayama, H., Stenoien, D.L., Fujii, S., Honda, R., Kimura, M., Okano, Y., Tatsuka, M., Suzuki, F., Nigg, E.A., et al. (2004). Aurora-C kinase is a novel chromosomal passenger protein that can complement Aurora-B kinase function in mitotic cells. Cell Motil. Cytoskeleton *59*, 249–263.

Sasai, K., Katayama, H., Hawke, D.H., and Sen, S. (2016). Aurora-C Interactions with Survivin and INCENP Reveal Shared and Distinct Features Compared with Aurora-B Chromosome Passenger Protein Complex. PLoS One *11*, e0157305.

Saunders, W.S., Chue, C., Goebl, M., Craig, C., Clark, R.F., Powers, J.A., Eissenberg, J.C., Elgin, S.C., Rothfield, N.F., and Earnshaw, W.C. (1993). Molecular cloning of a human homologue of Drosophila heterochromatin protein HP1 using anti-centromere autoantibodies with anti-chromo specificity. J. Cell Sci. *104 (Pt 2)*, 573–582.

Schlacher, K., Christ, N., Siaud, N., Egashira, A., Wu, H., and Jasin, M. (2011). Double-strand break repair-independent role for BRCA2 in blocking stalled replication fork degradation by MRE11. Cell *145*, 529–542.

Schlacher, K., Wu, H., and Jasin, M. (2012). A Distinct Replication Fork Protection Pathway Connects Fanconi Anemia Tumor Suppressors to RAD51-BRCA1/2. Cancer Cell *22*, 106–116.

Schröder, E. (2014). Dissecting the role of the radiation resistance factor survivin in DNA damage response. University Duisburg-Essen.

Schwaiger, M., Kohler, H., Oakeley, E.J., Stadler, M.B., and Schübeler, D. (2010). Heterochromatin protein 1 (HP1) modulates replication timing of the Drosophila genome. Genome Res. *20*, 771–780.

Sessa, F., Mapelli, M., Ciferri, C., Tarricone, C., Areces, L.B., Schneider, T.R., Stukenberg, P.T., and Musacchio, A. (2005). Mechanism of Aurora B activation by INCENP and inhibition by hesperadin. Mol. Cell *18*, 379–391.

Shaltieì, I.A., Krennin, L., Bruinsma, W., and Medema, R.H. (2015). The same, only different – DNA damage checkpoints and their reversal throughout the cell cycle. J. Cell Sci.

Shandilya, J., Medler, K.F., and Roberts, S.G.E. (2016). Regulation of AURORA B function by mitotic checkpoint protein MAD2. Cell Cycle *15*, 2196–2201.

Sheu, Y.-J., and Stillman, B. (2010). The Dbf4-Cdc7 kinase promotes S phase by alleviating an inhibitory activity in Mcm4. Nature *463*, 113–117.

Shibahara, K., and Stillman, B. (1999). Replication-Dependent Marking of DNA by PCNA Facilitates CAF-1-Coupled Inheritance of Chromatin. Cell *96*, 575–585.

Shiomi, Y., and Nishitani, H. (2013). Alternative replication factor C protein, Elg1, maintains chromosome stability by regulating PCNA levels on chromatin. Genes to Cells *18*, 946–959.

Shiomi, Y., and Nishitani, H. (2017). Control of Genome Integrity by RFC Complexes; Conductors of PCNA Loading onto and Unloading from Chromatin during DNA Replication. Genes (Basel). *8*.

Shogren-Knaak, M., Ishii, H., Sun, J.-M., Pazin, M.J., Davie, J.R., and Peterson, C.L. (2006). Histone H4-K16 acetylation controls chromatin structure and protein interactions. Science *311*, 844–847.

Shrestha, R.L., Conti, D., Tamura, N., Braun, D., Ramalingam, R.A., Cieslinski, K., Ries, J., and Draviam, V.M. (2017). Aurora-B kinase pathway controls the lateral to end-on conversion of kinetochore-microtubule attachments in human cells. Nat. Commun. *8*, 150.

Singh, P.B., Miller, J.R., Pearce, J., Kothary, R., Burton, R.D., Paro, R., James, T.C., and Gaunt, S.J. (1991). A sequence motif found in a Drosophila heterochromatin protein is conserved in animals and plants. Nucleic Acids Res. *19*, 789–794.

Sirbu, B.M., Couch, F.B., and Cortez, D. (2012). Monitoring the spatiotemporal dynamics of proteins at replication forks and in assembled chromatin using isolation of proteins on nascent DNA. Nat. Protoc. *7*, 594–605.

Smothers, J.F., and Henikoff, S. (2000). The HP1 chromo shadow domain binds a consensus peptide pentamer. Curr. Biol. *10*, 27–30.

Soboleva, T.A., Nekrasov, M., Pahwa, A., Williams, R., Huttley, G.A., and Tremethick, D.J. (2012). A unique H2A histone variant occupies the transcriptional start site of active genes. Nat.

Struct. Mol. Biol. *19*, 25–30.

Sogo, J.M., Lopes, M., and Foiani, M. (2002). Fork reversal and ssDNA accumulation at stalled replication forks owing to checkpoint defects. Science *297*, 599–602.

Song, J., Salek-Ardakani, S., So, T., and Croft, M. (2007). The kinases aurora B and mTOR regulate the G1–S cell cycle progression of T lymphocytes. Nat. Immunol. *8*, 64–73.

Speck, C., Chen, Z., Li, H., and Stillman, B. (2005). ATPase-dependent cooperative binding of ORC and Cdc6 to origin DNA. Nat. Struct. Mol. Biol. *12*, 965–971.

Stevens, F.E., Beamish, H., Warrener, R., and Gabrielli, B. (2008). Histone deacetylase inhibitors induce mitotic slippage. Oncogene *27*, 1345–1354.

Stodola, J.L., and Burgers, P.M. (2016). Resolving individual steps of Okazaki-fragment maturation at a millisecond timescale. Nat. Struct. Mol. Biol. *23*, 402–408.

Sullivan, R., Alatise, O.I., Anderson, B.O., Audisio, R., Autier, P., Aggarwal, A., Balch, C., Brennan, M.F., Dare, A., D'Cruz, A., et al. (2015). Global cancer surgery: delivering safe, affordable, and timely cancer surgery. Lancet Oncol. *16*, 1193–1224.

Suzuki, A., Hayashida, M., Ito, T., Kawano, H., Nakano, T., Miura, M., Akahane, K., and Shiraki, K. (2000). Survivin initiates cell cycle entry by the competitive interaction with Cdk4/p16INK4a and Cdk2/Cyclin E complex activation. Oncogene *19*, 3225–3234.

Taddei, A., Maison, C., Roche, D., and Almouzni, G. (2001). Reversible disruption of pericentric heterochromatin and centromere function by inhibiting deacetylases. Nat. Cell Biol. *3*, 114–120.

Tagami, H., Ray-Gallet, D., Almouzni, G., and Nakatani, Y. (2004). Histone H3.1 and H3.3 Complexes Mediate Nucleosome Assembly Pathways Dependent or Independent of DNA Synthesis. Cell *116*, 51–61.

Takahashi, T.S., Basu, A., Bermudez, V., Hurwitz, J., and Walter, J.C. (2008). Cdc7-Drf1 kinase links chromosome cohesion to the initiation of DNA replication in Xenopus egg extracts. Genes Dev. *22*, 1894–1905.

Takami, Y., Ono, T., Fukagawa, T., Shibahara, K., and Nakayama, T. (2007). Essential Role of Chromatin Assembly Factor-1–mediated Rapid Nucleosome Assembly for DNA Replication and Cell Division in Vertebrate Cells. Mol. Biol. Cell *18*, 129–141.

Takebayashi, S., Sugimura, K., Saito, T., Sato, C., Fukushima, Y., Taguchi, H., and Okumura, K. (2005). Regulation of replication at the R/G chromosomal band boundary and pericentromeric heterochromatin of mammalian cells. Exp. Cell Res. *304*, 162–174.

Tan, Y., Raychaudhuri, P., and Costa, R.H. (2007). Chk2 mediates stabilization of the FoxM1 transcription factor to stimulate expression of DNA repair genes. Mol. Cell. Biol. *27*, 1007–1016.

Tanaka, T., Kimura, M., Matsunaga, K., Fukada, D., Mori, H., and Okano, Y. (1999). Centrosomal kinase AIK1 is overexpressed in invasive ductal carcinoma of the breast. Cancer Res. *59*, 2041–2044.

Tang, A., Gao, K., Chu, L., Zhang, R., Yang, J., and Zheng, J. (2017). Aurora kinases: novel therapy targets in cancers. Oncotarget *8*, 23937–23954.

Tatsuka, M., Katayama, H., Ota, T., Tanaka, T., Odashima, S., Suzuki, F., and Terada, Y. (1998). Multinuclearity and increased ploidy caused by overexpression of the aurora- and Ipl1-like midbody-associated protein mitotic kinase in human cancer cells. Cancer Res. *58*, 4811–4816.

Terret, M.-E., Sherwood, R., Rahman, S., Qin, J., and Jallepalli, P. V. (2009). Cohesin acetylation speeds the replication fork. Nature *462*, 231–234.

Thangavel, S., Berti, M., Levikova, M., Pinto, C., Gomathinayagam, S., Vujanovic, M., Zellweger, R., Moore, H., Lee, E.H., Hendrickson, E.A., et al. (2015). DNA2 drives processing and restart of reversed replication forks in human cells. J. Cell Biol. *208*, 545–562.

Thiru, A., Nietlispach, D., Mott, H.R., Okuwaki, M., Lyon, D., Nielsen, P.R., Hirshberg, M.,

Verreault, A., Murzina, N. V, and Laue, E.D. (2004). Structural basis of HP1/PXVXL motif peptide interactions and HP1 localisation to heterochromatin. EMBO J. *23*, 489–499.

Todd, A.A., Groundwater, P.W., and Gill, J. (2018). Anticancer therapeutics : from drug discovery to clinical applications.

Trakala, M., Fernández-Miranda, G., Pérez de Castro, I., Heeschen, C., and Malumbres, M. (2013). Aurora B prevents delayed DNA replication and premature mitotic exit by repressing p21 Cip1. Cell Cycle *12*, 1030–1041.

Trembecka-Lucas, D.O., and Dobrucki, J.W. (2012). A heterochromatin protein 1 (HP1) dimer and a proliferating cell nuclear antigen (PCNA) protein interact in vivo and are parts of a multiprotein complex involved in DNA replication and DNA repair. Cell Cycle *11*, 2170–2175.

Trembecka-Lucas, D.O., Szczurek, A.T., Dobrucki, J.W., Szczurek, A.T., Dobrucki, J.W., and Dobrucki, J.W. (2013). Dynamics of the HP1β-PCNA-containing complexes in DNA replication and repair. Nucleus *4*, 74–82.

Trinkle-Mulcahy, L., Andersen, J., Lam, Y.W., Moorhead, G., Mann, M., and Lamond, A.I. (2006). Repo-Man recruits PP1 gamma to chromatin and is essential for cell viability. J. Cell Biol. *172*, 679–692.

Truong, L.N., and Wu, X. (2011). Prevention of DNA re-replication in eukaryotic cells. J. Mol. Cell Biol. *3*, 13–22.

Tsukahara, T., Tanno, Y., and Watanabe, Y. (2010). Phosphorylation of the CPC by Cdk1 promotes chromosome bi-orientation. Nature *467*, 719–723.

Uehara, R., Tsukada, Y., Kamasaki, T., Poser, I., Yoda, K., Gerlich, D.W., and Goshima, G. (2013). Aurora B and Kif2A control microtubule length for assembly of a functional central spindle during anaphase. J. Cell Biol. *202*, 623–636.

Ulrich, H.D., and Takahashi, T. (2013). Readers of PCNA modifications. Chromosoma *122*, 259–274.

Unruhe-Knauf, B., and Knauer, S.K. (2017). Analysis of HDACi-Induced Changes in Chromosomal Passenger Complex Localization. In Methods in Molecular Biology (Clifton, N.J.), pp. 47–59.

Uren, A.G., Wong, L., Pakusch, M., Fowler, K.J., Burrows, F.J., Vaux, D.L., and Choo, K.H.A. (2000). Survivin and the inner centromere protein INCENP show similar cell-cycle localization and gene knockout phenotype. Curr. Biol. *10*, 1319–1328.

Vader, G., Kauw, J.J.W., Medema, R.H., and Lens, S.M.A. (2006). Survivin mediates targeting of the chromosomal passenger complex to the centromere and midbody. EMBO Rep. *7*, 85–92.

Vagnarelli, P., Ribeiro, S., Sennels, L., Sanchez-Pulido, L., de Lima Alves, F., Verheyen, T., Kelly, D.A., Ponting, C.P., Rappsilber, J., and Earnshaw, W.C. (2011). Repo-Man coordinates chromosomal reorganization with nuclear envelope reassembly during mitotic exit. Dev. Cell *21*, 328–342.

Valton, A.-L., and Prioleau, M.-N. (2016). G-Quadruplexes in DNA Replication: A Problem or a Necessity? Trends Genet. *32*, 697–706.

Vashee, S., Cvetic, C., Lu, W., Simancek, P., Kelly, T.J., and Walter, J.C. (2003). Sequence-independent DNA binding and replication initiation by the human origin recognition complex. Genes Dev. *17*, 1894–1908.

Vermeulen, K., Van Bockstaele, D.R., and Berneman, Z.N. (2003). The cell cycle: a review of regulation, deregulation and therapeutic targets in cancer. Cell Prolif. *36*, 131–149.

Visconti, R., Della Monica, R., and Grieco, D. (2016). Cell cycle checkpoint in cancer: a therapeutically targetable double-edged sword. J. Exp. Clin. Cancer Res. *35*, 153.

Wang, F., Dai, J., Daum, J.R., Niedzialkowska, E., Banerjee, B., Stukenberg, P.T., Gorbsky, G.J., and Higgins, J.M.G. (2010). Histone H3 Thr-3 phosphorylation by Haspin positions Aurora B at centromeres in mitosis. Science *330*, 231–235.

Wang, Y., Zhao, Z., Bao, X., Fang, Y., Ni, P., Chen, Q., Zhang, W., and Deng, A. (2014). Borealin/Dasra B is overexpressed in colorectal cancers and contributes to proliferation of cancer cells. Med. Oncol. *31*, 248.

Warbrick, E. (2000). The puzzle of PCNA's many partners. Bioessays *22*, 997–1006.

Warbrick, E., Lane, D.P., Glover, D.M., and Cox, L.S. (1995). A small peptide inhibitor of DNA replication defines the site of interaction between the cyclin-dependent kinase inhibitor p21WAF1 and proliferating cell nuclear antigen. Curr. Biol. *5*, 275–282.

Watanabe, N., Broome, M., and Hunter, T. (1995). Regulation of the human WEE1Hu CDK tyrosine 15-kinase during the cell cycle. EMBO J. *14*, 1878–1891.

Welburn, J.P.I., Vleugel, M., Liu, D., Yates, J.R., Lampson, M.A., Fukagawa, T., Cheeseman, I.M., and Cheeseman, I.M. (2010). Aurora B phosphorylates spatially distinct targets to differentially regulate the kinetochore-microtubule interface. Mol. Cell *38*, 383–392.

Wold, M.S. (1997). REPLICATION PROTEIN A:A Heterotrimeric, Single-Stranded DNA-Binding Protein Required for Eukaryotic DNA Metabolism. Annu. Rev. Biochem. *66*, 61–92.

Wood, L., Booth, D.G., Vargiu, G., Ohta, S., deLima Alves, F., Samejima, K., Fukagawa, T., Rappsilber, J., and Earnshaw, W.C. (2016). Auxin/AID versus conventional knockouts: distinguishing the roles of CENP-T/W in mitotic kinetochore assembly and stability. Open Biol. *6*, 150230-.

Woodcock, C.L., and Ghosh, R.P. (2010). Chromatin higher-order structure and dynamics. Cold Spring Harb. Perspect. Biol. *2*, a000596.

Wreggett, K.A., Hill, F., James, P.S., Hutchings, A., Butcher, G.W., and Singh, P.B. (1994). A mammalian homologue of Drosophila heterochromatin protein 1 (HP1) is a component of constitutive heterochromatin. Cytogenet. Genome Res. *66*, 99–103.

Wu, L., Ma, C.A., Zhao, Y., and Jain, A. (2011). Aurora B interacts with NIR-p53, leading to p53 phosphorylation in its DNA-binding domain and subsequent functional suppression. J. Biol. Chem. *286*, 2236–2244.

Xu, M., Bai, L., Gong, Y., Xie, W., Hang, H., and Jiang, T. (2009). Structure and Functional Implications of the Human Rad9-Hus1-Rad1 Cell Cycle Checkpoint Complex. J. Biol. Chem. *284*, 20457–20461.

Yan, S., and Michael, W.M. (2009). TopBP1 and DNA polymerase-alpha directly recruit the 9-1-1 complex to stalled DNA replication forks. J. Cell Biol. *184*, 793–804.

Yang, C., Tang, X., Guo, X., Niikura, Y., Kitagawa, K., Cui, K., Wong, S.T.C., Fu, L., and Xu, B. (2011). Aurora-B mediated ATM serine 1403 phosphorylation is required for mitotic ATM activation and the spindle checkpoint. Mol. Cell *44*, 597–608.

Yang, D., Welm, A., and Bishop, J.M. (2004). Cell division and cell survival in the absence of survivin. Proc. Natl. Acad. Sci. U. S. A. *101*, 15100–15105.

Yang, K., Weinacht, C.P., and Zhuang, Z. (2013). Regulatory Role of Ubiquitin in Eukaryotic DNA Translesion Synthesis. Biochemistry *52*, 3217–3228.

Yeo, E.L.L., Chua, A.J.S., Parthasarathy, K., Yeo, H.Y., Ng, M.L., and Kah, J.C.Y. (2015). Understanding aggregation-based assays: nature of protein corona and number of epitopes on antigen matters. RSC Adv. *5*, 14982–14993.

Zeman, M.K., and Cimprich, K.A. (2014). Causes and consequences of replication stress. Nat. Cell Biol. *16*, 2–9.

Zeng, W., Ball, A.R., Yokomori, K., and Yokomori, K. (2010). HP1: heterochromatin binding proteins working the genome. Epigenetics *5*, 287–292.

Zhang, M., Yang, J., and Li, F. (2006). Transcriptional and post-transcriptional controls of survivin in cancer cells: novel approaches for cancer treatment. J. Exp. Clin. Cancer Res. *25*, 391–402.

Zhang, Y., Huang, L., Fu, H., Smith, O.K., Lin, C.M., Utani, K., Rao, M., Reinhold, W.C., Redon, C.E., Ryan, M., et al. (2016). A replicator-specific binding protein essential for site-specific initiation of DNA replication in mammalian cells. Nat. Commun. *7*, 11748.

Zhao, J., Tenev, T., Martins, L.M., Downward, J., and Lemoine, N.R. (2000). The ubiquitin-proteasome pathway regulates survivin degradation in a cell cycle-dependent manner. J. Cell Sci. *113 Pt 23*, 4363–4371.

Zhou, L., Tian, X., Zhu, C., Wang, F., and Higgins, J.M.G. (2014). Polo-like kinase-1 triggers histone phosphorylation by Haspin in mitosis. EMBO Rep. *15*, 273–281.

Zink, L.-M., and Hake, S.B. (2016). Histone variants: nuclear function and disease. Curr. Opin. Genet. Dev. *37*, 82–89.

Zou, L., and Elledge, S.J. (2003). Sensing DNA damage through ATRIP recognition of RPA-ssDNA complexes. Science *300*, 1542–1548.

Zuazua-Villar, P., Rodriguez, R., Gagou, M.E., Eyers, P.A., and Meuth, M. (2014). DNA replication stress in CHK1-depleted tumour cells triggers premature (S-phase) mitosis through inappropriate activation of Aurora kinase B. Cell Death Dis. *5*, e1253.

NHGRI Image Gallery - National Human Genome Research Institute (NHGRI). *2018-02–15*, https://www.genome.gov/imagegallery/.

Overview of the Cell Cycle - University of Tokyo. *2018-02–20*, http://csls-text3.c.u-tokyo.ac.jp/active/13_01.htm.

(2018). Duolink ® In Situ – Fluorescence User Manual.

Appendix

Amino Acids

Table 19: Amino acids.

one-letter code	three-letter code	amino acid
A	Ala	alanine
C	Cys	cysteine
D	Asp	aspartic acid
E	Glu	glutamic acid
F	Phe	phenylalanine
G	Gly	glycine
H	His	histidine
I	Ile	isoleucine
K	Lys	lysine
L	Leu	leucine
M	Met	methionine
N	Asn	asparagine
P	Pro	proline
Q	Gln	glutamine
R	Arg	arginine
S	Ser	serine
T	Thr	threonine
V	Val	valine
W	Trp	tryptophan
Y	Tyr	tyrosine

Vector maps

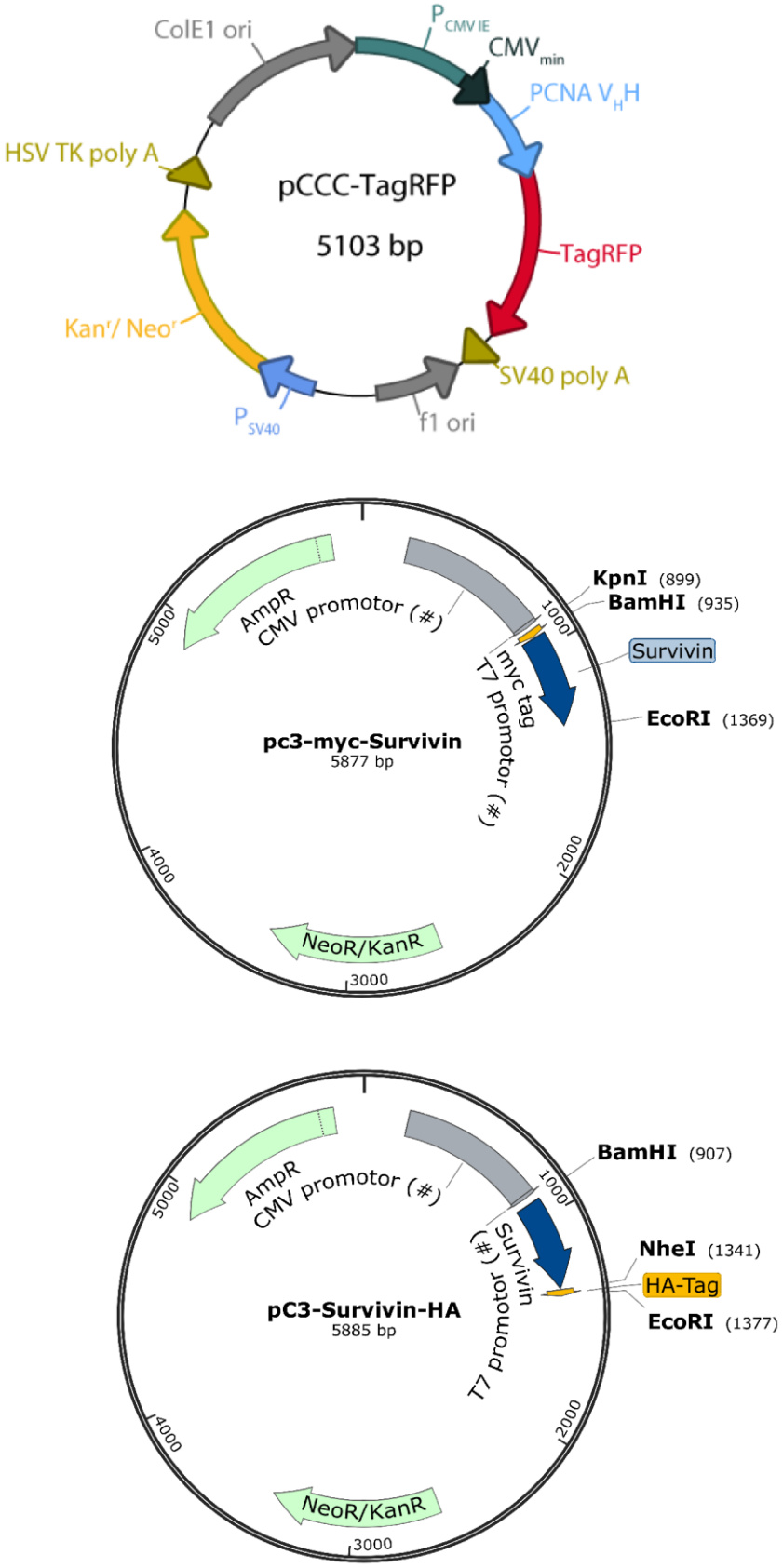

Figure 40: Vector maps.
Schematic representation of selected plasmid constructs.

Acknowledgement

First of all, I would like to express my gratitude to Prof. Dr. Shirley Knauer for giving me the opportunity to work on such an interesting project. Especially thanks for supervision, continuous support and advices as well as the faith in my work and me during the last years.

I also would like to thank the “Deutsche Forschungsgemeinschaft” for financial support of my thesis. As a member of the DFG graduate training program 1739 “Molecular determinants of the cellular radiation response and their potential for response modulation” I had the opportunity to fulfill a desire of mine to visit several conferences and to get in contact with other researchers of the field of replication or radiation sciences. Thanks to all the participants of the GRK 1739, whether students, PI’s or coordinators for teaching as well as critical and helpful comments during seminars and annual retreats, in particular to Prof. Dr. George Iliakis for mentoring and giving helpful advices.

I thank the actual and former „Shirley’s girlies and boys” for sharing the ups and downs during my scientific work and all the fun we have had in the last years. I could not have imagined having better co-workers. I want to thank especially Elisabeth for your comments on the thesis manuscript and Cecilia, the best room mate, for accepting my well-organized desk. Special thanks go also to Sarah for supporting me during the last year e.g. by establishing the iPOND assay.

Furthermore, I would like to thank Dr. Nina Schulze from the Imaging Centre Campus Essen for experimental and microscopic advices as well as for data analyses.

I also would like to thank Dr. Mao Li and Prof. Dr. Xiaoyu Hu that I could work with them on a different field of research, for numerous publications and very delicious Chinese food.

Zum Schluss möchte ich mich auch ganz herzlich bei meiner Familie bedanken die mich während der gesamten Zeit unterstützt hat. Ein ganz besonderer Dank gebührt hier meinem Ehemann, der mich immer wieder und besonders während der letzten Monate bestärkt und angespornt hat, sodass ich meine Ziele erreichen konnte.

Publications, oral presentations and poster presentations

Publications

Jiang, H., Hu, X.-Y., **Schlesiger, S.**, Li, M., Zellermann, E., Knauer, S.K., and Schmuck, C. (2017). Morphology-Dependent Cell Imaging by Using a Self-Assembled Diacetylene Peptide Amphiphile. Angew. Chemie Int. Ed. *56*, 14526–14530.

Li, M., **Schlesiger, S.**, Knauer, S.K., and Schmuck, C. (2015). A tailor-made specific anion-binding motif in the side chain transforms a tetrapeptide into an efficient vector for gene delivery. Angew. Chemie - Int. Ed. *54*, 2941–2944.

Li, M., **Schlesiger, S.**, Knauer, S.K., and Schmuck, C. (2016a). Introduction of a tailor made anion receptor into the side chain of small peptides allows fine-tuning the thermodynamic signature of peptide–DNA binding. Org. Biomol. Chem. *14*, 8800–8803.

Li, M., Ehlers, M., **Schlesiger, S.**, Zellermann, E., Knauer, S.K., and Schmuck, C. (2016b). Incorporation of a Non-Natural Arginine Analogue into a Cyclic Peptide Leads to Formation of Positively Charged Nanofibers Capable of Gene Transfection. Angew. Chemie - Int. Ed. *55*, 598–601.

Li, M., **Mosel, S.**, Knauer, S.K., and Schmuck, C. (2018). A dipeptide with enhanced anion binding affinity enables cell uptake and protein delivery. Org. Biomol. Chem. *16*, 2312–2317.

Oral presentations

09/07/2014 ZMB Lunch Seminar, Essen

08/05/2015 GRK1739, Annual Meeting 2015, Landhotel Straelener Hof, Straelen

09/06/2016 GRK1739, Annual Meeting 2016, Hotel Antoniushütte, Balve-Eisborn

26/10/2016 ZMB Lunch Seminar, Essen

18/05/2017 GRK1739, Annual Meeting 2017, Landhotel Voshövel, Schermbeck

19/09/2017 ERRS and GBS 2017, 43th Annual Meeting of the European Radiation Research Society and 20th Annual Meeting of the Society for Biological Radiation Research, Essen

25/09/2017 Molecular Basis of Life 2017 – International Fall Meeting of the German Society for Biochemistry and Molecular Biology, Bochum

Poster presentations

21/11/2014 Research day, University Hospital Essen

06/02/2015 EACR Conference ‘Radiation Biology and Cancer’, Essen

20/11/2015 Research day, University Hospital Essen

28/06/2016 ICGEB Conference “At the Intersection of DNA Replication and Genome Maintenance: from Mechanisms to Therapy”, Trieste, Italy

15/09/2016 14th Biennial Meeting of the DGDR “DNA Repair 2016”, Essen

18/10/2016 Network Meeting GRK1739 and GRK1657 Kloster Höchst, Höchst im Odenwald

04/04/2017	Keystone Symposia/Conference “Genomic Instability and DNA Repair” Santa Fe, NM, USA
25/09/2017	Molecular Basis of Life 2017 – International Fall Meeting of the German Society for Biochemistry and Molecular Biology, Bochum

Curriculum vitae

The curriculum vitae is not included in the online version for reasons of data protection.

Erklärungen

Die Erklärungen sind in der Online-Version aus Gründen des Datenschutzes nicht enthalten.